UNIVERSITY
of
GLASGOW

DEPARTMENT *of* GEOGRAPHY *and* GEOMATICS

The hydrology and dynamics of a glacier overlying a linked-cavity drainage system

Karin Grust

Submitted to the faculty of Physical Sciences
for the degree of Doctor of Philosophy

December 2004

"The real voyage of discovery consists not in seeking

new landscapes, but in having new eyes."

Abstract

This thesis investigates the links between glacier hydrology and ice dynamics at Glacier de Tsanfleuron, a small temperate glacier overlying a linked-cavity system in the Valais Alps, Switzerland. A better understanding of glacier hydrology and its interconnected research areas (e.g. glacier dynamics, hydrochemistry of glacial meltwaters, landscape erosion through sediment transport and solute acquisition) is important if we are to effectively predict how ice masses have responded to paleo-climatatic changes and how contemporary ice masses may respond to future climate change.

Fieldwork was undertaken at Tsanfleuron from 23 June to 5 September 2001 in order to capture the evolution of the glacier's hydrology over the course of a melt season and to establish how variations in hydrology influenced ice-dynamics. Glacier de Tsanfleuron is a remarkable site for studying inefficient drainage characteristics because Nye channels and cavities, incised into soluble bedrock have created a stable subglacial drainage structure. However, the inaccessibility and complexity of the glacio-hydrological processes require interdisciplinary research approaches. The areas of investigation in this study were snowpack hydrology, subglacial hydrology and glacier dynamics using techniques such as dye tracing, water level monitoring at the snow-ice interface, meteorological data recording, ablation measurements, discharge gauging, basic numerical modelling and survey of a stake network across the glacier.

The specific aims of the study were to investigate (i) intra-seasonal variations in drainage conditions within the supraglacial snowpack and the effect this has for meltwater delivery to the englacial and subglacial drainage system; (ii) the extent to which subglacial drainage conditions, as observed in the deglaciated proglacial bedrock, are representative of the current subglacial drainage conditions; (iii) the extent to which meltwater drainage into the glacier emerges from the snout of Tsanfleuron and the role karst sinkholes play for subglacial hydrology and (iv) the extent to which seasonal variations in glacier hydrology affect ice dynamics due to variations in water pressure and basal sliding.

The research results demonstrate that meltwater input to the englacial drainage system is significantly delayed by the supraglacial snowpack with travel velocities through the snowpack (0.08 to 0.32 mh^{-1}) more than an order of magnitude slower than the flow at the water-saturated snow-ice interface (7.7 mh^{-1} and 12.2 mh^{-1}). Since meltwater delivery is

critically influencing subglacial hydrology this has a significant impact on glacier sliding. Tracer return curves obtained from experiments in the subglacial drainage system showed low flow velocities (between 0.02 to 0.05 ms^{-1}) and high dispersivities (23 to 80 m) reflecting meltwater routing through an inefficient drainage system. This supports the existence of an inefficient linked-cavity drainage system beneath the present glacier. Results of the subglacial tracer experiments and basic modelling of Nye channel flow velocities indicate that subglacial meltwater travels most of the distance in Nye channels but spends most of the time in cavities.

Mean intra-seasonal surface velocities of 4 cm d^{-1} or 15 m a^{-1} respectively, were obtained form the survey of a stake network across the glacier. Horizontal surface velocities are generally higher at lower altitudes than at higher altitudes. There was no clear dynamic response (e.g. speed-up events due to increased subglacial water pressure) to seasonal meltwater inputs observed throughout the melt season, although large amounts of meltwater entered the englacial and subglacial systems in July and August. This suggested that higher water pressures were prevented by (i) the sufficient capacity of the Nye-channel and cavity configuration; (ii) water drainage into the karst bedrock or (iii) a too small meltwater input during the 2001 melt-season to attain pressurisation. An important finding of the research was the apparent loss of approximately 95 % of basal water into the bedrock karst. This is reflected in relatively low proglacial discharges from a limited catchment area. From the results obtained, it seems apparent, that the karstic bedrock and the linked Nye channel and cavity system play a critical role in limiting speed-up events.

Contents

List of Figures

List of Tables

Acknowledgements

A huge "thank you" to my supervisors Peter Nienow (University of Glasgow) and Martyn Tranter (University of Bristol). Thanks Pete, for your open-minded attitude, good discussions about research issues, constructive feedback and your patience with my English. I very much appreciated the opportunity of working on Glaciers in Greenland, Norway and Switzerland and I will always keep these exciting field experiences in good memory. Thanks to Martyn for the encouragement throughout my PhD time and discussions and advice in the field.

Special thanks go to my proof-readers Thomas Schuler and Russell Salisbury, who helped with their constructive comments, ideas and also with the English. This thesis benefited greatly from their thorough work. Throughout my PhD time, Thomas also provided constructive discussions via email and introduced me to the CXTFIT model. Furthermore, many thanks to "Nigel the duck" and "Dave the dog" for their clever remarks.

Many thanks to my field assistants at Glacier de Tsanfleuron Andrea Bull, Fay Campbell, Elena Dittmann, Jenny Dixon, Phillip Dunn, Anja Fleig, Christophe Hagedorn, Katie Hill, Daniela Kasbaur, Michael Moritz and Kerstin Wille, who helped collecting the data this thesis is based on and who made the field a fantastic place to be.

Sincere thanks are also due to Christian Dessimoz and colleagues of the Commune de Conthey, Switzerland, and Daniel Masotti for providing useful information and maps about the karst system and hydrological research area. Thank you for the interesting excursion to the Source des Glareys which helped me to understand the significant impact of the karst system beneath the glacier.

I would also like to thank Peter Chung for the help preparing the field equipment Pierre Schnegg for repairs and advice on the borehole-fluorometer and Brian Black for his assistance during times of computer problems. Many thanks to Uwe Hass for helping with Surfer plots in the "last minute" and Michael Trüber who helped with VBA programming that enabled me to progress field data more efficiently.

I gratefully acknowledge the financial support of Paul Bishop, Department of Geography and Geomatics, University of Glasgow and the British Geomorphological Research Group.

Thanks to my friends in Glasgow who made Scotland a great experience. Thanks to all my friends and family in Germany who came for visits to the field site or to Scotland, or provided pleasant times during my visits to Germany, who sent emails, letters and parcels and gave lots of encouragement during my writing-up time. ...and a monstrous "Thanks!" to Russell who gave great support during the final stages of my thesis and who made me think about other things than my thesis.

Declaration

This thesis embodies the results of original research carried out by the author. References to existing works are made as appropriate. Any remaining errors or omissions are the responsibility of the author.

Karin Grust

December 2004

1 Introduction

1.1 Rationale

Water movement within and beneath glaciers is of scientific interest, because it significantly influences glacier dynamics (Iken and Bindschadler, 1986; Mair et al., 2002), glacier outburst floods (Nye, 1976; Clarke, 1982; Björnsson, 1998; Fowler, 1999; Clarke, 2003) and landscape erosion through sediment transport (Swift et al., 2002; Alley, 2003) and solute acquisition (Collins, 1979; Tranter et al., 1996; Brown, 2002). Understanding how contemporary glaciers respond to varying meltwater inputs is critical if we are to effectively predict both how ice masses will respond to future climate change and what conditions have caused fluctuations in their spatial behaviour in the past.

It has been recognised that glacier hydrology plays a central role in glaciology (Stenborg, 1969; Röthlisberger and Lang, 1987; Nienow et al., 1998). Improved understanding of the links between glacier hydrology and glacier dynamics has important implications for other glacial research areas, such as hydrochemistry of glacial meltwaters and the mobilisation of subglacial sediments. For a comprehensive understanding of glacial hydrology, an advance in the understanding of glacial snowpack hydrology, the mechanisms of subglacial drainage and their relationship to glacier dynamics is essential. This thesis is concerned with the links between snow hydrology, subglacial hydrology and ice dynamics at Glacier de Tsanfleuron, a small temperate glacier in the Valais Alps, Switzerland.

The presence of a snowpack at the glacier surface cannot be ignored, since snow delays meltwater runoff and consequently introduces lags between meltwater production and delivery to the englacial and subglacial systems (Male and Gray, 1981). It has been demonstrated that the snowpack on glaciers influences discharge and water quality at the glacier terminus (Fountain, 1996) and thus plays a critical role in determining subglacial drainage conditions and consequently ice dynamics (Stenborg, 1969; Röthlisberger and Lang, 1987; Nienow et al., 1998). In order to fully understand subglacial hydrology, surface meltwater inputs to the englacial and subsequently subglacial drainage systems must be investigated. Water flow through snow is poorly understood regarding the temporal and spatial variations in meltwater storage and routing. Therefore, there is a need to investigate the effects of the supraglacial snowpack on meltwater delivery to the englacial and

subglacial drainage systems as part of a fully integrated investigation of hydrology and dynamics of a glacier.

Whilst supraglacial hydrology and permeability of the ice influences the delivery of surface meltwaters to the glacier bed, the subsequent impact of subglacial hydrology on the ice-bed interface initially controls basal water pressures, basal sliding and thus ice-dynamics (Kamb et al., 1985). It is generally recognised that a variety of different subglacial drainage configurations can exist beneath glaciers (e.g. Hooke, 1989), and these can vary both between glaciers and at individual glaciers over intra-seasonal timescales. Several research results have suggested an inefficient distributed drainage system exists at the start of the melt season, often described as a linked-cavity drainage system, which throughout the melt season evolves to an efficient, channelised drainage system (Fountain, 1992; Arnold et al., 1996; Nienow et al., 1996; Gordon et al., 1998; Nienow et al., 1998; Willis et al., 2002, Bingham, 2003).

In previously investigated cases of glaciers flowing over a hard, impermeable bed, large volumes of supraglacially derived meltwaters delivered quickly in the early stages of a melt season to a linked-cavity system cause increased subglacial water pressures (Nienow et al., 1998, Gordon et al., 1998). This pressure, if meltwater input increases continuously, can increase sufficiently to produce transient floating of a large proportion of the glacier above the glacier bed. This causes a speed-up event of enhanced basal sliding and vertical uplift, due to reduction of basal friction (Iken, 1981; Bindschadler, 1983; Iken et al., 1983; Iken and Bindschadler, 1986; Jansson, 1995; Hanson et al., 1998). Speed-up events cause instability of the distributed drainage system and the reorganisation of subglacial drainage causing the development of channelised conditions due to larger amounts of meltwater. The hydraulics of the subglacial linked-cavity system are distinct from those of a channelised system. Kamb (1987) developed a model describing the relationship between water discharge (Q) and subglacial pressure (P_W) of a channelised and linked-cavity drainage system. The schematic simplification of his theory (Figure 1.1) shows that, in the channelised system, the water discharge (Q) is a decreasing function of water pressure (P_W), whereas in a linked-cavity system it is an increasing function (Kamp, 1987). In the linked system, an increase in basal water pressure enlarges the cavities and therefore increases the basal water flux. Conversely, in a channelised system, an increase in basal

water flux results in a decrease in water pressure in the channel, once a steady state system is established (Kamb, 1987)

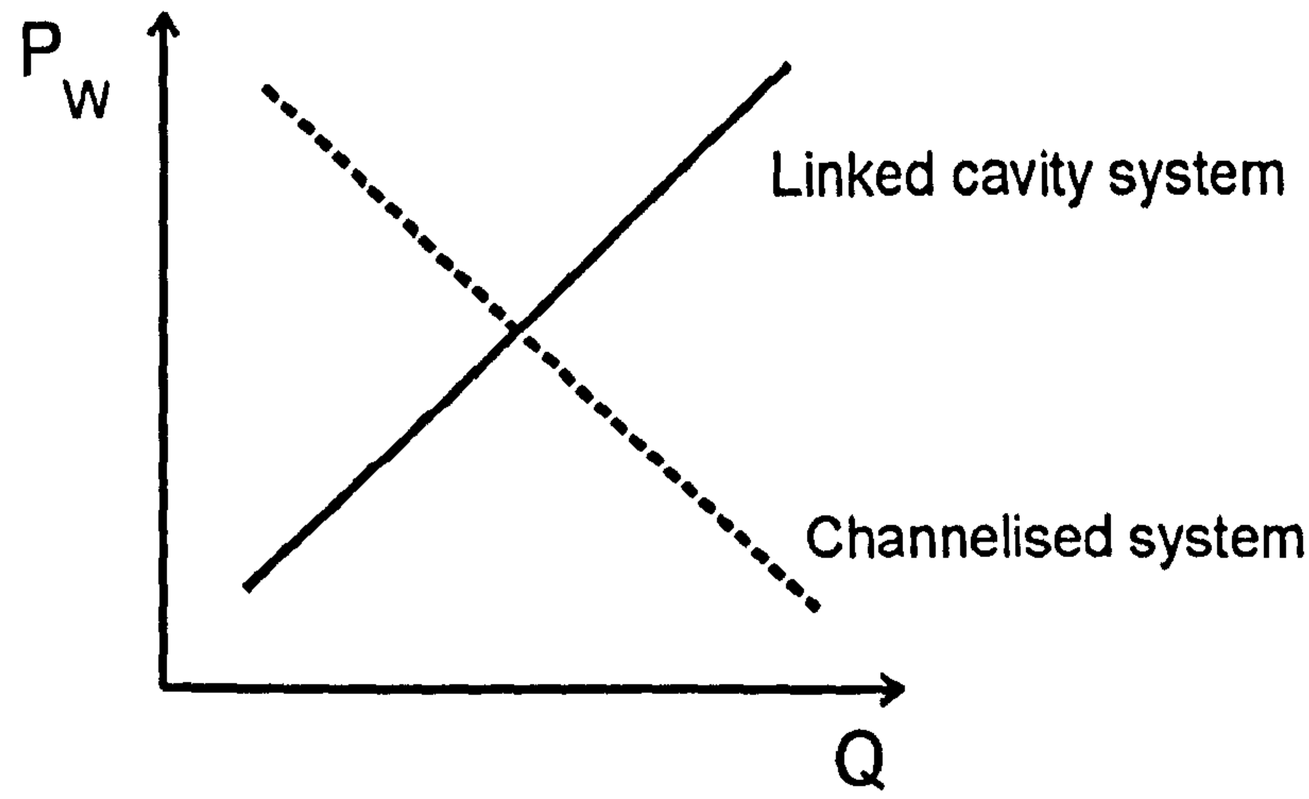

Figure 1.1: Schematic relationship between discharge (Q) and subglacial pressure (P w) of channelised and linked-cavity drainage system. The diagram shows the principle of increasing and decreasing limbs but they are not necessarily linear (Kamb, 1987).

The important role of the subglacial linked-cavity system in glacier hydraulics and dynamics has been recognised (Walder, 1986). However, at many glaciers it is difficult to study the hydraulic behaviour of a linked-cavity systems because they either drain so inefficiently that investigations are difficult (e.g. in winter) or they transform into a channelised system due to quickly increased meltwater input once the melt season has started and therefore only exist for a limited time period. However, it remains to be determined the degree to which links between hydrology and dynamics, observed at certain glaciers (e.g. at Haut Glacier 'd Arolla, Mair et al., 2002), are characteristic of other glaciers.

This study investigates links between glacier hydrology and ice dynamics at Glacier de Tsanfleuron. The glacier provides an ideal "laboratory" for innovative research because a relict of the subglacial drainage system is preserved in its forefield. Glacier de Tsanfleuron is underlain by highly soluble limestone bedrock, and thus the former subglacial drainage system structures become exposed as the glacier retreats (Sharp et al., 1989). The exposed structure consists of linked-cavities interconnected by subglacial passageways incised into the bedrock (Nye-channels) (Nye and Frank, 1973). It is likely that the structure continues subglacially beneath at least the lower part of the current glacier. This relict subglacial drainage system makes Glacier de Tsanfleuron an ideal research location for obtaining a

better understanding of linked-cavity drainage systems. To date, channelised systems including their hydraulic structure and seasonal evolution is better understood then that of linked-cavity systems. Since there is evidence for the existence of distributed, hydraulically inefficient drainage beneath many temperate glaciers (Lang et al., 1979; Brugman, 1986; Kamb, 1987; Nienow et al., 1998; Hock et al., 1999), an investigation of such a system should improve the understanding of subglacial drainage processes beneath these glaciers.

1.2 Objectives

The objective of this thesis is to contribute towards a better understanding of the links between glacier hydrology and ice dynamics. The evolution of the subglacial drainage system has been observed at many glaciers, but hydraulic characteristics of inefficient drainage configurations remain incomplete. Inefficient drainage configurations such as linked-cavity systems control meltwater drainage in the early melt season at many glaciers. The existence of inefficient subglacial drainage systems in conjunction with subglacial water storage has been linked to speed-up events (resulting from periods of enhanced basal sliding), particularly in the early melt season (Iken et al., 1983; Röthlisberger and Lang, 1987; Mair et al., 2002). When a linked-cavity system exists beneath a glacier, theory suggests there is a positive relationship between meltwater flux through that system and subglacial water pressure (Kamb, 1987) and thus a positive relationship between meltwater flux and rates of basal sliding. Thus given the presence of a linked-cavity system beneath Glacier de Tsanfleuron, the theoretical relationship observed by Kamb would be expected with the associated dynamic response to meltwater inputs.

The principal aim of the project, therefore, is to study the extent to which supraglacial and subglacial hydrology impacts on the ice dynamics of a glacier underlain by a linked-cavity subglacial drainage system. More specifically the aims of the study are to investigate:

(i) intra-seasonal variations in drainage conditions within the supraglacial snowpack and its effect this has for the meltwater delivery to the englacial and subglacial drainage system.

(ii) the extent to which subglacial drainage conditions, as observed in the deglaciated proglacial bedrock, are representative of the current subglacial drainage conditions.

(iii) the extent to which meltwater drainage into the glacier emerges from the snout of Glacier de Tsanfleuron and what role karst sinkholes play for subglacial hydrology.

(iv) the extent to which seasonal variations in glacier hydrology impact on the ice dynamics due to variations in water pressure and basal sliding.

To obtain these objectives a dye tracing programme investigating supraglacial and subglacial drainage conditions was undertaken in conjunction with surveys of glacier surface motion throughout the 2001 melt season. Additional information concerning glacial hydrology, runoff and meteorological conditions was also collected as will be discussed more fully in Chapter 3. The field work was undertaken from June to September with assistance of students from the Universities of Glasgow, Bristol and Aberystwyth (UK), Freiburg and Freiberg (Germany) and Innsbruck (Austria).

1.3 Research area: Glacier de Tsanfleuron, Switzerland

The aim of this section is to give an overall description of the field area. The characteristics of the research area are critical for achieving the goals outlined in the previous section. Therefore, in this section the field site and the hydrology of the catchment area are described and advantages and limitations of the field site are discussed. Furthermore, previous work concerning the hydrology of the area and the glacier forefield are summarised.

1.3.1 Field site description and characterisation

The devils legend

The legend tells that in ancient times Glacier de Tsanfleuron was beautiful, sunny pastures. These pastures of Tsanfleuron (flowery field) were damned since the day that a mean hearted shepherd refused his help to a needier person. The once pretty flowery field became a wild rocky and icy desert. It became the refuge for spiteful ghosts, a crossroads of the underworld; where the damned and all evil spirits gathered. In the valley, the shepherds heard the devils playing skittles. Hence the name "Quille du Diable" (Devil's Skittle) was given to the tower-shaped rock (Tour Saint Martin) at the southern border of Glacier de Tsanfleuron. This huge rock was meant to serve as target, goal or skittle for the various games of skill or brute force played by the devil and his demons. Thus, when stones rolled noisily down from this gigantic donjon the local people believed that diabolical players on the vast icy esplanade where throwing rocks with great force to knock over the skittle. The rocks bouncing down threatened the shepherds in the valley, as the devils played their heinous games of skittles. It is unlikely that Saint Martin would have approved!

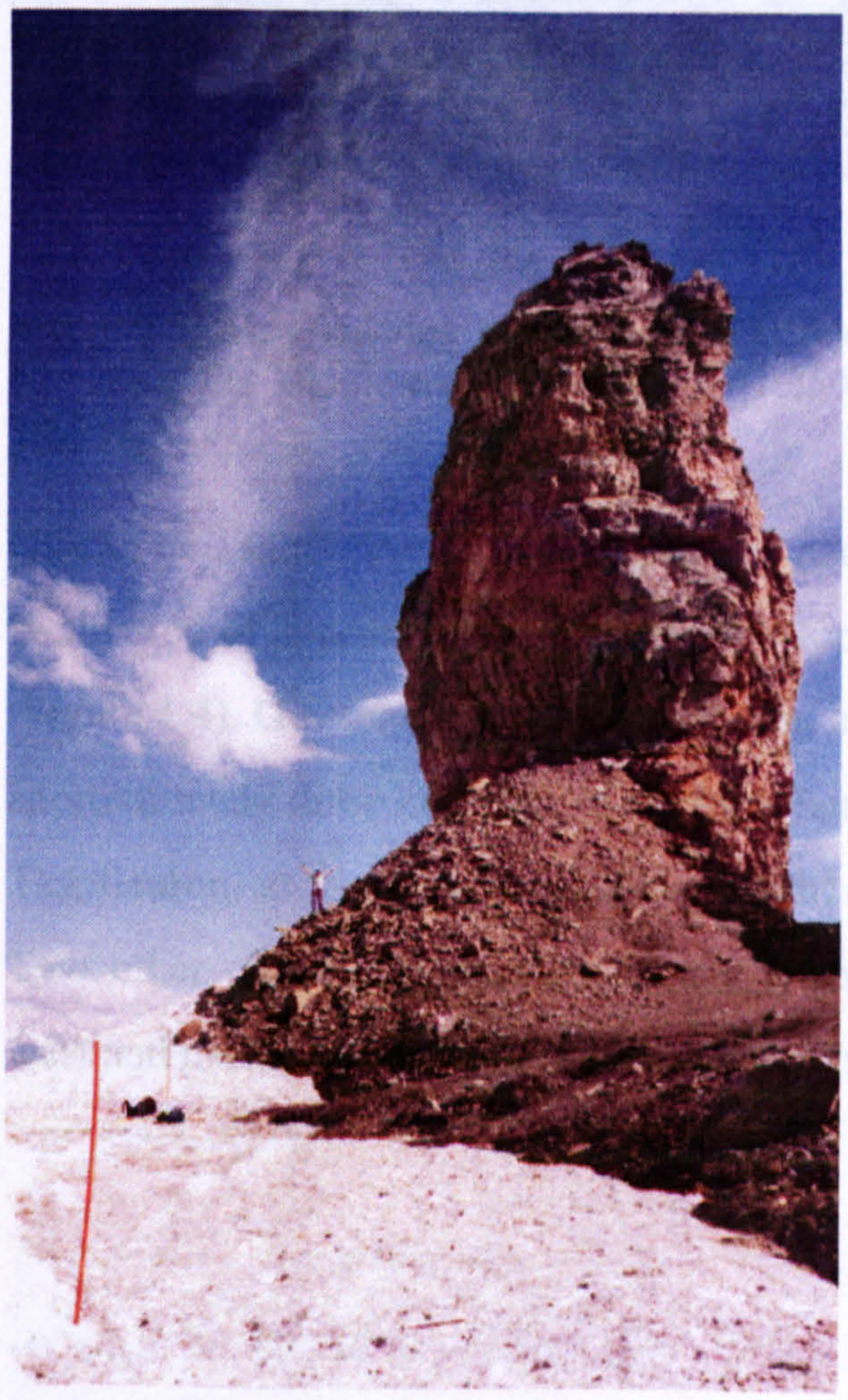

(Source: "Légendes des Alpes vaudoises" - "Diables et démons", de Ceresole).

Figure 1.2: "Quille du Diable" (Devil's Skittle) at Glacier de Tsanfleuron.

1.3.1.1 Location and general description

The site of this study, Glacier de Tsanfleuron (46° 19' N, 7° 14' E), is located on the massif des Diablerets-Suisse on the northern side of the Rhône valley northwest of the village Sion, in the Valais canton of western Switzerland (Figure 1.3).

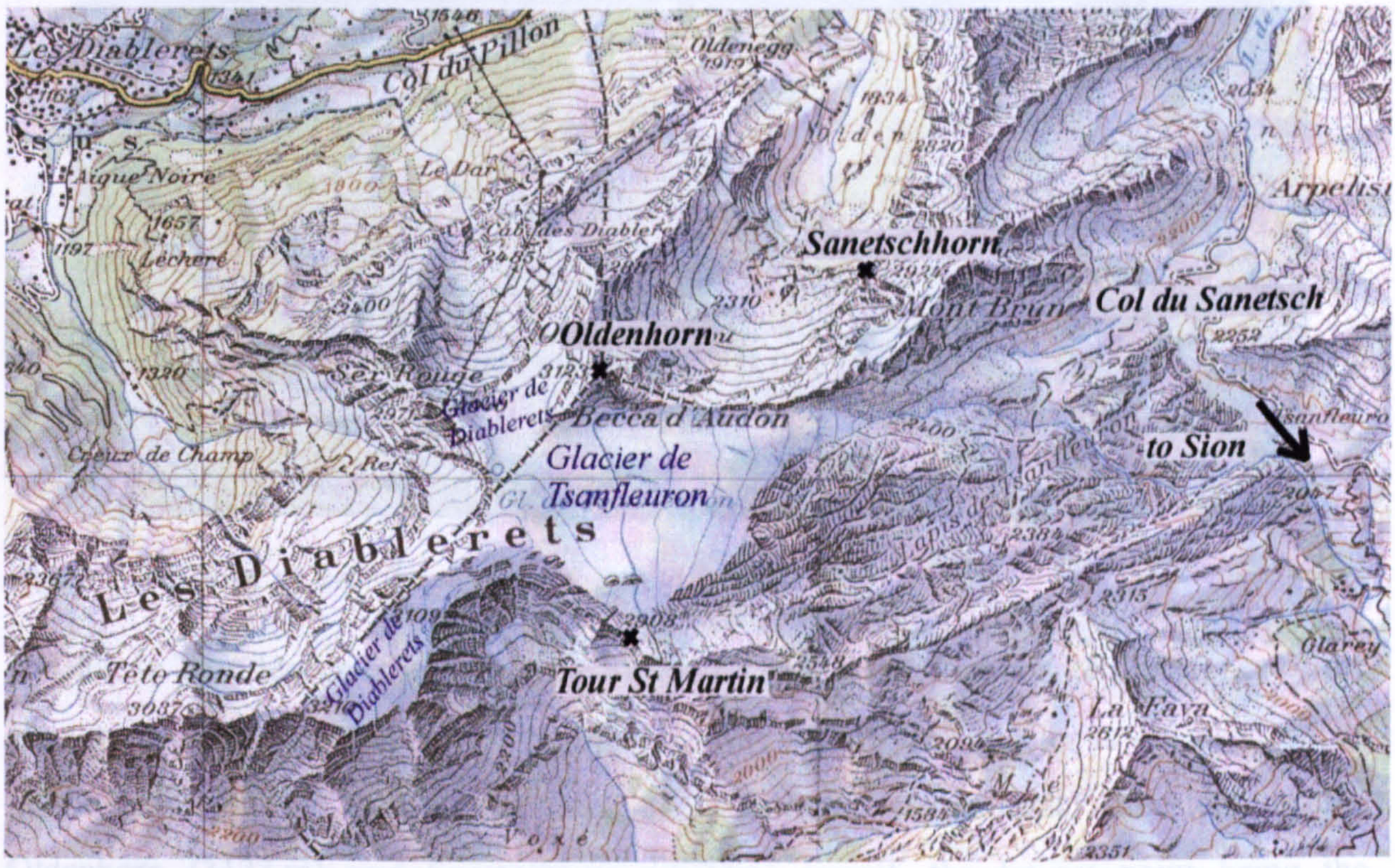

Figure 1.3: Map showing the location of Glacier de Tsanfleuron, Carte Nationale de la Suisse, No. 1285, Les Diablerets and No. 1286 (1:25000), St-Léonard (Office fédéral de topographie, 1992).

Glacier de Tsanfleuron is a small plateau glacier, flowing from west to east with an average inclination of approximately 5 degrees, steepening to around 15 degrees towards the snout (Figure 1.4). Glacier de Tsanfleuron has an area of about 4 km^2 and a present day length of approximately three km, from the glacier head, approximately 500 m south west of Col de Tsanfleuron, at an altitude of 2844m to the glacier snout at an altitude of about 2500 m. Two other outlet glaciers, Glacier des Diablerets and Glacier du Sex Rouge flow south west and north, respectively from the main Tsanfleuron plateau.

Figure 1.4: Glacier de Tsanfleuron from the proglac ial area.

Glacier de Tsanfleuron is underlain by Mesozoic and Tertiary carbonate limestones of the Hauterivian and Urgonian series (Fairchild et al., 1994). The glacier is enclosed on its northern margin by the scarped ridge of Hauterivian (Cretaceous) limestone of the Oldenhorn (3123 m) and Sanetschhorn (2923m) massif, the lowest point being the Oldensattel at 2737m. It is bounded to the south by the Urgonian (Cretaceous) limestone of Les Diablerets (3003m) and Tour Saint Martin (Quille du Diable) (2908 m). To the west the glacier is restricted by the south east arête of Sex Rouge (2971 m) and Le Dôme (3005 m). The equilibrium line (ELA) of the glacier is reported to be about 2700 m (Sharp et al., 1989), but has now probably increased in altitude due to further recession.

1.3.1.2 Geology and Hydrology

The catchment geology is dominated by Cretaceous and Tertiary limestones (Hubbard and Hubbard, 1998; Fairchild et al., 1999) in which a karstic drainage system has developed, the geology is an important aspect of the catchment hydrology and therefore influences the meltwater drainage of Glacier de Tsanfleuron.

The glacier terminates on a karstic limestone plateau which is near to the boundary between the top of a massive pure Cretaceous (Urgonian) limestone and thinly bedded Tertiary limestones (Figure 1.5 and Figure 1.6).

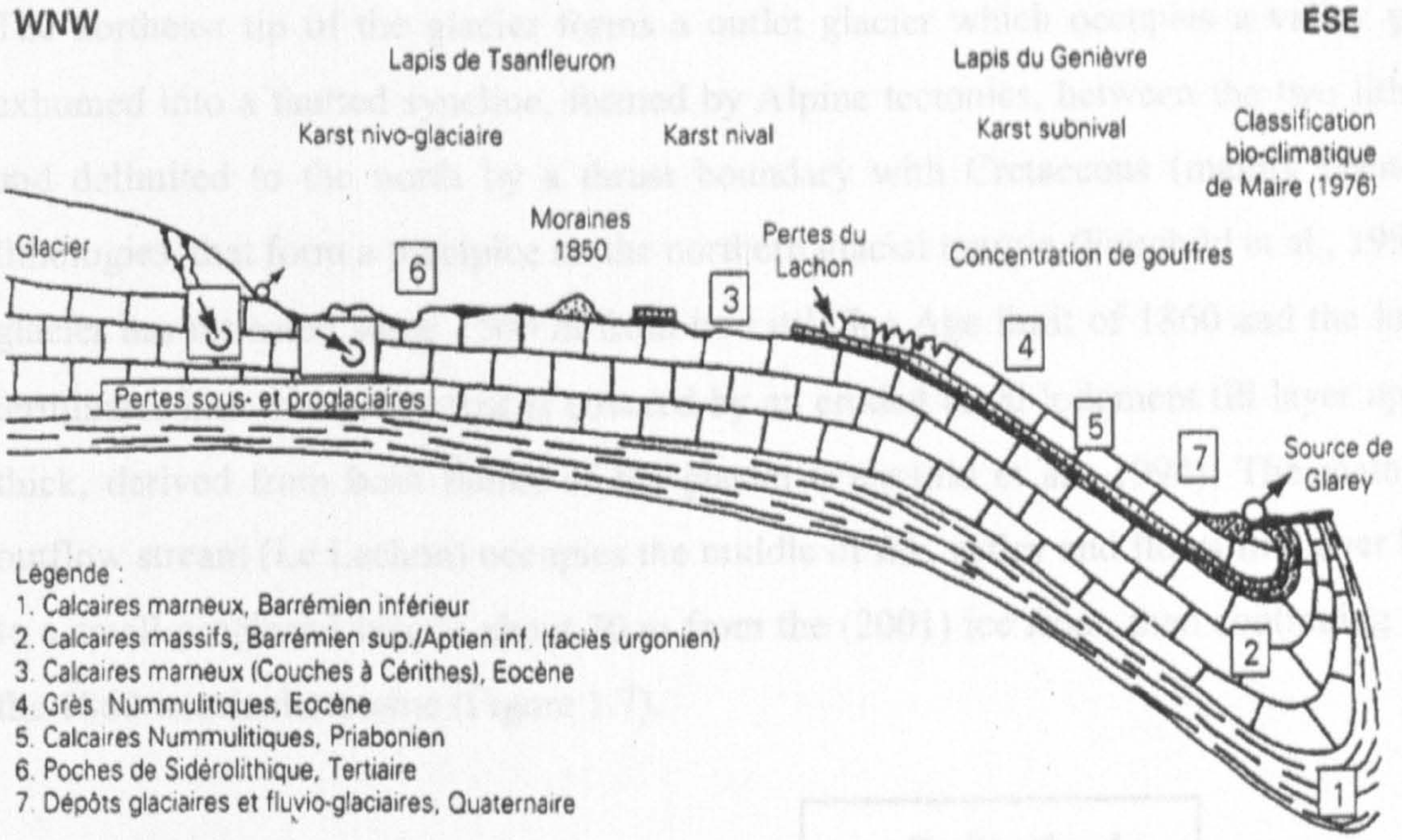

Figure 1.5: Location, geology and cross section of the proglacial area adjacent to Glacier de Tsanfleuron (after Fairchild et al., 1994)

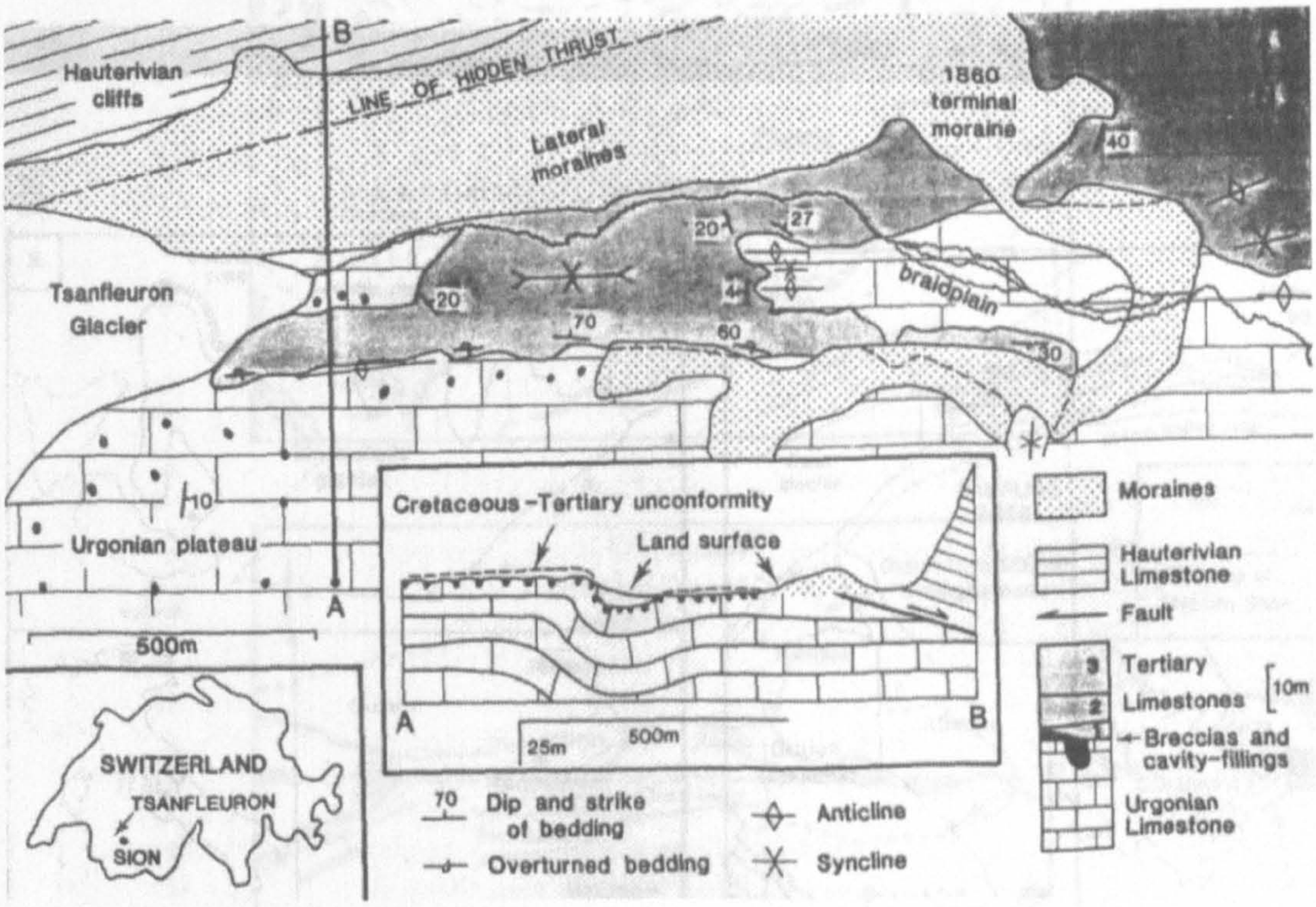

Figure 1.6: Schematic diagram showing the relation of Glacier de Tsanfleuron and its underlying karst (not to scale).

The northeast tip of the glacier forms a outlet glacier which occupies a valley glacially exhumed into a faulted syncline, formed by Alpine tectonics, between the two lithologies and delimited to the north by a thrust boundary with Cretaceous (mainly Hauterivian) lithologies, that form a precipice on the northern glacial margin (Fairchild et al., 1994). The glacier has retreated some 1500 m from its Little Ice Age limit of 1860 and the lobe now terminates into this valley that is covered by an eroded basal lodgment till layer up to 2 m thick, derived from both flanks of the glacier (Fairchild et al., 1994). The main glacier outflow stream (Le Lachon) occupies the middle of this valley and flows first over bedrock to a small proglacial lake at about 70 m from the (2001) ice front, then continuing through the 1860 terminal moraine (Figure 1.7).

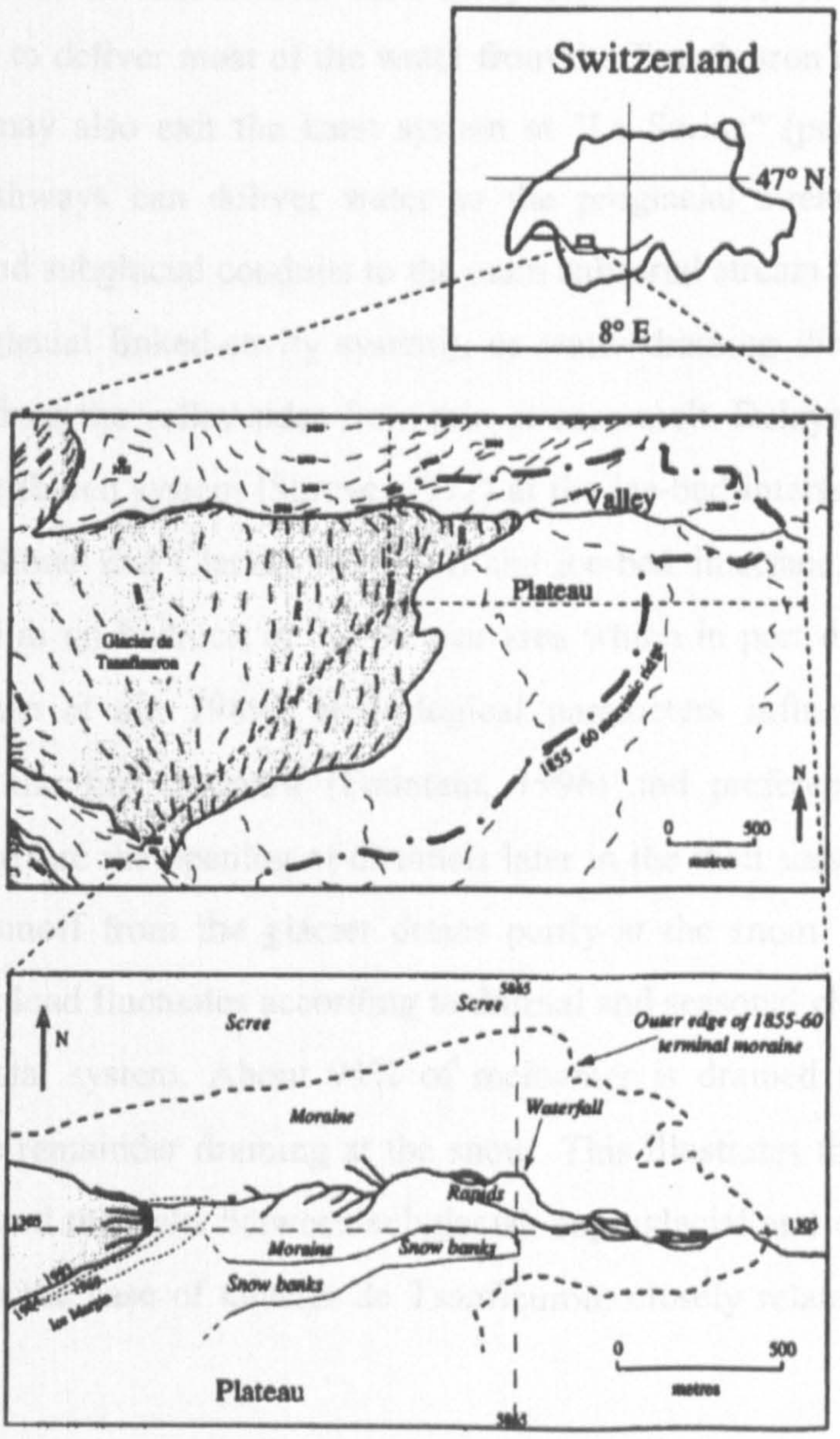

Figure 1.7: Location of Glacier de Tsanfleuron including the main subaerial meltstream "Le Lachon" (after Fairchild et al., 1999).

The exposition of the former subglacial bed, now proglacial area, gives a clue about the structure of the existing subglacial drainage system. The forefield is a vast a glacio-karst plateau environment of about 9 km^2 consisting of cavities linked by Nye-channels (of 0.1-0.2 m width and 0.1 m depth occurring at intervals of approximately 1.5 m across the glacier bed), 75% of which have a blind termination. They formed parallel to the former ice-flow direction and build a dissected network (Sharp et al., 1989). This Nye-channel and striated bedrock forefield has been exposed following the Little Ice Age retreat. This is underlain and bordered to the south by limestone karst. When water enters this system it is doubtful that it will re-emerge since the vertical karstic system has developed to considerable depth (Fairchild et al., 1999). However, a spring above the dammed lake "La Lixerne" (issuing from an inaccessible rock face) and at Source de Glarey, at 1547 m a.m.s.l are believed to deliver most of the water from the Tsanfleuron catchment. A minor quantity of water may also exit the karst system at "La Sarine" (pers comm., Massotti 2001). Various pathways can deliver water to the proglacial stream, waters draining through englacial and subglacial conduits to the main subaerial stream (possibly with some storage in the subglacial linked-cavity system), or water draining directly into the karst aquifer, or run off from the valley sides from rain or snowmelt. Delayed flow components spend time in a distributed system (Shreve, 1972) at the ice-bed interface, or as porewater in subglacial till (Stone and Clarke, 1996). At the ice-bed interface, the film reservoir represents a fluid film on bedrock in the plateau area which in part drains into a linked-cavity system (Sharp et al., 1989). Hydrological parameters influenced by snowmelt include storage in the firn reservoir (Fountain, 1996) and preferential routing into a distributed system before the opening of channels later in the melt season (Richards et al., 1996). Meltwater runoff from the glacier drains partly at the snout. The discharge and suspended sediment load fluctuates according to diurnal and seasonal changes of meltwater delivery to the glacial system. About 95% of meltwater is drained through the karstic bedrock system, the remainder draining at the snout. This illustrates that the hydrological system is complex and the links between subglacial, supraglacial and englacial hydrology are probably not, in the case of Glacier de Tsanfleuron, closely related to the proglacial outflow.

1.3.1.3 Snow conditions during the 2001 field season

At the start of the field season a thick snow layer that remained from the previous winter and spring snowstorm events covered the whole catchment. At the end of June snow thickness ranged from 2 m in lower to > 4 m in higher parts of the catchment. Summer 2001 was characterised by a late onset of snowmelt, but during July and August significant melting occurred and the snowpack was significantly reduced, August snow depth mainly between 0.5 and 1.0 m. However, due to the masses of deposited winter snow and two snowfall events in July and August more than 70 % of the glacier surface remained snow covered throughout the entire melt season and the snow line (ELA) did not rise above 2600 m. Moulins and crevasses through which supraglacial meltwater is drained did not open before the End of August 2001.

1.3.2 Previous research

This section briefly summarises previous work and gives an overview of the current knowledge of the hydrology, hydrochemistry, dynamics and geomorphology of Glacier de Tsanfleuron and its surrounds.

Glacier de Tsanfleuron has become a classic site principally for studies of subglacial hydrological processes involving carbonate dissolution and reprecipitation of distinctive carbonate crust deposits as exposed in the proglacial area (e.g. Fairchild et al., 1994; Fairchild et al., 1999; Hubbard and Hubbard, 1998). Also, as a by-product of other research, but by no means unique to Glacier de Tsanfleuron, isotopic evolution of basal ice in relation to refreezing events and Weertman regulation has been studied (Hubbard and Sharp, 1993). In this context the metamorphosis of clear-facies basal ice and its characteristics have also been evaluated at Tsanfleuron (Hubbard et al., 2000). The extensive proglacial area has been examined due to its unique glacio-karst geomorphology and hydrology by Masotti (1991), who demonstrated that a large quantity of the water entering the proglacial environment is given up to the underlying karst. However, perhaps of most relevance here is the previous work carried out on the hydrological characteristics of the forefield (Sharp et al., 1989) as well as the basal dynamics work of Hubbard (2002). Observations from the proglacial area of Glacier de Tsanfleuron suggest, by inference that this area was formerly subglacial, that the subglacial drainage system consists of a system

of cavities that are linked by numerous Nye-channels (Sharp et al., 1989). This cavity and Nye channel system covers approximately 50 % of the proglacial bedrock surface(Sharp et al., 1989), from this, it is not unreasonable to suggest that the contemporary subglacial area shares a similar configuration. Similarly, the number and distribution of sinkholes in the proglacial surface, where meltwater enters the karst drainage system, has also been mapped (Sharp et al., 1989), this will have impacts on the subglacial water pressure distribution at the glacier bed. Sharp et al., (1989) also suggested that the number of active channels would depend on meltwater fluxes and pressurised flow and would therefore occur episodically, activated by high meltwater inputs. Sharp et al.'s suggestions concerned what is in effect, a preserved or relict drainage system. Within such a subglacial system, an unknown, but certainly very large, volume of water would be required to fill and subsequently pressurise, and therefore influence basal dynamics, the channels, cavities and karstic system at the glaciers base.

More recently Glacier de Tsanfleuron has been the subject of research regarding the spatial differences in water content affects the flow characteristics of temperate glaciers (Hubbard et al., 2003). Hubbard (2002) has also made some very significant (to this study), direct measurements of basal ice flow velocities at Glacier de Tsanfleuron, using continuous logging, over a six day summer period, of fixed potentiometers. Also, and perhaps more esoterically Bates et al. (2003) have constructed numerical simulations of a three-dimensional hydro-dynamical model of pressurised and atmospheric flow in a Nye channel. This work may contribute to the improvement and calibration of computational fluid dynamics (CFD) models, but the contribution to obtaining an accurate digital elevation model (DEM) of the real sub-glacial system operating at Glacier de Tsanfleuron is doubtful.

1.4 Thesis outline

This thesis is composed of seven chapters. Chapter 1 describes the field site and gives the rationale and the aims of this study. Chapter 2 reviews the contemporary literature regarding glacial hydrology, snow hydrology and glacial dynamics. Methods (Chapter 3) gives detailed insight into the variety and execution of the various techniques and field observations made at Glacier de Tsanfleuron during the 2001 season and the subsequent analysis of the gathered data.

Chapters 4, 5 and 6 analyse of the results in detail and discuss the implications of the snowpack and subglacial hydrology together with the dynamic regime operating on and within the glacier during the 2001 ablation season. This thesis is concluded with Chapter 7 that gives a summary of the major findings of this research in context with previous research at both Glacier de Tsanfleuron and other similar environments. Suggestions for improvements and future research in subglacial hydrology and glacial dynamics are also discussed.

2 Hydrology and dynamics of glaciers: a review

2.1 Introduction

This chapter presents an overview of literature relevant to glacier hydrology and ice dynamics. Following the introduction, Section 2.2 summarises the energy flux considerations that control surface meltwater generation. Section 2.3 and 2.4 concern the hydrology of firn/snow and englacial/subglacial hydrology respectively. Section 2.5 summarises glacier dynamics and the extent to which hydrology impacts on glacier sliding mechanisms.

From a hydrological perspective, a glacier represents an aquifer consisting of ice, firn (snow older than one year) and snow. Glaciers differ from other aquifers in two main characteristics: (i) the aquifer is built by water in different phases and (ii) due to both glacier movement and the sensitivity of snow/ice to meteorological impacts, the system is highly dynamic. In most temperate glaciers, the main source of water contributing to glacier runoff is surface meltwater (Röthlisberger and Lang, 1987), which is drained through a variety of complex systems. The distribution of meltwater generation at the glacier surface is complex and varies spatially and temporally over the course of the melt season. Rates of meltwater generation vary in particular between snow and ice surfaces. In the accumulation area, annual snowfall exceeds snowmelt, thus snow cover remains all year around. By contrast in the ablation area, winter snow cover disappears during the summer and glacier ice becomes exposed. Consequently different melt characteristics (e.g. meltwater volumes) and mechanisms of meltwater drainage evolve in these areas. In the accumulation area, meltwater percolates through the snow and firn layer until it reaches glacier ice with significantly lower permeabilities. Water flow continues along the ice surface and during the ablation season often a saturated layer develops at the snow-ice interface (Meier, 1973; Ambach et al., 1981). Crevasses, moulins (e.g. Holmlund, 1988) and inter-granular veins (Nye and Frank, 1973) give meltwater access to the interior of the glacier and to the englacial drainage system. Once water reaches the glacier bed, it is transferred to the terminus through the subglacial drainage system. Since the interior of the glacier is virtually inaccessible (Röthlisberger and Lang, 1987), direct observations of englacial and subglacial drainage systems are generally restricted to the glacier surface,

natural or artificial cavities at the margins and at the terminus. Therefore, various indirect methods have been used to investigate the internal drainage system of glaciers resulting in our current understanding of the principle drainage pathways of a glacier as shown in Figure 2.1.

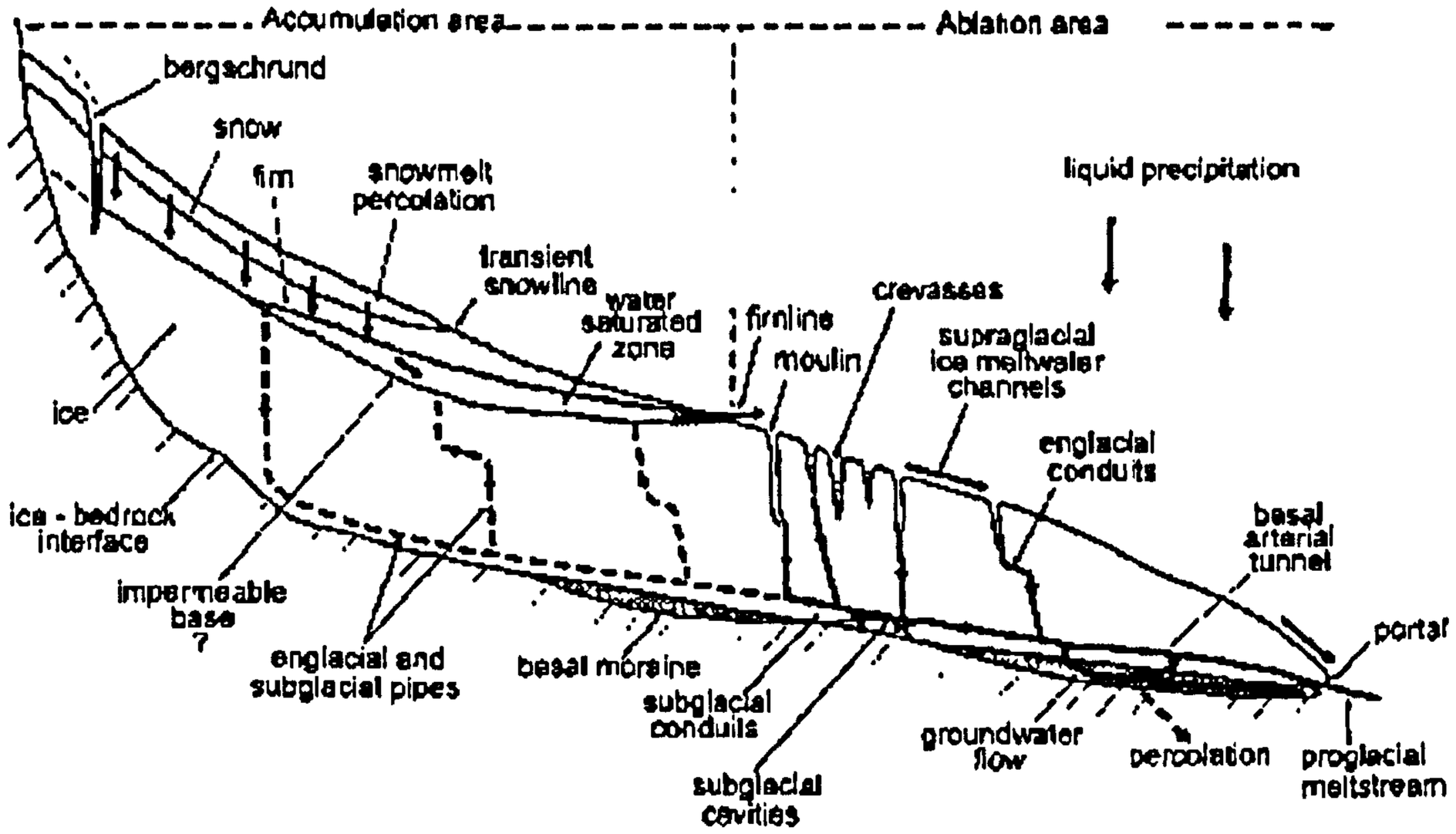

Figure 2.1: Schematic diagram of supraglacial, englacial and subglacial drainage pathways of a temperate glacier after Röthlisberger and Lang 1987, taken from Schuler 2002)

2.2 Surface energy fluxes and the generation of melt at the glacier surface

This chapter provides a brief overview of energy flux considerations at a glacier surface. A more detailed review of energy balance measurements on glaciers and the significance of the individual components is given by Ohmura (2001). Energy fluxes at the glacier surface control the generation of meltwater. Understanding these energy fluxes is therefore crucial to understanding runoff characteristics in glacierized areas (Röthlisberger and Lang, 1987). The physical basis of melt generation from a glacier is the energy balance of fluxes to and from the glacier surface:

$$Q_M = Q_N + Q_S + Q_L + Q_R + Q_G \tag{2.1}$$

where Q_M is the energy used to melt snow and ice or the energy gained from refreezing of meltwater, Q_N is the net radiation, defined as the balance of incoming and outgoing,

shortwave and longwave radiation (Röthlisberger and Lang, 1987), Q_S is the sensible heat flux, Q_L is the latent heat flux, Q_R is the sensible heat flux supplied by rain water and Q_G is the heat flux from the glacier surface to the ice or snowpack. For melt processes Q_N is the dominating term of the energy balance (Ohmura, 2001). It depends on slope, aspect and effective horizon, and Q_N reaches its maximum during noon on a sunny day when slope angle equals 90° relative to the incoming solar radiation. Because of the greater intensity of solar radiation with altitude, Q_N values increase at increasing altitudes. The quantity of absorbed shortwave radiation is controlled by the surface albedo (Male and Gray, 1981; McKay and Gray, 1981). Shortwave albedo values, which represent the ratio between incoming and reflected shortwave radiation, are highly variable and can range from about 10 % for a "dirty" ice surface at the end of the ablation season to more than 90 % for a fresh snow surface (Warren, 1982; Paterson, 1994). Therefore, snowfall events during the ablation increase the albedo and are associated with a sudden decrease in melt rate. Negative Q_N values occur during the night, due to the dominance of outgoing longwave radiation.

Q_S is caused by temperature differences between the glacier surface and the air immediately above, and is highest with large gradients between air and surface temperature. Q_L is positive for condensation and negative for evaporation and is dependent on the humidity gradient between air and glacier surface. Parallel to the temperature and humidity gradients between glacier surface and the atmosphere, the transfer of sensible and latent heat is influenced by wind speed, surface roughness and atmospheric stability (Paterson, 1994). For the surface energy budget, Q_S and Q_L are generally less significant compared to Q_N except during föhn events (or in the Arctic Chinook events). Because of the low temperature of the glacier surface, the air immediately above is generally well stratified and stable and consequently turbulent fluxes are suppressed. However, highest melt rates often occur with high turbulent fluxes (Hay and Fitzharris, 1988; Morris, 1989; Boon et al., 2003). Q_S and Q_L tend to decrease with altitude, because of the vertical lapse rate of air temperature and vapour pressure (Röthlisberger and Lang, 1987).

Q_R is the sensible heat flux supplied by rainwater. The energy balance may be dramatically affected by rain that is significantly warmer than the snow temperature and released in large volumes, e.g. during storm events. However, the influence of Q_R can mostly be neglected for melt generation at alpine glaciers (e.g. Lang et al., 1977). It typically plays a

significant role only if rainwater freezes within the supraglacial snowpack by forming an ice layer, thereby releasing latent heat (refreezing of one gram of water produces enough latent heat to raise the temperature of 160 grams of snow by one degree). This process represents the most efficient source for warming the snow (Marsh and Woo, 1984a; Marsh, 1990; Convey and Benedict, 1994; Paterson, 1994). For temperate glaciers, this is usually negligible during the ablation season.

It is commonly defined, that energy fluxes towards the surface (energy gains) are positive while fluxes away from the surface (energy losses) are negative. The components of the energy balance that constrain melting are Q_N, Q_S and Q_L. Maximum melt rates occur when these values are positive on warm, humid and sunny days with high Q_N and high fluxes of Q_S and Q_L (Röthlisberger and Lang, 1987).

During the ablation season, the surface of a temperate, alpine glacier is considered to be at the melting point and the energy balance is generally positive during melt periods. Melt rates M from the available energy are calculated by

$$M = \frac{Q_M}{\rho_w L_f} \tag{2.2}$$

where ρ_w represents the density of water and L_f the latent heat of fusion (L_f = 333.7 J g^{-1} at 0° C) (Röthlisberger and Lang, 1987). Highest melt rates on alpine glaciers occur in the ablation area during the summer. Furthermore, the albedo is a critical parameter for the melt rate at the glacier surface (Albert and Perron, 2000). A fresh snow surface reflects most of the incoming short-wave radiation back. Due to rocks and debris on the glacier imported from the catchment area and dust particles from the air and their deposition and accumulation on the snow surface over time, the short-wave albedo decreases rapidly and changes the surface energy-balance. The lower the albedo, the more melting occurs.

2.3 Firn and snow hydrology

2.3.1 Introduction

Snow is a source of meltwater, whilst also insulating the glacier ice beneath it thereby preventing melting. Glacier ice forms by the compaction and re-crystallisation of snow,

whilst firn represents an intermediate stage during the transformation of snow to ice. There is no clear characteristic boundary between snow and firn (Paterson, 1994). Firn becomes glacier ice, when the interconnecting air passages between the grains have been closed due to the pressure. Within the snowpack, water is temporarily stored causing a delay of meltwater delivery to the englacial drainage system. Snow and firn at the glacier surface also impact on the energy balance due to their significantly higher albedo than that of glacier ice.

In the accumulation area of a glacier, snow accumulation exceeds melting and snow is present all year around, even though the thickness of the snow layer typically decreases during the melt season. The ablation area is only snow-covered during "winter" and snowpack thinning, resulting in the disappearance of the snowpack, starts with the onset of melt at lower altitudes in spring. During the ablation season, the microstructure and hydraulic properties of snow change and the snowpack evolves on both temporal and spatial scales. In this chapter, the characteristic evolution of a snowpack is outlined. Findings of theoretical and empirical research are summarized and discrepancies between theory and field evidence are discussed.

2.3.2 Characteristic evolution of a glacial snowpack

When snow falls on glacier ice, the temperature of the glacier surface at 0°C or below prevents the snow from immediate melting, resulting in the accumulation and subsequent metamorphism of snow. Depending on where the snow falls on a glacier, it either melts during the melt season or evolves over several years undergoing continuous changes in microstructure, eventually forming glacier ice (accumulation area). Snowpack metamorphism generates characteristic transition phases that are apparent if a vertical profile is taken through several years of snow build-up in the accumulation zone (Østrem and Brugman, 1991).

When snow falls on the ground or the glacier surface, individual snow flakes are mechanically damaged, so that the dendritic crystal structure decomposes into fragments (Langham, 1981). Within a few days after snow is deposited its grain size, shape, density and strength as well as its optical properties change (Marsh, 1990). The density of freshly fallen snow is around 60 kg m^{-3}, increasing with time as the grains grow and the air spaces between them diminish. A settled snowpack reaches a typical density of 200 to 300 kg m^{-3};

it becomes firn at densities between 400 to 830 kg m^{-3} and is defined as glacier ice at densities greater than 830 kg m^{-3} (Table 2.1). Snow drifting and loading modifies the structure of the snow cover and can therefore affect snowpack evolution (McKay and Gray, 1981; Schmidt, 1982). Since snow crystal growth occurs differently under cold (below freezing) or melting conditions, metamorphism of the snowpack is separated into dry-snow processes (no meltwater involved) and wet-snow processes (meltwater involved). In glaciated areas, winter snowfall generally forms a dry snowpack. The metamorphism of the snow therefore usually starts under dry conditions and continues under wet conditions when meltwater percolates through the snowpack at the onset of the ablation season.

Table 2.1: Typical densities of snow and ice (Seligman, 1936) cited in (Paterson, 1994).

Type of snow or ice	Densities [kg m^{-3}]
New snow (immediately after falling in calm)	50 - 70
Damp new snow	100 - 200
Settled snow	200 - 300
Depth hoar	100 - 300
Wind packed snow	350 - 400
Firn	400 - 830
Very wet snow and firn	700 - 800
Glacier ice	830 - 917

2.3.2.1 Dry-snow processes

At temperatures below 0°C, snow cover development is dominated by dry-snow metamorphism (Marsh, 1990). Vapour sintering and heat sintering are the processes responsible for the growth of crystal fragments to more rounded snow grains in dry snowpacks (McKay and Gray, 1981). This rounding of grains is induced by a vapour flux from convex to concave zones where the water vapour pressure is lower. The net result of this vapour flux is rounding of the snow crystals (Colbeck, 1986 from Marsh, 1990). Vapour sintering occurs when, due to latent heat flux, airborne water vapour condenses onto crystal fragments and bonds form between them. When the latent heat flux is negligible and when the pressure of the overburden snowpack is high enough, heating bonds can form due to pressure heating. During both sintering processes, larger fragments grow at the expense of smaller ones (Langham, 1981). The development of more rounded snow grains decreases the ratio of surface area to volume, thus increasing the strength and

density of the snowpack (Paterson, 1994). Over time and under increasing pressure conditions snow grains transform into firn and later glacier ice (Langham, 1981). At the snow surface, the development may be enhanced due to the impacts of wind compression.

2.3.2.2 Wet-snow processes

Wetting front and flow finger development

Wetting of the snowpack starts with surface meltwater production, when the snow surface is at its melting point and the energy balance is positive. Before meltwater can start draining through the snowpack, the capillary deficit has to be filled. The capillary water content stays permanently retained by capillary forces around the grains (Gerdel, 1954; Colbeck, 1972).

Following initial meltwater production, a wetting front develops in the snow cover and advances downwards. In temperate snowpacks, the wetting front divides the snowpack into an upper and lower zone. The upper zone is wet and isothermal at 0°C and the lower zone is dry snow with temperatures below 0°C (Marsh and Woo, 1984a). Rapid growth of snow grains begins when liquid water is introduced to a dry snowpack. Due to preferential heat flow from small to large grains, larger grains grow and become rounded, whereas smaller ones disappear (Wakahama, 1968; Colbeck, 1979). The heat flux and grain growth rate also increase at higher water saturation (Wakahama, 1968; Marsh, 1990). Observations suggest that water from wetted snow can be released suddenly (Colbeck, 1986) due to grain growth reducing the overall capillary pressure. Relative to their volume, smaller snow grains have a greater surface area than larger grains, thus, the capillary pressure within a snowpack increases as grain size decrease. A snowpack of fresh, relatively small snow grains can hold more capillary water.

However, in a natural snowpack it is common to find grains at various stages of metamorphism. The development of a wetting front in a stratified snowpack is therefore inhomogeneous. Percolating meltwater interacts with stratigraphic horizons and, at locations of higher permeability, vertical flow fingers acting as preferential flowpaths evolve (Wakahama, 1975; Colbeck, 1979; Kattelmann, 1985, 1989; Marsh, 1990; Schneebeli, 1995; Kattelmann and Dozier, 1999; Albert and Perron, 2000). These are narrow in width and relatively evenly spaced (Wakahama, 1968; Marsh and Woo, 1984a)

and transfer meltwater efficiently. Due to an enhanced heat flux after rain fall the development of flow fingers can be significantly increased (Sturm and Holmgren, 1993). Generally, flow fingers reach the base of the snowpack before the wetting front (Gerdel, 1954; Schneebeli, 1995). Flow fingers are responsible for the fast component of meltwater percolation until the entire snowpack has changed to a wet snowpack (Marsh and Woo, 1984a). If a moving meltwater front is overtaken, a shock front develops with large fluxes above and smaller fluxes below it (Colbeck, 1978). Also, if the snowpack temperature generally remains below 0°C, water flow may occur due to flow fingers (Marsh and Woo, 1984a; Pfeffer and Humphrey, 1996). The overall permeability of wet snow depends on snow density and mean grain diameter (Shimizu, 1970). The flow accelerates due to gravity and the rate of flow increases with the meltwater flux. Therefore, during a diurnal melt cycle, meltwater fluxes are faster in the afternoon than in the morning.

When the wetting front reaches the base of the snowpack, meltwater percolates laterally along the snow-ice interface driven by the local hydraulic gradient. The snowpack reaches water saturation at a water content of about 20 % by volume (Colbeck, 1978; Denoth, 1999). The routing of water through the snowpack is influenced by the metamorphic changes of individual snow particles and the overall stratigraphy, including the formation and decay of ice layers. These impacts are discussed in the next section.

Snowpack stratigraphy and ice layers

Snowpacks are naturally stratified, because every snowfall event produces a new layer of snow. A snowpack often consists of various layers of snow which differ in grain size, porosity, strength, density and therefore permeability. The heterogeneous, layered structure of a snowpack and the formation of internal and surface ice layers influence meltwater drainage through the snowpack. Ice layers on the snow surface are mostly a result of rain or meltwater refreezing on the surface, but they can also develop from a wind or sun crust or hoar due to sublimation (Colbeck, 1978; Marsh, 1990). These surface ice layers are subsequently incorporated by further snowfall events (Langham, 1981). Ice layers can also form when percolating rain or meltwater within the snowpack becomes frozen overnight or when the water reaches a sufficiently cold environment. Thick ice layers can also develop when water, percolating through the snow, accumulates and refreezes at impermeable layers (Nakawo and Hayakawa, 1998)

If water reaches an impermeable layer, flow occurs laterally down-slope until a break in this layer occurs where upon vertical gravitational flow continues. Meltwater accumulating on ice layers within the snowpack may induce ice layer destruction (Gerdel, 1954; Convey and Raymond, 1993). This can occur when meltwater accumulates at the ice layer, inducing melting and resulting in the ice layer becoming permeable. Where the ice layer is penetrated, vertical drainage channels develop (Gerdel, 1954). The permeability of an ice layer can vary diurnally, because variations in size of veins between ice crystals depend on temperature (Langham, 1975; Marsh, 1990). Furthermore, refreezing of percolating or stored water within the snowpack can destroy preferential passageways (Pfeffer and Humphrey, 1996). After cold periods during the melt season, new paths need to develop.

Water flow through mature snowpacks

After several weeks of melting and snowpack thinning, the remaining snow will have reached a grain size of approximately 1 to 2 mm, after which metamorphism continues very slowly, unless the pressure of the overlying snowpack activates further metamorphism (Wakahama, 1968; Colbeck, 1978; Jordan, 1983a). As the snowpack matures, it becomes more homogeneous, resulting in an increased mean flow velocity. However, the fastest moving water molecules through snowpacks occur in freshly wetted snow (due to the presence of flow fingers) and not in ripened, melt-metamorphosed snowpacks (Marsh, 1990). The factors controlling the hydrograph from ripe snowpacks are snow depth and melt rate (Dunne et al., 1976).

At the end of the melt season, residual water held within the remaining snow cover drains out gradually. The remaining coarse snow and firn in the accumulation area will become increasingly consolidated as air and free water are reduced and will gradually develop into glacier ice. This process of pressure metamorphism is induced by the weight of the overlying snowpack.

The hydrological behaviour of a snowpack is variable both temporally and spatially. Thus, different processes may occur contemporaneously in the same glacial system with wet snow processes occurring at lower elevations and dry-snow-processes at higher elevations.

2.3.3 Research in snowpack hydrology

As demonstrated in the previous section, meltwater flow through natural snowpacks is a complex, inhomogeneous process and many of the physical aspects remain poorly understood (Colbeck, 1975; Williams et al., 1999). The importance of the physical determination of water routing through snow has long been recognised, but because of the complex nature of the processes, field evidence has been difficult to achieve. Indeed, Colbeck had already remarked the need for more field studies in the early 1970's. However, only limited data from investigations of meltwater flow processes from experiments under natural field conditions are available to date. Theoretical considerations also play an important role in understanding snowpack hydrology and these, in addition to the most important empirical achievements, are summarized below.

2.3.3.1 Theoretical work

In a sequence of publications in the 1970's Colbeck (1972; 1974; 1975; 1976; 1977) developed a theory to describe the main features of meltwater flux waves through snow. Colbeck (1972) applied Darcian flow theory, which describes the flow of fluids through porous media to explain the vertical drainage of water through snow. He used Darcy's law by considering entirely wet snow conditions, under which capillary effects are negligible and gravitational forces are dominant. However, using Darcy's law in order to identify mechanisms and characteristics of snowpack hydrology is limited, because the conditions of stable and homogenous conditions considered in the model are not given in natural environments. However, it may provide a model of approximation.

An advanced theoretical approach resulted in the basic theory of saturated flow at the snow-ice interface and a two-layer model describing unsaturated and saturated water flow through snow (Colbeck, 1974). Colbeck's model was tested in Canadian sub-arctic snowpacks over frozen, impermeable soils using micro-meteorological measurements to obtain meltwater production at the surface as well as measurements of snow density and grain size (Dunne et al., 1976). Measured and predicted total runoff including peak discharge were similar under various conditions, although the time lag from melt generation to discharge was overestimated by the model.

The observation that a temperate snow cover usually contains inhomogeneities such as ice layers and flow channels inspired Colbeck to develop a model describing the percolation of

water through inhomogeneous and layered snow (Colbeck, 1975). Overall, the goal of Colbeck's research was the prediction of water flow through snowpacks, taking into account their transient variability due to processes of snow metamorphism processes. His theoretical work provided the basis for subsequent modelling of meltwater flow through snow (e.g. Marsh and Woo, 1984b; Illangasekare et al., 1990; Pfeffer et al., 1990; Sellers, 1999; Lehning et al., 2002a; Lehning et al., 2002b). More detailed descriptions of the principles of snowpack properties and the derivation of meltwater flow theories are given in Colbeck (1978), Wankiewicz (1979), Male (1980), Male and Gray (1981) and Marsh (1990).

2.3.3.2 Empirical work

Fieldwork is essential to investigate snowpack hydrology and the properties of snowpacks because natural conditions in snow are extremely complex and they cannot be reproduced in laboratories or by computer simulation (Marsh, 1999). Snowpacks are sensitive to external influences such as temperature, albedo variations, wind impact and rain. These external conditions vary and together with the continuously evolving microstructure of the snow make this a complex research area. Various field methods have been applied (often by parallel, complimentary methods) to a wide range of snowpacks at different levels of maturity as outlined below.

Dye tracing

Early dye tracing experiments showed that large spatial inhomogeneities exist within the snowpack (Hughes and Seligman 1939 cited by Colbeck 1972; Gerdel 1954). Dye tracer experiments have been used to investigate preferential flowpaths (Marsh and Woo, 1984a; Schneebeli, 1995; Kattelmann and Dozier, 1999), to measure the hydraulic conductivity (Behrens et al., 1979) and flow velocities at the snow-ice interface (Ambach and Eisner, 1979). From the latter study, water flow velocities in the saturated firn aquifer between 0.3 and 0.6 m h^{-1} were obtained (Ambach and Eisner, 1979). A major limitation of dye tracer experiments is the artificial introduction of water to the snowpack by spreading a dye solution, since this additional water input will influence the considered system (Albert et al., 1999). The use of very fine dye powder is especially unsuitable under the often windy conditions that occur on glaciers because of the likelihood of contamination over a large area yielding spurious results. If the tracer is injected at the snow surface, the tracer could

change the natural albedo of the snow surface and therefore, induce accelerated melting (Albert et al., 1999).

Lysimeter method

Lysimetry is used to collect and measure the volume of water draining through the snowpack investigate meltwater discharge from snowpacks (Colbeck and Anderson, 1982; Jordan, 1983a; Albert et al., 1999). The meltwater discharge from snow at different densities was examined by Harrington and Bales (1983a) and arrays of lysimeters have been used to measure spatial variability of meltwater discharge from snowpacks (Kattelmann, 1989; Sommerfeld et al., 1994; Williams et al., 1999). Multi-compartment lysimeters have been used to compare the daily volume of flow in isolated flow fingers and in the background of the wetting front (Marsh and Woo, 1984a). It has become apparent that the amount of water transported by a flow finger is controlled by the dynamic micro-structure of the snow and the water availability (Marsh and Woo, 1984a, 1984b).

Water level monitoring at the firn-ice interface

The saturated layer at the base of glacial snowpacks reacts to meltwater inputs and outputs by water level changes in a local aquifer and represents an important temporary water storage (Schneider, 2001).

Pumping and slug tests

Pumping tests or slug tests are a common method to determine hydraulic conductivity in aquifers (Freeze and Cherry, 1979). The hydraulic conductivity is a parameter that describes the porosity of a porous medium. A known quantity of water is removed or added to the aquifer and changes in water levels are recorded over time. Pumping and slug tests in the firn aquifer have been undertaken on different temperate glaciers (Schommer, 1978; Oerter and Moser, 1982; Fountain, 1989; Schneider, 1999).

Capacitance meter measurements

The storage of liquid water in snowpacks has been measured by capacitance meters using the dielectric properties of snow (Gerdel, 1954). Using a similar method, Singh et al. (1999) measured the liquid water content above ice layers, demonstrating how ice layers

impede water flow and therefore delay runoff. It has also been observed how liquid water over ice layers can result in the disintegration of these layers (Gerdel, 1954; Langham, 1975; Convey and Raymond, 1993). However, since ice layers reduce the permeability of a snow cover, Albert and Perron (2000) measured the permeability of ice layers using a "permeameter". Intrinsic permeabilities of ice layers ranged from between 1 to 19 x 10^{-10} m^2 and the permeability of the surface crust in the early melt season is increased to around 70 to 120 x 10^{-10} m^2, although this is not necessarily controlled by an increase of snow density.

Thermistor technique

In order to measure meltwater infiltration and storage processes, thermistors have been used to measure snow temperature gradients. Snow temperature measurements enable the tracking of meltwater infiltration e.g. after rain events, causing heat flux changes in the snowpack (Convey and Raymond, 1993; Sturm and Holmgren, 1993; Convey and Benedict, 1994).

Aerial photography

Aerial photographs of the melting snow surface have been used to reveal areas of high water content by quantifying the snow surface brightness (Sommerfeld et al., 1994) also, near infrared aerial photographs, (in conjunction with dielectric capacitance measurements) (Williams et al., 1999), were used and to characterise the spatial distribution of meltwater flowpaths.

Snow pit observations

Additional information about grain size, hardness of a snowpack and snow densities have been measured from snow pits at different locations across the glacier. This information is useful, because small changes in the snow microstructure (grain sizes) have a significant impact on snow permeability. Crystal type and grain size of snow particles can be classified by using grain size charts or the "International Classification for Seasonal Snow on the Ground" (Colbeck et al., 1990). The hardness of snow can be classified using a hardness scale from 1 (one finger for high density) to 5 (fist for low density) or by using a

"penetrometer" that uses spring pressure to quantify the force necessary to penetrate into the substrate (Schneebeli et al., 1999).

Laboratory experiments

Laboratory experiments are of very limited value for investigating snowpack hydrology because of the difficulty of preparing conditions analogous to nature. However, a series of laboratory experiments by Wakahama (1968) gave evidence that the metamorphism of snow grains in wet snow depended on the degree of water saturation and the overburden pressure of the snowpack. Overall, a major outcome from this research was a demonstration of the highly variable nature of most snowpack parameters (melt rate, velocity, heat flux) (Sturm and Holmgren, 1993; Harrington and Bales, 1998a).

2.3.4 Discussion

Theoretical work in hydrological snow research has generally preceded empirical justification. Theoretical work attempts, necessarily, to simplistically explore the mechanisms controlling natural processes, whereas empirical work attempts to observe and quantify the character of these natural processes. The limitations of field experiments are due to the changing and highly variable natural conditions and complex linkages between interconnected processes. Field experiments also often influence natural conditions, and consequently the obtained parameters are unrepresentative. A limitation for glacial hydrological research is that snowpack hydrology has predominantly been studied in non-glacial snowpacks and can therefore only partly characterise processes in glacial environments since the snowpack may respond differently when sitting on an ice bed. Glacial snowpack is clearly not influenced by snow-soil temperature regimes and energy transport through the snow-soil interface. Ice surface temperature is always 0°C or below. Therefore no melting processes controlled by the underlain ice-surface occur, also the hydrological properties if ice differs from soil. The ice surface is apart from inter-granular veins (Nye and Frank, 1973) impermeable and only at moulins and crevasses can meltwater run off. Conversely on soil substrates water can permeate anywhere so long as the soil is not water logged and/or frozen.

There are also no studies available describing snow-hydrological processes at retreating glacial snowpacks during the ablation season. On glaciers, the snowpack has a particularly

high impact on meltwater runoff during years with (i) large winter accumulation, ii) late onset of melt, (iii) cold summers or (iv) the occurrence of snow fall during the ablation season.

Differences in research findings are expected, according to differences between individual glaciers, time of year or the location on a given glacier. However, the general aim of investigation into snowpack hydrology is to clarify the effects of the snowpack on meltwater runoff. If models are used, the theoretical description of the processes has to be simplified. It has been recognised that meltwater delivery from a snowpack to the englacial and subglacial drainage system also has impacts on glacier dynamics. Therefore, the development of models that can predict meltwater delivery through a heterogeneous and continuously evolving snowpack will be useful. This is problematic because snowpack properties are very complex and highly variable in time and space, so that simplifications may not necessarily represent natural conditions.

An effective model of supraglacial snowpack hydrology must include all relevant parameters, but in real world situations this is seldom, if ever possible. There have been many attempts to model different aspects of snow hydrological processes, e.g. meltwater infiltration in subfreezing snow (Marsh and Woo, 1984b; Illangasekare et al., 1990; Pfeffer et al., 1990). Detailed simulations of the evolution of snowpack at a micro-structural level including grain size, shape and bonding effects of the snow grains has been undertaken to predict avalanches (Lehning et al., 1999; Lehning et al., 2002a; Lehning et al., 2002b). Work remains to be carried out in terms of field interpretation, modelling and improvement of theoretical understanding of glacial hydrological systems. In particular, there is a requirement for a better understanding of the role of water storage changes within snow, firn and at the base of glaciers, in particularly at the beginning of the melt season (Arnold et al., 1998).

2.4 Englacial and subglacial hydrology

2.4.1 Introduction

Numerous research projects have investigated processes of meltwater drainage through glaciers. This section provides an overview of the scientific literature concerning englacial and subglacial drainage. Water that drains from temperate glaciers is predominantly meltwater from the glacier surface (Röthlisberger and Lang, 1987). Other sources of water which contribute to glacier runoff are basal melt due to frictional and geothermal heat and extraglacial surface runoff or groundwater. Understanding subglacial drainage systems is of fundamental importance to glaciology due to its influence on glacier movement, sediment evacuation, water chemistry and landform evolution.

Theoretical considerations (e.g. Weertman, 1964; Röthlisberger, 1972; Shreve, 1972; Weertman, 1972; Hooke, 1984) in conjunction with a variety of direct and indirect methods have advanced our understanding of englacial and subglacial hydrology. Examples and limitations of different field techniques for investigating englacial and subglacial drainage systems are shown in Table 2.2.

Table 2.2: Research methods for investigating englacial and subglacial hydrology

	Method	Limitations	Reference
Direct methods	Decent into or mapping of moulins	Observation of an isolated location.	(Reynaud, 1987) (Holmlund, 1988)
	Entering englacial channels	Maybe not representative, because only accessible at glacier margins.	(Röthlisberger, 1980)
	Investigation of natural basal cavities or tunnels	Limited accessibility and representativeness unclear.	(Kamb and LaChapelle, 1964) (Anderson et al., 1982) (Andreason, 1983)
	Investigation of artificial tunnels/ access of glacier bed through artificial tunnels	Only limited access to the glacier bed (at the margins).	(Vivian and Bocquet, 1973) (Vivian, 1980) (Hagen et al., 1983) (Boulton and Hindmarsh, 1987)
	Water pressure measurements in boreholes	Point observations.	(Engelhardt et al., 1978) (Hodge, 1979) (Hantz and Lliboutry, 1983) (Iken and Bindschalder, 1986) (Stone et al., 1993) (Fountain, 1994) (Gordon et al., 1998) (Hubbard et al., 1995)
	Down-borehole photography and TV-videos	Poor visibility in sediment rich waters.	(Harrison and Kamb, 1973) (Pohjola, 1994) (Harper and Humphrey, 1995) (Copland et al., 1997b) (Harbor et al., 1997)
Indirect methods	Tracer experiments	Difficulty of interpreting the structure of distributed subglacial systems. Difficulty in separating englacial and subglacial drainage.	(Behrens et al., 1975) (Burkishmer, 1983) (Brugman, 1986) (Seaberg et al., 1988) (Willis et al., 1990) (Fountain, 1993) (Nienow, 1993) (Hock and Hooke, 1993) (Hock et al., 1999) (Schuler, 2002)
	Geochemical analyses	Exact sources and routing of meltwater unclear.	(Brown, 2002) (Tranter et al., 1996) (Collins, 1979) (Behrens et al., 1971) (Collins, 1979)
	Sediment analyses	Complexity of storage-release mechanisms. Representative samples are difficult to achieve.	(Gurnell et al., 1996) (Swift, 2002)
	Mapping of recently deglaciated bedrock	Condition under which bedrock morphology generated unknown.	(Walder and Hallet, 1979) (Sharp et al., 1989) (Hallet and Anderson, 1980)
	Deductions from runoff hydrographs	Complex integration of all parts of the meltwater system.	(Gurnell, 1993) (Hannah et al., 1999) (Hannah et al., 2000)

2.4.2 Englacial drainage

There are two pathways by which water can enter the englacial drainage system, (i) through crevasses and moulins (Röthlisberger and Lang, 1987), and (ii) through intergranular veins (Nye and Frank, 1973; Raymond and Harrison, 1975; Hooke, 1989). The most efficient way for meltwater to enter the glacier is through crevasses and moulins. A detailed description of the water drainage through moulins is given by Holmlund (1988). Seepage of water through intergranular veins, about 25 μm in size (Hooke, 1989), occurs as capillary drainage and the dimension of the veins results in the low permeability of glacier ice (Lliboutry, 1971; Raymond and Harrison, 1975). Intergranular veins drain limited volumes of meltwater, when compared to crevasses and moulins, but due to the release of potential energy in the seeping water, they may be important in enabling the development of englacial conduits (Shreve, 1972) that eventually drain larger volumes of water. The englacial drainage system has been likened to an upward-branching arborescent network of interconnecting conduits linking the surface to the glacier bed (Shreve, 1972) (Figure 2.2). Drainage of filled boreholes before the glacier bed (Fountain and Walder, 1998) and observations from borehole videos (Pohjola, 1994; Copland et al., 1997a) provide evidence for a high density of englacial channels.

The structure of the englacial drainage system is critically dependent on counteracting processes between ice-overburden pressure enforcing plastic deformation and channel closure on one side, the water pressure in the channels and the melt rate of the channel walls due to frictional heat generated by flowing water on the other.

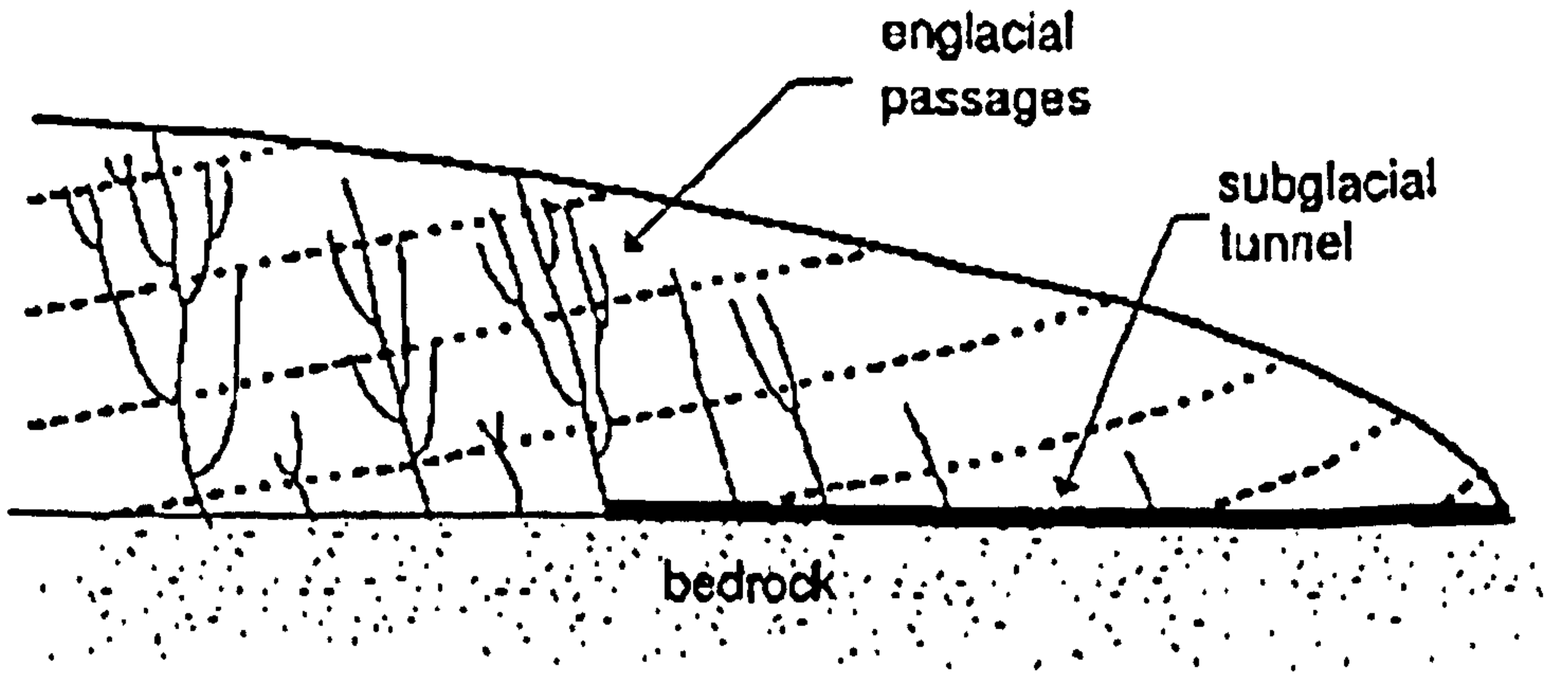

Figure 2.2: Equipotential surfaces of the glacier ice (dashed lines) and hypothetic network of englacial drainage pathways developing perpendicular to equipotential surfaces (after Shreve, 1985).

Hooke (1984) postulated that in englacial channels > 4 mm diameter, wall melting is greater than the closure rate, whereby conduits enlarge faster than ice deformation can close them resulting in open channel flow (non-pressurised, atmospheric conditions). Under open channel conditions, water flows at the base of englacial conduits, enhancing the development of steeper channels. It is most likely that englacial passageways, fed by an overlaying firn- or snow-aquifer, are water filled and develop under pressurised conditions. This is because meltwater input through a snow or firn layer dampens the discharge from the firn area and is less variable than runoff from the ablation area (Fountain and Walder, 1998).

The evolution of englacial conduits occurs in the ablation area earlier than in the accumulation area, because the melting of snow in the ablation area starts earlier in the season and meltwater volumes are larger due to the elevated temperature at lower altitude. Since meltwater volumes control the development and size of moulins, greater meltwater input locations are expected lower down-glacier, where further up-glacier not enough meltwater is generated to expand moulins. The distribution and number of moulins and crevasses is important for the development of the englacial and subglacial drainage systems, because these features divert water input directly into these englacial and subglacial systems (Stenborg, 1969; Nienow et al., 1998).

2.4.3 Subglacial drainage

Meltwater, delivered from the englacial drainage system is subsequently routed at the ice-bed interface before leaving the glacier at the snout in one or more glacial streams. The hydraulic efficiency of the meltwater drainage at the transition between englacial and subglacial drainage and whether the meltwater delivery to the bed is spatially concentrated or distributed will subsequently affect the structure of the subglacial drainage system.

Several theories have been proposed to explain subglacial flow characteristics and channel geometries (e.g. Weertman, 1964; Röthlisberger, 1972; Shreve, 1972; Weertman, 1972; Nye, 1973; Hooke, 1984). According to their geometry, subglacial drainage paths can be divided into two main categories: (i) channelised drainage systems and (ii) distributed drainage systems (Fountain and Walder, 1998). The different geometries develop in response to the physical properties of the ice, the character of the glacier bed and the nature and variability of the meltwater input (Röthlisberger and Lang, 1987). Field observations at

different glaciers provide evidence for the existence of different subglacial drainage systems. Also, the co-existence of different systems has been recognised beneath a number of glaciers e.g. at Variegated Glacier (Humphrey et al. 1986), Storglaciären (Hooke et al., 1988; Seaberg et al., 1988), Midtdalsbreen (Willis et al., 1990) and South Cascade Glacier (Fountain, 1993). The main components of channelised and distributed subglacial flowpaths (Figure 2.3) are briefly described below, whilst detailed reviews on subglacial hydrology can be found in Hooke (1989), Hubbard and Nienow (1997) and Fountain and Walder (1998).

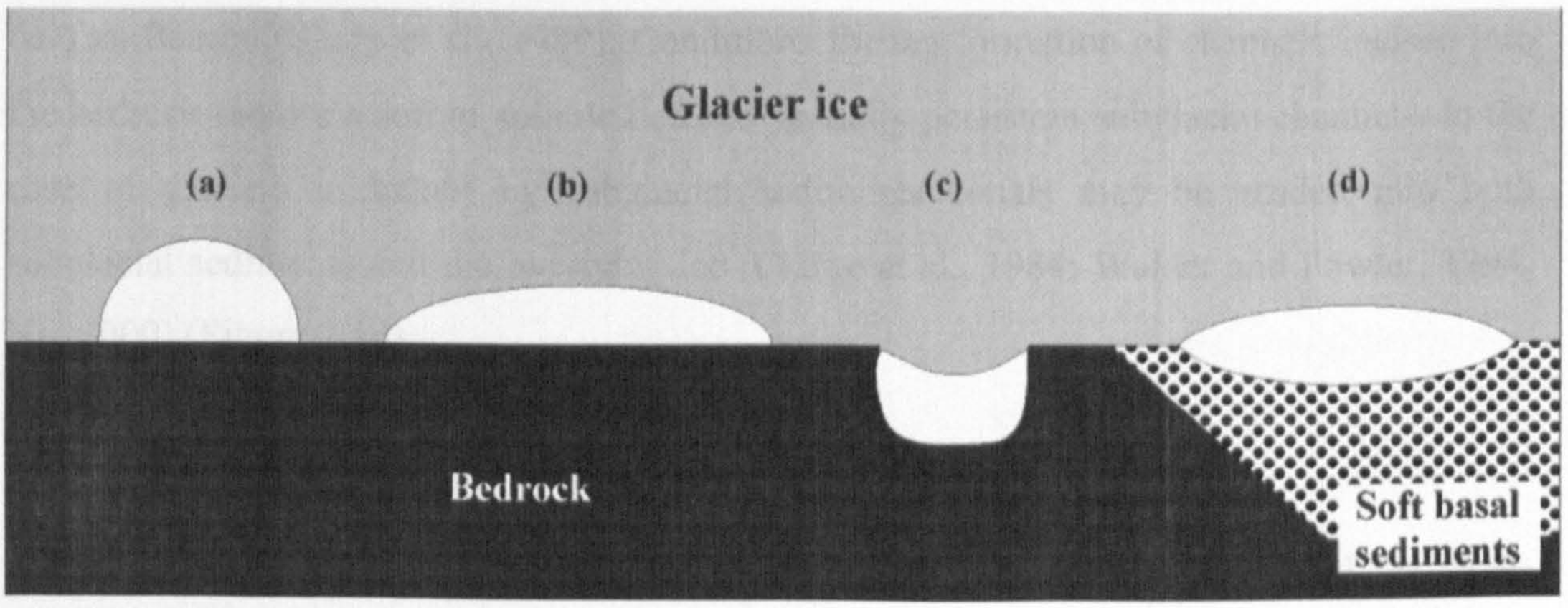

Figure 2.3: Idealised channel geometries at the glacier bed a) a semi-circular R-Channel; b) a broad, low, elliptical channel; c) a Nye-Channel, incised into bedrock d) a canal eroded into subglacial sediment (after Nienow, 1993).

2.4.3.1 Channelised drainage systems

Several forms of subglacial channelised drainage systems have been suggested (Figure 2.3), which adjust their form according to the hydraulic conditions at the ice-bed interface. Channelised systems preferentially evolve where locally high volumes of water reach the glacier bed and they are hydraulically efficient and typically arborescent ("tree-like") in form (Fountain and Walder, 1998). Semi-circular subglacial channels incised upwards into the ice (Figure 2.3a) are commonly described as "R-channels", after Röthlisberger (1972). Röthlisberger's theory was formulated considering full channel flow under steady-state conditions, with a balance between melt and closure rates. Since this approach is commonly unrealistic for typical subglacial drainage conditions, it has been extended to an instationary subglacial water flow (Nye, 1976; Spring, 1980; Clarke, 1982; Walder and Fowler, 1994; Schuler, 2002; Clarke, 2003). The semi-circular shape of R-channels was

questioned by Hooke and co-workers (Hooke, 1989; Hooke et al., 1990) who argued that during non-pressurised conditions, channels enlarge due to melting at the base of the channel walls, rather than ceilings. They postulated the theory of broad, low channels at the glacier bed ("H-channels") (Figure 2.3b).

Subglacial channels which are incised downwards into the underlying bedrock are called "N-channels" after (Nye, 1973) (Figure 2.3c). They have been observed on deglaciated glacier forefields consisting of highly soluble carbonate bedrock at Blackfoot Glacier (Walder and Hallet, 1979), Castleguard Glacier (Hallet and Anderson, 1980) and Glacier de Tsanfleuron (Sharp et al., 1989). Conditions for the formation of channels incised into the bedrock require a soft or soluble bed and spatially persistent subglacial channels. In the case of glaciers underlain by subglacial sediments canals may be eroded into both subglacial sediments and the overlying ice (Clarke et al., 1984; Walder and Fowler, 1994; Ng, 2000) (Figure 2.3d).

2.4.3.2 Distributed drainage systems

A fundamental characteristic of distributed drainage systems is that individual flowpaths are spatially distributed and basal waters are drained from areas not directly connected to a channelised system. Water transport in distributed systems is usually slower than in channelised drainage systems (Hubbard and Nienow, 1997). This is predominantly because meltwater, which enters the distributed subglacial system, is routed through hydraulically inefficient passageways and is often stored in cavities and the pore spaces of subglacial sediment layers. At high water pressures, the entrapment of basal water by the distributed network can be greatly increased by separation of basal ice from the bedrock. Furthermore, flowpaths through the distributed system are rather convoluted and indirect, delaying the subglacial flow to the glacier terminus. In contrast, water through single, well developed channels, follows more direct passageways and incidences of subglacial storage are fewer.

Various types of distributed drainage structure have been proposed. Weertman (1964; 1972) suggested that when glaciers overly impermeable bedrock, a thin film of basal meltwater, usually only a few μm thick, can form. Such a water film presumably drains only a small proportion of meltwater, but they might be of consequence in terms of basal lubrication, recession flow hydrochemistry (during the winter and overnight, when there is little surface melting) and as a primary component of glacier sliding by regelation

(Hubbard and Nienow, 1997). If permeable sediments underlie the glacier, meltwaters may drain into the till until saturation occurs (Boulton and Jones, 1979; Boulton and Hindmarsh, 1987; Alley, 1989) whereupon flow through the pore space of the saturated sediment layer occurs (Shoemaker, 1986; Walder and Fowler, 1994). If the meltwater input exceeds the drainage capacity of the sediment layer, either a Weertman water film may develop at the sediment-ice interface (Shoemaker, 1986; Alley, 1989) or broad, shallow canals may incise into the sediment layer (Figure 2.3d) (Walder and Fowler, 1994; Ng, 2000).

It is generally believed that most of the meltwater in the distributed system is drained through a complex network of cavities linked by narrow passageways (Kamb, 1987). From proglacial bedrock mapping, field evidence for the existence of such a linked-cavity system was derived (Walder and Hallet, 1979; Hallet and Anderson, 1980; Sharp et al., 1989). Development of the system is the result of several processes. A mechanism described as regelation (Weertman, 1957) occurs, when ice moves over an uneven, rough bed. The higher pressure on the upstream side of a bedrock bump causes melting and the generated meltwater flows downwards, around the bump and refreezes at the lee side (Weertman, 1957). If glacier flow is rapid enough, ice will separate from the bed in the lee of bedrock bumps, thereby forming a cavity which may fill with subglacial meltwater (Lliboutry, 1968). If the water pressure exceeds ice pressure, water spreads out at the glacier bed into neighbouring cavities and linkages between individual cavities can develop. In a network of interconnected cavities, the linkages enlarge by energy dissipation in the flowing water, while the size of the cavities is primarily determined by the sliding speed. The stability of the network depends mainly on the effects of the sliding velocities (Walder, 1986; Fowler, 1987; Kamb, 1987). If sliding velocities drop, or meltwater discharge and thus water pressures suddenly increase, melt enlargement will exceed creep-closure (Kamb, 1987) and the linked-cavity system can collapse into a channelised drainage system (Nienow et al., 1998).

To summarise, the coexistence of channelised and distributed water flow is most likely beneath temperate glaciers. Pressurised as well as open-channel flow conditions can occur in both, the channelised and the distributed drainage system. However, there are still limitations in our understanding of the complexity of subglacial drainage systems and as Willis (1995: 79) highlighted, "the relative importance of the drainage components in

discharging waters from beneath the glacier is not fully known and the degree to which these components interact with each other has not been clearly established."

2.4.4 Seasonal evolution of the subglacial drainage system

The seasonal evolution of the subglacial drainage system is related to several processes including snowline retreat, meltwater storage, discharge variations and fluctuations in glacier sliding rate. Understanding the seasonal variations of these processes and their linkage to the evolution of the subglacial drainage system is therefore critical for the interpretation of glacier hydrology and ice dynamics.

At the start of the melt season, the subglacial drainage system at temperate glaciers typically consists of a distributed drainage system, characterised by relatively high water pressures with small diurnal variations (Nienow et al., 1998). The flow connections are poorly developed and cannot efficiently drain larger amounts of meltwater generated at the glacier surface. Subglacial flow connections from the previous year are closed or reduced in size, hence the basal drainage system cannot cope with the increased water flux (Fountain and Walder, 1998). The first meltwater that reaches the glacier bed through the englacial system is stored subglacially. At many glaciers, speed-up events have been observed in the early melt season often termed "spring-events" (Iken et al., 1983; Iken and Bindschalder, 1986; Mair et al., 2001). These "spring-events" result from enhanced basal sliding due to a significant increase in basal water pressures (Seaberg et al., 1988; Stone and Clarke, 1996) and as this pressure reduces travel friction, fast sliding can take place (Iken et al., 1993).

With increasing subglacial water pressure and energy dissipation from meltwater, the cavities will enlarge and interconnect (Kamb, 1987). Subglacial channel walls begin to melt, thus increasing the drainage capacity by enlarging the cross-sectional area. Since the water pressure in the larger channels is lower than in smaller channels, water flow is directed towards the larger conduits and these grow at the expense of smaller ones (Röthlisberger and Lang, 1987). As the snowline retreats up-glacier, larger areas of glacier ice become exposed, so that meltwater generation increases due to a reduced albedo of the melting surface. Accordingly, a channelised system evolves up-glacier to drain the increasing meltwater flux efficiently (Stone and Clarke, 1996; Gordon et al., 1998; Nienow et al., 1998). As long as the meltwater supply is large enough to counteract the channel

closure rate due to the overburden ice pressure, the drainage channels developed will remain open. The transition between the channelised and distributed system is expected in the area of the transient snowline (Nienow et al., 1998). The number and distribution of moulins and crevasses through which water is routed to the glacier base has an influence on the distance between snowline and the location where channelised flow occurs. During the ablation season englacial and subglacial channels remain open and transport water due to the balance between wall-melting and inward ice creep caused by the overburden ice pressure (Röthlisberger, 1972; Sharp et al., 1993). The drainage channels increase in size down-glacier due to the higher discharges (Arnold et al., 1998; Gordon et al., 1998; Nienow et al., 1998).

At a diurnal time scale, basal water pressures vary sinusoidally in response to the typical diurnal variations in surface meltwater inputs. During peak discharge, the water pressure in the channelised system often exceeds that of the distributed system (Weertman and Birchfield, 1983; Hubbard et al., 1995) and therefore water flows into the distributed system to be stored temporarily (Walder, 1982; Fowler, 1987). At times of lower discharges, the hydraulic gradient is reversed and water flows towards bigger channels with lower pressure. Once the channelised system has been established, open channel flow can occur during times of low discharge. In areas where meltwater inputs to the glacier bed are limited, the flow passageways of the distributed system remain during the ablation season and drain the water slowly down-glacier until they transect with channelised flowpaths nearer to the glacier snout (Nienow et al., 1998).

The meltwater drainage system reaches its maximum efficiency by late-summer and usually the channelised system dominates the routing of surface derived meltwaters through the subglacial drainage (Sharp et al., 1993; Nienow et al., 1998). With the first snowfall, meltwater inputs from the glacier surface drop dramatically resulting in closure of channels as creep closure rates exceed the rates of frictional melting needed to keep channels open (Röthlisberger and Lang, 1987). When the efficient, channelised system is shut, the inefficient, distributed system becomes dominant and remains throughout the winter draining meltwaters generated internally and basally by frictional and geothermal heat (Röthlisberger and Lang, 1987).

To summarise, during the melt season, the glacial drainage system evolve from a hydraulically inefficient, distributed drainage system to a hydraulically efficient,

channelised system (Hock and Hooke, 1993; Gordon et al., 1998; Nienow et al., 1998). The system continuously adjusts itself to the supraglacial, englacial and subglacial discharge conditions and the ice overburden pressure. This vision of seasonal evolution has been verified by extensive dye tracer experiments at Haut Glacier d'Arolla, Switzerland (Nienow et al., 1998).

The seasonal evolution of the drainage system as described above has been suggested for glaciers on non carbonate bedrock (Fountain and Walder, 1998; Nienow et al., 1998). However, little is known about the drainage evolution of glaciers on limestone bedrock, which is highly soluble and therefore can form a karstic system that may have an effect on the water drainage. In particular, the stability of the Nye-channels may mean that there is a low dramatic change in drainage system structure between winter and summer.

2.5 Glacier dynamics

2.5.1 Introduction

The two major components of glacier motion are internal ice deformation and basal motion, where basal sliding can be the result of deformation of the glacier bed (Paterson, 1994). It has been shown that basal motion is the most important mechanism for controlling short-term variations in glacier motion (Raymond, 1980; Paterson, 1994) and sliding rates are critically controlled by the subglacial water pressure (Bindschadler et al., 1977; Iken et al., 1983; Harrison et al., 1986; Iken and Bindschalder, 1986; Kamb and Engelhardt, 1987; Richards et al., 1996; Iken and Truffer, 1997; Sharp et al., 1998; Gudmundsson et al., 2000). However, most parts of the glacier bed are inaccessible and therefore, measurements of basal sliding are often achieved indirectly at the glacier surface.

The sliding of glaciers is mainly influenced by slope angle, bed substrate, topography, climate, glacier geometry (including ice thickness) and subglacial hydrology. Ice sliding velocities can vary enormously from slow rates of < 0.02 m per day to high rates, at the most extreme, of > 100 m per day (Kamb et al., 1985; Paterson, 1994 referring to Reynaud et al, 1988). Glacial dynamic processes are highly variable in space and time and are exceptionally complicated phenomena, although it is likely that similar behaviour at different temperate glaciers can be caused by similar factors (Paterson, 1994; Willis, 1995). Diurnal and seasonal variations are related to the conditions at the ice-bed interface and

most importantly, variations in water pressure. Spatially, glaciers move faster along the centre-line, primarily because of the higher frictional drag the at margins relative to the centre (Meier, 1960). Furthermore, shear stress and internal deformation are reduced at locations with thinner ice such as the margins and the terminus (Raymond, 1971). The remainder of this section examines the methods used for inferring ice dynamics and then looks at the links between subglacial hydrology and basal sliding. Further insight into glacier dynamics are given in extensive reviews by Paterson (1994), Willis (1995), Van der Veen (1999) and Fischer and Clarke (2001).

2.5.2 Observation techniques

Monitoring basal motion is difficult, because the glacier bed is in the main inaccessible. Therefore, direct measurements (Table 2.2) can only be undertaken at the glacier margins and snout or via boreholes. Mechanical instruments such as the "drag spool" (Blake et al., 1994) and "ploughmeter" (Fischer and Clarke, 1994) have been developed to measure basal sliding velocities and deformation in basal sediments respectively. Such instruments are installed at the glacier bed in natural or artificial cavities, excavated tunnels or through boreholes. Direct observations of vertical strain rates within the ice body have been undertaken by inserting magnetic rings through boreholes at fixed depths (Gudmundsson, 2002; Sugiyama and Gudmundsson, 2003). Qualitative observations have been made by time-lapse photographic methods where the movement of a glacier section can be visually observed (Vivian et al., Alpine Glaciology Meeting (AGM), Grenoble, 2003).

Indirect observation techniques (Table 2.3) are predominantly surface velocity measurements, considering that variations in basal motion are reflected by variations in surface dynamics (e.g. Willis, 1995; Mair et al., 2001). However, due to the coupling of longitudinal stress-gradients, through which motion from the glacier bed is transferred to the surface, signals of local basal anomalies may be delivered to a wide area of the glacier surface and may therefore not reflect the local anomaly appropriately. To differentiate between real changes at the glacier bed and the spatial averaging at the surface, studies of glacier dynamics at surface require extensive measurements over large areas and at spatially and temporally high resolution (Jansson, 1995; Mair et al., 2001). Borehole inclinometry measurements for investigations of internal ice deformation have also been used (Blake and Clarke, 1992). The study of surface motion using repeat surveying of

marker networks on the glacier surface at different glaciers has made a major contribution to the understanding of glacier dynamics. The advantage of surface measurements as opposed to spatially limited basal measurements is that temporal variations can be investigated over a wide area. The spatial and temporal resolution of the measurements depends on the number of markers within the network and the frequency of measurements. The ratio between basal and surface ice velocities varies widely, but at temperate glaciers basal motion accounts for, on average, about half of the displacement observed at the glacier surface (Theakstone, 1967; Paterson, 1994).

The resolution of surveying instruments has been continuously improved and therefore the accuracy of surface motion measurements has been significantly enhanced.

Table 2.3: Observation techniques of glacier dynamics

	Method	Aims	Problems and limitations	Reference
Direct methods	"Drag spools" in natural or artificial subglacial cavities or boreholes	Horizontal basal movement and vertical uplift from glacier bed	Cavities are near the margins or at ice falls and do perhaps not represent typical basal movement.	(Theakstone, 1967) (Blake et al., 1994)
	"Ploughmeters" in boreholes	Horizontal basal movement Sediment strength	Hard to control from glacier surface.	(Fischer and Clarke, 1994) (Fischer et al., 1998) (Fischer et al., 1998)
	Magnetic rings drilled in the ice body at different depth	Vertical strain rates	Due to deformation of the borehole only observable for a limited period.	(Gudmundsson, 2002) (Sugiyama and Gudmundsson, 2003)
	Automatic series of photographs of surface motion	Visualisation of glacier movement	No a quantitative results.	(Moreau, 2003)
	Strain gauges and sensors in subglacial till in excavated tunnels	Subglacial sediment deformation	Building tunnels is hard and costly, velocity gradients within till can be measured, but not the absolute velocity.	(Fischer and Clarke, 2001) (Iverson et al., 2003) (Blake and Clarke, 1992) (Iverson et al., 1994)
Indirect methods	Survey of a marker-network at the ice surface	Horizontal and vertical surface motion	May not be representative for basal sliding processes.	(Iken and Bindschalder, 1986) (Hooke et al., 1989) (Willis, 1995) (Mair et al., 2001) (Bingham et al., 2003?)
	Borehole inclinometry	Internal ice deformation	Only monthly-daily variations can be observed. The technique can only represent basal motion if the borehole reaches the glacier bed (this is not always guaranteed).	(Blake and Clarke, 1992)

2.5.3 Impacts of subglacial hydrology on basal sliding processes

It has been recognised that the subglacial drainage system plays a key role for basal sliding processes and the most important driving factor are variations in the subglacial water pressure (Boulton, 1974; Bindschadler, 1983; Iken et al., 1983; Iken and Bindschalder, 1986; Humphrey, 1987; Kamb and Engelhardt, 1987; Hooke et al., 1989; Hanson et al., 1998). Variations of subglacial water pressure may affect hard-bedded glaciers, differently than soft-bedded glaciers (Willis, 1995). However, both types will react to rising water pressures with increased basal movement. Hard bedded glaciers will react to an increase of water pressure, resulting in separation from the bed, due to vertically lifting if a large enough proportion of the glacier is affected. Subsequently the glacier "floats" on subglacial water due to reduced basal friction and as a consequence enhanced basal sliding will occur (Iken and Bindschalder, 1986; Hooke et al., 1989). At soft-bedded glaciers high subglacial water pressures can lead to sediment weakening and enhanced deformation. Intergranular sediment friction is reduced (Boulton and Jones, 1979; Boulton and Hindmarsh, 1987; Alley, 1989; Kamb et al., 1994; Iverson et al., 1995; Fischer et al., 1999). However, differentiating between hard and soft-bedded glaciers is not always clear, because both types can occur under the same glacier.

High water pressures are likely to develop at the onset of the melt season, after rainstorm events and during times of high discharge as a result of increased meltwater input and inefficient subglacial drainage. It has been observed that during events of rapid sliding the subglacial water pressure rises and basal water levels significantly drop afterwards (Willis, 1995). The efficiency of the subglacial system depends largely on the configuration, size and geometry of the dominant drainage system beneath the glacier, the extent to which differing types of systems interact, how flowpaths and cavities are spatially interconnected and the degree to which one type of regime is superseded by another during the melt season (Willis, 1995). The configuration of the subglacial drainage system also defines the capacity for water storage. It has been found that a positive correlation between high ice motion velocities and englacial and subglacial water storage exists (Willis, 1995). The impacts of the englacial and subglacial drainage passage ways, i.e. the system structure and hydraulic behaviour, have a significant influence on the sliding mechanisms of a glacier (Willis, 1995). As the melt season develops, diurnal velocity fluctuations reach locally their

greatest amplitude. These peaks are induced by supraglacial meltwater-inputs of the high diurnal variation due to high subglacial water pressure during late summer.

The character of meltwater input to the englacial and subglacial drainage system is critically influenced by the distribution of moulins and crevasses. If the glacier has numerous moulins and crevasses enabling widespread meltwater inputs to the glacier bed, it is more likely that water in the subglacial drainage system will be pressurized over an area large enough to lift up the glacier or parts of it and hence induce glacier sliding.

2.5.4 Temporal variations of glacier sliding

Horizontal and vertical glacier movement can vary significantly in long-term time scales of hundreds and thousands (or even millions) of years as well as in short-term time scales of decades and intra-annual measures. Long-term variations are recognized as a response to climate change that generally occurs due to changes in precipitation, temperature and/or solar radiation and leads to an increase or decrease of the amount and the distribution of accumulation and melt (Hooke, 1998).

Long-term dynamics are studied, because glacier movement is a reflection of medium and long-term climatic fluctuations and the proxy record of these changes is preserved in the landforms that they alter or deposit. The prediction of climatic change is of critical contemporary importance because of growing concerns on the effects of global climate chance on the Earth's ecosystems and its impact on the human population. Short-term variations of glacier dynamics predominantly reflect local seasonal and diurnal impacts. These are studied to understand the processes that cause glacier movement. This knowledge is used to facilitate the interpretation of long-term climatic dynamics patterns. Intra-annual variations of glacier dynamics have been investigated at various field sites and patterns of vertical and horizontal glacier movement in short-term time scales have been reviewed in detail by Willis (1995). The main findings of previous studies are: (i) Flow velocity in summer are generally higher than in winter (e.g. Raymond, 1980; Iken et al., 1983; Iken and Bindschalder, 1986; Gudmundsson et al., 1997; Gudmundsson et al., 2000), although exceptions showing an opposite trend have also been measured (e.g. Meier, 1960). (ii) During the ablation season horizontal ice motion velocities decrease up-glacier (e.g. Schimpp, 1958; Hodge, 1974; Hooke et al., 1989; Willis, 1995) and the amplitude of seasonal velocity variation also decreases, up-glacier (Willis, 1995). (iii) Vertical

movement occurs due to increasing water pressure in the subglacial drainage system (Hooke et al., 1983; Iken et al., 1983; Iken and Bindschalder, 1986; Kamb and Engelhardt, 1987) and also due to the internal deformation during glacier motion causing compression and extension of the ice body (Gudmundsson et al., 1997; Gudmundsson, 2002). However, since subglacial hydrology is the driving factor of basal motion (Section 2.5.3), basal sliding processes rather than internal deformation of the ice are responsible for changes in the movement of ice masses (Willis, 1995). (iv) At a diurnal or weekly scale, most glaciers show a correlation between horizontal surface velocity variations and melt- or rainwater input (Iken et al., 1983; Kamb and Engelhardt, 1987). (v) Kinematic waves of high velocities can move down-glacier (Schimpp, 1958; Hodge, 1974; Krimmel and Rasmussen, 1986; Krimmel and Vaughn, 1987) as well as up-glacier (Hooke et al., 1983; Andreason, 1985; Hooke et al., 1989).

2.6 Limitations identified from existing work

From the sections above further research is required in snow hydrology, subglacial hydrology and glacier dynamics to fully understand these interconnected glacial processes and reactions. The importance of snow hydrology has been recognised for many years and theoretical as well as empirical approaches have advanced our understanding of the processes occurring within a snowpack. It is apparent that snowpacks are heterogeneous and highly metamorphosed and they are therefore difficult to predict or to generalise with respect to their evolution and properties. Features occurring during the evolution of a glacial snowpack such as the wetting front, flow fingers and ice lenses have been studied in detail but the interconnections of these elements and their impacts on meltwater delivery to the englacial drainage system remain largely unknown. There is a requirement for empirical data from meltwater investigations and flow processes under natural conditions i.e. in the glacial environment. An important research question that has previously not been addressed arises:

How do drainage conditions within the snowpack develop throughout the melt season and how does this affect the meltwater delivery to the subglacial drainage system?

Subglacial hydrology has been studied extensively at a variety of glaciers on non carbonate bedrock. Drainage conditions on highly soluble carbonate bedrock where Nye-channels are incised into the rock create a stable meltwater drainage system may be different from those

described above. The seasonal evolution of such a subglacial drainage system remains poorly understood. At Glacier de Tsanfleuron the subglacial drainage conditions were assessed by studying and mapping features in the proglacial area such as Nye channels and cavities. This leaves the following questions open:

To what extent are the subglacial drainage conditions, as observed in the deglaciated proglacial area, representative of the current subglacial drainage conditions of Glacier de Tsanfleuron?

What role do limestone bedrock and karst sinkholes play for subglacial hydrology at Glacier de Tsanfleuron?

Recent research in glacier dynamics has recognised that the hydraulic structure of the subglacial drainage system critically affects of glacier dynamics through the influence of subglacial water pressures. It remains unclear how a glacier overlying a linked-cavity drainage system responds to meltwater input to the subglacial system. The following research question has previously not been addressed:

Do seasonal variations in glacier hydrology impact on the ice dynamics of a glacier overlying a Nye channel linked-cavity drainage system?

To answer these questions and to focus on the objectives of the research (Section 1.2), a variety of field methods were utilised and a detailed research programme was developed to be undertaken at Glacier de Tsanfleuron, Switzerland, during the 2001 field season. This field research programme concentrated on dye tracer experiments in the snowpack, subglacial dye tracer experiments and detailed observations of glacier dynamics (Chapter 3).

3 Field methods

3.1 Introduction

The fieldwork at Glacier de Tsanfleuron was carried out from 23 June to 5 September 2001 in order to capture the evolution of the glacier hydrological system over the course of a melt season and to establish how variations in hydrology impacted on ice-dynamics. Because of the inaccessibility and variability of the structure of englacial and subglacial drainage systems, the use of a single method cannot be relied upon to determine behaviour in glacial drainage systems. Therefore, due to the complexity of the glacio-hydrological system, an interdisciplinary research approach is required utilizing a number of different techniques, this philosophy is adopted in this thesis. This chapter summarises the field techniques used during the melt-season.

In this thesis, dye-tracing has been used as the key technique to determine the characteristics of meltwater flow through both the supraglacial snowpack and subglacial drainage system. Five dye tracer injections were undertaken in the snowpack between 27 July and 17 August, three of which were undertaken on the snow surface and two at the snow-ice interface. Dye-tracing methodology is discussed in Section 3.2 and considers the principles of the tracer technique (Section 3.2.1), basics of tracer injection and detection, methods of analysing tracer experiments and the value of multiple tracer experiments. To investigate the water flow through the subglacial snowpack, dye injections were undertaken at both the snow surface and the snow-ice interface (Section 3.2.3). In order to investigate of the subglacial drainage system, dye tracers were injected into moulins where freely draining surface meltwater entered the interior of the glacier (Section 3.2.4). At the glacier snout, a gauging station was installed to monitor the proglacial stream water level, electrical conductivity and temperature as described in Section 3.3. This additional information was needed in conjunction with the dye tracing results to make inferences about the glacier's hydrology. The dynamics of the glacier during the melt-season was investigated from surveys of a stake network established across the glacier surface (Section 3.4). Surface melt data was obtained from ablation measurements undertaken across the glacier as described in (Section 3.5) and variations in the water table at the base of the snowpack were recorded.

Concentrations throughout this thesis are given in $\mu g\, l^{-1}$, which is equivalent to the concentration in parts per billion [ppb] as used in other literature.

3.2 Dye tracer experiments

3.2.1 Principles of the tracer technique

In glacial environments tracer experiments have been undertaken for more than 100 years. The tracer technique has often been used to investigate hydraulic conditions in and the structure of subglacial drainage systems and to quantify water transport and storage mechanisms (e.g. Theakstone and Knudsen, 1981; Behrens et al., 1982; Burkishmer, 1983; Moeri and Leibundgut, 1986; Seaberg et al., 1988; Hooke, 1989; Willis et al., 1990; Fountain, 1993; Hock and Hooke, 1993; Nienow, 1993; Hock et al., 1999; Schuler, 2002). Dye tracing has contributed significantly to our current knowledge of glacial hydrology. The method involves labelling water, which enters an unknown system and the detection of this tracer after passage through the system. The interpretation of the tracer breakthrough curve provides information about the passage of water through the system. The tracer technique is "likely to provide the best data" (Hooke, 1989: 231) to investigate the complex structure of glacial drainage systems.

3.2.1.1 Requirements of tracers

Tracers have to meet certain requirements to be of use in investigating hydrological systems. An ideal tracer should behave identically to the water in the system being investigated and whilst "perfect" tracers do not exist, modern tracers have excellent properties enabling hydrological investigations. The most commonly used tracers in glaciology are fluorescent dyes and common salt (NaCl). Detailed information about the properties of different tracers and various applications can be obtained from Käss (1998) and Smart and Laidlaw (1977).

Tracers used in glacial hydrology require a high solubility in water, physical and chemical stability and resistance to adsorption onto sediments or other substratum. They should also have good detectability at very low concentrations in the generally turbid waters of glacial streams, independence of water temperature and *p*H of the water, a low natural background

concentrations, ecological harmlessness (non-toxic) and cost effectiveness (Smart and Laidlaw, 1977; Käss, 1998).

3.2.1.2 Tracer injection

In glaciology, the most commonly used injection sites are moulins and crevasses where waters enter the glacier naturally (e.g. Ambach et al., 1972; Stenborg, 1973; Behrens et al., 1975; Theakstone and Knudsen, 1981; Burkishmer, 1983; Willis et al., 1990; Fountain, 1993; Hock and Hooke, 1993; Nienow et al., 1996a; Schuler, 2002). Tracer injections are also undertaken through boreholes directly into the firn aquifer (Ambach and Eisner, 1979; Behrens et al., 1982; Oerter and Moser, 1982; Schneider, 2001) or into the subglacial drainage system (Hooke et al., 1988; Hock et al., 1999). Furthermore, tracers have been spread out over the snow or firn surface of the glacier (Krimmel et al., 1973; Behrens et al., 1982; Fountain, 1989).

The injections at Glacier de Tsanfleuron were undertaken into moulins as well as at the snow surface and at the snow-ice interface. To avoid the contamination of the injection area, the tracer injection solutions were prepared in advance away from the research area.

3.2.1.3 Tracer detection

Fluorescent tracers have unique optical properties and are visible to the human eye at extremely low concentrations. Sodium-fluorescein (also known as uranine) for example is visible at about 40 $\mu g\, l^{-1}$ in clear water (Käss, 1998). Thus, early glacier-hydrological investigations detected fluorescent tracers visually (Forel, 1898; Mercanton, 1916). Modern instruments can accurately detect fluorescent tracers in even lower concentrations and sodium-fluorescein is detectable at 0.002 $\mu g\, l^{-1}$ in the laboratory measurement (Käss, 1998). This makes these dyes very effective quantitative investigations. Dye detection is undertaken using either filter fluorometers, which are most suitable for field investigations due their robust design, or spectro-fluorometers that are commonly used in laboratories.

At Glacier de Tsanfleuron filter fluorometers were used for the detection of emerging dyes at chosen sampling sites. These operate by exciting fluorescent molecules, which absorb light at a specific wavelength from a light source in the instrument. Almost immediately following excitation (10^{-8}s later) light is emitted at a longer wavelength and this "fluorescence" is measured (Turner, 1997). Excitation and emission wavelengths are

constant and specific for each fluorescent tracer and therefore allow identification through their spectral properties. At the concentrations at which the return curves at Glacier de Tsanfleuron were measured (< 100 $\mu g\ l^{-1}$), the intensity of the emitted light is proportional to the dye concentration in the tracer solution.

The collection of extensive amounts of data is problematic if individual samples have to be collected and returned to the laboratory for subsequent laboratory analyses. However, if the field conditions do not allow immediate recording, individually collected samples can be collected and measured subsequently (Bingham, 2003). The availability of modern filter fluorometers with a continuous flow-through cuvette enables more comprehensive tracer investigations including detailed diurnal and seasonal observations of the hydrological system since automatically recorded *in situ* measurements provide high resolution data series at intervals of only a few seconds. Furthermore, there is no risk degradation of tracer concentrations during storage due to instability.

In order to obtain accurate estimates of dye concentrations, the fluorometers must be calibrated. The calibration procedure used for the fluorometers at Glacier de Tsanfleuron is described in Appendix A.

3.2.1.4 Rationale for tracer experiment analyses

The key to quantitative tracer experiments is the rigorous analysis and interpretation of tracer return curves that can provide information about the characteristics of the drainage system. The tracer return curve provides integrated information concerning the route taken by the dye cloud from the injection to the detection point.

Useful information about drainage system characteristics can be achieved from visual inspection of a return curve (Nienow, 1993). However, this approach is limited and further quantitative analyses are necessary to examine the main flow parameters characterising the drainage system. This can be achieved using transport models that simulate tracer return curves and to calculate parameters such as flow velocity and dispersion coefficient, which can then be further analysed. The proportion of injected tracer that is recovered can also be used to make inferences about the drainage system structure.

3.2.1.5 Multiple tracer experiments

The characteristics and detection properties of many tracers do not interfere with each other and different tracers can therefore be used simultaneously. This is of great value for collecting comprehensive sets of temporal and spatial data since different tracers can be injected in parallel at different locations across the glacier.

3.2.2 Tracers used at Glacier de Tsanfleuron

During summer 2001 at Glacier de Tsanfleuron three fluorescent tracers (sodium-fluorescein, rhodamine WT and sulphorhodamine B) and a salt tracer (lithium chloride) were used. The properties of these tracers are shown in Table 3.1 and this section explains the reasons for selection of these four tracers.

Table 3.1: Overview about the properties of the tracers used at Glacier de Tsanfleuron, summarised from Käss (1998) and Smart and Laidlaw (1977).

	Sodium-fluorescein (uranine)	Rhodamine WT	Sulpho-rhodamine B	Lithium chloride
Detectability at Glacier de Tsanfleuron field season	≈ 0.01 µg l^{-1} (*in situ*)	≈ 0.05 µg l^{-1} (*in situ*)	≈ 0.05 µg l^{-1} (*in situ*)	≈ 0.1 µg l^{-1} (lab analysis)
Solubility in water (20°C)*	> 600 g l^{-1}	comes as 20 % solution	10 g l^{-1}	832 g l^{-1}
Adsorption onto limestone sediments (at 2 g l^{-1} sediment conc.) **	2 %	7 %	3 %	-
Physical stability *	stable	stable	stable	stable
Photo-chemical decay*/**	high	low	low	stable
Chemical/*p*H stability */**	best at *p*H > 8.5	best at *p*H > 5.5	best between *p*H 3.5 and 10	Li-cations associate strongly with water molecules when dissolved in water and are therefore chemically very stable. *p*H independent
Temperature dependence [% per °C] *	0.4 (low)	2.7 (high)	2.9 (high)	independent
Toxicity */**	low	low in low concentrations	low in low concentrations	low in low concentrations
Costs (2000) [£/kg]	≈ 19	≈ 41 (20% solution)	≈ 27	≈ 8

* from (Käss, 1998), ** from (Smart and Laidlaw, 1977)

All these tracers used at Glacier de Tsanfleuron (Table 1) are detectable at low concentrations and are sufficiently soluble in water. The tracers also require a high

resistance to adsorption since tracer loss due to adsorption onto sediments may affect the flow parameters derived from tracer tests, thereby offering interpretation of the traced hydrological system. At Glacier de Tsanfleuron the suspended sediment concentration was mainly below 1 g l^{-1} and during peak discharge up to 2 g l^{-1}. The tracers show low adsorption losses for the observed range of sediment concentrations and therefore satisfy the criterion of resistance to adsorption. However, high suspended sediment concentrations, reflected by high turbidities of the stream water, can cause light scattering within the fluorometer resulting in misleading measurements. Complications caused by turbidity of the proglacial stream during dye-tracer experiments have been discussed in the literature (Smart and Laidlaw, 1977; Brugman, 1986; Nienow, 1993). This general problem of continuous fluorometry in highly turbid water is only avoidable by taking individual samples (grab samples) and allowing the sediment to settle before analysis. However, the advantages of the *in situ* measurement method are lost if grab sampling is used.

The tracers selected were chemically and optically sufficiently stable for the purpose of this study. During the experiments at Glacier de Tsanfleuron, the low photolytic stability of sodium-fluorescein was not critical for the following reasons. i) During experiments investigating the subglacial drainage system, the tracer was only briefly exposed to direct sunlight between emergence at the glacier snout and arrival at the sampling point in the proglacial area (a distance of about 50 m). ii) During snowpack experiments, photo-chemical decay was unimportant because the loss of a small quantity of tracer did not affect the results since estimation of tracer recovery rates was not possible because water discharge at the snow-ice interface was unknown. The tracer was always injected at concentrations high enough to generate a measurable signal at the snow-ice interface, even on days with high ultraviolet light.

Meltwater temperatures in glacial environments show minimal variations and ranged between 0°C and 3°C at Glacier de Tsanfleuron during summer 2001. Operating in fairly stable temperatures is clearly advantageous for the use of temperature dependent tracers such as rhodamine dyes. The effect of temperature on the fluorescence of rhodamine tracers is insignificant if the instrument operates in stable stream temperatures and is calibrated with water at stream temperature or if the laboratory calibration is temperature compensated. Equations for temperature correction are available in the literature (Smart and Laidlaw, 1977; Käss, 1998).

The *p*H in the proglacial streams was measured at various locations with a portable *p*H-meter (Jenway 3150) and ranged between *p*H 9 and 10, the alkaline *p*H was expected due to the limestone bedrock. The *p*H of the meltwater in the snowpack, which has not had bedrock contact, was about *p*H 7. At these *p*H ranges, the fluorescence of most of the tracers is at its maximum (Smart and Laidlaw, 1977; Käss, 1998). A fluorescence reduction of about 20 % for sodium-fluorescein due to the neutral *p*H values of the snowmelt water was expected during the snowpack experiments. This affects the strength of the signal, but not the actual appearance and shape of the return curve if an adequate tracer concentration was injected.

Lithium chloride (LiCl) was chosen as a promising tracer for undertaking simultaneous injections with rhodamine WT or sulphorhodamine B and sodium-fluorescein. Lithium chloride has been successfully used in groundwater research (Käss, 1998) with the first tracer test reported by Vortmann and Timeus (1910). However, applications of LiCl in glacier hydrology have not been published to date. Lithium chloride is easily soluble in water and due to the very small ionic radius of the lithium ion, it builds strong covalent bonds when dissolved in water (Mortimer, 1987). This covalent association between the lithium cation and the hydroxyl anion inhibits the likelihood of the lithium ion from reacting with bedrock or basal and suspended sediments within the subglacial drainage system (Käss, 1998).

Rhodamine WT and sulphorhodamine B both have similar emission wavelengths and therefore cannot be used simultaneously. However, three independent tracers were available and used for simultaneous injections since rhodamine dyes (rhodamine WT or sulphorhodamine B), sodium-fluorescein and lithium chloride can be detected in the same sample without any interferences.

3.2.3 Tracer experiments in the snowpack

In this study, we investigated the water flow in the snowpack by tracer tests. In order to characterise flow through the snowpack and at the snow-ice interface, different experiments were carried out with dye released at the snow surface and/or at the snow-ice interface. Dye detection took place at the snow-ice interface some distance downstream of the injection point. The procedure and difficulties of this method are outlined in this section.

Five experiments were undertaken near Stake 20 between 27/07/01 and 17/08/01. The snowpack at this location had a thickness of about 2 m at the onset of the tests. During the melting of the snowpack, it was hoped to establish whether evolution of preferential passageways occurred during the melt season. For the snowpack experiments, sodium-fluorescein and rhodamine WT were used as tracers.

3.2.3.1 Injections at the snow surface

In order to investigate natural water flow through the snowpack, it is necessary to undertake tracer tests in a natural, unaltered snowpack. An even and minimal distribution of tracer solution was achieved by sprinkling a dye solution (500 ml total volume) across a $1m^2$ area using a watering can (Figure 3.1).

Figure 3.1: Injection at the snow surface using a watering can.

The injection method was tested on an adjacent snowpack separate area to ensure that an even spread of dye could be delivered to the snow surface. The experimental set-up (Figure 3.2) shows the location of the injection area a few metres upstream from the detection site.

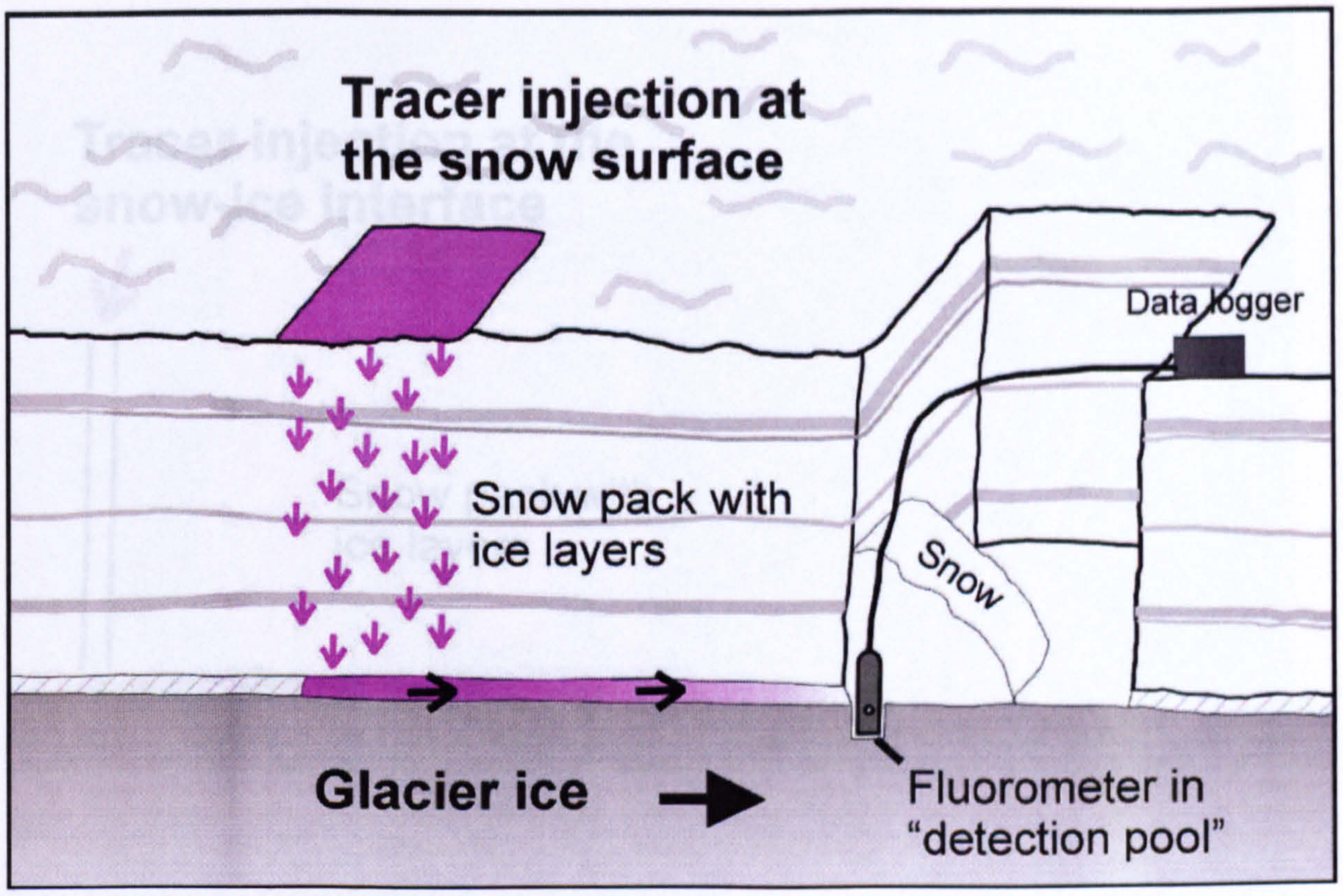

Figure 3.2: Experimental set-up for injections at the snow-surface.

The hydrological effects associated with adding the "water" solution to the snowpack are considered to be small since only 500 ml solution (containing 0.5 g of dye) was used in each test, which is the equivalent of a 0.5 mm water film, spread over the $1m^2$ injection area. Dye at the snow surface decreases the albedo of the snowpack thereby increasing the melt rate, so each injection may had a very slight effect on the initial infiltration rate, depending on solar radiation at the time of injection.

3.2.3.2 Injections at the snow-ice interface

To investigate water flow along the snow-ice interface, dye injections at the snow-ice interface were undertaken a few metres upstream of the detection site (Figure 3.3). For each injection, a condom with 0.2 g of dye in a solution of 10 ml water was dropped into a borehole to the snow-ice interface (bottom of borehole) and burst at injection time (instantaneous injection).

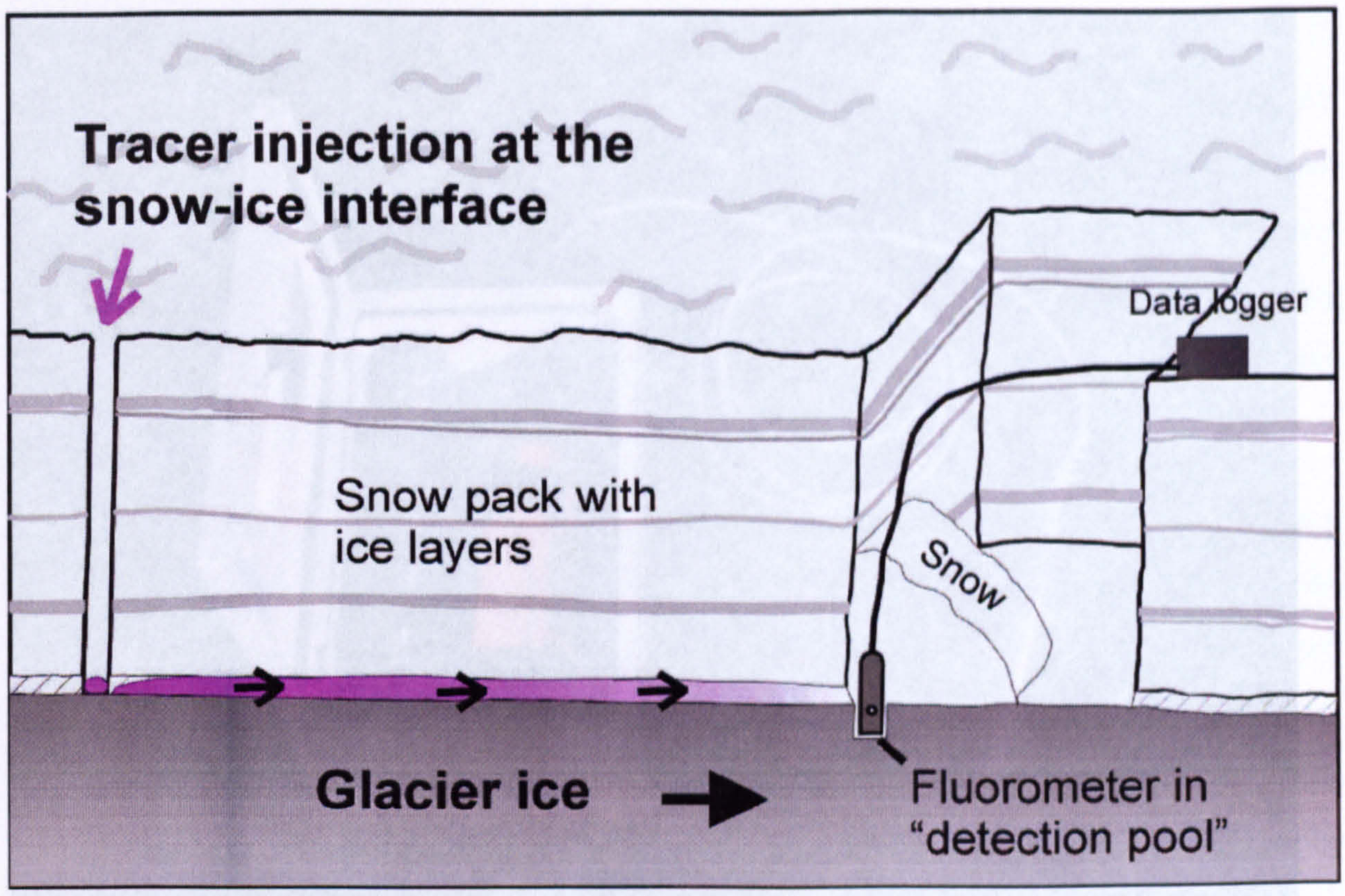

Figure 3.3: Experiment set-up for snow-ice interface injections.

3.2.3.3 Tracer detection at the snow-ice interface

A down borehole GGUN-FL fluorometer (Figure 3.4) was installed at the snow-ice interface down-glacier of the injection site in order to detect the dye tracers emerging from both the snow surface and snow-ice interface injections. Before starting each experiment, the stratigraphy of the undisturbed snowpack was recorded from the up-glacier wall of the fluorometer pit. Ice layers critically influence water flow through snow (Section 2.3.2.2) and information about the number of ice layers and their thickness may clarify the interpretation the tracer breakthrough curve. Tracers spread at the surface will initially percolate vertically downwards as meltwater flows through the snowpack (Colbeck, 1972). If the meltwater encounters an impermeable horizon, it will flow almost horizontally until a permeable weakness enables continuous downward percolation (Albert and Perron, 2000). Once it reaches the impermeable ice, water flows along the snow-ice interface towards the detection site, where the tracer concentrations were recorded.

Figure 3.4: GGUN-FL downhole fluorometer with logger and memory cards.

The down borehole fluorometer (GGUN-FL) was installed at a known distance down-glacier of the injection area at the bottom of a snow pit (Figure 3.2 or Figure 3.3) in order to record the dye return curves. Since the fluorometer head has to be continuously submerged in water (about 4 cm deep), a small core was taken from the ice surface to create a small "pool". The fluorometer must be set-up vertically to avoid air bubbles accumulating in the optical cell since they scatter light and degrade the signal quality by producing spurious peaks (Geomagnetism-Group, 2000). During surface injections, the snow surface between injection area and pit was undisturbed to ensure natural conditions. Dye concentrations were measured and logged automatically at 10 s intervals.

The overall establishment of an effective dye detection method was challenging. Similar tracer tests have not been undertaken in a supraglacial snowpack and a suitable experimental set-up was therefore developed during the field season at Glacier de Tsanfleuron. A problem with the fluorometer set-up resulted from the "detection pool" becoming larger during the experiment due to melt and subsequently the fluorometer falling over. The fluorometer was therefore covered with snow to prevent the "pool" from

melting and also to hold the fluorometer in a stable position (Figure 3.2 or Figure 3.3). Another problem occurred when the fluorometer sensor became blocked by snow such that the passage of the dye was not recorded. To prevent this problem, the fluorometer head was covered with a perforated plastic bottle and then covered with snow. This may have impeded water circulation and mixing during times of very little water flow such as during the night (gap in return curves, see below). Following the establishment of an effective snowpack tracing protocol, the first return curve was monitored successfully on 27 July.

Due to a connection failure, the instrument was not fully available before 09 August (repaired at the University of Neuchâtel, Switzerland). The subsequent calibration of the instrument was undertaken with deionised water at a temperature of 0 °C in the laboratory at Glasgow University. The calibration conditions were chosen to mimic the situation on the glacier where the fluorometer was mainly used in snowmelt water of very low mineral and negligible sediment content. The calibration of the fluorometer was undertaken by submerging the fluorometer in samples of known concentrations of 0, 10 and 100 $\mu g\ l^{-1}$ rhodamine WT and sodium-fluorescein. The calibration function, achieved by linear regression is shown in the Appendix A.

3.2.3.4 Analyses of tracer return curves

The tracer returns curve provides information on the hydrological system through which the traced water has flowed. Water flow through snowpacks is extremely complicated and is effected by various factors including meltwater fluxes from the surface, water saturation of the snowpack, snow grain size distribution, ice layers, preferential flow fingers and snow temperature. However, freezing/refreezing processes, that for simplicity are disregarded here, also complicate water travelling through snow. Figure 3.5 shows different idealised types of return curves that might be expected after the percolation of tracer labelled water through the snowpack from a single point at the snow surface. For the experiments at Glacier de Tsanfleuron square injections onto the snow surface were undertaken rather than point injections to provide a broader representation of the overall structure of the snowpack. The following provides summaries of hypothetical snowpack conditions likely to generate the return curves presented in Figure 3.5.

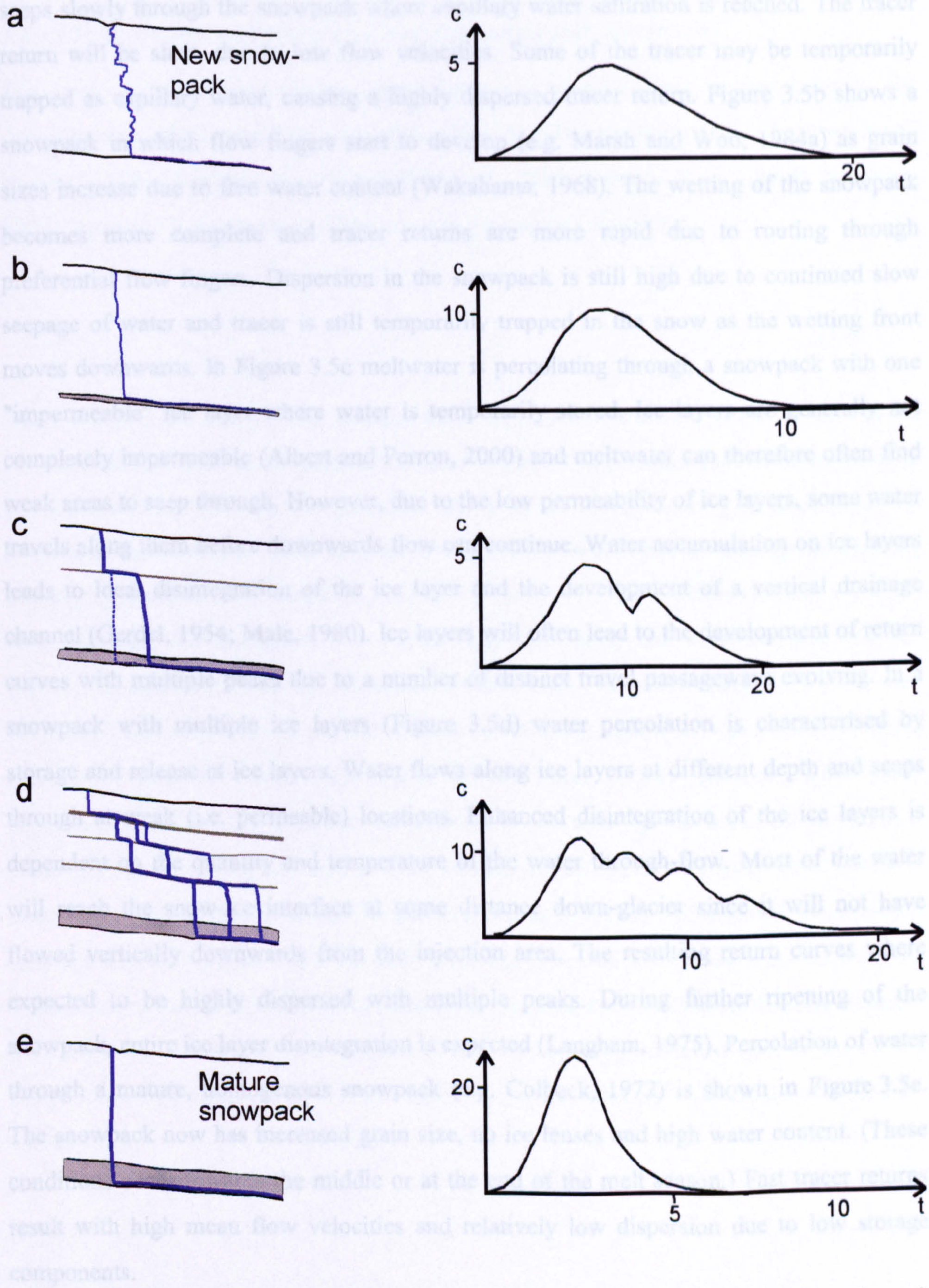

Figure 3.5: Idealised return curves from the passage of tracer through different configurations of glacial snowpacks.

In Figure 3.5a, tracer is percolating through a relatively fresh snowpack without ice lenses. The wetting of the snow has started, but flow fingers have not been developed. Meltwater

seeps slowly through the snowpack where capillary water saturation is reached. The tracer return will be slow, due to low flow velocities. Some of the tracer may be temporarily trapped as capillary water, causing a highly dispersed tracer return. Figure 3.5b shows a snowpack in which flow fingers start to develop (e.g. Marsh and Woo, 1984a) as grain sizes increase due to free water content (Wakahama, 1968). The wetting of the snowpack becomes more complete and tracer returns are more rapid due to routing through preferential flow fingers. Dispersion in the snowpack is still high due to continued slow seepage of water and tracer is still temporarily trapped in the snow as the wetting front moves downwards. In Figure 3.5c meltwater is percolating through a snowpack with one "impermeable" ice layer where water is temporarily stored. Ice layers are generally not completely impermeable (Albert and Perron, 2000) and meltwater can therefore often find weak areas to seep through. However, due to the low permeability of ice layers, some water travels along them before downwards flow can continue. Water accumulation on ice layers leads to local disintegration of the ice layer and the development of a vertical drainage channel (Gerdel, 1954; Male, 1980). Ice layers will often lead to the development of return curves with multiple peaks due to a number of distinct travel passageways evolving. In a snowpack with multiple ice layers (Figure 3.5d) water percolation is characterised by storage and release at ice layers. Water flows along ice layers at different depth and seeps through at weak (i.e. permeable) locations. Enhanced disintegration of the ice layers is dependent on the quantity and temperature of the water through-flow. Most of the water will reach the snow-ice interface at some distance down-glacier since it will not have flowed vertically downwards from the injection area. The resulting return curves where expected to be highly dispersed with multiple peaks. During further ripening of the snowpack, entire ice layer disintegration is expected (Langham, 1975). Percolation of water through a mature, homogenous snowpack (e.g. Colbeck, 1972) is shown in Figure 3.5e. The snowpack now has increased grain size, no ice lenses and high water content. (These conditions occur towards the middle or at the end of the melt season.) Fast tracer returns result with high mean flow velocities and relatively low dispersion due to low storage components.

3.2.3.5 Hydrological parameters derived from snowpack tracer tests

The most common quantitative flow parameter derived from tracer tests is the determination of "throughflow velocity". This velocity represents (e.g. Theakstone and Knudsen, 1981; Burkishmer, 1983; Willis et al., 1990; Nienow et al., 1996b; Bingham, 2003) "apparent flow velocity". Flow velocity (v) was calculated by:

$$v = \frac{x}{t} \qquad (3.1)$$

where x (m) is the straight-line distance between injection and detection site and t is the flow time of the tracer to the peak of the return curve. This distance does not correspond to the real travelling distance, but gives the minimum possible travelling distance (and thus minimum flow velocity), as it is more likely that the water travels through meandering drainage passageways of unknown lengths (Käss, 1998). Flow characteristics vertically down through the snowpack (x_1, Figure 3.6) and along the snow-ice interface (x_2, Figure 3.6) differ significantly. Therefore, in this study, flow velocities at x_1 and x_2 are considered separately. Since the travel route of water through a snowpack can be highly variable (Figure 3.5) and exact routes of the tracer remain unknown from tracer experiments as described here, the calculation of flow velocity was based on an idealised pathway (Figure 3.6). In addition to snow surface injections, tracer experiments were also undertaken directly at the snow-ice interface. From the transit time along the snow-ice interface (t_2) at distance (x_2) the flow velocity (v_2) was calculated. Furthermore, the subtraction of the transit time at the snow-ice interface for a measured distance obtained from injections at the snow-ice interface allows the separation of t_1 and t_2, from the overall travel time (t) by using $t_1 = t - t_2$. Then equation 3.1 was applied to obtain the vertical flow velocity (v_1).

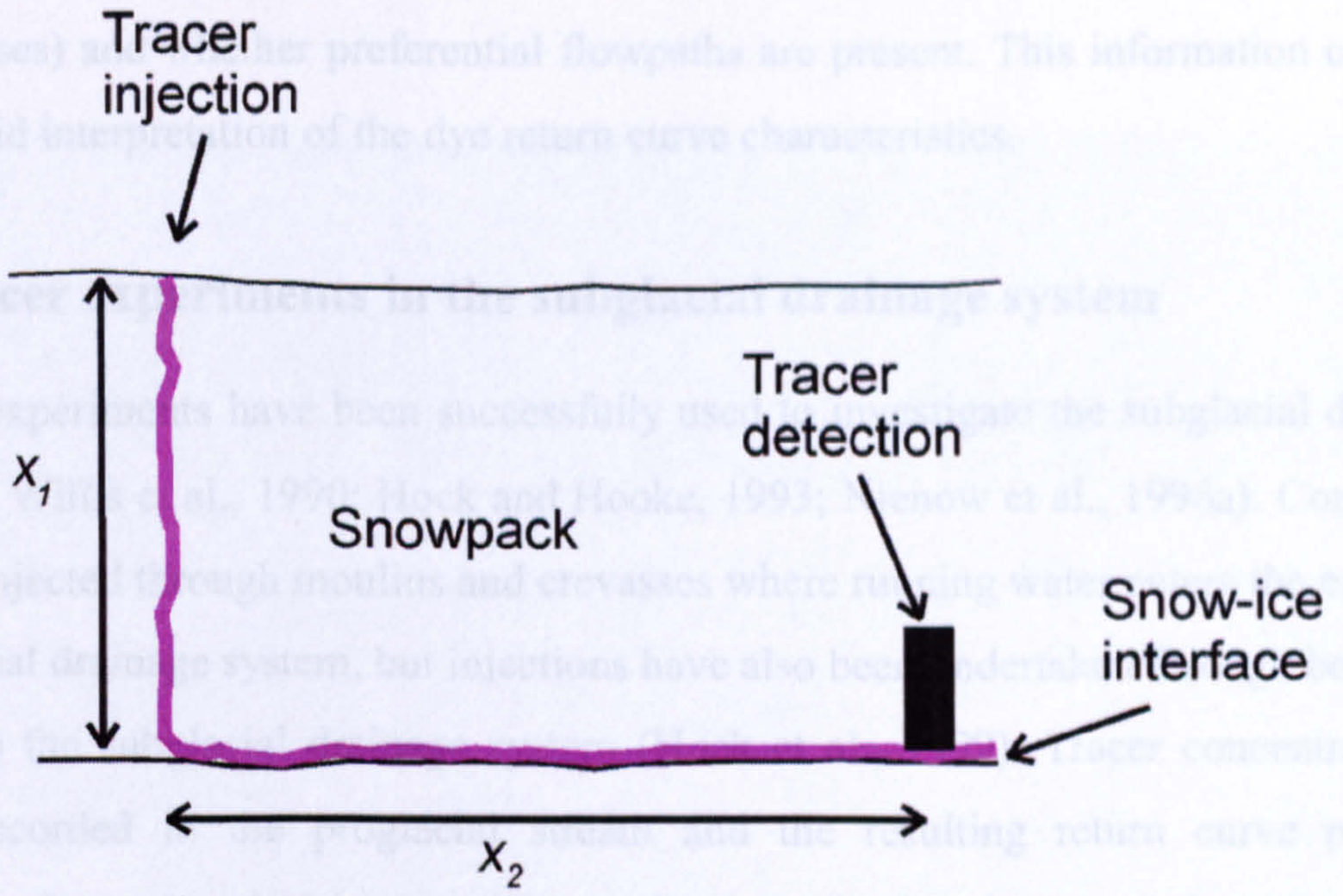

Figure 3.6: Idealised and simplified travel pathway through the snowpack for the isolation of travel characteristics vertically through the snowpack and at the snow-ice interface. x_1 represents the vertical travel distance through the snowpack and x_2 the travel distance at the snow ice interface.

The tracer return curves from both the snow surface and snow-ice interface injections were interpreted by analysing the tracer return curve shape and calculated flow velocities in conjunction with meteorological observations. The information derived can be used to infer snowpack flow. The time to the first appearance of tracer and to first and second peaks (if applicable) was used to calculate specific throughflow velocities.

Due to the complex shapes of the return curves, the application of advection-dispersion models was inappropriate and dispersion coefficients were not obtained. Recovery rates of the experiments could also not be calculated due to the unknown discharge at the snow-ice interface.

3.2.3.6 Visual observation of surface injection

The pattern of dye percolation through the snowpack, from a different tracer experiment was observed visually in a separate pit. Between one and three hours after an injection, a section was cut beneath the injection area to display the flowpaths from the surface downwards. This approach does not provide quantitative results, but highlights the travel passageways of the dyed meltwater providing information about potential storage locations

(e.g. ice lenses) and whether preferential flowpaths are present. This information can then be used to aid interpretation of the dye return curve characteristics.

3.2.4 Tracer experiments in the subglacial drainage system

Dye tracer experiments have been successfully used to investigate the subglacial drainage system (e.g. Willis et al., 1990; Hock and Hooke, 1993; Nienow et al., 1996a). Commonly tracers are injected through moulins and crevasses where running water enters the englacial and subglacial drainage system, but injections have also been undertaken through boreholes directly into the subglacial drainage system (Hock et al., 1999). Tracer concentration is generally recorded in the proglacial stream and the resulting return curve provides information about the drainage conditions in and characteristics of the investigated drainage system.

At Glacier de Tsanfleuron the tracer method was used to investigate the subglacial drainage system and to determine whether the current drainage system is hydraulically similar to the relict system exposed in the proglacial area. Ten experiments were undertaken at the end of the field season between 28 and 31 August from seven different moulins or crevasses in the ablation area of the glacier. Earlier injections were not possible because the un-seasonally thick snowpack prevented the location of moulins fed by supraglacial meltwater streams. Injections were not possible from the lowest part of the glacier tongue as it was highly crevassed and supraglacial meltwater channels were absent. All sites in the ablation area where considerable amounts of meltwater (≥ 0.1 l s^{-1}) entered the englacial drainage system were tested.

3.2.4.1 Injections into moulins or crevasses

A known quantity of tracer solution was poured into a meltwater channel flowing directly into a freely draining moulin or crevasse (Figure 3.7). The supraglacial water input to the moulin can critically influence the tracer transport (Nienow et al., 1996b) and the quantity of water input was therefore estimated. The location and elevation of the injection sites was surveyed with a hand-held Garmin Summit eTrex GPS, which achieved accuracy at this site of between 1-10 m. The barometric altimeter of the GPS was calibrated regularly at point 2417 m as shown on Carte Nationale de la Suisse, No. 1286 (1:25000), St-Léonard (Office fédéral de topographie, 1992).

Figure 3.7: Manual injection into a moulin, Experiment 3 on 29 August 2001.

3.2.4.2 Tracer detection

At Glacier de Tsanfleuron a Turner Designs 10-005 field fluorometer was used to detect the emerging rhodamine WT or sulphorhodamine B and a Turner Designs 10-AU field fluorometer (similar to Turner Designs 10-005 field fluorometer) was used to detect the emerging sodium-fluorescein at the proglacial stream. Both instruments are equipped with a flow through cuvette for continuous monitoring. Dye emergence was monitored in the proglacial stream about 50 m from the glacier's snout where water was routed by gravity flow through the fluorometer. Uphill flow to the fluorometer was started and maintained by a suction-driven siphon system. Hosepipes of 1.5 cm diameter and about 10 m length were attached to the flow-through cuvette at both sides enabling water to flow from a higher to a lower elevation. The hosepipe intake was placed within the main flow of the stream, not too close to the stream bed to reduce sediment concentrations, but sufficiently below the stream surface to ensure permanent submergence over a diurnal discharge cycle. Furthermore, the intake was in a position with low turbulence to avoid air bubbles entering the hose that would affect the fluorescence measurement.

The fluorometer was connected to a Campbell Scientific Ltd. CR 21X datalogger programmed to read the dye concentrations every second and store average values each minute. Both Turner fluorometers and the datalogger were supplied by separate 12 V car batteries, which were kept fully charged using a 20 W solar panel. To prevent the data logger and fluorometers from excess voltage (> 16 V), a solar shunt regulator was connected into the power system. A petrol-powered generator was available and occasionally used as back up.

During the 2001 field season, the salt tracer lithium chloride (LiCl) was used in addition to the dye tracers. Water samples were collected with an automatic ISCO vacuum-pump sampler at typically 10-30 minute intervals. The water samples were subsequently analysed for lithium cations in the laboratory by flame-photometry at the 670.8 nm line (Käss, 1998). In order to remove the calcium ions occurring in natural waters that hinder detection of the lithium spectrum, ammonium oxalate powder (1000 mg l^{-1}) was added to the samples to precipitate the calcium. This procedure increases the lithium emission by approximately 25 % (Käss, 1998).

The ISCO vacuum-pump sampler was also used to collect water samples from the long tailing edge of dye returns when the battery power was too low to keep the Turner fluorometers continuously powered, especially during lengthy return times. To check tracer concentrations in samples comparable with the *in situ* record, a few samples were collected during the *in situ* measurement. The pump sampler was typically used over night obtaining water samples at 30-60 minute intervals which were run through the fluorometer the following morning after shaking them to obtain original sediment concentrations.

3.2.4.3 Tracer return curve shapes

The shape of the tracer return curve contains information about characteristics of the investigated drainage system (Nienow, 1993). Figure 3.8 provides examples of idealised subglacial drainage system configurations and the resulting tracer return curves expected from the flow through these systems. These models of return curve generation are made on the basis of equal tracer injection masses, equal straight line distances between injection and detection point and equal discharge regimes during the time of tracer passage.

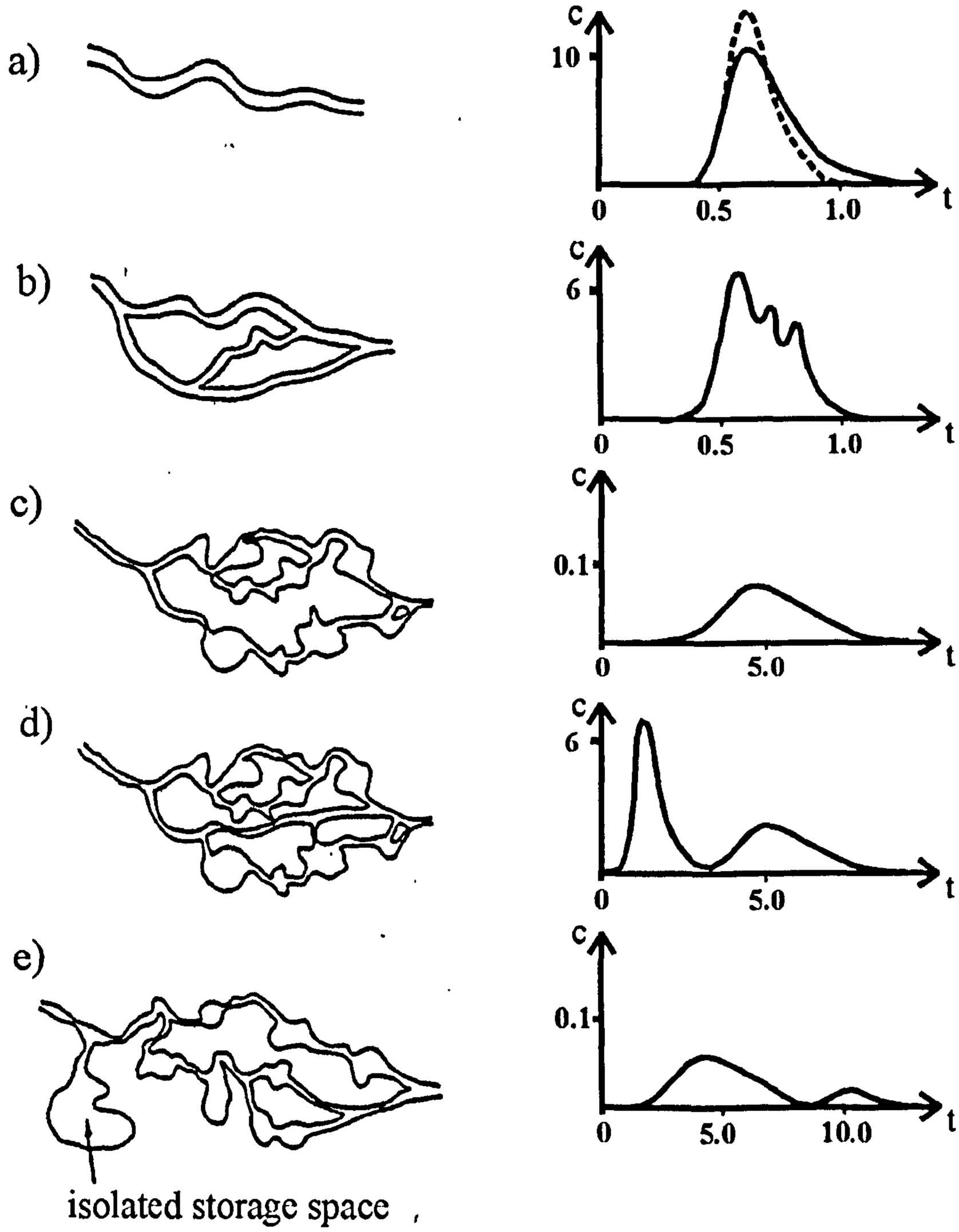

Figure 3.8: Idealised tracer return curves from the passage of dye through hydraulic ally distinct subglacial drainage systems (after Nienow, 1993).

A narrow single-peaked curve with limited tailing suggests a well-developed, hydraulically smooth and efficient englacial and/or subglacial drainage system (Burkishmer, 1983; Seaberg et al., 1988). The roughness of the channel clearly influences the hydraulic efficiency of the system (Richards et al., 1996), whereby a hydraulically "smoother" channel is more efficient than a rougher channel, thereby producing a more peaked curve (dashed line) (Figure 3.8a). A pronounced tail could be produced by reversible sorption of the tracer or by retention in storage zones such as eddies. Multiple peaks can result from flow through an anabranching channel system, representing differing tracer pathways

(Figure 3.8b) (Collins, 1982; Burkishmer, 1983; Seaberg et al., 1988). The more complex the drainage system is and the more the tracer is dispersed during transit, the wider the resulting return curve becomes. These conditions are expected in inefficient distributed drainage systems such as linked-cavity systems (Lliboutry, 1968; Kamb and Engelhardt, 1987) or water film Figure 3.8c) (Weertman, 1972). Drainage through systems possessing multiple flowpaths are likely to have low velocities and often produce long lasting highly dispersed tracer returns. If a main channel exists within a complex drainage system, it is likely to produce a tracer return curve with a rapidly increasing limb and a pronounced tailing or a secondary peak at the Figure 3.8d). If the drainage system includes cavities that connect to flow passageways during high discharge, tracer can be isolated and thus stored there during low discharge and subsequently released at the next high discharge producing a secondary peak (Figure 3.8e) (Willis et al., 1990; Nienow, 1993).

3.2.4.4 Quantitative analysis of tracer return curves

Flow parameters can be derived from raw data (recovery rates) and modelled data (mean flow velocity, dispersion coefficient). Furthermore, from mean flow velocities and dispersion coefficient the dispersivity can be calculated. The model used and the parameters obtained are explained in this section.

Tracer transport model

A number of different models can be used to model return curves to quantitatively evaluate the curve characteristics. In this project, the curves were modelled using a tracer transport model that was implemented in the CXTFIT 2.1 code provided by the U.S. Salinity Laboratory. The advection-dispersion model was applied in this study to estimate solute transport parameters from observed tracer concentrations (Toride et al., 1999). The model considers tracer transport as one-dimensional along the flow direction. The tracer concentration c at a location downstream of the injection site is described by

$$c(t) = \frac{m}{Q} \frac{x_1}{\left(4\pi D t^3\right)^{1/2}} \exp\left(-\frac{(x_1 - vt)^2}{4Dt}\right) \tag{3.2}$$

where m is the total injected tracer mass, Q is discharge and x_1 is the transport distance (Kreft and Zuber, 1978). The values of the parameters flow velocity (v) and dispersion

coefficient (D) were iterated using a non-linear least-square method (Marquardt, 1963) to obtain optimum agreement between measured and simulated tracer concentrations.

The background level was subtracted from the raw fluorescence data of the moulin experiments and the fluorometer data was converted into actual tracer concentrations using the calibration functions (Appendix A). In order to compare the results from the application of the CXTFIT 2.1 model to each of the return curves, the measured concentrations were standardised. To this end, the tracer load $c(t)\,Q(t)$ at the detection site was calculated and normalised with the mass of injected tracer (m). This procedure allows the comparison of different tracer return curves independent of the discharge conditions and the quantity of detected tracer.

Flow velocity

The flow velocity (v) corresponds to the mean flow velocity along the flowpath. Information about the flow conditions and hydraulic characteristics of the subglacial drainage system can already be inferred from the flow velocity (Hooke, 1989; Hubbard and Nienow, 1997; Fountain and Walder, 1998). Rapid throughflow velocities of more than 0.2 ms^{-1} indicate tracer transport through a hydraulically efficient drainage system, while low flow velocities of less than 0.2 ms^{-1} suggest a hydraulically inefficient drainage system (Hubbard and Nienow, 1997). However, this value is only an approximate indicator for the efficiency of the drainage system. Other flow parameters such as the dispersion of the tracer cloud have to be considered for a more reliable interpretation of the drainage configuration.

Dispersion coefficient

Two main processes are responsible for the dispersal of the tracer during its travel down-glacier, molecular diffusion and mechanical dispersion (advection). Fischer (1968) and Taylor (1954) explained the processes of diffusion and dynamic dispersion in detail. Both can be described by a diffusion equation including a hydrodynamic dispersion coefficient (Taylor, 1954). The dispersion coefficient (D), which can be determined from a tracer breakthrough curve, evaluates the degree of tracer dispersal and can be used to make inferences regarding the drainage system configuration. However, the dispersion coefficient provides a quantitative measure of the tracer return curve shape, its independence from v concludes that analyses of D alone do not give consistent indicators

of drainage system configuration (Nienow, 1993). It is possible to produce identical values of D from breakthrough curves with disparate values of v (Figure 3.9), which imply that equal values of D can be derived from complementary flow through drainage system configurations. Therefore, it is essential to analyse D in combination with v, hence the derivation of the dispersivity parameter (d).

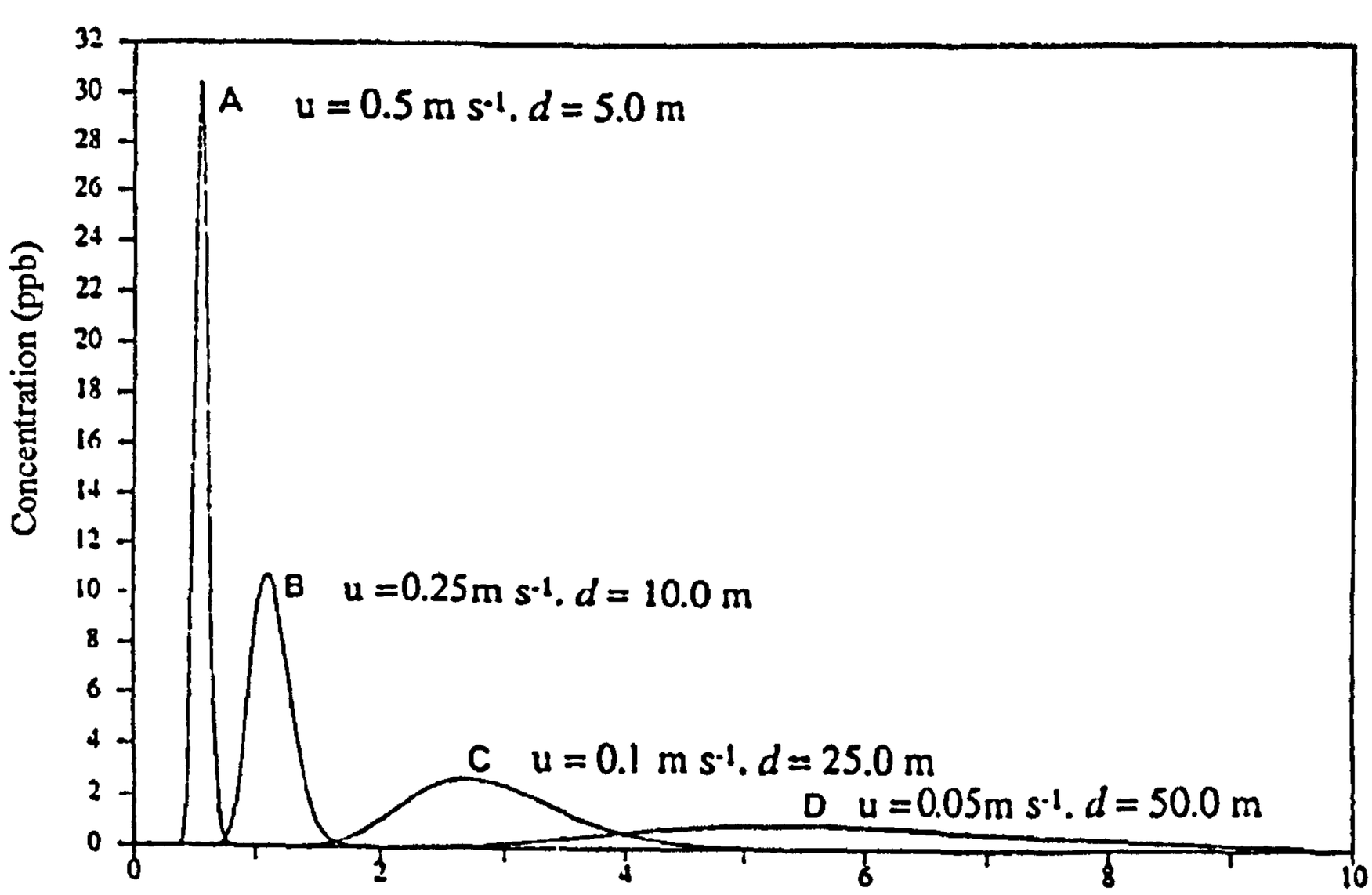

Figure 3.9: Hypothetical return curves resulting from flow through a 1 km drainage system with a constant injection mass and discharge. The dispersion coefficient (D) is constant at 2.5 m^2s^{-1}, but variations in throughflow velocities (v) give varying return curves that are revealed by altering values of dispersivity (d) (After Nienow, 1993).

Dispersivity

In a channel with an even roughness and constant hydraulic radius, dispersion coefficient (D) is approximately proportional to the flow velocity (v) (Taylor, 1954; Fischer, 1968; Behrens et al., 1975; Maloszewski, 1992). In many applications in glacier hydrology, the dispersivity (d) is therefore calculated after Brugman (1986) as

$$d = \frac{D}{v}. \tag{3.3}$$

The dispersivity or dispersion length describes the rate of dispersion of a tracer cloud relative to its rate of advection through the glacier (Seaberg et al., 1988; Hock and Hooke,

1993). Dispersivity illustrates the dependence of the longitudinal dispersion coefficient on the throughflow velocity (Käss, 1998), or the rate of dispersion of a dye cloud in relation to its rate of advection through a hydrological system (Fischer, 1968; Seaberg et al., 1988; Hubbard and Nienow, 1997). As a general indication, high dispersivities (d >10 m) suggest flow through hydraulically inefficient, distributed drainage systems (Seaberg et al., 1988), whereas low dispersivities (d < 10 m) curves reflect flow through hydraulically efficient, channelised drainage systems (Hubbard and Nienow, 1997). However, care is required in the interpretation of drainage system structure based on analyses of only one parameter such as d. High values of d may occur due to increasing flow divergence in the drainage pathway, increase in storage within the system and/or varying turbulence along the drainage pathway (Nienow, 1993). If turbulence along a channelised drainage path is responsible for increasing values of d, then flow velocities might remain consistently high despite large variations observed in d (Nienow, 1993). It is therefore essential to examine not only d, but also variations in v and D, to obtain a clear impression of the processes incident in the englacial and subglacial drainage systems (Hubbard and Nienow, 1997).

Tracer recovery rate

The tracer recovery rate (M), expresses the ratio of recovered to injected tracer mass

$$M = \int_{t_0}^{t_1} \frac{c(t)Q(t)}{m} dt \,. \qquad (3.4)$$

The recovery rate of perfect tracer experiments would be $M = 1$, but due to tracer loss within the glacier-hydrological systems this is rarely obtained. Tracer loss can be caused by tracer adsorption onto sediments (Bencala et al., 1983; Brugman, 1986), storage in isolated spaces (e.g. cavities) or tracer outflow at concentrations below detection limits (Theakstone and Knudsen, 1981; Willis et al., 1990). Further sources of errors in estimates of tracer recovery include uncertainties in the mass of tracer injected and/or errors in the discharge measurements, especially where a stable discharge station with a defined cross-section is not available. As a result, calculated recovery rates are often unreliable and care is required with interpretations derived from recovery rates. To optimise the quality of the parameter

estimation in this study, the actual recovered tracer mass was used instead of the injected tracer mass hence, to normalise tracer load (t_{norm})

$$t_{norm} = \frac{c(t)Q(t)}{\int_{t_0}^{t_1} c(t)Q(t)dt} \tag{3.5}$$

3.3 Gauging station monitoring

3.3.1 Introduction

The proglacial stream at Glacier de Tsanfleuron was the only subaerial outflow emerging from the subglacial drainage system (Figure 1.6). An unknown proportion of the meltwater from the glacier drains into the karst bedrock system. The characteristics of proglacial meltwaters including the discharge hydrograph can provide information about englacial and subglacial drainage mechanisms and the system efficiency. To this end, a gauging station was installed at the proglacial stream to record the water's level, temperature and electrical conductivity plus air temperature and precipitation.

At the start of the field season, on 25 June 2001, snow thickness in the proglacial area was between 1.5 m and 2.0 m. The proglacial stream and its surrounding area subsequently went through major changes during the first four weeks of the field season. The proglacial stream was covered with snow until mid July, and glacial runoff was draining through the snowpack within a saturated bottom layer. During times of maximum runoff, water would drain briefly over the surface of the snowpack within the main "drainage area". A pit was dug to observe variations of the water table in the saturated snow layer from 26 June to 20 July. After the snow in the proglacial area had melted, the gauging station was reinstalled for the rest of the field season (23 July to 05 September) in the proglacial stream. Suitable sites for installing the gauging station were limited, because the stream was braiding. The most suitable gauging site was located about 50 m from the glacier snout where a large boulder partially buried in an exposed moraine defined the stream channel on its northern bank. All water was here routed through a single channel before braiding again and draining into a small proglacial lake. At the outflow of the lake, the water percolated into proglacial sediments and reappeared at the surface after about 100 m Figure 3.10.

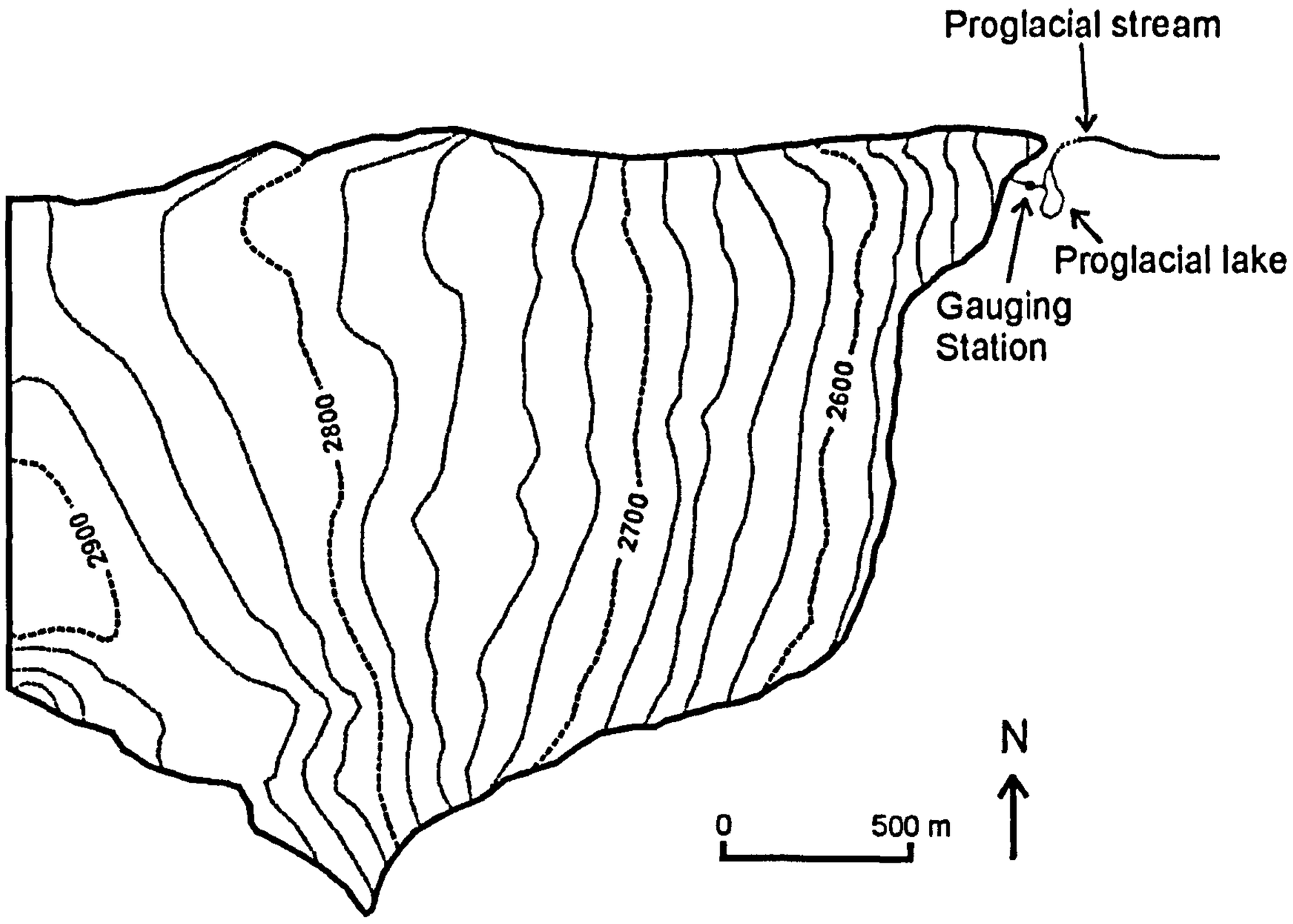

Figure 3.10: Glacier de Tsanfleuron with proglacial stream, proglacial lake and gauging station

At the gauging station a Dexion structure was mounted with the gauging instrumentation attached. The structure reached about 0.2 m into the flow (approximately 25 % of the channel width). Water level variations for bulk discharge calculations (Section 3.3.2) and water temperature (Section 3.3.3) were continuously monitored. Water level was measured with a Druck PD CR 830 pressure transducer every 10 seconds and average values were recorded at 15-minute intervals. The pressure transducer used for water level gauging was installed at about 0.05 m from the channel bed with the combined temperature/electrical conductivity probe at about 0.07 m. All instruments were connected to a Campbell Scientific CR 23X data logger. During times of low water discharge the instruments were not always completely submerged, thereby generating gaps in the data, especially at the end of the melt season. Air temperature and precipitation were recorded near the gauging station (Section 3.3.3).

3.3.2 Stream discharge

The discharge of the proglacial stream of Glacier de Tsanfleuron is mainly influenced by surface meltwaters generated from the glacier surface, rainfall on the glacier and rainfall and snow melt input from the un-glaciated part of the basin. The shape of the discharge hydrograph reflects characteristics of the glacier drainage system (Baker et al., 1982; Gurnell, 1993) and monitoring the outflow of water at the glacier snout is therefore of major importance for glacial-hydrological investigations (Meier and Tangborn, 1961; Mathews, 1963; Elliston, 1973). To estimate the proportion of meltwater draining into the karstic bedrock system beneath Glacier de Tsanfleuron, bulk discharge was also measured in conjunction with ablation rates. Furthermore, discharge values are required for the calculation of recovery rates from tracer experiments into moulins and crevasses.

Discharge measurements in proglacial streams with their turbulent and unstable character are often not easy to obtain. The most suitable method in such an environment is the tracer-dilution method (Käss, 1998; Grust, in press). The principle of the tracer dilution method as illustrated in Figure 3.11 involves the injection of a known quantity of tracer into the stream and the detection of the diluted concentration some distance downstream. The distance between injection and detection site must be long enough to ensure uniform mixing of the tracer over the entire cross-section. From the tracer dilution in the stream, the runoff (Q) can be calculated from

$$Q = \frac{m}{\int_{t_0}^{t_1} (c_1 - c_0)\,dt} \tag{3.6}$$

where Q [$m^3\ s^{-1}$] is the discharge, m [g] the mass of injected tracer, t_0 [s] the start of tracer return, t_1 [s] the end of the tracer return, c_0 [$\mu g\ l^{-1}$] the background concentration and c_1 [$\mu g\ l^{-1}$] the monitored tracer concentration. The requirements for reliable measurements are stationary discharge conditions and no water sources or sinks between injection and detection point.

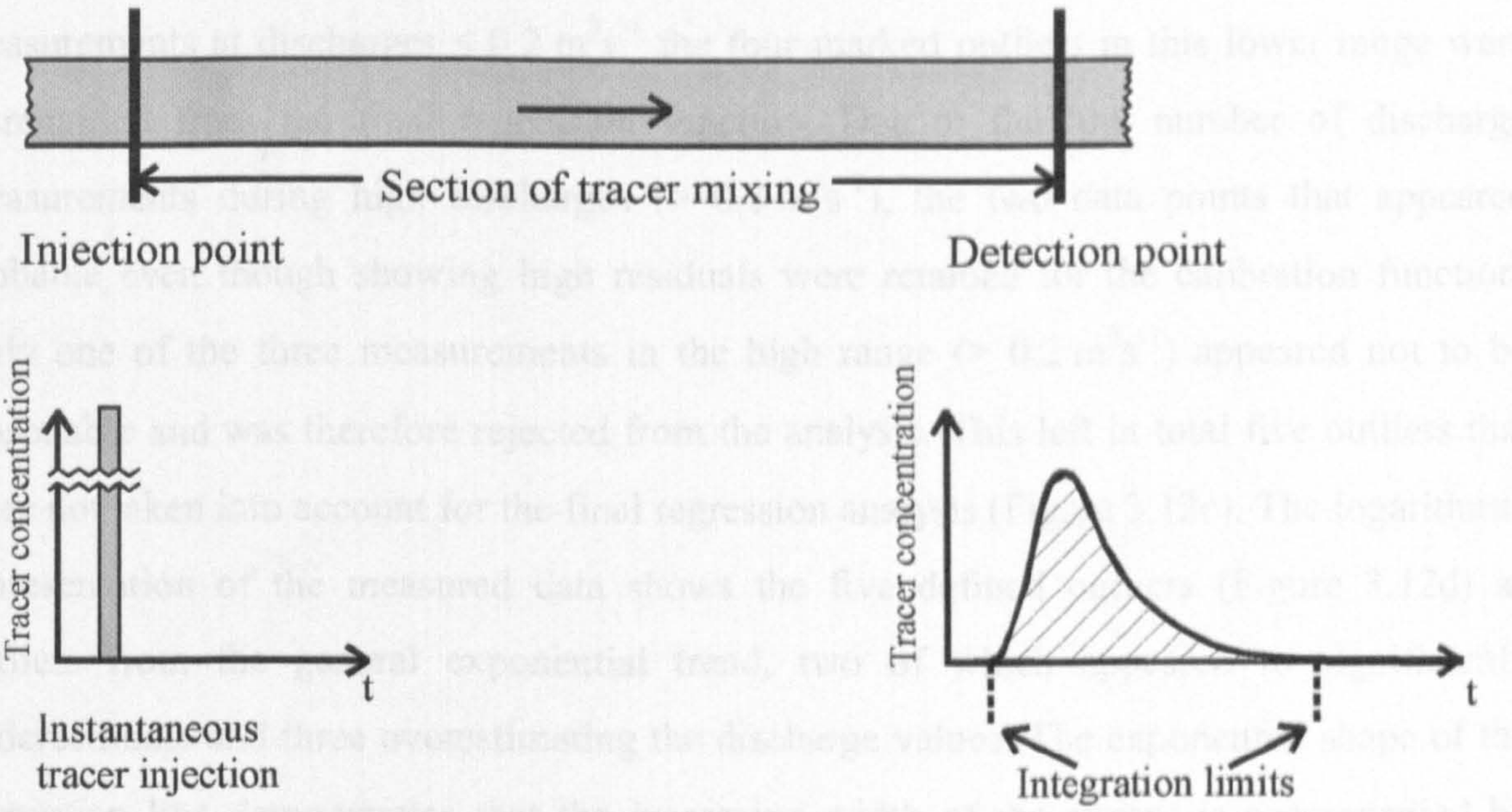

Figure 3.11 Principle of the tracer dilution method.

To relate water level to discharge during summer 2001, a total of 49 individual discharge measurements (tracer-dilution method) were undertaken throughout the season at a wide range of discharges (Figure 3.12). The distance between injection and detection point at Glacier de Tsanfleuron was about 50 m, which was sufficient to achieve complete mixing of the tracer. Rhodamine WT (20 % solution) was used and injected in volumes of between 0.1 and 0.8 ml depending on the water level during the measurement. The tracer concentration at the detection site in the proglacial stream was measured with a Turner 10-005 filter fluorometer at intervals of one second and average values were stored on a Campbell Scientific CR 23X data logger every minute. To ensure an accurate identification of the peak the data logger was programmed for 10 second averaging when the tracer concentration rose above the background concentration. Dye concentrations for each experiment were recorded until the background concentration was reached again. Background concentrations were defined as stable concentrations, measured before and after the passage of the tracer. The calibration function for transforming the recorded water levels into discharge values as presented in Figure 3.12c was obtained by fitting an exponential regression curve to 44 (out of 49) measured discharges and corresponding water levels. Five outliers were defined using the following procedure. The exponential function of all data points (Figure 3.12a) was used to calculate the absolute residuals of each measurement. Residuals of > 0.05 m were regarded as outliers and this applied to seven data points which are marked red in Figure 3.12b. Due to a high coverage of

measurements at discharges < 0.2 m^3s^{-1} the four marked outliers in this lower range were disregarded from the final regression function. Due to the low number of discharge measurements during high discharges (> 0.2 m^3s^{-1}), the two data points that appeared probable even though showing high residuals were retained for the calibration function. Only one of the three measurements in the high range (> 0.2 m^3s^{-1}) appeared not to be reasonable and was therefore rejected from the analysis. This left in total five outliers that were not taken into account for the final regression analysis (Figure 3.12c). The logarithmic representation of the measured data shows the five defined outliers (Figure 3.12d) as outliers from the general exponential trend, two of which appeared to significantly underestimate and three overestimating the discharge values. The exponential shape of the regression line demonstrates that the increasing width of the stream is accompanied by increasing water level. Due to a number of repeated calibration experiments during low discharges (< 0.2 m^3s^{-1}) errors in the proglacial discharge estimation are probably reasonably low (< 15 %). Errors of 15 % to 30 % are possible during higher discharges (> 0.2 m^3s^{-1}) due to the limited number and therefore poor reliability of the discharge calibration function in the upper area. For further applications of the discharge record, a mean estimated error of 23 % was used.

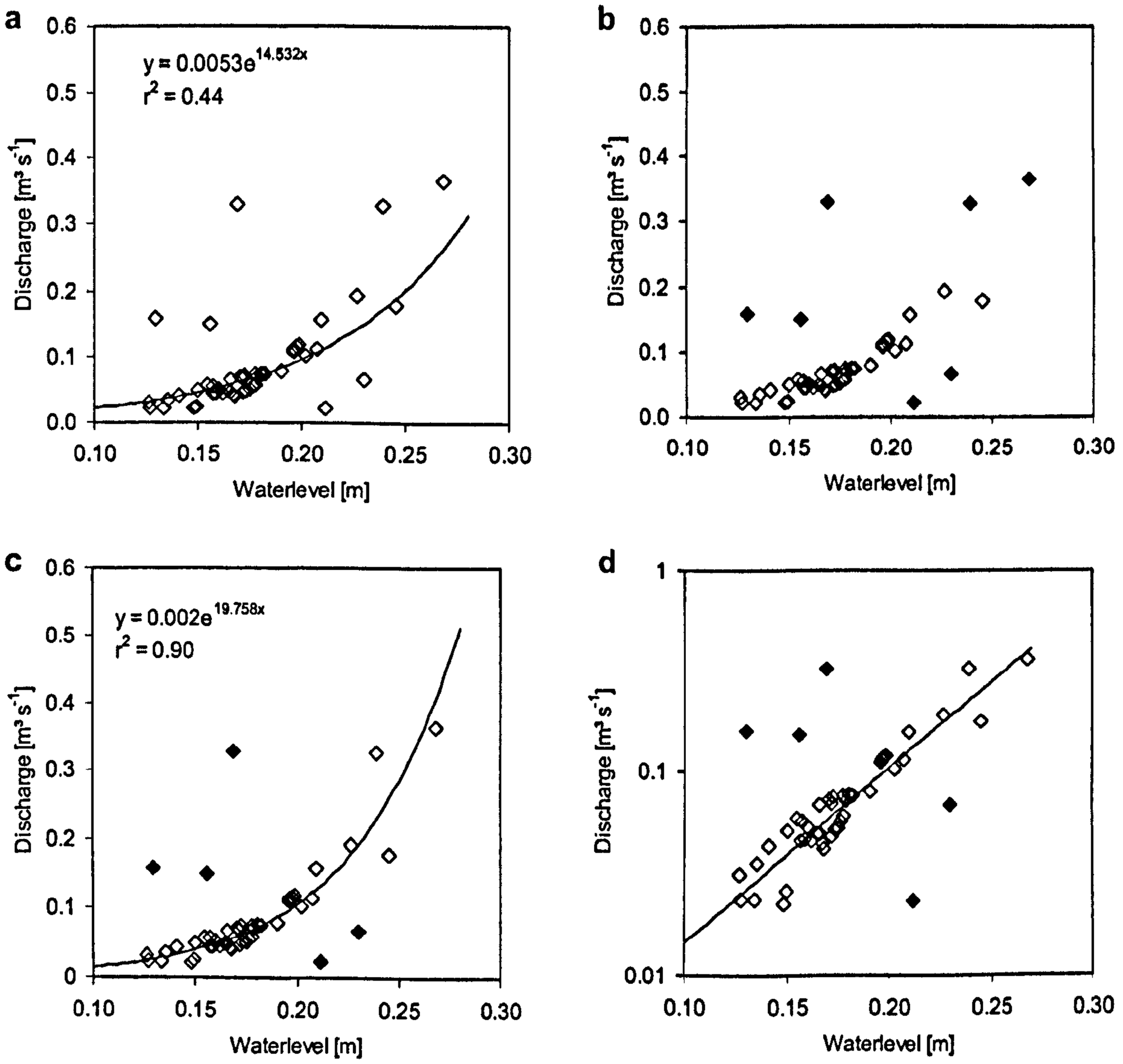

Figure 3.12: (a) Bulk discharge calibration measurements and their exponential relationship; (b) discharge calibration measurements. Residuals of data points > 0.5 are marked as filled symbols; (c) bulk discharge calibration curve for the proglacial stream of Glacier de Tsanfleuron during the summer season 2001. Outliers are marked as filled symbols and were no t taken into account for the calculation of the calibration function; (d) logarithmic presentation of discharge calibration measurements, outliers are marked as filled symbols.

A possible reason for outliers is the none-uniform mixing of tracer between injection and detection sites that may have occurred during times of slow or less turbulent flow conditions. The discharge would be underestimated if the tracer were detected in higher than average concentrations and overestimated if detected at lower than average concentrations. A further extension of the distance between injection and detection point was not possible due to site limitations. Errors are also introduced because the gauging station was installed in a stream with a sediment bed and therefore its cross section was variable.

A further weakness of the obtained calibration function results from the poor constraint of discharges larger than 0.36 m^3s^{-1}. Values higher than the measured maximum were therefore derived by extrapolation. Additionally, the correlation of higher discharge measurements is weak because only a few measurements were undertaken and these were all on the same day (26 July 2001) with a maximum discharge of about 0.36 m^3s^{-1}. Furthermore, the high correlation coefficient ignoring outliers ($r^2 = 0.89$) is reinforced by repeated experiments shortly after each other, disguising the fact that the streambed is continuously evolving, especially after high discharge events when changes of the channel geometry are expected. The established series of bulk discharge in the proglacial stream at Glacier de Tsanfleuron is valuable from the end of July until the start of September. The discharge curve obtained needs to be treated with caution and with the awareness of errors especially at higher discharges. However, they give a valuable indication of the variation and approximate magnitude of proglacial stream discharge.

3.3.3 Temperature and precipitation records

In order to understand and interpret hydrological behaviour of the glacier, meteorological data is required. Because longwave incoming radiation and sensible heat flux components are closely related to air temperature (e.g. Braithwaite and Olesen, 1987; Lang and Braun, 1990) the variations in meltwater production is largely explained by the variations of air temperature (Ohmura, 2001).

Observations were undertaken at Glacier de Tsanfleuron including temperature measurements and the observation of precipitation. Air temperature was measured at the gauging station about 50 m from the glacier snout at 15 minute-intervals throughout the field season. The temperature probe was placed within a shielded sensor and located on a pole about one meter above the ground.

Rain influences the hydrology of the glacier due to the relatively warm water input altering the temperature flux. Runoff is the sum of ablation and precipitation in the catchment area minus evaporation. Whilst our precipitation measurements at a single point give only a rough measure of precipitation in the catchment, it gives useful information for the interpretation of the hydrological conditions at the glacier.

Precipitation was monitored at base camp and the glacier snout using basic rain gauges with funnel diameters of 20 cm and 13 cm respectively. The rain gauge was placed on the ground. Regular readings were carried out in the morning and sometimes during an event if more frequent measurements were necessary to prevent the container from overflowing. Precipitation fell as snow during the summer season on 16 July, 20 July and 11 August. Snow fell on 1 September and during the first week of September, leading to snow accumulation of about 50 cm in the proglacial area, indicating the end of the summer melt season.

3.4 Glacier dynamics

A survey programme was undertaken at Glacier de Tsanfleuron in order to monitor diurnal and intra-seasonal variations of the surface motion and to identify flow characteristics related to the glacier's hydrology. It has been observed at different glaciers that increasing rates of supraglacial meltwater penetration to the subglacial drainage systems was followed by an increase in subglacial water pressures that enhanced basal motion (Iken et al., 1983; Willis, 1995; Nienow et al., 1998). Therefore, the research at Glacier de Tsanfleuron was undertaken to investigate coupling between meltwater drainage through the glacial drainage systems and glacier motion. A network of twenty-six velocity stakes was distributed across the glacier surface at the start of the field season (Figure 3.13). The position of each stake was measured repeatedly from a stable survey station situated on bedrock. Surface ice-velocities at Glacier de Tsanfleuron prior to the field season of 2001 were unknown. The set-up of the stake network, the procedure of the survey and the focus of the analyses are outlined below.

3.4.1 Stake network

All survey stakes were 2 m long with sections of red and white colouring altering every 50 cm. Most stakes were aluminium with a few of wood with a plastic cover. A pink painted wooden target board with a centrally fixed reflecting prism was mounted at the top of each stake. This was used to locate the position of the stake by reflecting the infrared signal of the surveying instrument back to the surveying station; all reflectors were oriented towards the surveying station. The stakes were individually drilled vertically into the glacier surface to a depth of about 1.7 m and in staggered rows. The centre stakes in the

longitudinal profile are numbered 10, 20, 30 etc. to 80. These stakes are about 200 m apart from each other and counted up-glacier (from west to east). Intermediate stakes are numbered with 15, 25, 35 etc. according to their location. Stakes in the transverse profiles (if applicable) are additionally labelled with N_1 on the north side of the centre line and S_1, S_2, S_3 on the south side (Figure 3.13). Initially, due to the thick snowpack on the glacier, all stakes were drilled into snow. Later, near the end of the field season the stakes in the lower ablation area were drilled into the ice. The network did not cover the entire glacier. There were no stakes at altitudes below 2580 m due to the slope angle in that area they would not have been observable from the surveying station. There were no stakes in the southern part of the glacier, because of a ski lift running for parts of the season and therefore there was a risk that skiers could damage or manipulate the stakes.

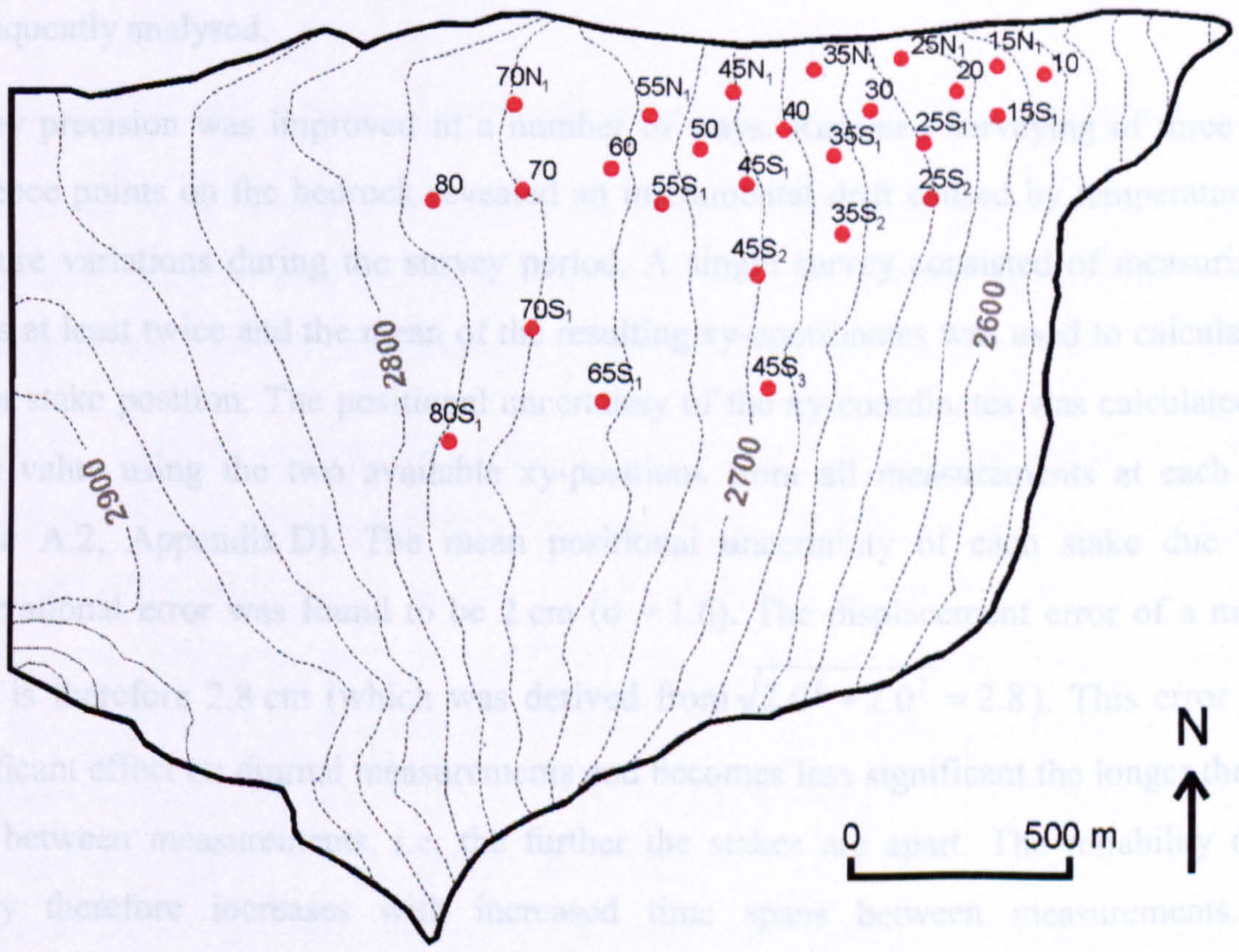

Figure 3.13: The stake network across Glacier de Tsanfleuron.

3.4.2 Surveying procedure

The survey of the stake network was undertaken with a Geodimeter System 400 (Total Station). The instrument combines the functions of a theodolite and an electronic distance meter, thus measuring horizontal and vertical angles as well as the straight-line distance of a target point relative to the position of the survey station. In this study the relative position in three-dimensions of each stake was regularly determined throughout the season and from

this the ice surface movement was quantitatively determined. All stakes but one (Stake $80S_1$, 1100 m) were within the optimal one kilometre range of the Geodimeter. The stability of the Geodimeter was maintained by surveying from a permanently established tripod set-up on bedrock. However, during a stormy day and night on 6/7 July the tripod was displaced by wind, producing a data gap.

3.4.3 Survey analysis and analytical precision

Trigonometric calculations of the straight-line distance and angles enabled the position of each stake to be determined relative to the survey station. Horizontal velocities and vertical displacements of each stake between two surveys were thus calculated using basic trigonometry and variations of the glacier motion both temporally and spatially were subsequently analysed.

Survey precision was improved in a number of ways. Repeated surveying of three fixed reference points on the bedrock revealed an instrumental drift caused by temperature and pressure variations during the survey period. A single survey consisted of measuring all stakes at least twice and the mean of the resulting xy-coordinates was used to calculate the planar stake position. The positional uncertainty of the xy-coordinates was calculated as a mean value using the two available xy-positions from all measurements at each stake (Table A.2, Appendix D). The mean positional uncertainty of each stake due to an observational error was found to be 2 cm ($\sigma = 1.6$). The displacement error of a moving stake is therefore 2.8 cm (which was derived from $\sqrt{2.0^2 + 2.0^2} = 2.8$). This error has a significant effect on diurnal measurements and becomes less significant the longer the time span between measurements, i.e. the further the stakes are apart. The reliability of the survey therefore increases with increased time spans between measurements. The significance of this error on horizontal surface velocities over different time scales (diurnal, weekly and seasonal) has to be considered for the interpretation of the data. The size of the possible error related to the measuring period is presented in Figure 3.14.

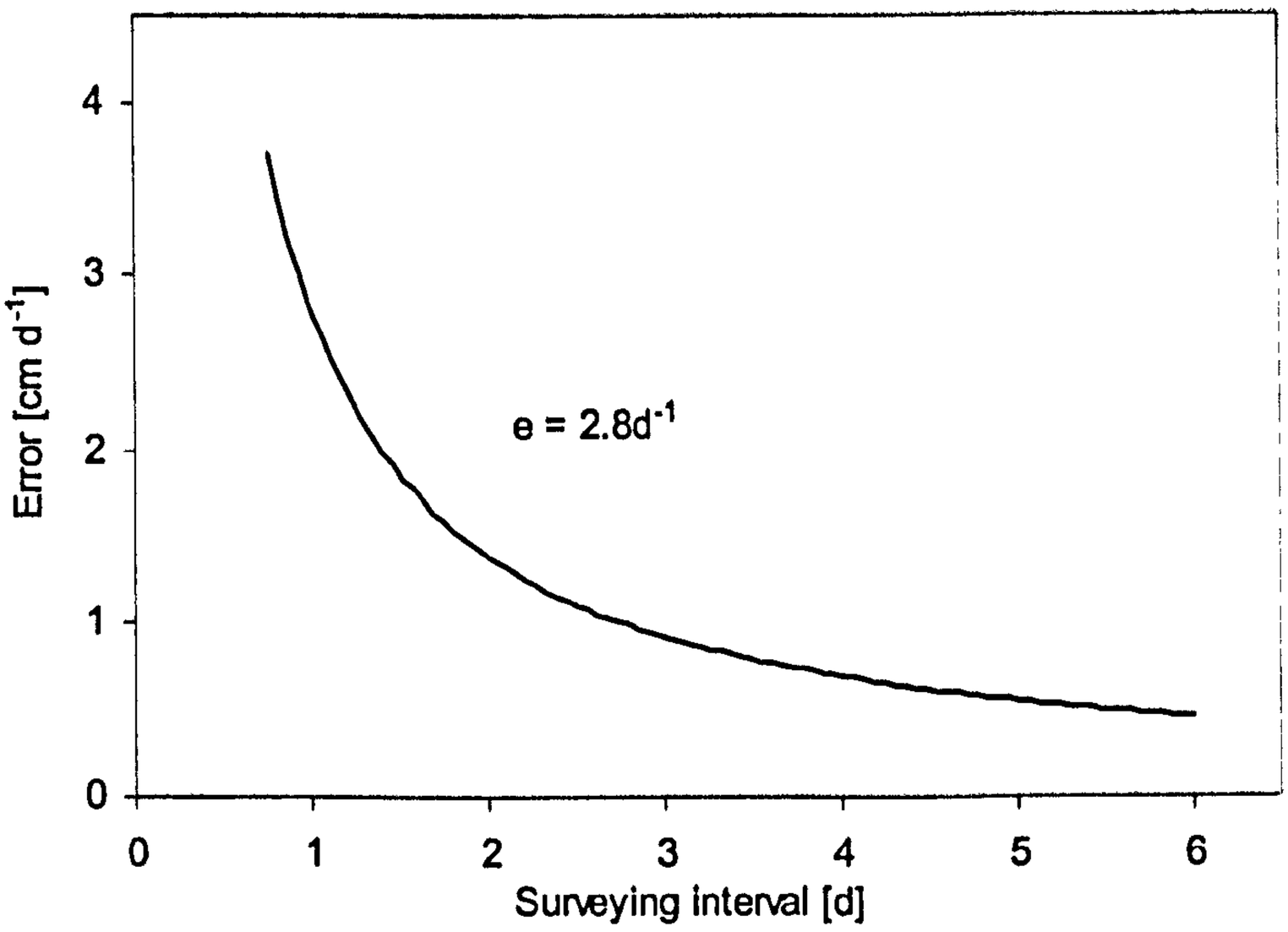

Figure 3.14: Correlation between surveying interval and error in stake velocities.

Instrumental errors derived from the survey station itself were neglected since they are significantly smaller than the measurement error and therefore inconsequential. The systematic error of the horizontal displacement was between 0.1 and 0.4 cm ($\sigma = 0.5$).

During the ablation season, the stakes started to melt out of the snow/ice and were therefore redrilled at regular intervals. The position of the stake was surveyed immediately before and after redrilling to achieve a continuous data record. For most of the season surveys were undertaken every two or three days, weather permitting. This is an adequate interval to successfully elucidate intra-seasonal variations linked to glacio-hydrological conditions as shown by other workers (Iken, 1981; Bindschadler, 1983; Iken et al., 1983; Iken and Bindschalder, 1986; Jansson, 1995; Hanson et al., 1998). Consistently throughout the season, most measurements were undertaken in the afternoon and in the same order, thus improving the temporal consistency of the data.

The full survey of all stakes (the network of stakes measured twice with reference points) typically took between one and two hours and provided surface motion data across the glacier that were used for the analysis of temporal and spatial variations of the glacier surface motion.

3.5 Ablation measurements

Ablation at the glacier surface is a critical component of glacier hydrology since in temperate glaciers this melting generates the majority of water within the glacier hydrological system. Rates of melting vary throughout the day, depending on the energy balance at the surface (Section 2.2). Generally melt rates decrease with increasing altitude. Furthermore, melt rates of ice are higher than for snow under similar conditions due to the higher albedo of snow surfaces (Röthlisberger and Lang, 1987).

In order to estimate actual melt-rates, the density of the surface snow layer is required (Appendix B). Snow density measurements were undertaken frequently at different altitudes and different times of the season.

Rates of lowering of the snow or ice surface due to melting were calculated from ablation measurements during the entire field season at 26 stakes positioned across the glacier. These stakes were the same as those used for the investigation of the surface dynamics of the glacier and their positions are shown in Figure 3.13 and the stakes were located in both ablation and accumulation zones. Measurements were taken from the top of each of the 2 m long stakes to the snow or ice surface (accuracy of 0.5 cm) at the down-glacier side of the ablation stake. If the glacier surface topography was uneven a meter stick was used to "integrate" the glacier surface. Surface depositions often occur around stakes due to increased melt rates in the immediate neighbourhood of the stake. The repeated measurement of the thinning snowpack or lowering ice surface during the melt season enables calculation of local melt rates. The initial thickness of the snowpack was determined using an avalanche probe. Ablation rates at each stake were typically measured every day or every second day.

Ablation measurements were analysed in order to determine the contribution of the lower glacier tongue to the overall melt-generation from the glacier. By doing so, it was hoped to define the area of the glacier that contributes to runoff at the glacier snout as opposed to meltwater that is routed through the karst bedrock system.

3.6 Water level measurements at the snow-ice interface

The thickness of the saturated layer at the snow-ice interface has been suggested to be proportional to the runoff from the snowpack (Colbeck, 1974). This implies that there is a

higher water delivery to the englacial and subglacial drainage systems during periods of high water levels at the snow-ice interface. In order to obtain information about variations of the water table in the snowpack and thus supraglacial melt-water storage and runoff, a pressure transducer was set-up at the snow-ice interface near Stake 20 at about 2620 m a.m.s.l. (This is the same location as snowpack tracer experiment, Section 3.2.3). Data was recorded for approximately three weeks from 29 July to 18 August continuously measuring water pressures at 10-second intervals and averaging the records every 15 minutes that were later transformed into a water level stage record due to pressure and water depth being directly proportional.

The water level measurement at the snow-ice interface may not be accurate because the pressure transducer was placed in the saturated snow rather than in free water. This probably affected the response of the instrument that was only calibrated in free water.

4 Snowpack hydrology

4.1 Introduction

The manner by which snowpack hydrology controls meltwater delivery to the englacial drainage system is, at present inadequately understood. Investigations of water flow through the snowpack require the application of indirect methods. Dye tracing and measurements of the water table in the snowpack are adequate techniques. Tracer return curves generated from the passage of tracer through the snowpack can characterise percolation mechanisms, their local and temporal variations as well as storage effects.

Specific aims of the research therefore are:

i) To develop a dye tracer technique as a quantitative method to investigate the evolution of snowpack hydrology using an *in situ* borehole fluorometer;

ii) To determine rates of water flow through a thinning snowpack;

iii) To investigate water flow rates/conditions at the snow-ice interface.

iv) To determine how flow through snowpack varies temporally as the melt season develops.

v) To investigate the ablation of the glacier surface and to determine the area from which meltwater is drained to the glacier snout by comparing it with the bulk discharge in the proglacial stream

An 'idealised' evolution of snowpack hydrology is discussed in Section 4.3. Since the snow conditions on glaciers vary from year to year, the snowcover and melt conditions at Glacier de Tsanfleuron during the melt season 2001 are described in Section 4.4. The analyses of ablation measurements are described in Section 4.5. Dye tracer experiments undertaken at the snow surface and at the snow-ice interface are discussed in Section 4.6. In Section 4.7 the record of water level variations at the snow-ice interface is presented. Data from the field season and theoretical considerations are compared and improvements of the tracer methods are discussed in Section 4.8. Conclusions from the research are summarised in Section 4.9.

4.2 Significance of glacial snowpack hydrology research

Most water that drains through glaciers is meltwater that is produced at the glacier surface at rates of between 0.1 and 10.0 m a^{-1} compared to the basal melt rate of only about 0.01 m a^{-1} (Röthlisberger and Lang, 1987). These figures demonstrate the relative importance and high variability of surface melt generation. The supraglacial snowpack is, especially at the start of the melt season, a major source of meltwater production. Snowpack buffers meltwater delivery to moulins and crevasses due to temporary storage, this significantly impacts on hydrological processes within the englacial and subglacial drainage systems (Nienow et al., 1998). Due to the coupling between subglacial hydrology and glacier movement (Section 2.5.3) the supraglacial snowpack indirectly influences glacier dynamics.

Water storage in snowpack plays an important role for the water balance of temperate glaciers (Röthlisberger and Lang, 1987) and refreezing of stored water within the snowpack is a significant factor influencing mass balance. This is because melt from the snow surface can be retained in the snowpack at the end of the hydrological year (Pfeffer et al., 1991). Refreezing of percolating meltwater requires low temperatures within the snowpack and the rate of percolation will impact on the proportion of melt that can runoff before refreezing takes place. The impact of supraglacial hydrological processes on mass balance is therefore a result of internal accumulation and infiltration into the remaining snow and firn layer and refreezing during cold periods (Pfeffer et al., 1991; Schneider, 2001).

4.3 Theoretical considerations

In this chapter, a basic model of meltwater residence time in the snowpack is formulated. It is based on theoretical considerations influencing the behaviour of the hydrological parameters within the snowpack and the snow-ice interface from the start of melt until complete removal of the snowpack (Figure 4.1). Snowpack melt is driven by a number of variable parameters and the air temperature represents a indicator for the development of summer melt (Braithwaite and Olesen, 1987).

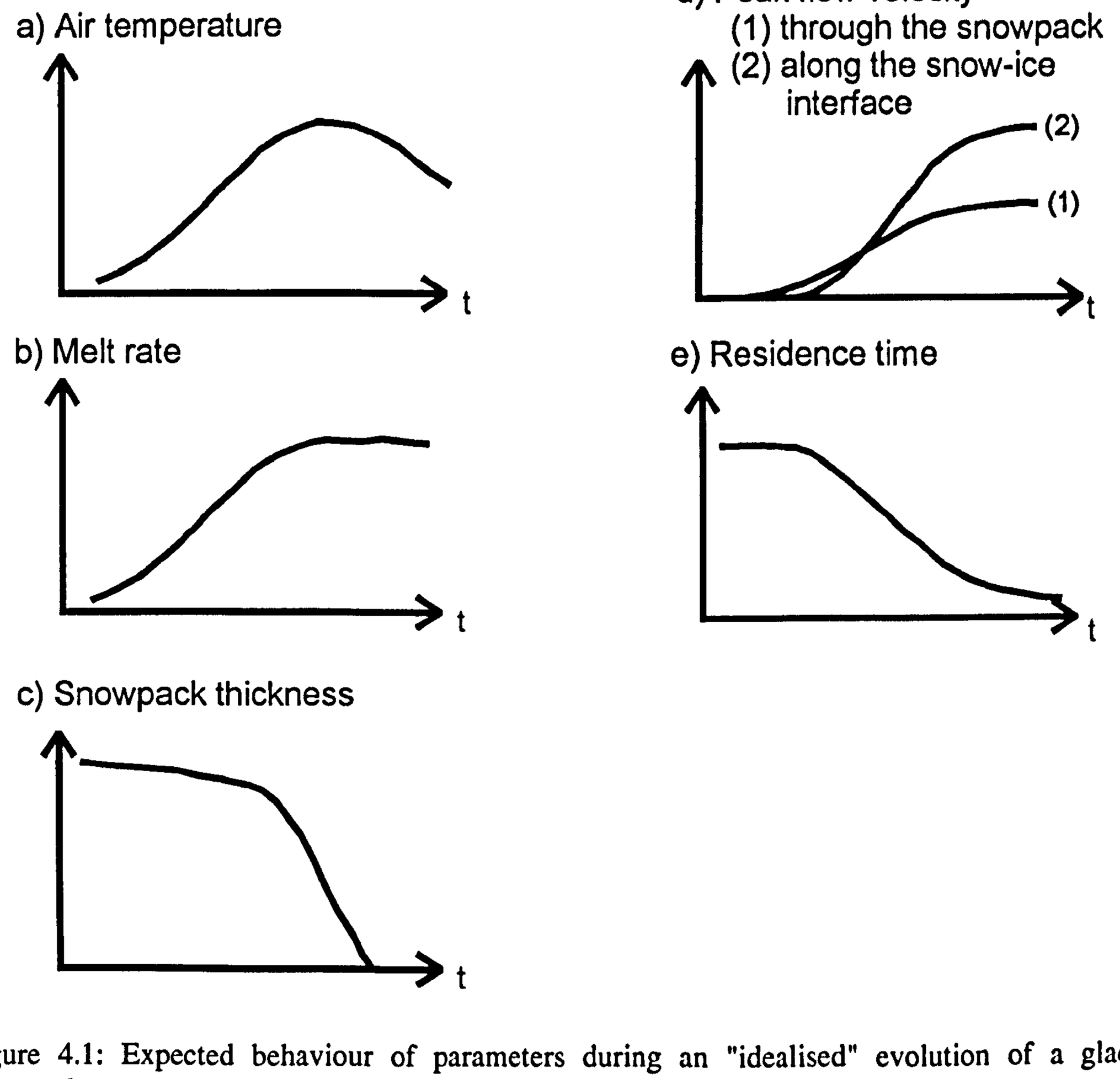

Figure 4.1: Expected behaviour of parameters during an "idealised" evolution of a glacial snowpack.

According to the climate diagrams from meteorological stations nearby, Montana (46.32°N, 7.40 °E at 1508 m) and Sion (46.22°N, 7.30 °E at 482 m) (Climate in Switzerland, 2004) the air temperature is expected to show an approximately sinusoidal variation over the melt season (Figure 4.1a).

The melt rate (Figure 4.1b) of the snowpack is expected to increase approximately sinusoidally, mainly influenced by factors such as increasing air temperature, solar radiation and decreasing albedo. The low albedo at the late season complicates, to some extent, the effect of the temperature decrease as the season progresses, which explains the flattening of the melt rate curve towards the end of the season. However, this pattern can be disturbed if a summer snowfall event occurs. The snowpack thins parallel to the melt rate, slowly at the start of the melt season in response to the air temperature increase. As air temperature and melt rates increase a rapid thinning of the snowpack is expected until midsummer. Due to stable melt rates after midsummer, the snowpack thickness should

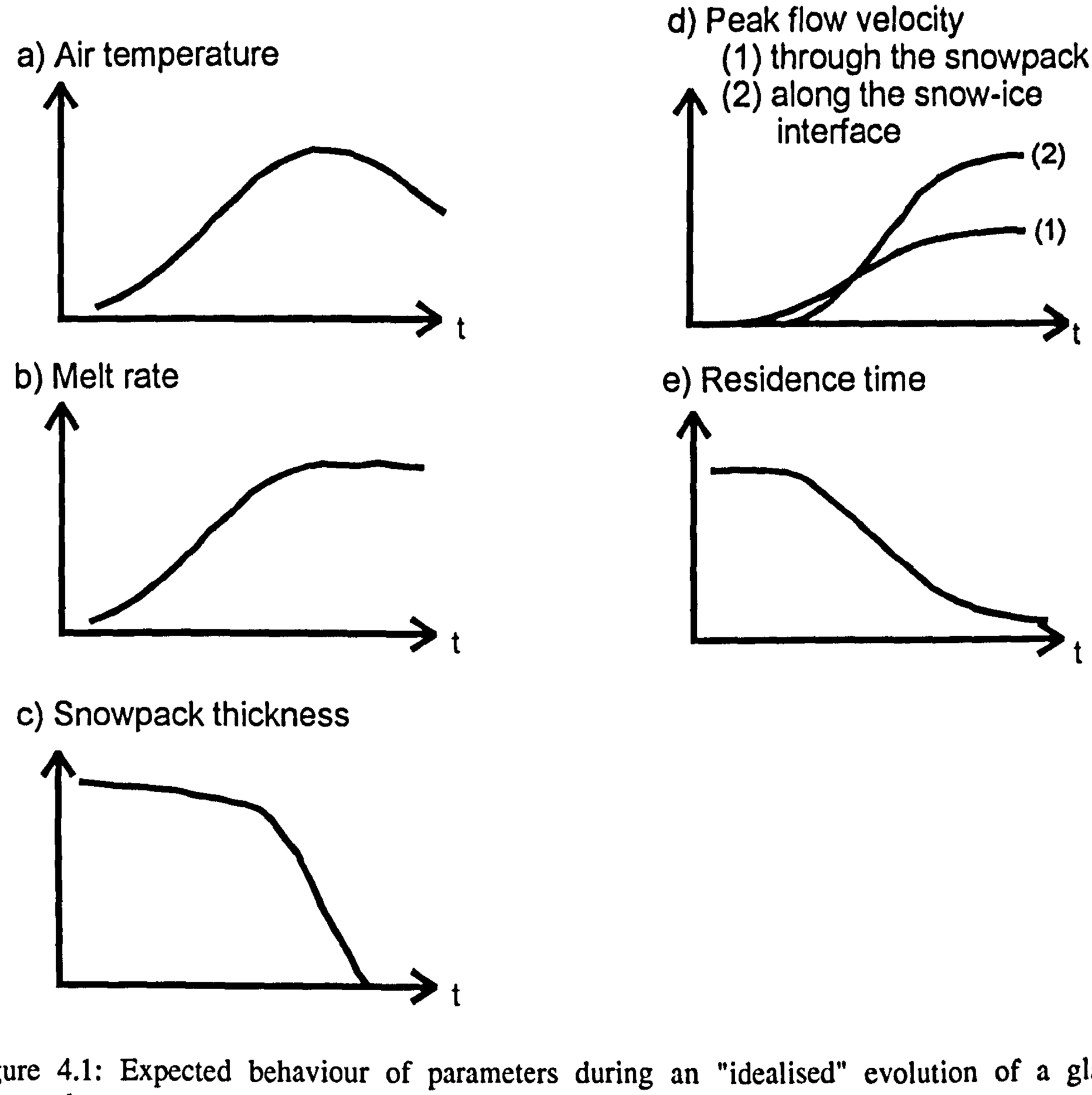

Figure 4.1: Expected behaviour of parameters during an "idealised" evolution of a glacial snowpack.

According to the climate diagrams from meteorological stations nearby, Montana (46.32°N, 7.40 °E at 1508 m) and Sion (46.22°N, 7.30 °E at 482 m) (Climate in Switzerland, 2004) the air temperature is expected to show an approximately sinusoidal variation over the melt season (Figure 4.1a).

The melt rate (Figure 4.1b) of the snowpack is expected to increase approximately sinusoidally, mainly influenced by factors such as increasing air temperature, solar radiation and decreasing albedo. The low albedo at the late season complicates, to some extent, the effect of the temperature decrease as the season progresses, which explains the flattening of the melt rate curve towards the end of the season. However, this pattern can be disturbed if a summer snowfall event occurs. The snowpack thins parallel to the melt rate, slowly at the start of the melt season in response to the air temperature increase. As air temperature and melt rates increase a rapid thinning of the snowpack is expected until midsummer. Due to stable melt rates after midsummer, the snowpack thickness should

decrease linearly (Figure 4.1c). The wetting of the snowpack plays an important role for the percolation of water through snow. As outlined in the literature review (Section 2.3.2) some time is required for the wetting of the snowpack until saturation of capillary water surrounding snow grains is reached. The development of flow fingers at the start of the melt period leads to meltwater transfer to the snow-ice interface and meltwater delivery to the englacial and subglacial drainage systems (Wakahama, 1968; Marsh and Woo, 1984a; Albert and Perron, 2000). Mean flow velocities in both the snowpack and at the snow-ice interface are expected to increase parallel with the melt rate, but with some time lag due to the buffering effect of the snowpack (Figure 4.1d). However, due to water saturation and larger snow grain sizes (and therefore increasing water permeability) flow velocities along the snow-ice interface are expected to be higher than flow through the unsaturated upper snow layers. According to an increase in flow velocity, meltwater residence times (Figure 4.1e) decrease exponentially (inverse to flow velocity). A thick, inhomogeneous snowpack at the start of the melt season has a higher storage capacity than a more mature thin snowpack at the end of the season. This is, apart from the actual thickness, a consequence of the increased grain size lowering the capillary pressure of mature snowpacks, therefore holding less water than small-grained snowpacks. Hence, as the snowpack thins, ice layers and lens density decrease, thereby allowing increased water flow.

The characteristics of the development of these theoretical parameters affecting snowpack hydrology, during a summer melt season, must be considered as conditions that would appear in an average or typical year. Variations are likely to occur in exceptional years, and since these parameters are co-dependent, different patterns of hydrological development can occur.

4.4 Snowcover and melt conditions at Glacier de Tsanfleuron in summer 2001

4.4.1 General conditions

As outlined in Section 1.3.1.3, the onset of the melt season in 2001 was characterised by unexpectedly large amounts of deposited winter snow. This winter snow and three snowfall events in July and August resulted in snow coverage of more than 70 % of the glacier surface throughout the entire melt season and that the snow line was not rising above 2650 m a.m.s.l.. This shows a lower end-of-summer snowline for summer 2001 than it was

reported by Sharp et al. (1989) of about 2700 m a.m.s.l, although the general trend during the last decade has probably been increased due to further recession. The position of the transient snowline was determined from ablation measurements throughout the season from a network of stakes across the glacier (Section 3.5), the snowcover depth and snowline retreat is shown in Figure 4.2. The snow depths across the glacier (Figure 4.2) are obtained by interpolation of measured snow depth at individual data points (stakes) and the boundaries of the glacier.

reported by Sharp et al. (1989) of about 2700 m a.m.s.l, although the general trend during the last decade has probably been increased due to further recession. The position of the transient snowline was determined from ablation measurements throughout the season from a network of stakes across the glacier (Section 3.5), the snowcover depth and snowline retreat is shown in Figure 4.2. The snow depths across the glacier (Figure 4.2) are obtained by interpolation of measured snow depth at individual data points (stakes) and the boundaries of the glacier.

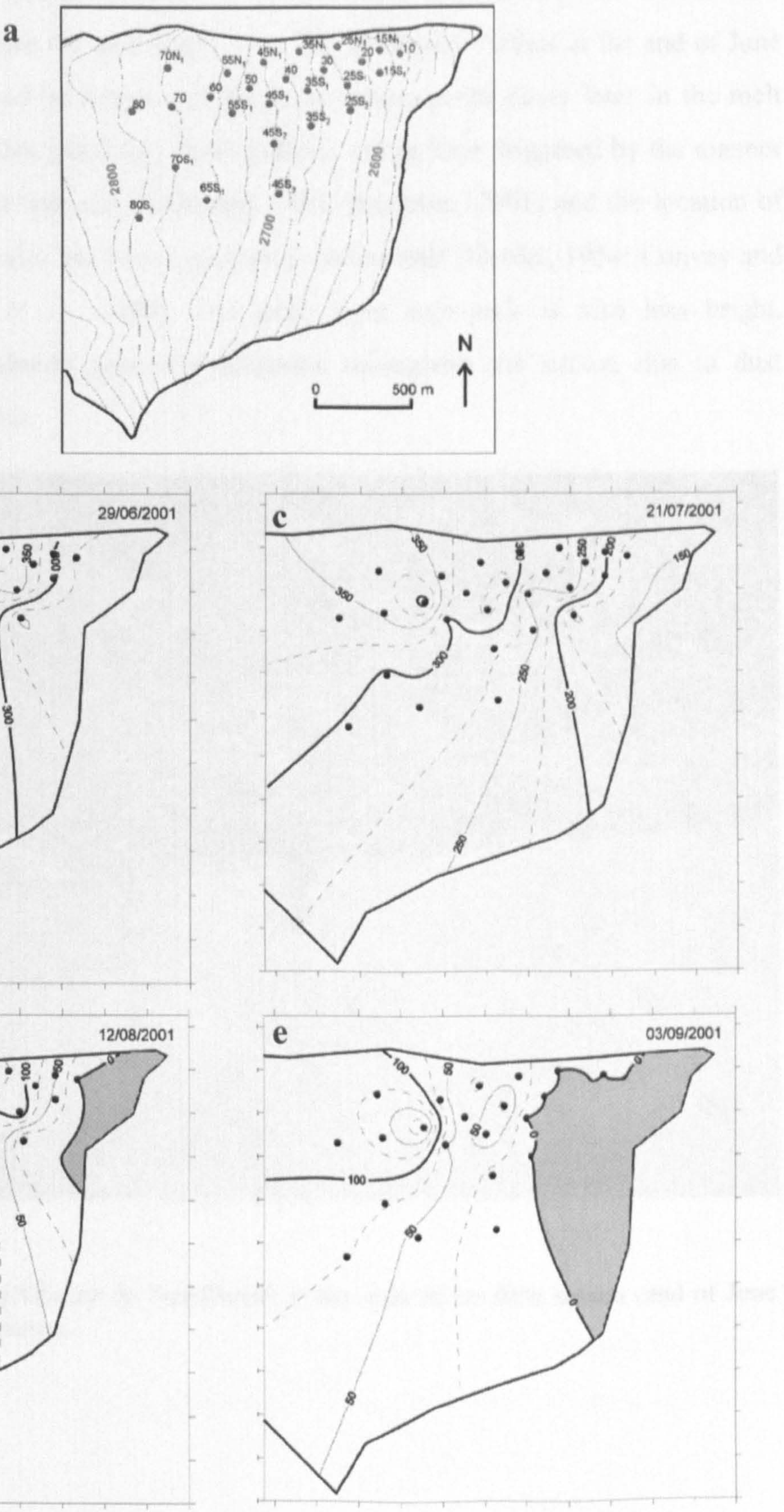

Figure 4.2: Spatial distribution of the snowcover on Glacier de Tsanfleuron during the summer season 2001 in [cm], 0 = transient snow line. (a) showing the location of the measuring points from which the spatial snow depth distribution was extrapolated, (b) snowd epth at end of June, (c) mid July, (d) mid August and (e) start of September. Grey areas are snow -free.

Changes of the snow surface are apparent if pictures from the start and end of the field season are compared (Figure 4.3 and Figure 4.4). The snowpack surface at the end of June is smoother than at the end of August (small surface depressions occur later in the melt season in apparently random patterns). These patterns are perhaps triggered by the manner in which the snow surface had settled (Jordan, 1981; Betterton, 2001) and the location of flow fingers where meltwater has been percolating downwards (Gerdel, 1954; Convey and Benedict, 1994; Albert et al., 1999). The later, riper snowpack is also less bright, demonstrating that the albedo generally decreases throughout the season due to dust accumulating on the surface.

Figure 4.3: Snow surface of Glacier de Tsanfleuron at the start of the field season (end of June 2001) (photograph by P. Nienow).

Figure 4.4: Snow surface of Glacier de Tsanfleuron at the end of the field season (end of August 2001).

To obtain a visual impression of tracer passageways through snowpack vertical profiles were cut through the snow one to three hours after the injection Figure 4.5 shows an example of a section about one and two hours after injection. The pattern of infiltration and the effects of stratigraphy become visible, as dye accumulates on the upper surface of the ice lenses. Flow through the snowpack occurs obviously in an inhomogeneous manner. Previous dye tracer tests support this finding of meltwater percolation occurring in a highly irregular manner (Male, 1980; Kattelmann and Dozier, 1999). The appearance of a more intense colour of dye demonstrates the accumulation of water at ice layers but colouring beneath ice layers gives evidence that water flow is not completely blocked by these ice layers. After flowing along thin layers of ice, water eventually penetrates through or passes by them. Ice lenses would therefore appear to play an essential role for routing meltwater through the snowpack.

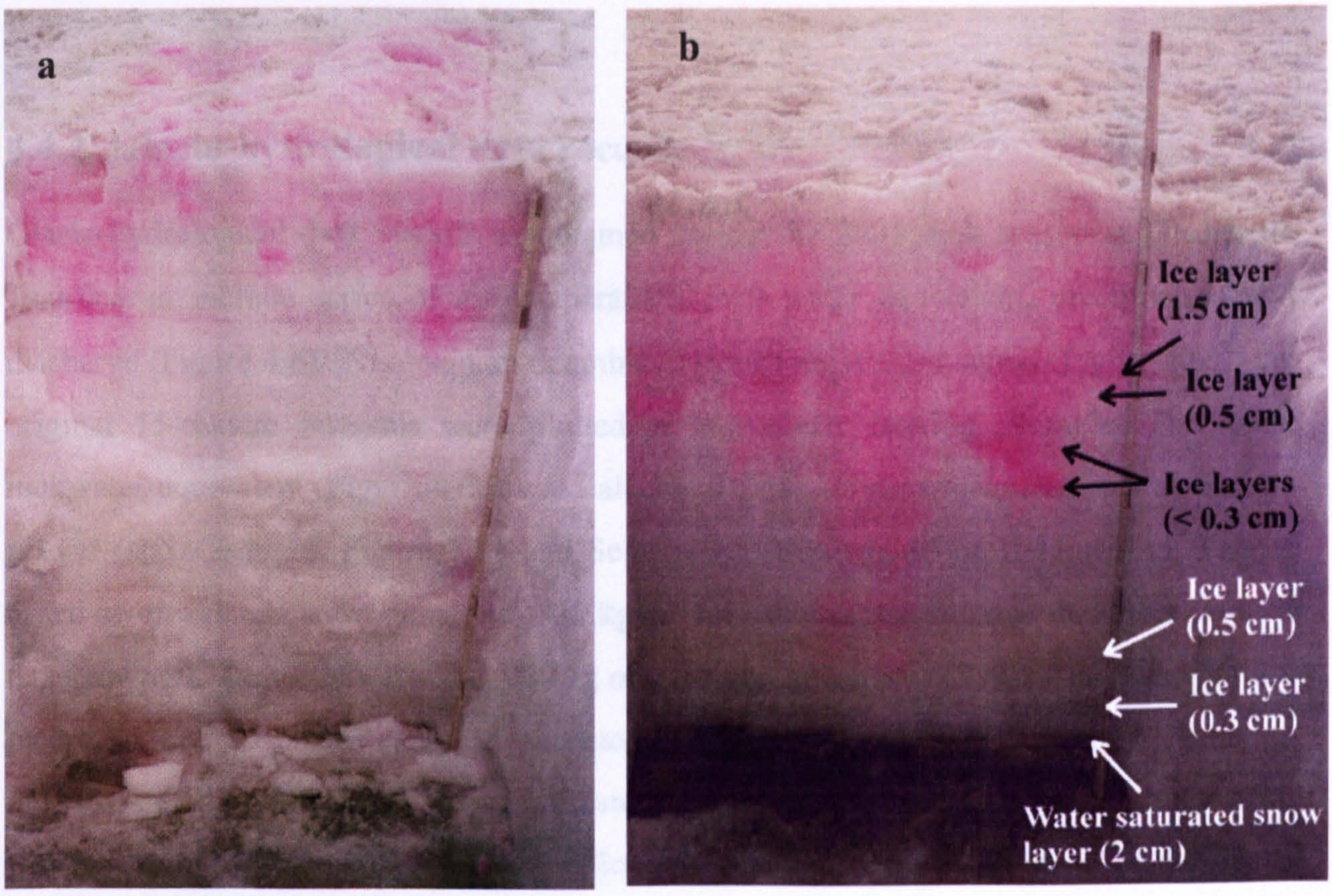

Figure 4.5: Pit section (a) about one hour and (b) about two hours after rhodamine WT surface injection. Dye penetrates inhomogeneously and accumulates at ice layers but is not completely blocked by these layers (photographs by F. Campbell). Stratigraphy notes are presented in Table 4.1.

Table 4.1: Stratigraphy of the snowpack from top to bottom as shown in Figure 4.5. N.B. Coarse snow is defined as grain size > 0.2 mm.

Snow depth [cm]	Stratigraphy notes
109	Snow surface
84 - 104	Coarse snow (grain size 0.3 - 0.5 cm)
83	Thick ice layer (1.5 cm)
78	Ice layer (0.5 cm)
68 - 78	Coarse snow (grain size ~ 0.3 cm)
68	Ice layer (< 0.3 cm)
65	Ice layer (< 0.3 cm)
26 - 65	Ice layer (0.5 cm)
26	Coarse snow
11 - 26	Ice layer (0.3 cm)
11	Coarse snow (grain size 0.2 - 0.3 cm)
2 - 11	Water saturated snow layer
0 - 2	Coarse snow with ice lenses

4.4.2 Glacio-hydrological data records

Glacio-hydrological data records as obtained during the 2001 melt season at Glacier de Tsanfleuron include series of air temperature, melt water equivalent, precipitation and discharge (Figure 4.6). To obtain an unambiguous air temperature signal (Figure 4.6a), the original 15-minute intervals were plotted as two-hourly moving averages. The mean meltwater equivalent (Figure 4.6b) was calculated from ablation measurements across the glacier (stake network Figure 3.14 and Section 3.5) throughout the field season. This is based on an average snow density of 530 kg m^{-3} for snow as measured at the upper layer of the snowpack (Appendix B) and 900 kg m^{-3} for ice (Paterson 1994). The precipitation record, monitored at base camp, is presented in Figure 4.6c, intra-seasonal snow events on 16 July, 20 July and 11 August are indicated. The amount of precipitation from snowfall was estimated from the depth of newly fallen snow at camp and an average snow density of 150 kg m^{-3} for damp new snow (Paterson 1994). Furthermore, a discharge record, monitored at the glacier snout is presented in Figure 4.6d. Glacial runoff, is characterised by variability both on a seasonal and diurnal timescale. Seasonal variability is a response to air temperatures and solar radiation variations, but is also influenced by the evolution of the supraglacial, englacial and subglacial drainage systems and their water storage capacities. During the 2001 field season, discharge was highest at the end of July (Figure 4.6d). The highest discharges were estimated as up to 0.6 m^3s^{-1}, but due to uncertainty in the discharge calibration function for upper discharge values, an error of 15 to 30 % may be possible (Section 3.3.2). Highest discharges at the end of July and at the start of August were caused by high melt water input from extraglacial snowmelt within the catchment area and not just from the glacier surface melt. Later in the season the discharge was much lower due to the zero snowmelt input from the extraglacial catchment. Typical diurnal variations with high amplitudes were observed at Glacier de Tsanfleuron throughout the season.

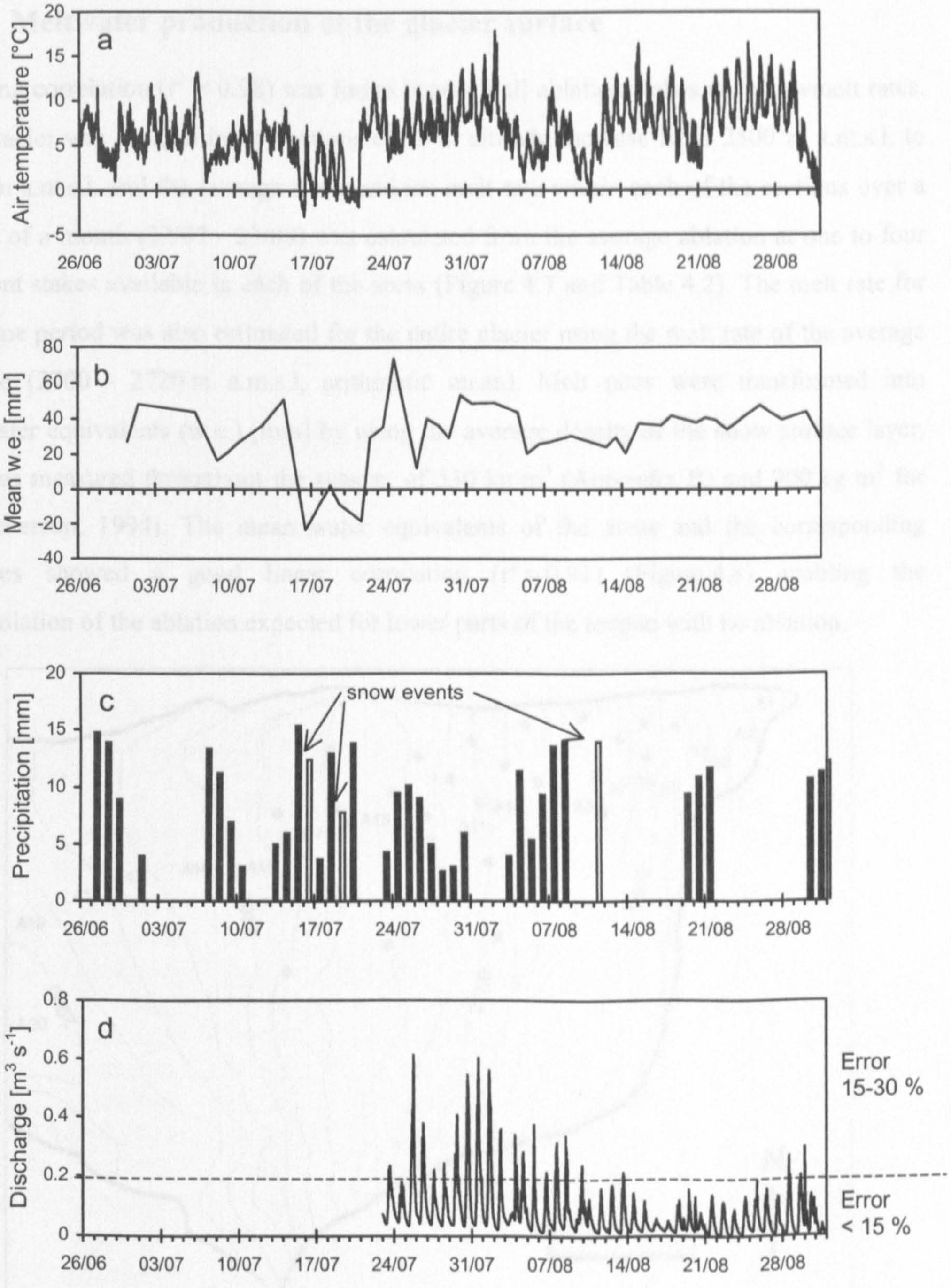

Figure 4.6: (a) Air temperature at the glacier snout (b) Mean melt water equivalent (c) precipitation at the glacier snout [mm]; snow fall events on 16/07, 20/07 and 11/08 are labelled as unfilled columns (d) bulk discharge at the proglacial stream during the 2001 melt season at Glacier de Tsanfleuron. The estimated error for lower discharges ($< 0.2\ ms^{-1}$) is < 15 %, for higher discharges ($> 0.2\ ms^{-1}$) 15 -30 %.

4.5 Analyses of ablation measurements

4.5.1 Meltwater production at the glacier surface

A strong correlation ($r^2 = 0.98$) was found between all ablation stakes and snowmelt rates. The glacier was divided in 16 sections of 20 m altitude increase from 2500 m a.m.s.l. to 2780 m a.m.s.l. and the average snow and ice melt rate within each of the sections over a period of a month (22/07 - 23/08) was calculated from the average ablation at one to four different stakes available in each of the areas (Figure 4.7 and Table 4.2). The melt rate for the same period was also estimated for the entire glacier using the melt rate of the average altitude (2700 - 2720 m a.m.s.l, arithmetic mean). Melt rates were transformed into meltwater equivalents (w.e.) [mm] by using the average density of the snow surface layer, that was measured throughout the season, of 530 kg m^3 (Appendix B) and 900 kg m^3 for ice (Paterson, 1994). The mean water equivalents of the areas and the corresponding altitudes showed a good linear correlation ($r^2 = 0.91$) (Figure 4.8) enabling the extrapolation of the ablation expected for lower parts of the tongue with no ablation.

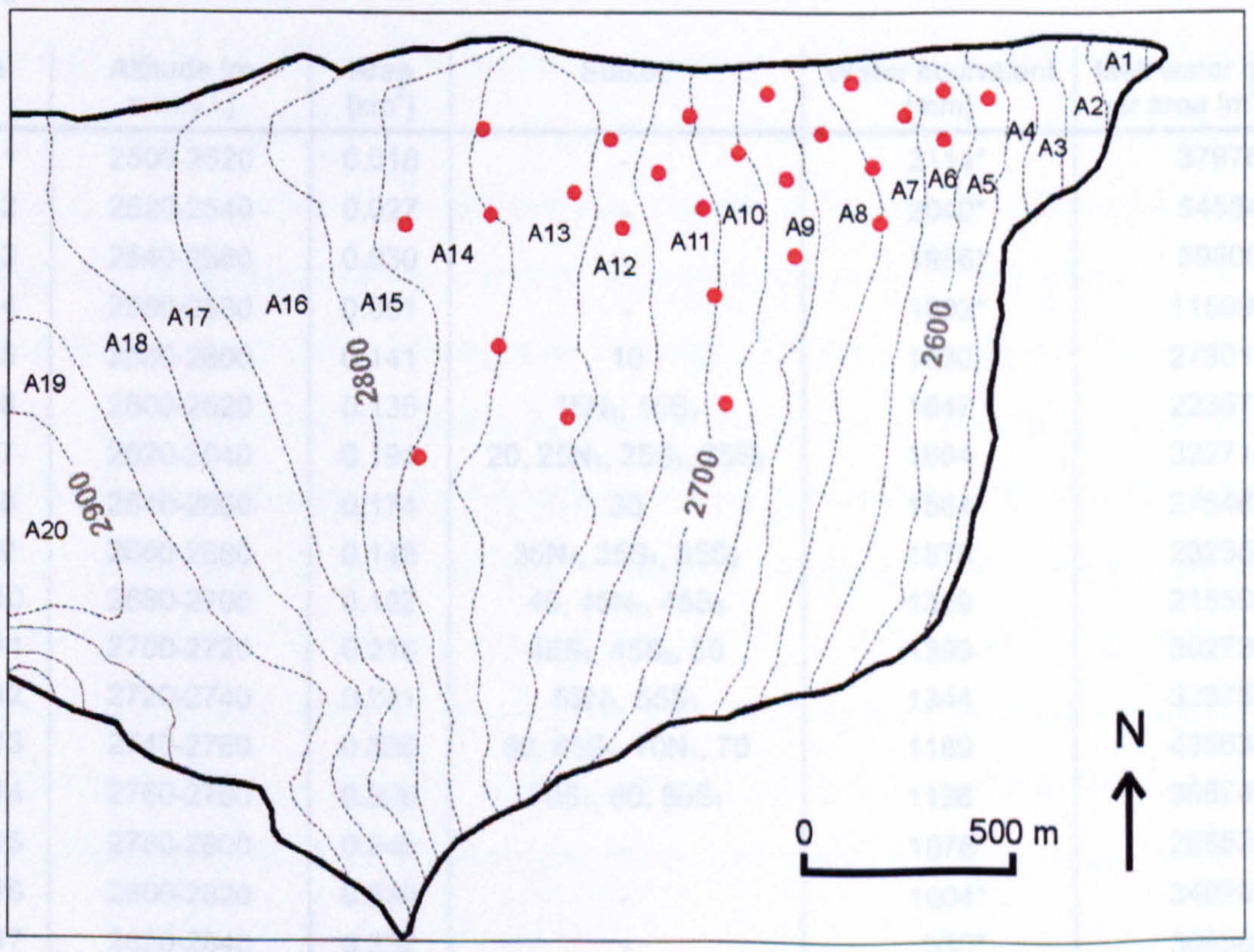

Figure 4.7: Map of Glacier de Tsanfleuron showing the division of the glacier surface area into areas according to 20 m altitude intervals.

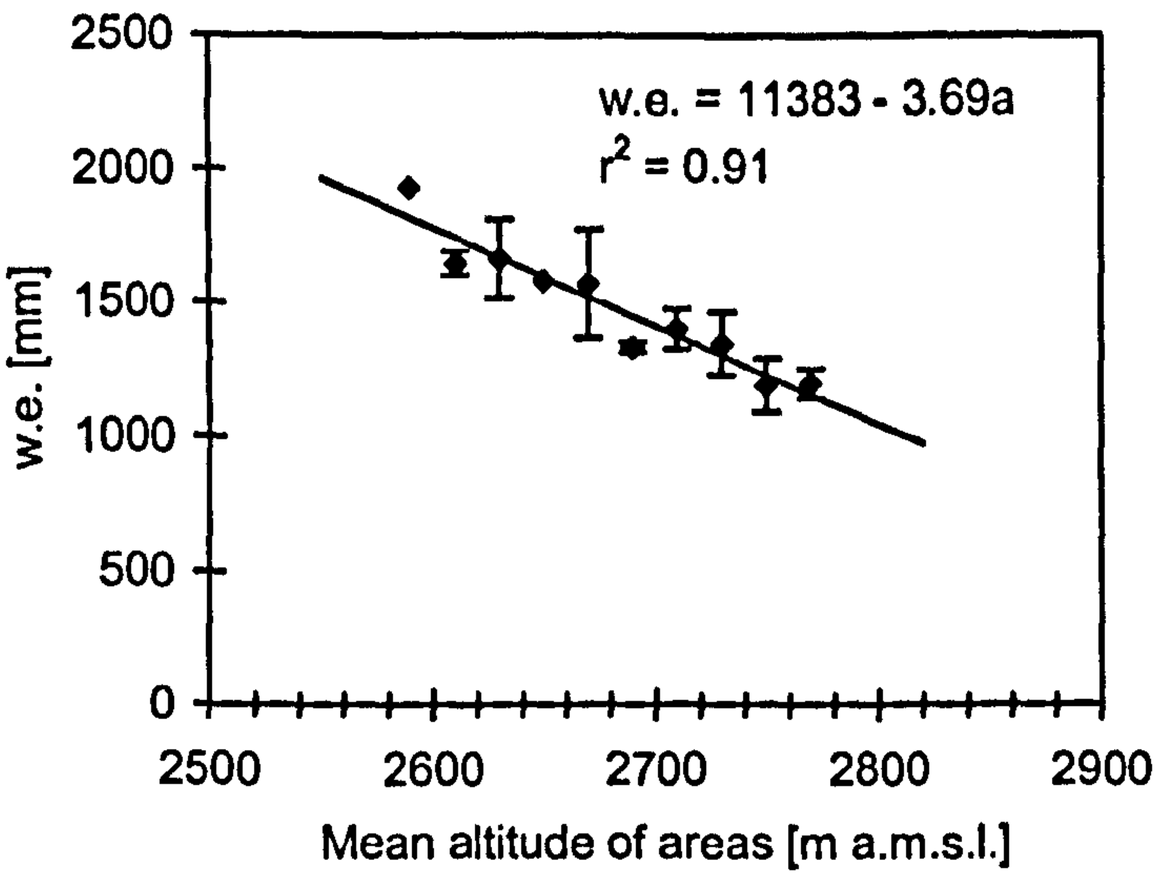

Figure 4.8: Linear correlation between the average water equivalent (w.e.) of differing areas and the mean altitude of the areas (Table 4.2). The error calculation is based on the standard deviation of two to four ablation stakes within each area. The average error was 90. 1 mm or 7 %. Areas 5 (2580-2600 m.a.s.l) and 8 (2640-2660 m.a.s.l) do not show error bars, because only one ablation stake was available.

Table 4.2: Meltwater production from 22 July to 23 August for different altitude levels and the whole glacier.

Area	Altitude [m a.m.s.l.]	Area [km^2]	Stakes	Water equivalent [mm]	Melt water quantity per area [m^3] ± 7%
Area 1	2500-2520	0.018	-	2114*	37976
Area 2	2520-2540	0.027	-	2040*	54554
Area 3	2540-2560	0.030	-	1966*	59800
Area 4	2560-2580	0.061	-	1892*	115099
Area 5	2580-2600	0.141	10	1930	273018
Area 6	2600-2620	0.136	$15N_1$, $15S_1$	1647	223571
Area 7	2620-2640	0.194	20, $25N_1$, $25S_1$, $25S_2$	1664	322714
Area 8	2640-2660	0.174	30	1584	276481
Area 9	2660-2680	0.148	$35N_1$, $35S_1$, $35S_2$	1570	232356
Area 10	2680-2700	0.162	40, $45N_1$, $45S_3$	1329	215590
Area 11	2700-2720	0.216	$45S_1$, $45S_2$, 50	1399	302739
Area 12	2720-2740	0.241	$55N_1$, $55S_1$	1344	323752
Area 13	2740-2760	0.366	60, $65S_1$, $70N_1$, 70	1189	435638
Area 14	2760-2780	0.306	$70S_1$, 80, $80S_1$	1196	366240
Area 15	2780-2800	0.249	-	1078*	268524
Area 16	2800-2820	0.339	-	1004*	340297
Area 17	2820-2840	0.332	-	930*	308580
Area 18	2840-2860	0.252	-	856*	215868
Area 19	2840-2880	0.358	-	782*	280254
Area 20	2880-2900	0.072	-	708*	51328
Whole glacier	2500-2920 (mean = 2710)	3.823		1399	4704378

* extrapolated values (error± 7 %)

4.5.2 Response of bulk discharge to ablation

The accumulative discharge total volume measured at the gauging station during the period from 22 July (17:00) to 23 August (17:00) was about 2.8 x 10^5 m^3. The average discharge error is about 23 % (Section 3.3.2). If the discharge measurements were overestimated or underestimated by about 23 %, the total accumulative discharge during the period 22 July to 23 August would be 2.2 x 10^5 m^3 or 3.4 x 10^5 m^3, respectively. For comparison, the quantity of meltwater that was generated during this period from each area was calculated from the area sizes and the measured melt water equivalent (Section 4.5.1). From this, the meltwater generated at the entire glacier surface was calculated to be approximately 4.7 x 10^6 m^3 ± 7 % (Table 4.2).

From the estimated discharge quantity at the glacier snout (2.8 x 10^5 m^3 ± 23 %), and the snowmelt rate at the glacier surface (47.0 x 10^5 m^3 ± 7 %), it is clear that only a small proportion of the meltwater generated at the glacier surface is drained at the snout. Meltwater therefore must enter the karst system beneath the glacier in significant quantities. The configuration of this system, especially the number and size of sinkholes beneath Glacier de Tsanfleuron is unknown. However a large karst sinkhole was observed in the proglacial catchment area (Figure 4.9). This sinkhole with subglacial and supraglacial water input at the south-western margin of the glacier indicated a division of the subglacial drainage between northern and southern parts of the glacier. Due to the inaccessibility of englacial and subglacial drainage systems it is impossible to define the area of the glacier surface that drains into the snout precisely. Therefore, the most likely division between the drainage of the southern and northern parts of the glacier surface was considered from the observed sinkholes, surface topography and valley shape. The estimated watershed (Figure 4.9) defines the glacial catchment area that drains at the glacier snout. This area was used to calculate snow surface melt rates for the northern part of the glacier. Melt rates obtained from this area are probably closer to the true melt rate that contributed to the bulk discharge at the snout than using the entire surface area.

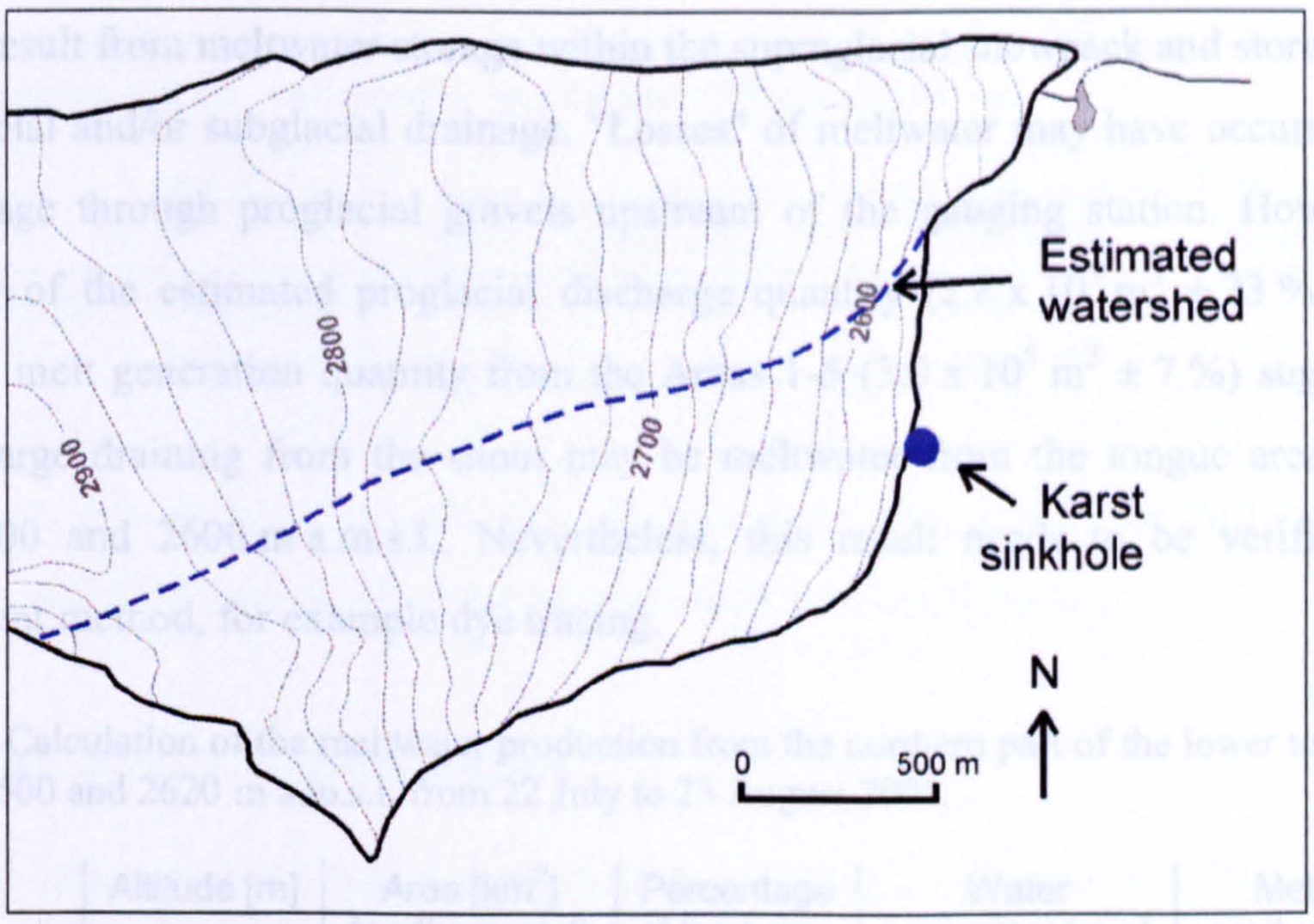

Figure 4.9: Map of Glacier de Tsanfleuron showing the location of the sinkhole at the southwestern glacier margin and the estimated watershed of the proglacial catchment area.

4.5.3 Definition of proglacial stream catchment area

From the above, it is likely that surface snow and ice melt water from only the northern part of the glacier contributed to bulk discharge at the snout. In order to estimate the surface area from which meltwater runs off at the glacier snout, the melt water generation was calculated.

The total melt water quantity from the northern part of the lower tongue area up to 2580 m a.m.s.l. (Areas 1-4) between 22 July and 23 August was approximately 2.1×10^5 m^3 ± 7 % (Table 4.3). During the same time, the meltwater production between 2500 m a.m.s.l. and 2600 m a.m.s.l. (Areas 1-5) was approximately 3.0×10^5 m^3 ± 7 % (Table 4.3) and between 2500 m a.m.s.l. and 2620 m a.m.s.l. (Areas 1-6) approximately 4.1×10^5 m^3 ± 7 % (Table 4.3). As described above, the total accumulative discharge from the glacier snout during this time period (considering an error of the bulk discharge of 23 %) was approximately 2.8×10^5 m^3 ± 23 %. Note that the calculated meltwater quantity generated at the glacier surface is surface meltwater only, whereas the discharge data also includes rainwater. The snowmelt contribution from the non-glacierized parts of the catchment was considered to be small since the glacier adjoins to the north with a steep rock flank where hardly any snow deposits remained. Discrepancies between estimates of surface meltwater and bulk proglacial discharge can be due to measurement errors as suggested above and

can also result from meltwater storage within the supraglacial snowpack and storage during the englacial and/or subglacial drainage. "Losses" of meltwater may have occurred due to the drainage through proglacial gravels upstream of the gauging station. However, the proximity of the estimated proglacial discharge quantity (2.8×10^5 m^3 ± 23 %) and the estimated melt generation quantity from the Areas 1-5 (3.0×10^5 m^3 ± 7 %) suggests that the discharge draining from the snout may be meltwater from the tongue area between about 2500 and 2600 m a.m.s.l.. Nevertheless, this result needs to be verified by an independent method, for example dye tracing.

Table 4.3: Calculation of the meltwater production from the northern part of the lower tongue area between 2500 and 2620 m a.m.s.l. from 22 July to 23 August 2001.

Area	Altitude [m]	Area [km^2] (northern part)	Percentage of total area	Water equivalent [mm]	Melt water production from area [m^3] ± 7 %
Area 1	2500-2520	0.018	0.5	2115*	0.38×10^5
Area 2	2520-2540	0.027	0.7	2041*	0.55×10^5
Area 3	2540-2560	0.030	0.8	1967*	0.60×10^5
Area 4	2560-2580	0.029	0.8	1893*	0.54×10^5
Area 5	2580-2600	0.050	1.3	1930	0.97×10^5
Area 6	2600-2620	0.063	1.7	1647	1.04×10^5
Areas 1-4	2500-2580	0.104	2.8	2004* (mean)	$\Sigma = 2.1 \times 10^5$
Areas 1-5	2500-2600	0.154	4.1	1989* (mean)	$\Sigma = 3.0 \times 10^5$
Areas 1-6	2500-2620	0.217	5.7	1932* (mean)	$\Sigma = 4.1 \times 10^5$
Whole glacier	2500-2920	3.8	100	1238*	47.0×10^5

* extrapolated values (± 7 %)

Furthermore, the proportion of the surface area of the whole glacier that drains at the snout was calculated using the results presented in Table 4.3. The area of the whole glacier is about 3.8 km^2, the area between 2500 and 2600 m a.m.s.l. is about 0.15 km^2. If meltwater from the tongue area between 2500 and 2600 m a.m.s.l. is drained to the glacier snout, this suggests that the meltwater of the proglacial stream is derived from an area covering only about 4 % of the total surface area (Table 4.4). The considered volume of meltwater produced at the surface of the whole glacier between 22 July and 23 August is about 47.0×10^5 m^3 ± 7 %, whereas the meltwater quantity produced between 2500 and 2600 m a.m.s.l. is 3.0×10^5 m^3 ± 7 % m^3. Thus, only about 6 % (Table 4.4) of the total melt water produced at the glacier surface runs off at the glacier snout and about 94 % of meltwater would appear to run off into the karst system or is lost elsewhere.

Table 4.4: Comparison between meltwater generation during the period of 22 July to 23 August for the whole glacier and the lower tongue area between 2500 and 2600 m.

Area	Altitude [m]	Area [km^2]	Proportion of total area [%]	Melt water volume [m^3] ± 7%	Proportion of total melt [%]
Whole glacier	2500-2920	3.8	100	47.0×10^5	100
Areas 1-5	2500-2600	0.154	4	3.0×10^5	6

In this study, 6 % of the total melt seems to have come from 4 % of the total glacier area. This is a reasonable finding due to higher melt rates at lower altitudes.

4.6 Dye tracer experiments

A general description of tracer methodology is given in Section 3.2. The dye tracer experiments undertaken at Glacier de Tsanfleuron to investigate snowpack hydrology included injections from the snow surface and at the snow-ice interface near Stake 20. Recovery rates cannot be calculated for those experiments, because the rate of water flow is unknown. The air temperature at the altitude of Stake 20, about 150 m above the snout, is expected to be about 0.7° to 1.0° colder assuming a typical temperature lapse-rate of 0.5° to 0.8° per 100 m of altitude increase (Weischet, 1991). Furthermore, a data record of water level measurements at the snow-ice interface near Stake 20 is available for the period during the dye tracer experiments.

4.6.1.1 Dye tracer experiments on the snow surface

As described in Section 3.2.3, dye was injected across a $1m^2$ area on the snow surface (Table 4.5). For quantitative observations, the return curve of the injected tracer was measured at the snow-ice interface a few meters down-glacier. Three experiments from snow surface injections are available between 27 July and 17 August.

Table 4.5: Injections undertaken at the snowpack surface.

Date	Mean snow density [kg m^{-3}]	Tracer	Distance to pit [m]	Vertical flow distance in snowpack [cm]
27/07/01	590	Sodium-fluorescein	4-5	200
05/08/01	530	Sodium-fluorescein	4-5	115
17/08/01	530	Rhodamine WT	9-10	40

4.6.1.2 Dye tracer experiments at the snow-ice interface

Experiments at the snow-ice interface were undertaken as described in Section 3.2.3. Two return-curves from injections at the snow-ice interface on 31 July and 17 August are available (Table 4.6).

Table 4.6 Injections undertaken at the snow-ice interface

Date	Snow depth [m]	Tracer	Distance to pit [m]
31/07/01	160	Sodium-fluorescein	6.7
17/08/01	37	Sodium-fluorescein	11.0

4.6.2 Tracer return curves from snowpack experiments

The return curves obtained from three surface injections between 27 July and 17 August are presented in (Figure 4.10). The plots show the dye concentration and the air temperature measured at the glacier snout during the experiments. The tracer return curves were recorded at 10 second intervals and the air temperature at 15 minute intervals.

The return curve from the injection on 27 July (Figure 4.10a) was obtained after an injection on the surface of the 2 m thick snowpack and the centre of the injection area 4.5 m from the fluorometer pit. The data gap in the curve was due to a full memory card that was not exchanged in time. Also, data that did not make sense during the morning hours when no or little water flowed through the "fluorometer pool" and the dye was not properly mixed with the water in the "pool" has been omitted. The dye return started about 4 hours after injection. Peaks occurred after about 6 and 27 hours. The fastest flowing water molecules flowing down vertically into the snow-ice interface at the shortest snowpack distance may explain the first peak. The flowpath of these molecules seemed to be the most direct and least influenced by ice layers. Some molecules may even find a travel path straight through ice layers, since consolidated coarse crusty layers (Gerdel, 1954) and often ice layers are not completely impermeable (Figure 4.5).

The dispersion of the dye return curve from snow surface injections is also caused by temporary storage within the snowpack. A small, slow flowing quantity of water that penetrates into the "fluorometer pool" was possibly not flowing turbulent enough to homogeneously mix with the pool water impeding detection by the downhole fluorometer. The second, dominant peak occurred on the following day and was induced by increasing melt rates, which enhanced the water flow through the snowpack. After the peak, the

concentration decreased rapidly due to high dilution effects in the "fluorometer pool". The dilution effect was probably also enhanced by melt water from the pit area. The experiment was finished after about 30 hours.

During the second experiment on 05 August the snowpack at Stake 20 was 115 cm thick and the centre of the injection area was located 4.5 m up-glacier from the fluorometer pit. The dye return curve (Figure 4.10b) shows rapidly increasing dye concentrations from about 3.9 hours after injection. The first, dominant, peak appeared after 4.2 hours and the dye concentration decreased rapidly again due to dilution effects from the pit area. The data gap is, again, due to a full memory card and unreliable data during periods of low melt rates. The following day a second peak occurred. The peak was followed by a rapid concentration decrease most likely due to dilution effects from the pit area and the experiment was finished after about 35 hours.

It is notable that the dye return for both experiments on 27 July and 5 August started after about four hours in spite of an approximate 50 % reduction of snowpack (vertical travel distance) between the experiments due to rapid melting. The injection times for both experiments were similar (11:31 and 11:06), but meteorological conditions differed significantly and can perhaps explain the unexpectedly similar maximum transit times. The morning of 27 July was sunny with a low (about 1/8), although increasing cloud cover (to about 6/8) during the day. Whereas, the morning of 5 August was misty with complete cloud cover remaining all day. It rained on both days during the afternoon (slightly more on 5 August) and the local rain quantities may have influenced water percolation through the snow. The air temperatures measured at the snout on 27 July at 11:00 and at 15:00 were 7°C and 10°C as opposed to temperatures of about 5°C on 5 August at 11:00 and 15:00 with a cooling trend towards 4°C in the afternoon. Therefore, during the experiment on 27 July the air temperature was significantly higher than during the experiment on 5 August, consequently a higher melt rate can be presumed, unless equally high melt rates occurred on 5 August due to the diffuse longwave solar radiation that day. From analyses of mean diurnal melt rates at individual stakes it was recognised that ablation measurements, as undertaken during the field season 2001 at Glacier de Tsanfleuron, were not of sufficiently high resolution to give support for the inferred higher melt rates on 27 July.

The third experiment at the snow surface was undertaken on 17 August. The 3 weeks between the first and third surface injection were characterised by intensive melting and a

significant snowpack thinning. The snowpack at the time of the last experiment was only 37 cm thick. The centre of the injection area was 9.5 m up-glacier from the fluorometer pit. The resulting dye return curve (Figure 4.10c) is relatively smooth probably due to a more homogeneous structure of the snowpack than earlier in the season. Due to high melt rates during the previous weeks, and especially during the five days previous to the experiment it can be inferred that hydrological passageways are well developed. The dye return started after 1.7 hours and after about 2 hours the concentration increased slightly and remained fairly constant for about one hour. After an abrupt, rapid rise, the peak occurred about 3.5 hours after injection. The experiment was finished after about 7 hours.

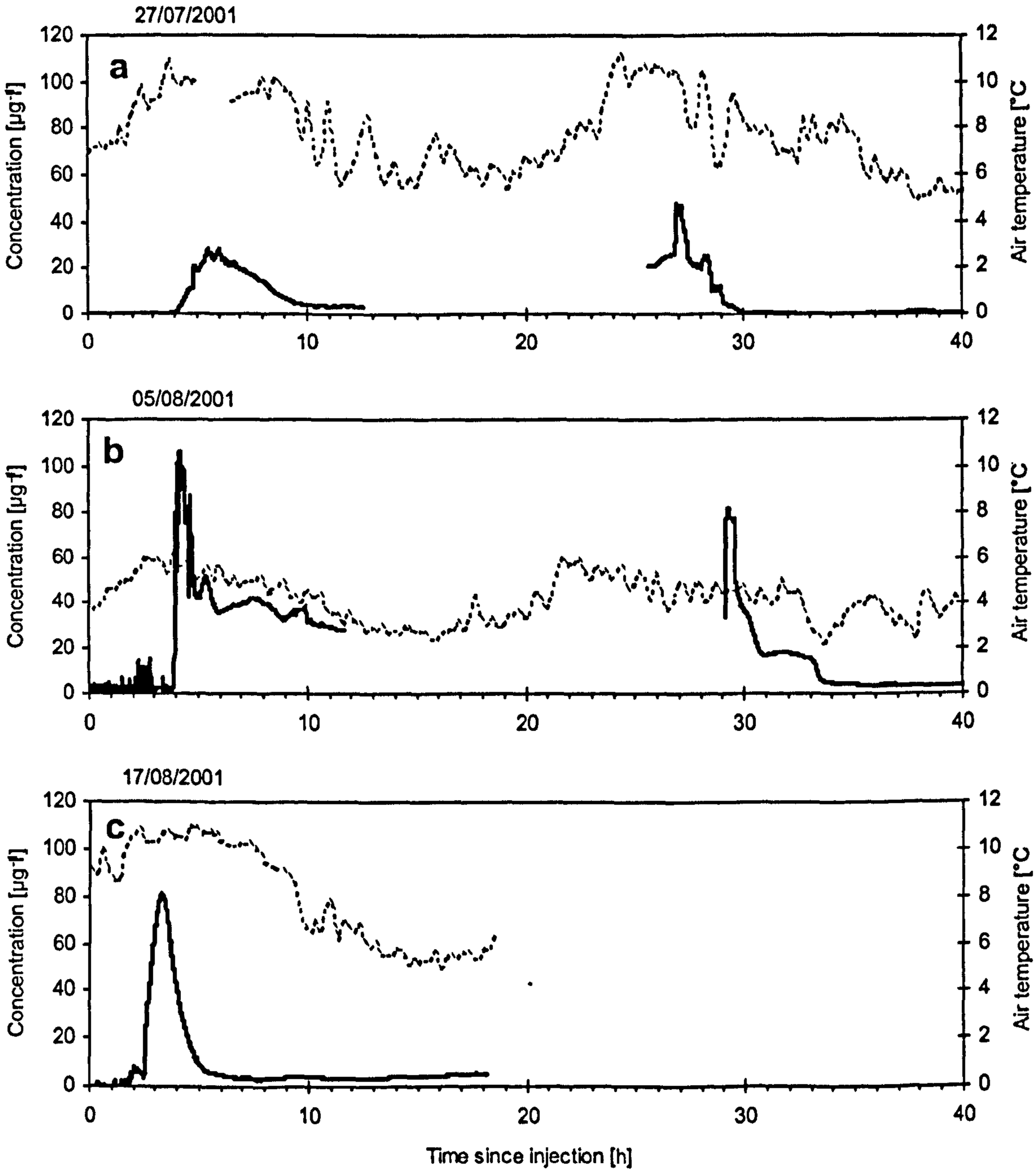

Figure 4.10: Return curves from snow surface experiments (measuring interval = 10 seconds), (a) on 27 July, (b) on 05 August and (c) 17 August. The dashed line indicates the air temperatur e during the experiment (measuring interval = 15 minutes).

Generally, the tracer return curve reflects the hydraulic evolution of the snowpack. Water percolating through a thick snowpack disperses more and lower flow velocities occur as if water is percolating through a declined snowpack. This is demonstrated by the more dispersed curves on 27 July and 5 August compared to the more peaked return curve on 17 August.

4.6.3 Tracer return curves from snow-ice interface experiments

The return curves and air temperature at the glacier snout during experiments at the snow-ice interface are shown in Figure 4.11. The first injection was undertaken on 31 July with a straight flow distance of 6.7 m. The snow thickness at the injection area was 160 cm. About 48 minutes after injection a rapid concentration increase started at the dye detection point and a double peaked return curve was recorded (Figure 4.11a). The first peak was reached 52 minutes after injection and was followed by a rapid concentration decrease. Shortly after the first, dominant peak, probably due to the inhomogeneous nature of the water saturated snow aquifer, more dye was released and a second peak occurred after only 12 minutes. Again the concentrations decreased rapidly to background values and the experiment was finished after 1.3 hours.

Another injection at the snow-ice interface was undertaken on 17 July. The distance to the fluorometer pit was 11 m; the snow depth had declined to only 37 cm. The return curve (Figure 4.11b) was also double peaked and is characterised by rapid increase and decrease of the tracer concentrations. The return started 0.7 hours after injection. The first, dominant peak occurred after less than 1 hour and a second peak after 1.2 hours. The experiment was finished after about 2 hours.

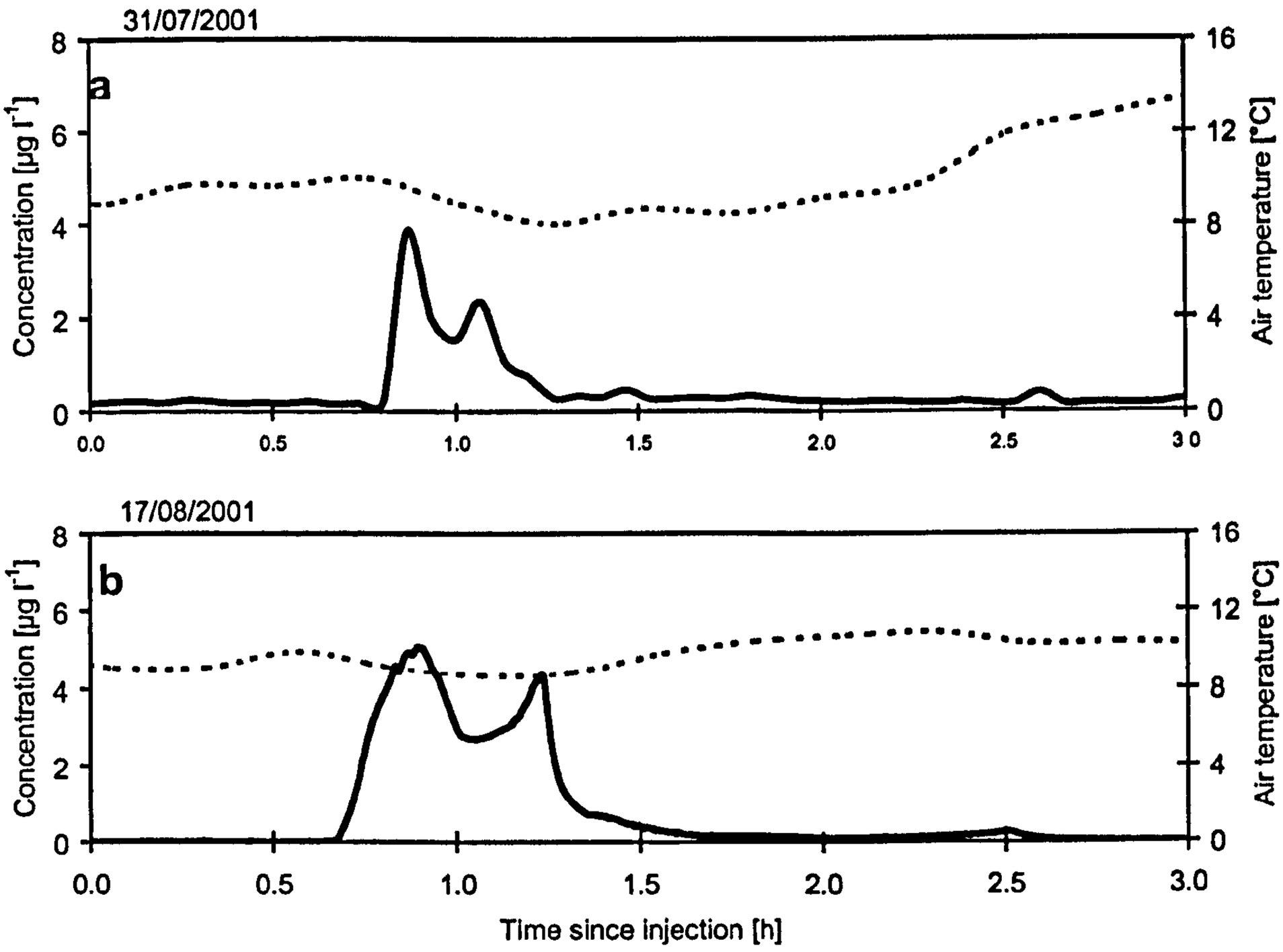

Figure 4.11: Tracer return curves from snow-ice interface injections (measuring interval = 10 seconds), (a) on 31 July 2001 and (b) on 17 August 2001. The dashed line indicates the air temperature during the experiment (measuring interval = 15 minutes).

4.6.4 Flow velocities along the snow-ice interface

Flow velocities along the snow-ice interface are significantly faster than the percolation through the snowpack. The two experiments on 31 July and 17 August (Table 4.7) show maximum flow velocities of 8.4 and 17.7 mh^{-1}. Peak flow velocities were 7.7 and 12.2 mh^{-1}

Table 4.7: Flow velocities from experiments at the snow -ice interface.

Date	Travel distance [m]	Maximum flow velocity [mh^{-1}]	Peak flow velocity [mh^{-1}]
31/07/01	6.7	8.4	7.7
17/08/01	11.0	15.7	12.2

The water drainage at the snow-ice interface is mainly influenced by the effective saturation of the layer, the quantity of meltwater input from the unsaturated snowpack

above and the slope inclination (Colbeck, 1974). Higher flow velocities at the end August probably occurred due to an increased effective saturation at the snow ice interface. Even though the water level at the snow ice interface was slightly higher on 17 August (2.6 cm as opposed to 1.5 cm during peak times of the experiment), it is likely that the meltwater input to the saturated layer at the snow-ice interface was lower due to lower air temperatures measured during the time of the experiment. Therefore, this cannot explain faster flow velocity on 17 August.

4.6.5 Flow velocities through the snowpack

The most significant flow velocities for the interpretation of water flow through snow used were the maximum and peak flow velocities. Maximum flow velocities represent the velocity of the fastest moving tracer particles, i.e. velocities calculated from the tracer that first appeared at the detection point. Peak flow velocities represent water flow velocities calculated from the main peak of the tracer return.

The dye tracer injected at the snow surface first percolates down through the snowpack and continues its flow along the snow-ice interface to the detection point in the snow pit (Figure 3.3). Flow velocities through the snowpack (Section 3.2.3.5, Table 4.8) were obtained by subtracting measured travel times at the snow-ice interface (experiments at the snow-ice interface) from total travel times (experiments at the snow surface). These calculations were based on the measured maximum–flow velocities at the snow-ice interface of 12.2 mh^{-1}. For the first two experiments (27 July and 05August) the flow velocity through the snowpack did not significantly vary regardless of the measured transit times at the snow-ice interface that was used to calculate the total flow velocity. During the experiment on 17 August the flow velocity of 12.2 mh^{-1} at the snow-ice interface was more likely than 7.7 mh^{-1} due to the progress of the melt season and the increased proportion of time the water flows at the snow-ice interface.

Table 4.8: Flow velocities for dye tracer flow through the snowpack only.

Date	Snow depth [m]	Maximum flow velocity [mh^{-1}]	Peak flow velocity [mh^{-1}]
27/07/01	2.00	0.54	0.08*
05/08/01	1.15	0.34	0.32
17/08/01	0.40	0.50	0.16

* Velocity based on the time of the second peak

Flow velocity through snowpack determined from previous studies range between 0.1 to 0.17 mh^{-1} (Krimmel et al., 1973a; Behrens et al., 1982; Oerter and Moser, 1982) and results from the experiments undertaken at Glacier de Tsanfleuron show peak velocities in a similar range (0.08 - 0.32 mh^{-1}). Maximum flow velocities do not vary with snow thickness, even in a melting and thus changing snowpack. This may be a result of efficient flow passageways already in the early snowpack, which enabled to maximum flow velocities similar to those through the more homogenous, entirely wetted snowpack later in the season. However, the peak flow velocity was significantly delayed in the thicker snowpack earlier in the season compared to the peak flow velocities later appeared to be at least twice as fast. It is likely that delays in the thicker snowpack were enhanced by storage and retardation due to the stratigraphy of an early snowpack. The variation of flow velocities at the experiments on 5 August and 17 August can be caused by a higher magnitude of meltwater input as this effect was investigated in earlier experiments by Colbeck (1978). Due to the small number of experiments performed the results presented here should, however be treated with caution.

4.7 Water level record at the snow-ice interface

At temperate glaciers during the melt season above the snowline, a water-saturated snow layer develops at the snow-ice interface. The meltwater flow at the snow-ice interface presents an important component of meltwater drainage through temperate glaciers. The "aquifer" at the snow-ice interface is an intermediate storage for meltwater through the glacial drainage systems and significantly delays meltwater runoff from glaciers (Stenborg, 1969, 1973). The aquifer at the snow-ice interface is analogous to a porous groundwater aquifer with the main difference that in saturated snow the storage medium and the fluid stored have the same composition in different phases (Krimmel et al., 1973b). Additionally, the permeability of the aquifer can rapidly change due to snow metamorphism (Röthlisberger and Lang, 1987).

At Glacier de Tsanfleuron variations of the water level at the snow-ice interface (W) near Stake 20 at about 2620 m a.m.s.l. were measured from 29 July to 18 August. Spatial and temporal variations of meltwater generation at the snow surface (influenced by energy balance and albedo) and the routing of meltwater through the snowpack are responsible for the W hydrograph. The asymmetrical shape of the W hydrograph is caused by the dispersion

of water during its travel through the snowpack. Variations of *W* are plotted and discussed together with air temperature variations (Figure 4.12a). To obtain an unambiguous air temperature signal, the original 15-minute intervals were plotted as two-hourly moving averages. Furthermore, *W* variations are plotted and discussed below in comparison to the bulk discharge at the snout (Figure 4.12b). Since meltwater flow at the snow-ice interface controls water input into the englacial and therefore also to the subglacial drainage system, variations of *W* may be reflected by variations of the bulk discharge (*Q*).

As indicated in Figure 4.12, the observation period was also examined under the aspect of precipitation influences. Rain occurred on 29 and 30 July and between 03 and 10 August. It snowed in the early morning of 11 August. Dry periods occurred from 31 July to 02 August and from 12 to 18 August. The data record of *W* presents clear diurnal cyclicity. In this 19-day observation period, the *W* varied between 0.7 and 5.3 cm. The individual diurnal cycles are influenced by rain events and the occurring smaller spikes are a clear response to intense rain events.

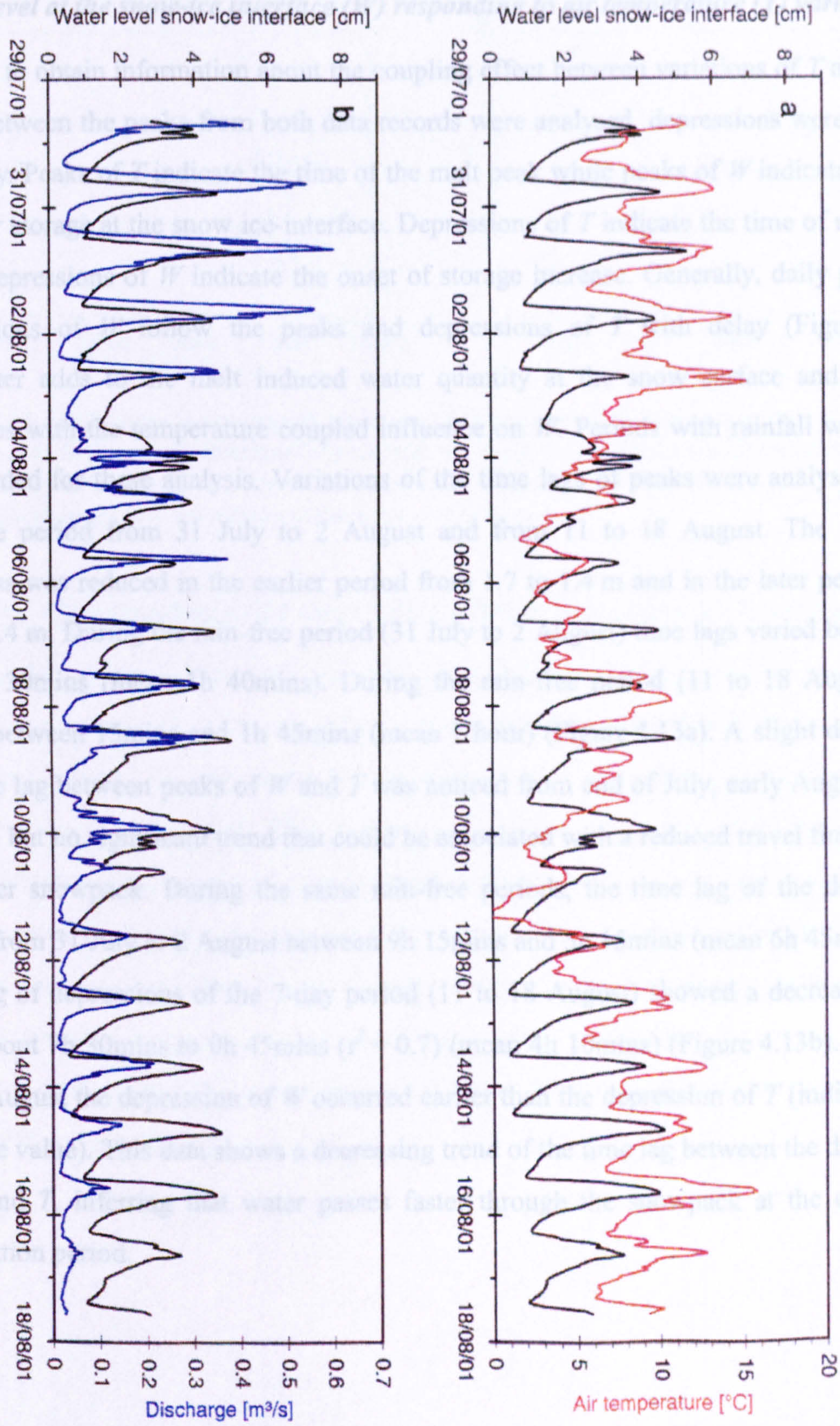

Figure 4.12: Water table record of the snow-ice interface near Stake 20 from 29 July to 18 August (black lines). (a) shows the water-levels at the snow-ice interface (black line) and the temperature record at the snout (red line) and (b) the water-levels at the snow-ice interface (black line) and the bulk discharge at the snout (blue line). The temperature data is plotted as a two-hourly moving average of 15-minute interval measurements.

Water level at the snow-ice interface (W) responding to air temperature (T) variations

In order to obtain information about the coupling effect between variations of *T* and *W*, lag times between the peaks from both data records were analysed, depressions were analysed similarly. Peaks of *T* indicate the time of the melt peak while peaks of *W* indicate the peak of water storage at the snow ice-interface. Depressions of *T* indicate the time of melt onset while depressions of *W* indicate the onset of storage increase. Generally, daily peaks and depressions of *W* follow the peaks and depressions of *T* with delay (Figure 4.12a). Rainwater adds to the melt induced water quantity at the snow surface and therefore interferes with the temperature coupled influence on *W*. Periods with rainfall were hence disregarded for these analysis. Variations of the time lags of peaks were analysed for the rain-free period from 31 July to 2 August and from 11 to 18 August. The snowpack thickness was reduced in the earlier period from 1.7 to 1.4 m and in the later period from 0.8 to 0.4 m. During the rain-free period (31 July to 2 August) time lags varied between 2h and 1h 30mins (mean 1h 40mins). During the rain-free period (11 to 18 August) they varied between 15mins and 1h 45mins (mean 1 hour) (Figure 4.13a). A slight decrease of the time lag between peaks of *W* and *T* was noticed from end of July, early August to mid August, but no significant trend that could be associated with a reduced travel time through a thinner snowpack. During the same rain-free periods, the time lag of the depressions varied from 31 July to 2 August between 9h 15mins and 5h 15mins (mean 6h 45mins). The time lag of depressions of the 7-day period (11 to 18 August) showed a decreasing trend from about 7h 30mins to 0h 45mins ($r^2 = 0.7$) (mean 4h 10mins) (Figure 4.13b). However, on 16 August the depression of *W* occurred earlier than the depression of *T* (indicated by a negative value). This data shows a decreasing trend of the time lag between the depressions of *W* and *T*, inferring that water passes faster through the snowpack at the end of the observation period.

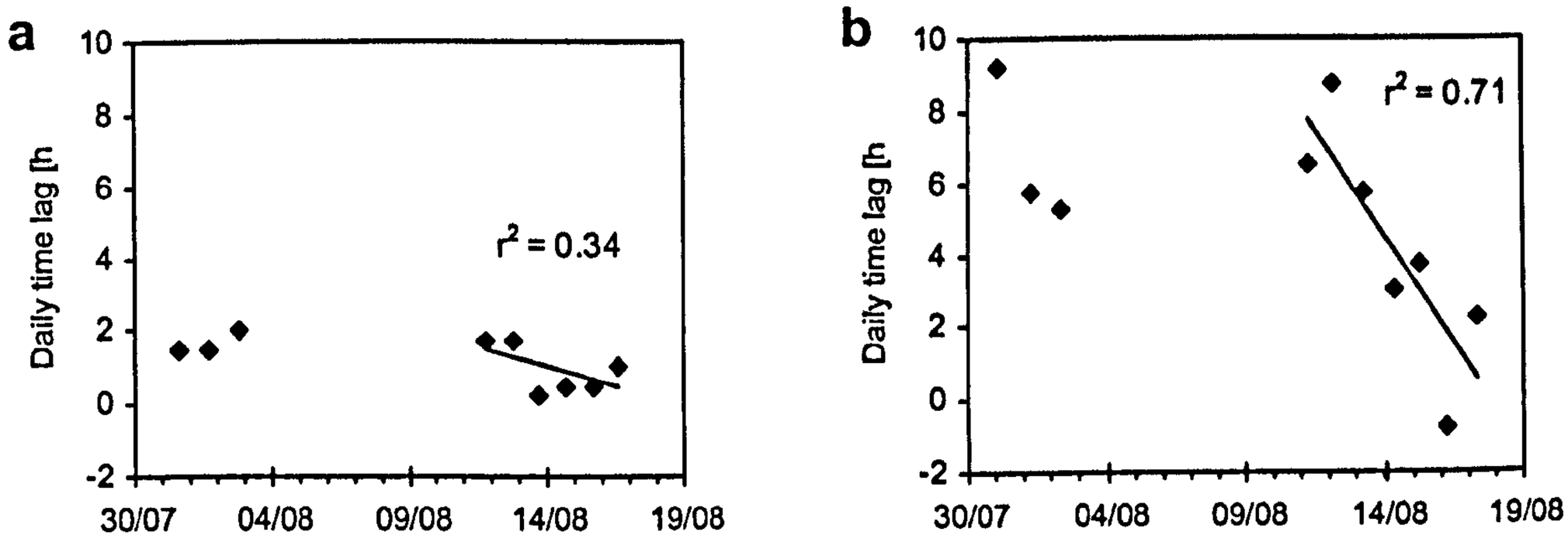

Figure 4.13: Daily time lags between peaks and depressions of the air temperature (*T*) and the water level at the snow-ice interface (*W*) records. (a) Daily time lag between air temperature peaks and water level peaks at the snow-ice interface. (b) Daily time lag between air temperature minimum and water level minimum at the snow-ice interface.

Discharge (Q) responding to the water level variations at the snow-ice interface

The time lags between the peaks and depressions of *W* and *Q* may help to identify links between the water level variations at the snow-ice interface (*W*) and bulk discharge (*Q*). As shown in Figure 4.12b, daily peaks and depressions of *Q* occur predominantly before daily peaks and depressions of *W*. This is because the observation site of *W* is at about the furthest distant of the proglacial stream catchment area (Figure 4.14). Due to shorter travel distances bulk discharge at the gauging station received most surface meltwater from lower altitudes quicker than from higher altitudes. Furthermore, the glacier surface at lower altitudes became snow-free earlier than upper areas responding in increased surface meltwater production. This is an effect of the lower albedo of ice surfaces compared with snow surfaces (Section 2.2).

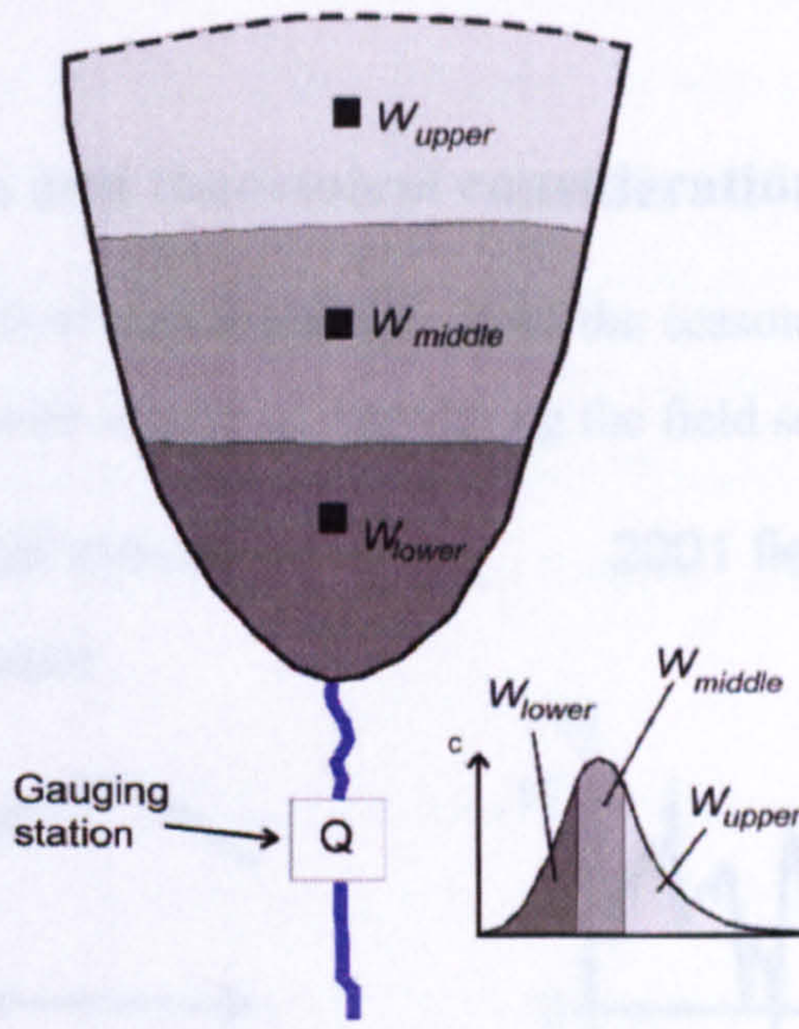

Figure 4.14: Hypothetical catchment area of a glacier and hypothetical stations for the observation of the water level variations at the snow-ice interface in the lower, middle and upper area. The contribution of different areas to bulk discharge is presented under the assumption of consistent discharge quantities.

Understanding why W occurs delayed to Q is crucial for the analyses of the time lags between W and Q. Variations of time lags of peaks were analysed from 31 July to 18 August. During the period of observation the snowpack decreased from about 1.9 m to 0.4 m. Time lags between W and Q peaks varied between 5h and 0h 45mins (mean 2h 30mins), but with no significant trend (Figure 4.15), but a decreasing trend of the time lags between daily W and Q minima from 5h 45mins to 2h was observed ($r^2 = 0.6$). Time lags between daily W and Q minima varied between 6h and 1h 15mins (mean 3h 50mins).

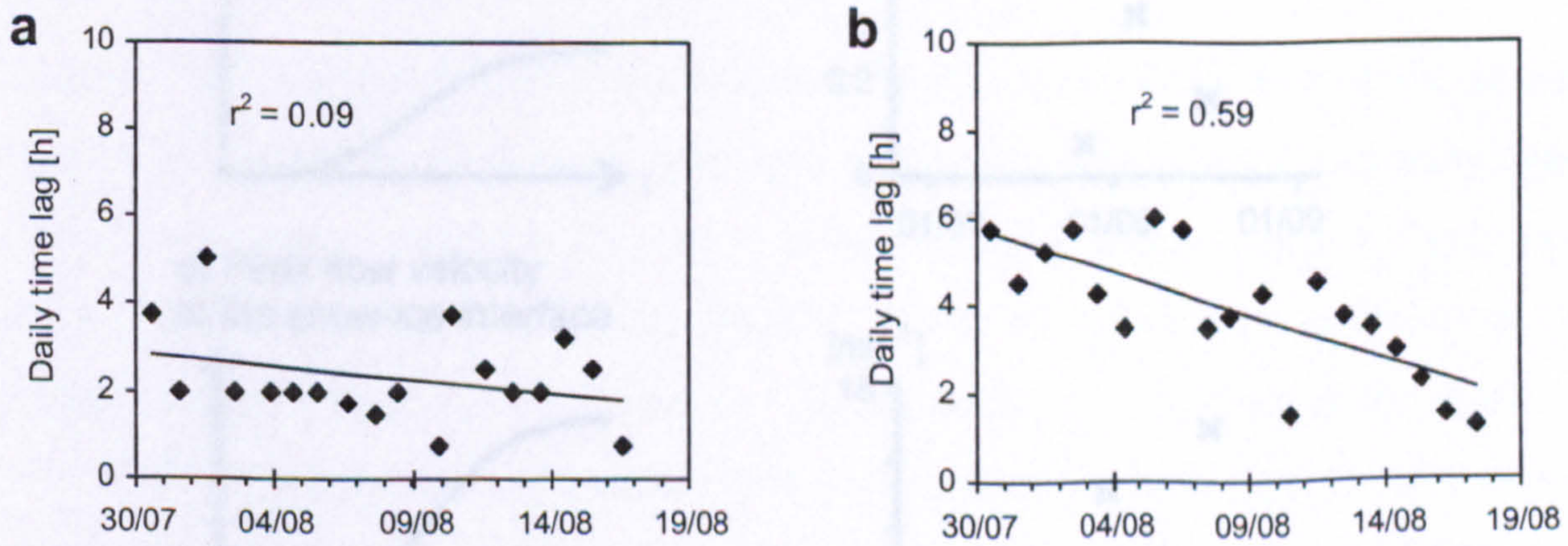

Figure 4.15: Daily time lags between peaks and depressions of the bulk discharge (Q) and the water level at the snow-ice interface (W) records. (a) Daily time lag between bulk discharge peaks and water level peaks at the snow-ice interface. (b) Daily time lag between bulk discharge minimum and water level minimum at the snow-ice interface.

4.8 Discussion

4.8.1 Measured data and theoretical considerations

In this chapter the theoretical considerations about the seasonal development of snowpack hydrology are compared with measured data during the field season.

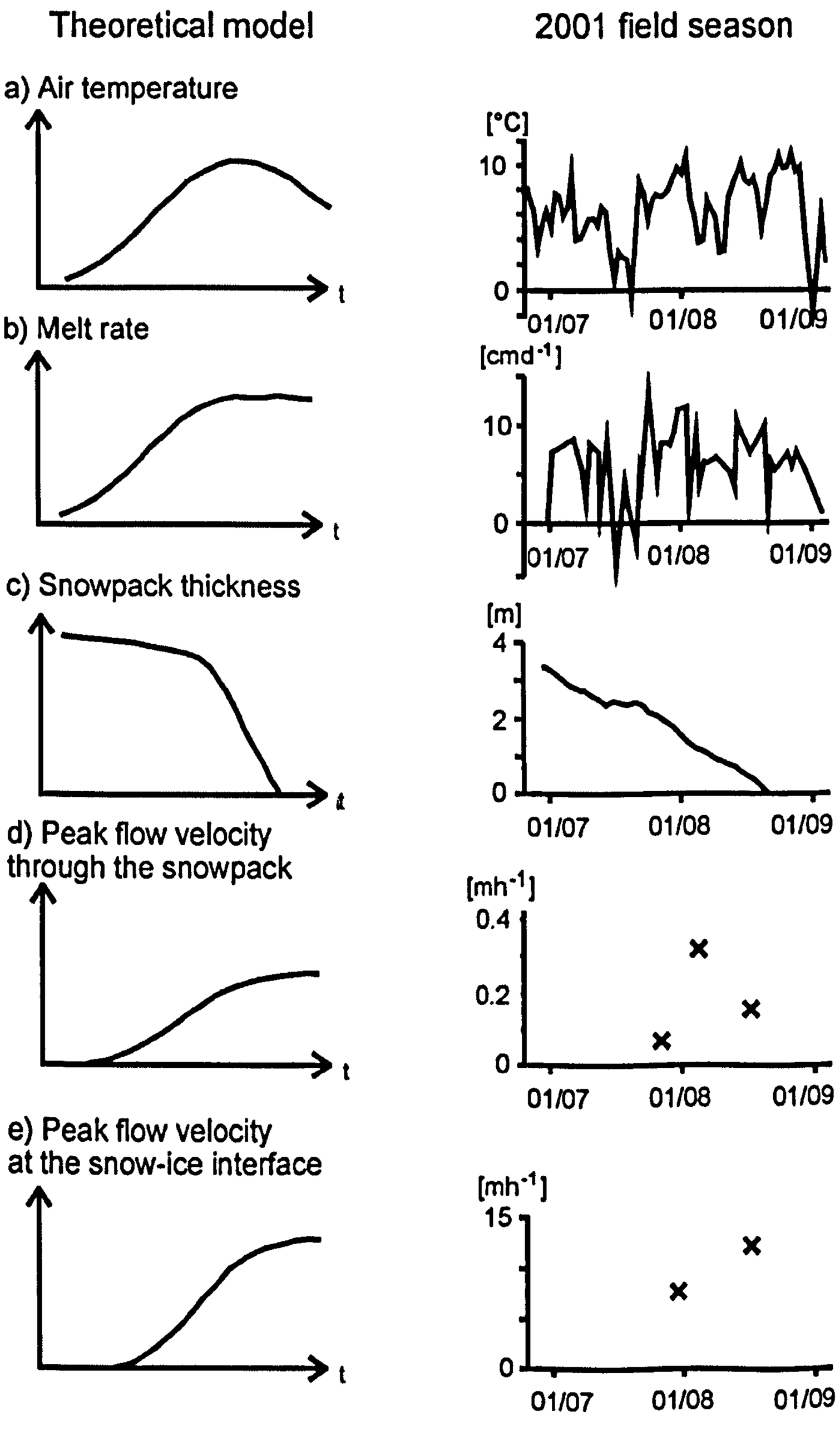

Figure 4.16. Model predictions compared to data of the 2001 field season.

The air temperatures from end of June to start of September 2001 at Glacier de Tsanfleuron were highly variable. They did not show a trend of a sinusoidal increase and decrease as expected from the idealised climate graphs for the region (Figure 4.16a). Twice during the summer season the temperature went below 0 °C and it snowed on the glacier. To obtain the expected sinusoidal temperature time series, measurements over several years, shown as averages in climate diagrams, would be required. The melt rate, which is predominantly modulated by variations of air temperature, solar radiation and albedo, was highly variable (Figure 4.16b).

The decrease of the snowpack thickness at Stake 20 (Figure 4.16c) throughout the season was approximately linear and this trend was observed at all 26 locations of the stake network across the glacier. The snowfall event and cold temperatures in mid July clearly affected the thinning of the snowpack due to a negative melt rate (accumulation). The snowpack thickness remained stable for a few days before thinning continued following a linear trend until depletion at this location on 22 August. Peak flow velocities in the snowpack (Figure 4.16d) varied between 0.08 and 0.32 mh^{-1}. The faster flow velocities could be related to greater meltwater generation at the snow surface, reflected by a higher water level at the snow-ice interface. This is critically dependent on both the diurnal temperature cycle and the seasonal variation. There is not enough data available for definite inferences to be made about the seasonal development of peak flow velocities. Flow velocities do not increase continuously throughout the season; they may dependent on short-term temperature variations, which may trigger the evolution of ice-lenses, and a variable meltwater production rate at the snow surface.

Peak flow velocity at the snow-ice interface increased towards the end of the season (Figure 4.16e), possibly due to better-developed travel paths. The inferred increasing trend of the flow velocity throughout the season cannot be made because there are only two experimental results available. During the melt season the water level at the snow-ice interface is expected to increase, therefore influencing the flow velocity at the snow-ice interface. The thickness of the water-saturated lower part of the snow layer (snow aquifer) varies mainly depending on local variations of the hydraulic gradient (Schneider, 2000).

The measured data at Glacier de Tsanfleuron does not closely match the theoretical model. The reasons for this are a lack of comprehensive and continuous data sets over the whole melt season. With the amount of data available, it was not possible to investigate

weaknesses of the theoretical model, which may also have contributed to discrepancies between the theoretical model and measured data. The theoretical model can probably be improved given further future research and data in this direction. However, combining theory and field observations does give valuable information about the meltwater flow and evolution of the snowpack during this particular season at Glacier de Tsanfleuron.

4.8.2 Improvements of the method and future research

Repeated surface dye injections at the same location throughout a diurnal melt cycle or over longer periods of time (e.g. entire melt season) could be used to rationalise the glaciers temporal behaviour related to variations of meltwater generation measured at the glacier surface. Although, this needs also to take into account that the upper boundary of the snowpack is changing as well as the internal snowpack properties. Additionally, two or more fluorometers at the snow-ice interface a small distance apart could be used to gather information about the dispersion of the tracer cloud and the local variations of this cloud. Water flow velocity measurements at the snow-ice interface could be correlated with water level data at the snow-ice interface. These data could perhaps help elucidate the evolution of the snow-ice interface drainage system, and thus meltwater delivery to the englacial and subglacial drainage systems throughout the ablation season.

Valuable information can also be given by visual observations of dye injections in a separate pit close to the injection area. These observations might reinforce and supplement results obtained from dye tracer return curves. Digging sections at the side of the injection area and not just in front might also prove useful, because the routing of dye from the surface to the snow-ice interface will possibly be seen more clearly at the pit sides.

Furthermore, measuring surface melt rates using an ultrasonic depth gauge (UDG) at a high resolution as opposed to daily stake readings could be used to continuously monitor the local meltwater input into the snowpack given that the actual snow density is measured frequently. A correlation between the melt rate and the water level at the snow-ice interface could provide information about water storage times within the snowpack. Since melt processes at the glacier surface are controlled by meteorological parameters, automatic weather stations at different elevations on the glacier measuring air temperature, relative humidity, wind speed, shortwave and longwave radiation and precipitation would be advantageous. Even though measuring precipitation accurately is difficult, a record of

precipitation would be useful because rain enhances water percolation through snowpack and also provides energy for melting.

Covering the fluorometer head with expanded polystyrene would improve the tracer detection set-up by protecting the "detection pool" from further melting and would also help to keep the fluorometer in position. To reduce the retention or buffering effects of the "pool" it would be advantageous to reduce its size, for example by reconstructing a fluorometer so it can measure concentrations at shallow water tables. This would be especially valuable at the start and end of the melt season when only small melt rates occur, this factor impeded the measurements carried out in this study. A square injection area as opposed to the injection in a line has the advantage of smoothing out local effects, for example ice layer inconsistencies within the snowpack. However, it can be argued that the "line injection" technique would reduce the disruptive effects that occur due to the experiment locally affecting albedo, the smaller the injection area is, the less significant are the potential effects of the injection.

Using dye as a tracer will influence the albedo at snow surface injections. A suitable tracer for snowpack experiments that would not affect the albedo has not been found to date. Covering the injection area with a thin layer of snow after injection brings the albedo, during experiments, closer to its natural albedo. Although, it is possible that as a result of the disturbed snow layer more melt water was produced that penetrated through the snowpack. Alternatively the snow surface could be left and the effects on the albedo acknowledged and perhaps compensated for. Both methods influence the snowpack, unless a clear tracer which does not affect the albedo or the melt rate of the snow, for example by increasing the pressure-melting point of the snow. The problem of changing the albedo following dye injections on the snow surface can be reduced by the injection of a very sensitive tracer at (nearly) invisible concentrations. To ensure that the dye appears in measurable concentrations after it has travelled through the snowpack, it would be useful to test the dilution effects during dye transport. If low injection concentrations were used, the duration at which dye has an affect on the snow surface albedo would be minimised.

Simultaneous tracer injections would be useful to investigate the spatial variability of melt water flow through the snowpack under the actual meteorological conditions at different locations on the glacier. Also, due to the range of altitudes in mountainous areas, significant spatial differences of snowpack evolution and snowpack thickness are expected

at altitudinal different locations and will critically influence meltwater discharge. This could be, similarly, investigated by simultaneous tracer injections at different altitudes. Due to the decreasing temperature and increasing solar radiation with altitude changes of snow properties and melt characteristics are expected at different altitudes. Snowpack injections could be undertaken simultaneously at one high and one low altitude location, allowing interpolation of intermediate locations (depending on the glacier size and character of the glacier intermediate stations may be useful).

4.9 Conclusions

4.9.1 Conclusions from dye tracing

Although, every effort was made to minimise the experimental impacts upon the study area, it is very difficult, if not impossible to investigate a natural snowpack without somehow influencing either the structure or other physical and chemical properties of the pack. Despite the difficulties in obtaining an ideal fluorometer set-up together with other side effects such as dye injections influencing the natural albedo, the experiments undertaken at Glacier de Tsanfleuron allow some valuable conclusions about snowpack hydrology. Consequently, the tracer technique has proven to be a valuable method to study water percolation within a melting snowpack. The interpretation of dye return curves gives information about processes occurring within the snowpack, which cannot directly be observed.

From the experiments conducted in this study, travel times through the snowpack (between 0.08 and 0.32 mh^{-1}) are more than an order of magnitude slower than flow at the water-saturated snow-ice interface (7.7 mh^{-1} and 12.2 mh^{-1}), indicating that the saturation of the layer at the snow-ice interface plays a major role for the meltwater delivery to the englacial and subglacial drainage systems. It is considered that the structure of the saturated snow-ice interface is more homogeneous than the structure of the unsaturated snowpack (Colbeck, 1979) inducing increased flow velocities. The main factors influencing water residence times are the thickness of the snowpack and its physical properties (ice layers, grain size, water saturation) (Chapter 2.3.2). For a better understanding of the complex behaviour and spatial variation of snowpack hydrology more experiments are required. In order to gain

spatial information about the evolution of the snowpack at different altitudes, simultaneous experiments are required as suggested in the previous chapter.

The evolution of the snowpack, reflected in tracer return curves from broad, dispersed to peaked curves, reflects the input regime of meltwater to the englacial and subglacial drainage systems. Colbeck (1974) suggested the thickness of the saturated layer at the snow-ice interface to be proportional to the runoff from the snowpack. The snowpack is declining during the melt season and therefore the impact of the snowpack on glacial hydrology is highest at the start of the melt season, furthermore, water travels more slowly and is stored for longer periods in fresher and thicker snowpacks.

Finding a general pattern of the evolution of meltwater flow through snowpacks and quantifying the meltwater delivery to the englacial and subglacial drainage systems may be possible, but more detailed investigations need to be undertaken at individual supraglacial snowpacks independently because the processes are very complex and are influenced by many parameters, some of which maybe only locally significant.

4.9.2 Links between air temperature, water level variations at the snow-ice interface and discharge

During the 19-day observation period (29 July - 17 August) of water level variations at the snow ice interface (W) at about 2625 m a.m.s.l., the water level varied between 0.7 and 5.3 cm. The air temperature ranged between 1 °C and 18 °C (mean 7.3°C) and the bulk discharge varied from 0.01 to 0.61 $m^3 s^{-1}$ (mean 0.09 $m^3 s^{-1}$). During the same time period, the snowpack decreased by about 1.5 m from about 1.9 m to 0.4 m (795 mm w.e). This period was characterised by relatively warm air temperatures, high melting and high bulk discharge. However, the high bulk discharge demonstrates a decreasing trend during this period which was caused by the decreased impact of meltwater input from non-glacierised catchment area after these became increasingly free of snow.

Time lags between W and Q peaks varied between 5h and 0h 45mins (mean 2h 30mins), but with no significant trend. Conversely, a decreasing trend of the time lags between daily W and Q minima from 5h 45mins to 2h was observed ($r^2 = 0.6$). Time lags between daily W and Q minima varied between 6h and 1h 15mins (mean 3h 50mins).

The analyses of the time series of water level variations at the snow-ice interface (W) in relation to Temperature (T) and bulk discharge (Q) variations show clear patterns of coupling. However, increases and decreases of the curves occur with time lags. Analyses of the time lags between peaks and depressions of the daily W and T peaks and also of W and Q peaks showed a slight decreasing time lag (Section 4.7), but significantly decreasing trends for the time lags between W and T minima as well as between W and Q minima. This suggests that the transit time of meltwater through the thinning supraglacial snowpack is increasing, inferring decreasing storage times. This supports the findings from dye tracer tests, which suggested increased flow velocities through an evolving snowpack. Due to the tailing of diurnal W cycles, decreasing time lags between W and T or W and Q minima are more pronounced than the lag times between W and Q or W and T peaks respectively. Heavy rain events are reflected in both W and Q time series by additional spikes within the diurnal cycle. The strength of the Q amplitudes decrease towards the end of the observation period, while the strength of the W amplitudes remains similar. This is because the bulk discharge is also fed by meltwater from the non-glacierized catchment area and the delivered quantities of meltwater from these areas decrease significantly during the melt season. The diurnal melt signal shown in the shape of W keeps preserved during englacial and subglacial drainage, because the flow through these drainage systems is faster than the drainage through the snowpack. Therefore, the shape of the bulk discharge hydrograph is dependent on supraglacial meltwater input (Chapter 3.3.2).

The study of water level variations at the snow-ice interface has shown that such data series provide valuable information for glacial hydrology as the snow-ice interface presents a linking element at the transition of supraglacial and englacial hydrological systems. Extended water level measurements from the start to the end of the melt season for more than one year and across the glacier are required for reasonable predictions about the seasonal development of the water level at the snow-ice interface of a temperate glacier. This is in general agreement with (Schneider, 1999, 2000).

4.9.3 Glacier catchment area of the proglacial stream

Studying the ablation of Glacier de Tsanfleuron during the 2001 melt-season in conjunction with bulk discharge measurements at the snout suggest that the water draining from the glacier into the proglacial stream is melt water generated from the areas between

2500 and 2600 m a.m.s.l. This area presents only about 6 % of the glacier surface and implies that 94 % of surface meltwaters drain through the karst system beneath the glacier. However, there is uncertainty in the true proglacial stream catchment area represented by the estimated watershed shown in Figure 4.9 (Section 4.5.2). Also, uncertainties are introduced by the probability of storage within the snowpack, supraglacially (e.g. surface pools), englacially and subglacially during meltwater drainage, as well as inaccuracies of the discharge measurement (Section 3.3.2). Therefore, the apparent 94 % deficit of meltwater discharge at the glacier snout cannot count as the true value, but this gives an indication that only a small amount of water actually runs off at the glacier snout. Further evidence for this conclusion can be obtained from dye tracer experiments into moulins and crevasses at the glacier surface. Tracer tests as undertaken at the subglacial drainage system at Tsanfleuron glacier in summer 2001 are described in the following chapter.

5 Subglacial hydrology

5.1 Introduction

Observations in the proglacial area of Glacier de Tsanfleuron, where the former bed lies exposed, suggest that the subglacial drainage system consists of cavities that are linked by numerous Nye-channels (Section 1.3.1.2). Within such a system, a certain volume of water is required to fill the channels and to generate pressurised conditions at the glacier base. The number and distribution of sinkholes, where meltwater enters the karst drainage system beneath the glacier, will impact on the water pressure distribution at the glacier bed. However, it is unknown how many sinkholes are beneath the glacier and to what proportion the glacial meltwater drains to the glacier terminus. Previous investigations (Section 1.3.2) suggested atmospheric pressure in the subglacial drainage system at discharges < 5 m^3s^{-1}. The number of active channels would depend on meltwater fluxes and pressurised flow would therefore occur episodically, triggered by high meltwater inputs. In order to determine whether the previously described conditions are representative of the current subglacial drainage system, a number of tracer tests were undertaken in the summer 2001 melt-season. The procedure for these experiments was explained in Section 3.2.4.

The specific aims of the tracer tests were to determine:

(i) the flow conditions within the subglacial drainage system;

(ii) the surface area of the entire glacier from which meltwater drains to the proglacial stream (as opposed to draining into the subglacial bedrock via sinkholes);

(iii) whether drainage through a linked-cavity system (connected by Nye-channels) as exposed in the proglacial area is consistent with current subglacial conditions and

(iv) the proportion of the time and distance that water spend in Nye-channels and cavities respectively.

Details and results of the tracer experiments are presented in Section 5.2. Theoretical considerations regarding the proportion of the subglacial water flow in Nye-channels or

cavities are presented and discussed in Section 5.3. The role that sinkholes may play in controlling the conditions of the subglacial drainage system is discussed in Section 5.4. In the discussion (Section 5.5) both practical (tracer experiments) and theoretical approaches are examined. Conclusions are presented in Section 5.6.

5.2 Tracer experiments

Heavy winter snowfall and little early summer melt ensured that the snowpack was slow to disappear from Glacier de Tsanfleuron in summer 2001. As a result, the tracer experiments into exposed moulins/crevasses were only possible during a limited period late in the melt-season. Thus, freely draining moulins and crevasses because exposed as late as August and a total of ten injections were conducted on four days, between the 28 and 31 of August 2001, into small moulins or crevasses across the lower tongue of the glacier. In order to enable simultaneous tracer tests at different injection points, different tracers were used (rhodamine WT or sulphorhodamine B, sodium-fluorescein and lithium chloride) (Section 3.2.2). The locations of the injection points and the gauging station where the tracer was detected in the proglacial stream are shown in (Figure 5.1).

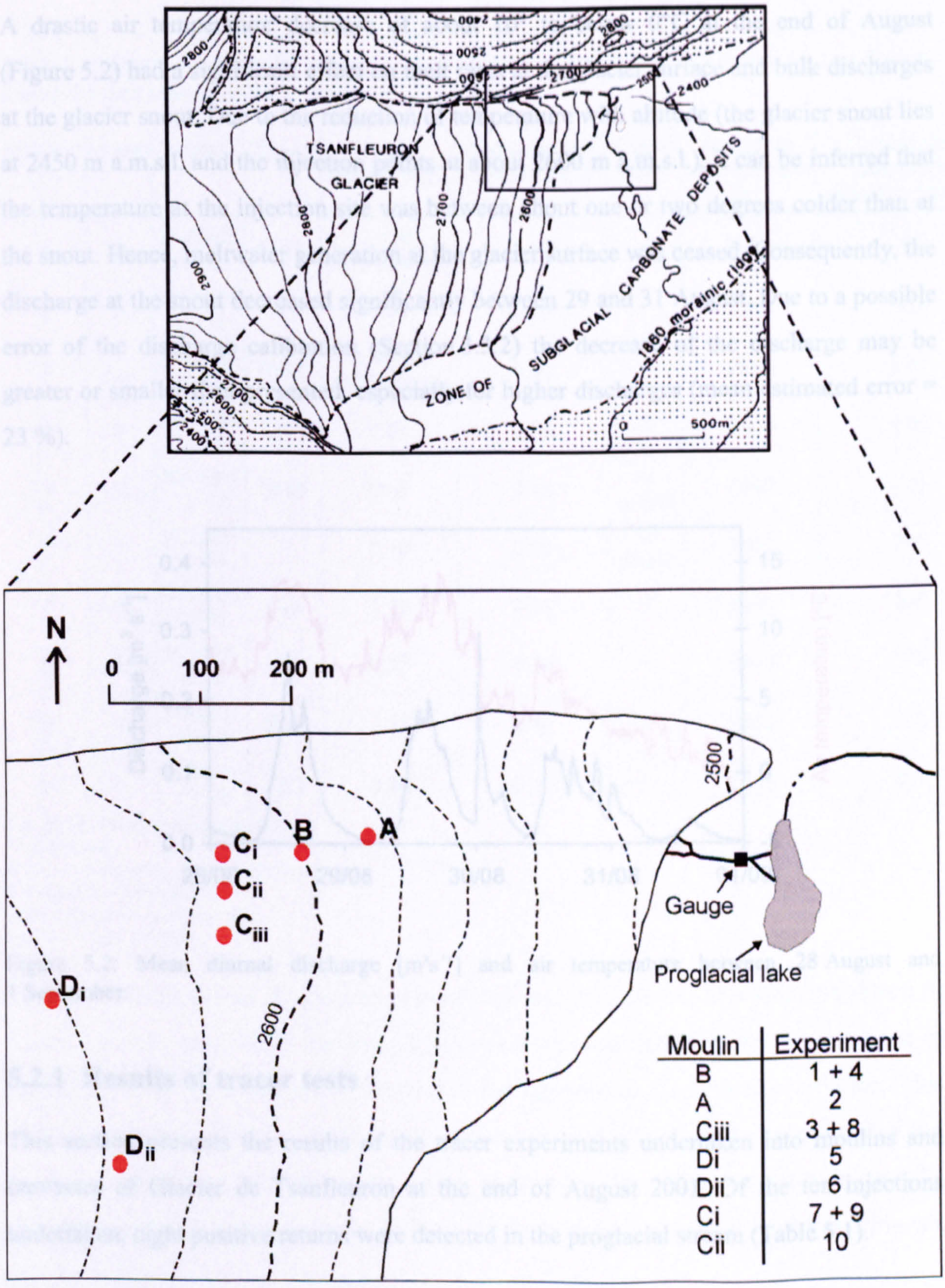

Figure 5.1: Tracer injection points at Glacier de Tsanfleuron. The moulins are labelled A to D according to increasing altitude. Subscripts (i to iii) differentiate between different moulins at similar altitudes. The table in the right hand corner explains which experiment(s) were undertaken at which moulin.

A drastic air temperature decrease of about 10° to below 0°C at the end of August (Figure 5.2) had a significant effect on melt rates at the glacier surface and bulk discharges at the glacier snout. Due to the reduction of temperature with altitude (the glacier snout lies at 2450 m a.m.s.l. and the injection points at about 2600 m a.m.s.l.), it can be inferred that the temperature at the injection site was between about one or two degrees colder than at the snout. Hence, meltwater generation at the glacier surface was ceased. Consequently, the discharge at the snout decreased significantly between 29 and 31 August. Due to a possible error of the discharge calibration (Section 3.3.2) the decrease of the discharge may be greater or smaller than presented, especially for higher discharges (mean estimated error = 23 %).

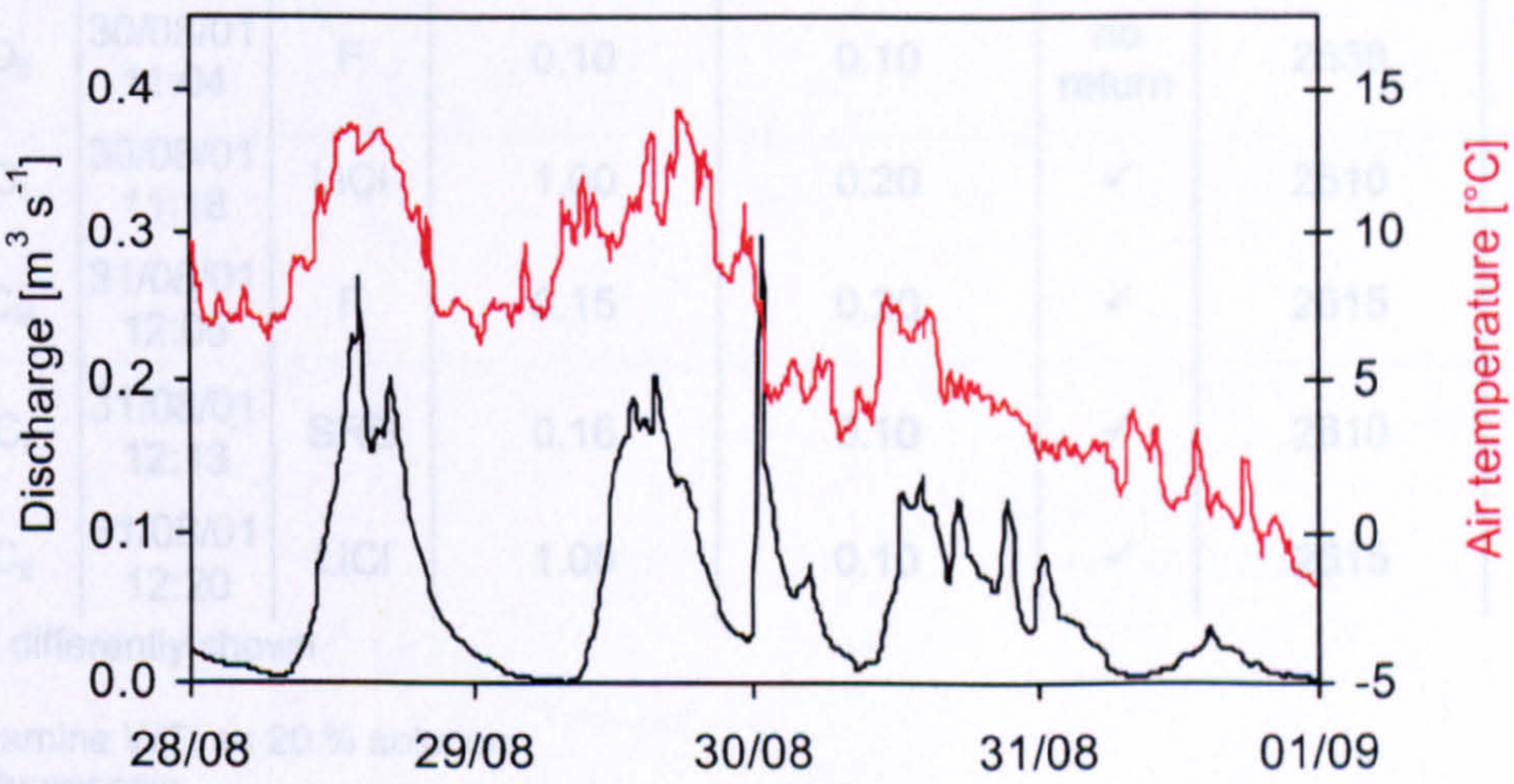

Figure 5.2: Mean diurnal discharge [m^3s^{-1}] and air temperature between 28 August and 1 September.

5.2.1 Results of tracer tests

This section presents the results of the tracer experiments undertaken into moulins and crevasses of Glacier de Tsanfleuron at the end of August 2001. Of the ten injections undertaken, eight positive returns were detected in the proglacial stream (Table 5.1).

Table 5.1: Tracer experiments undertaken into moulins and crevasses at Glacier de Tsanfleuron during the melt season 2001.

Injection No.	Moulin	Date	Tracer	Tracer quantity [kg]*	Discharge into crevasse [ls^{-1}]**	Tracer return	Altitude of injection point [m]	Straight-line distance to detection site [m]
1	B	28/08/01 15:07	RWT	≈ 0.04 (200 ml 20%)	0.10	✓	2600	480
2	A	28/08/01 15:18	F	0.03	0.15	✓	2585	405
3	C_{iii}	29/08/01 11:08	RWT	≈ 0.08 (400 ml 20%)	0.50	✓	2615	570
4	B	29/08/01 11:14	F	0.07	0.20	✓	2600	480
5	D_i	30/08/01 10:47	SRB	0.08	0.15	no return	2642	770
6	D_{ii}	30/08/01 11:04	F	0.10	0.10	no return	2638	765
7	C_i	30/08/01 11:18	LiCl	1.00	0.20	✓	2610	565
8	C_{iii}	31/08/01 12:05	F	0.15	0.20	✓	2615	570
9	C_i	31/08/01 12:13	SRB	0.16	0.10	✓	2610	565
10	C_{ii}	31/08/01 12:20	LiCl	1.00	0.10	✓	2615	565

* in [kg] if not differently shown
** estimated
RWT = Rhodamine WT, as 20 % solution
F = Sodium-fluorescein
SRB = Sulphorhodamine B
LiCl = Lithium chloride

The tracer return curves obtained from injections into moulins and crevasses are shown in Figure 5.3. As explained in Section 3.2.4.3, the tracer concentrations were normalised to the quantity of recovered tracer, providing the appropriate tracer load over time. This allows comparison between tracer return curves independently of discharge conditions and the tracer mass detected. The return curves obtained in this study are generally broadly dispersed, asymmetric and complex in form. Multiple peaks occur in all of the experiments (Figure 5.3).

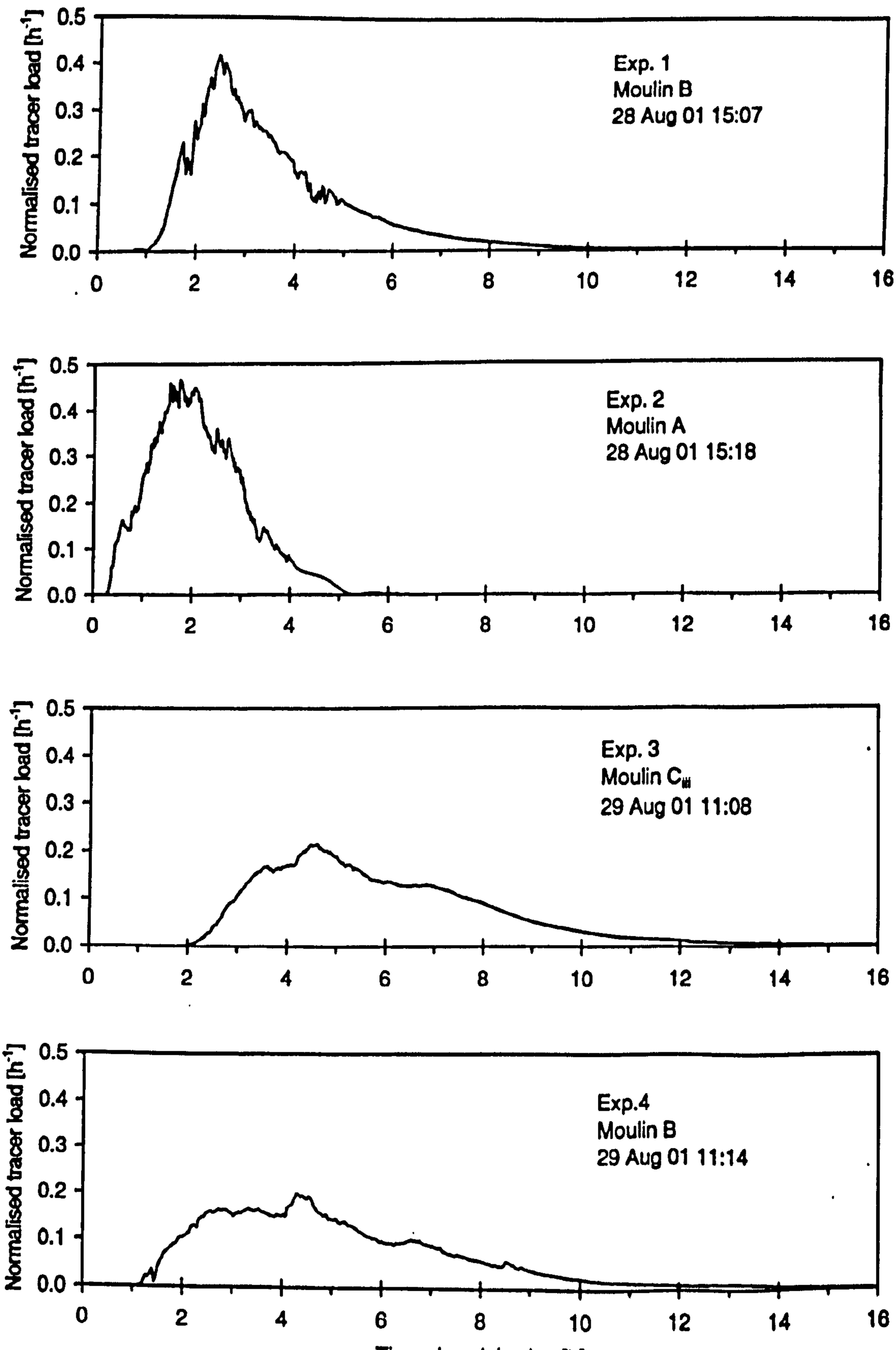

Figure 5.3: Normalised tracer return curves of the Experiments 1 to 4 and 8 to 10 undertaken between 28 and 31 August (for further information refer to Table 5.1). Experiment number and date and time of the injection are shown.

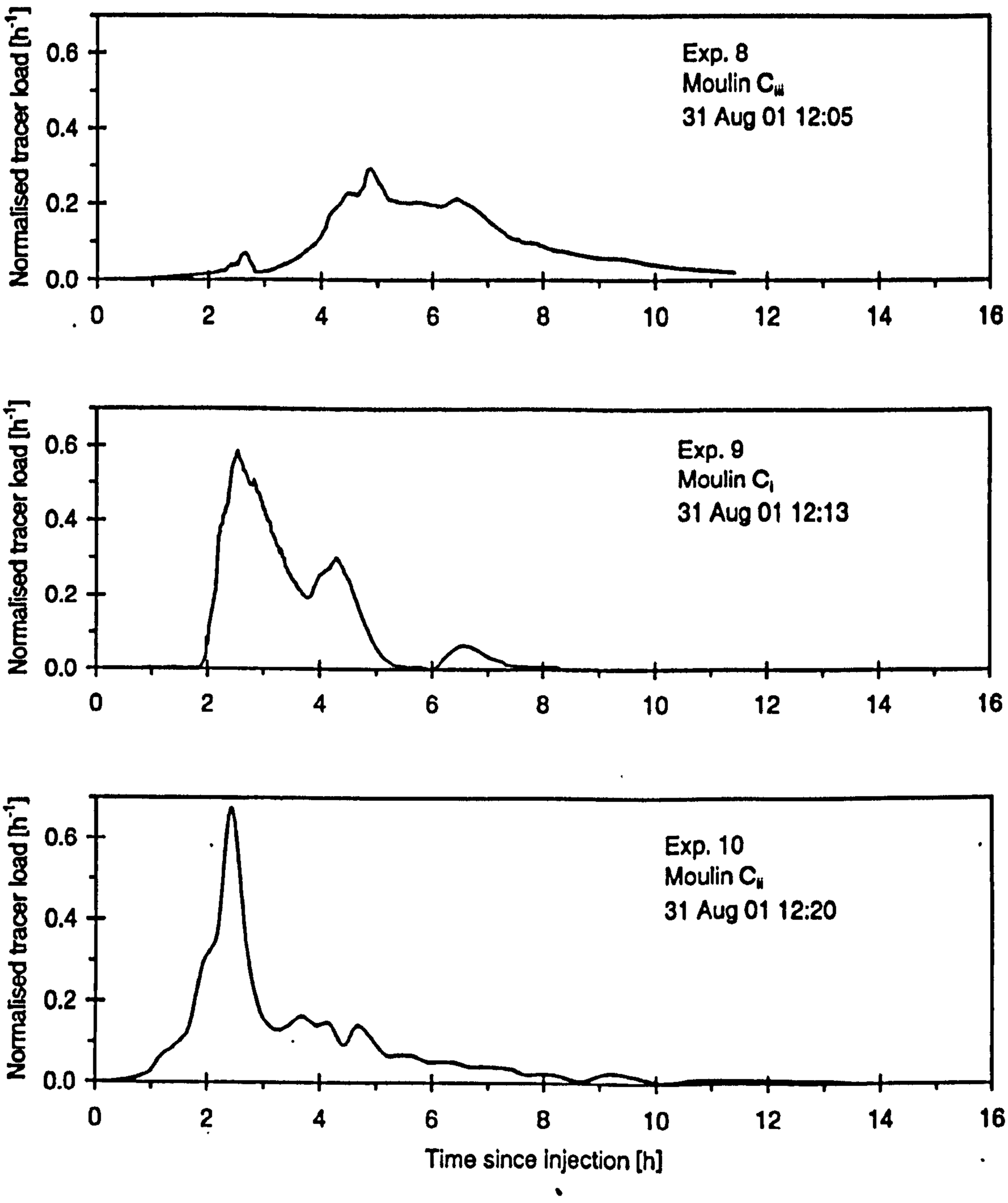

Figure 5.3 cont.: Normalised tracer return curves of the Experiments 1 to 4 and 8 to 10 undertaken between 28 and 31 August (for further information refer to Table 5.1). Experiment number and date and time of the injection are shown.

Despite the relatively short "straight-line" travel distances (about 400 to 600 m) the tracer cloud took between 6 to 15 hours to completely pass the sampling site from the time of injection to end of detection. The occurrence of multiple peaks indicates tracer transport through several flowpaths. Experiment 9 for example shows at least three separate peaks (Figure 5.4). However, because of the complexity of the tracer return curves it is difficult to determine degree of overlap between individual tracer breakthrough (Schuler, 2002b)

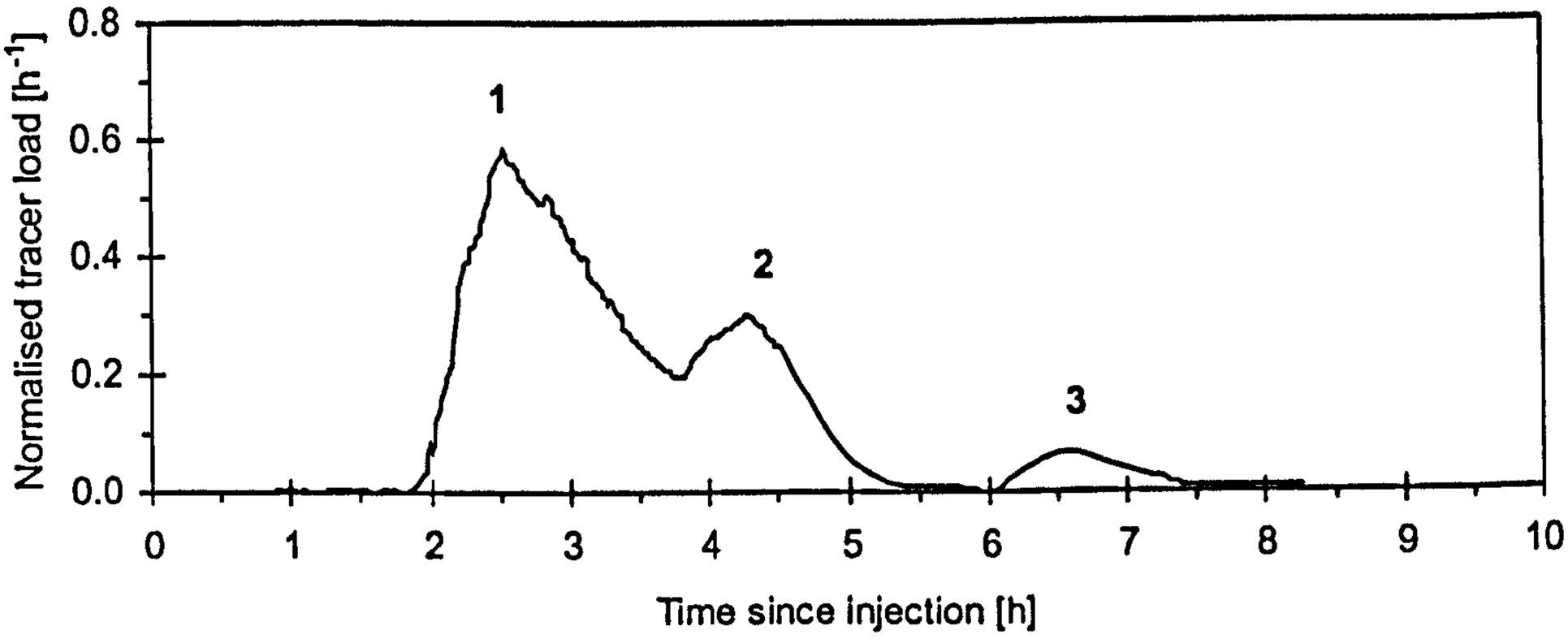

Figure 5.4: Tracer concentrations (measured at one-minute intervals) from Experiment 9, illustrating at least three separate flowpaths.

Since visual interpretation of tracer return curves provides only limited information, flow parameters such as velocity, recovery rate, dispersion coefficient and dispersivity were calculated from tracer test results to obtain parameters that can be used to characterise the subglacial drainage system.

5.2.2 Flow parameters

Flow parameters determined from quantitative analysis of tracer breakthrough curves are commonly used to characterise the englacial and subglacial drainage systems of the studied glacier. In this section, parameters derived from the tracer experiments at Glacier de Tsanfleuron are defined and discussed.

In order to determine flow velocities and the dispersion coefficients, the individual tracer return curves were fitted by an advection-dispersion model implemented in the CXTFIT 2.1, provided by the U.S. Salinity Laboratory (Toride et al., 1999). Results from fitting the model to the measured tracer return curves are presented in (Figure 5.5). For further information about the parameter analysis see Section 3.2.4.4.

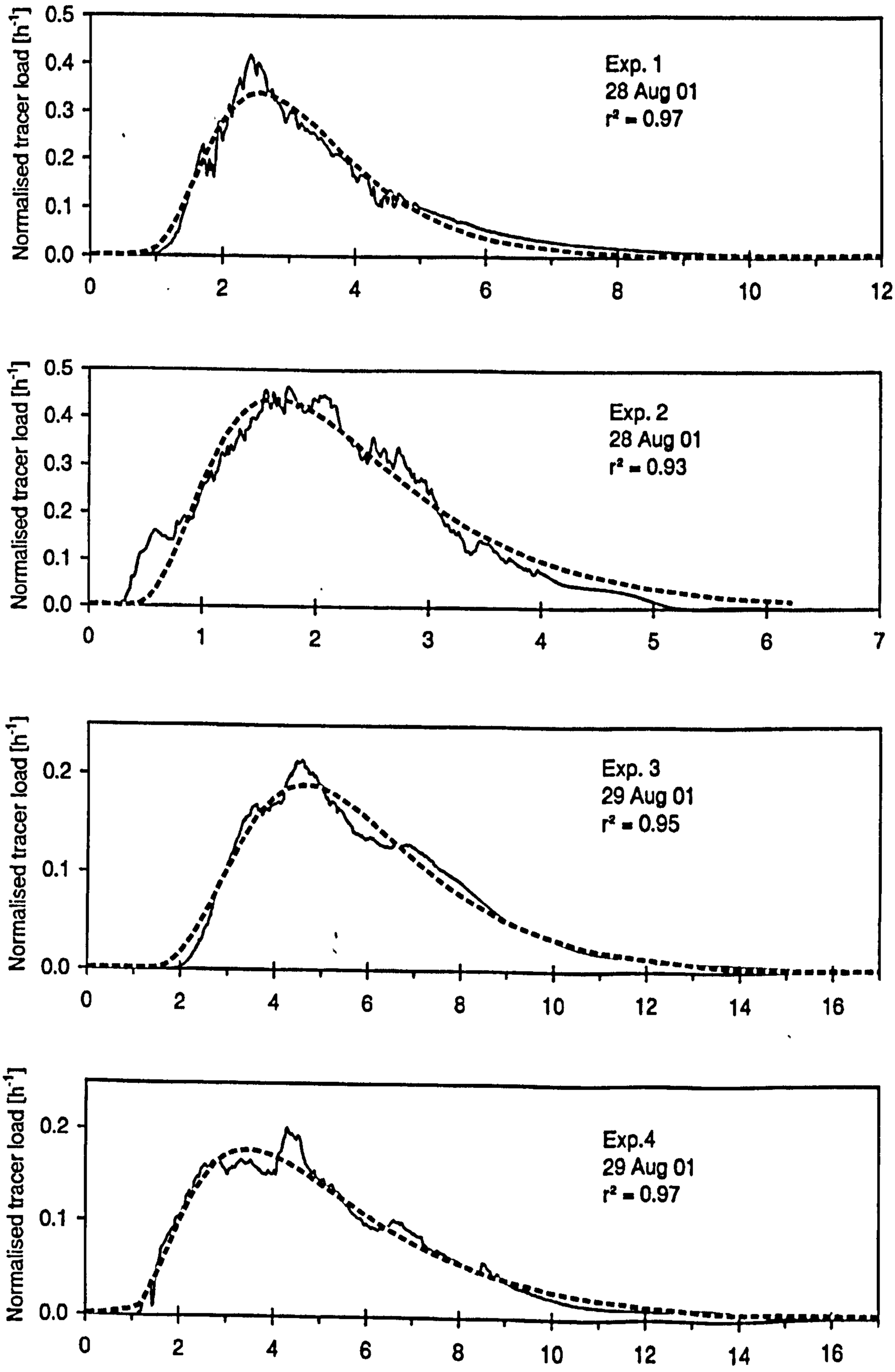

Figure 5.5: Best fit of the normalised tracer return curves (Experiments 1 to 4) using the advection - dispersion model. Experiment number, date and time of the injection and the correlation coefficient (r^2) between measured and modelled curve are shown.

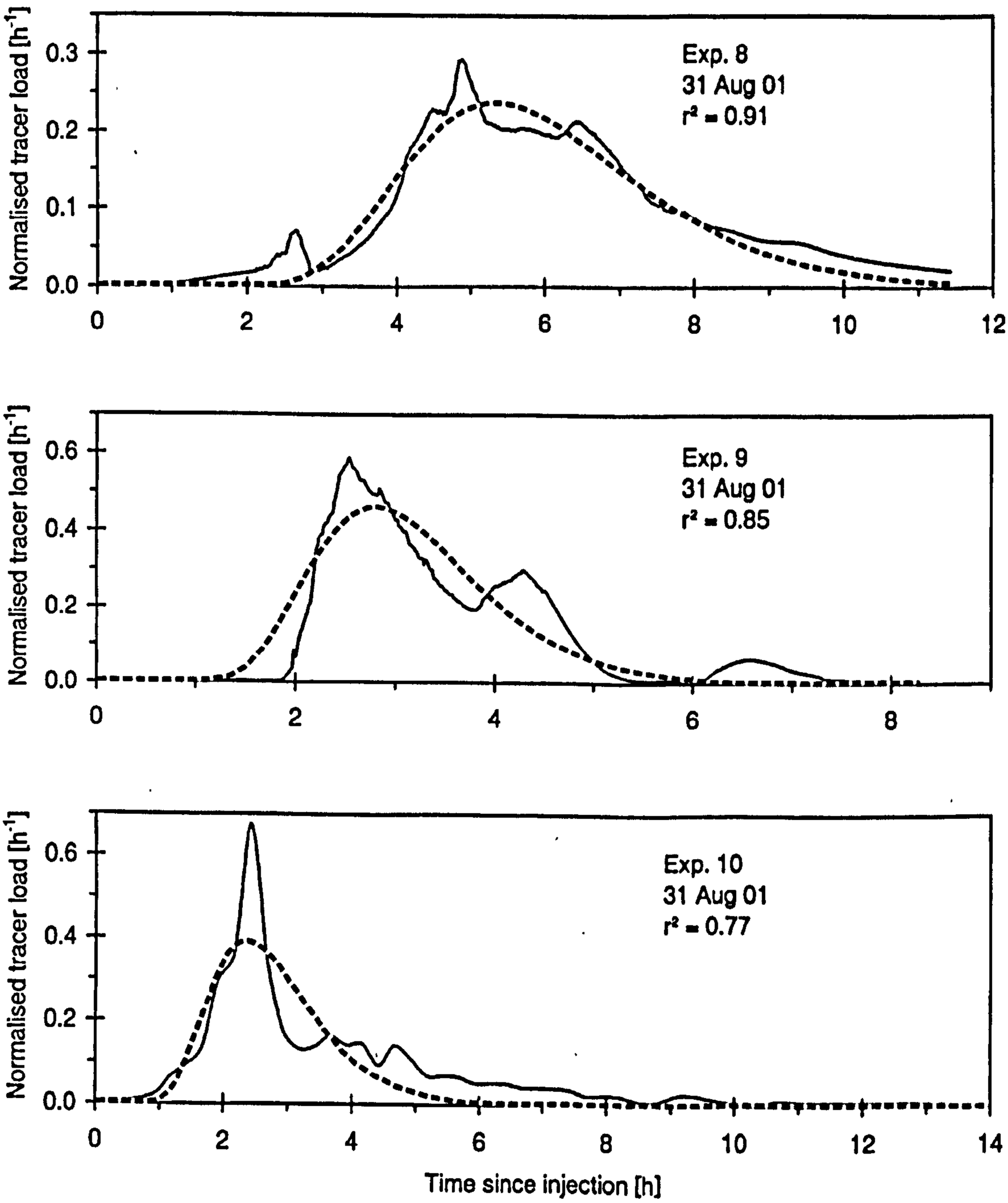

Figure 5.5 cont: Best fit of the normalised tracer return curves (Experiments 8 to 10) using the advection-dispersion model. Experiment number, date and time of the injection and the correlation coefficient (r^2) between measured and modelled curve are shown.

Table 5.2: Calculated parameters derived from tracer breakthrough curves.

Injection No	Date and time of injection	Flow distance [m]	Mean discharge [m^3s^{-1}]*	Flow velocity [ms^{-1}]**	Dispersion coefficient [m^2s^{-1}]	Dispersivity [m]	Estimated tracer recovery [%]***
1	28/08/01 15:07	480	0.075	0.040	1.65	41.2	60
2	28/08/01 15:18	405	0.118	0.045	2.56	76.1	34
3	29/08/01 11:08	570	0.116	0.026	1.31	49.4	75
4	29/08/01 11:14	480	0.116	0.024	1.86	76.8	90
5	30/08/01 10:47	770	n/a	-	-	-	-
6	30/08/01 11:04	765	n/a	-	-	-	-
7	30/08/01 11:18	565	n/a	-	-	-	16
8	31/08/01 12:05	570	0.014	0.026	0.61	23.0	2
9	31/08/01 12:13	565	0.018	0.049	1.19	24.1	1
10	31/08/01 12:20	565	0.016	0.046	1.74	79.6	1

* Mean proglacial discharge during the time of tracer recovery, measured at 15-minute intervals.

** Determined by fitting the advection-dispersion model CXTFIT 2.1 provided by the U.S. Salinity Laboratory to the individual tracer return curves (Toride et al., 1999).

n/a = not applicable

*** The calculated tracer recovery rates are unreliable because of potential capture losses at the snout and discharge estimation errors (Sections 3.2.4.4 and 3.3.2) but provide useful indicators for the estimation of englacial/subglacial storage and other losses from the system.

5.2.2.1 Flow velocities

The flow velocity obtained from modelling the tracer return curves represents the mean flow velocity along the flow passageway (Table 5.2). Flow velocities from experiments undertaken at Glacier de Tsanfleuron range from 0.02 to 0.05 ms^{-1}. When compared to flow velocities found at other glaciers (Table 5.3), these values are amongst the lowest that have been measured. This demonstrates that the tracer has been routed through a hydraulically inefficient drainage system at Glacier de Tsanfleuron as flow velocities of $< 0.2\ ms^{-1}$ generally reflect flow through a hydraulically inefficient distributed drainage system (Hubbard and Nienow, 1997).

Table 5.3: Flow velocities from tracer experiments at different glaciers. n = number of injections, abl = experiments undertaken in the ablation area, acc = experiments undertaken in the accumulation area, m = injections into moulins, c = injections into crevasses, b = injections into boreholes (subglacial).

Glacier	Injection site	n	Flow velocity [ms^{-1}]	Reference
Mikkaglaciären (Sweden)	abl (m, c)	36	0.5-0.7	(Stenborg, 1969)
Hintereisferner (Austria)	abl (m, c)	19	0.2-0.7	(Ambach et al., 1972)
	abl (m)	16	0.5-1.1	(Behrens et al., 1975)
South Cascade Glacier (USA)	abl (m)	14	0.1-0.7	(Krimmel et al., 1973)
	abl + acc (c, m, b)	46	0.02-0.3	(Fountain, 1993)
Aletschgletscher (Switzerland)	abl (m)	2	0.8-1.7	(Lang et al., 1979)
	abl (m, b)	4	0.3-0.9 (m)	(Hock et al., 1999)
Austre Okstindbreen (Norway)	abl (m)	13	0.1-1.8	(Theakstone and Knudsen, 1981)
Pasterzengletscher (Austria)	abl (m)	57	0.03-1.1	(Burkishmer, 1983)
Peyto Glacier (Canada)	abl (m)	18	0.1-0.4	(Collins, 1982)
Findelengletscher (Switzerland)	abl (b in winter)	2	0.008-0.097	(Moeri and Leibundgut, 1986)
Storglaciären (Sweden)	abl (m)	12	0.03-0.16	(Seaberg et al., 1988)
	abl (b)	2	0.01-0.02	(Hooke et al., 1988)
	abl (m)	10	0.07-0.29	(Hock and Hooke, 1993)
	abl (m)	92	0.1-0.5	(Kohler, 1992)
Midtdalsbreen (Norway)	abl (m, c)	19	0.007-0.2	(Willis et al., 1990)
Haut Glacier d'Arolla (Switzerland)	abl + acc (m, c)	533	0.06-0.83	(Nienow, 1993)
Glaciar Zongo (Bolivia)	abl (c)	4	0.1	(Schuler, 1997)
Vernagtferner (Austria)	abl (m, c)	10	0.1-0.9	(Grust, 1998)
Dokriani glacier (India)	abl (m)	10	0.1- 0.5	(Hasnain et al., 2001)
Unteraargletscher (Switzerland)	abl (m)	23	0.2-0.8	(Schuler, 2002)

5.2.2.2 Recovery rates

The tracer recovery rate that is the ratio between recovered and injected tracer mass, can provide information on water storage in the englacial or subglacial drainage system. The recovery rate of a perfect, conservative tracer test would be 100%.

During the 2001 melt-season at Glacier de Tsanfleuron, low surface meltwater input and low bulk discharge appeared to have significantly influenced the recovery rates of the experiments. Tracer recovery rates for the experiments of 28 and 29 August are between 34 % and 90 %, whereas the experiments from 31 August achieved only 1% to 2 % recovery (Table 5.2). The proportion of tracer recovered depends upon a number of factors including tracer adsorption onto sediments (Bencala et al., 1983; Brugman, 1986), retardation or "loss" in storage spaces (e.g. in subglacial cavities) and the quantity of tracer that emerges below the detection limit due to high dispersion of the tracer or an inadequate injection mass (Theakstone and Knudsen, 1981; Willis et al., 1990). Furthermore, recovery rates depend on the precision of the measurements of tracer concentration (instrument and calibration errors) as well as on the accuracy of the discharge measurements (Section 3.3.2).

As discussed in Section 3.2.2, the tracers used at Glacier de Tsanfleuron are suitable tracers under the prevalent field conditions. Tracer concentrations measurements are of high accuracy due to the use of highly sensitive instruments and a meticulous calibration procedure. The factor most likely to introduce inaccurate estimates of tracer recovery rates at Glacier de Tsanfleuron is an imprecise discharge calibration, especially during maximum discharges (Section 3.3.2). Overestimates of discharges would clearly lead to an overestimate in recovery rates and underestimates of discharge having the opposite effect. Any inaccuracies in the discharge record are probably due to the discharge measurements being undertaken in a stream cross-section of unstable geometry. However, the discharge estimates are believed to be accurate to ± 23 % (estimated mean error) and the tracer recovery results can therefore give an approximation of the tracer mass recovered. It is therefore concluded that most of the tracer from Experiments 8 to 10 was delayed in either temporary or long-term storage during decreased meltwater discharge. This is especially likely, given that meltwater inputs at all three injection sites used on 31 August were continuously decreasing after the injection and ceased completely by 01 September after snow fall on the glacier. This drop in meltwater input would likely lead to the isolation of

meltwaters in the subglacial drainage system due to the disconnection of pools and cavities or over-deepenings within Nye-channels during the Experiments 8 to 10.

The high recovery rate of 90 % from Experiment 4 is possibly a result of overlap between Experiments 2 and 4. Experiment 2 was undertaken 20 hours before Experiment 4 and only 34 % of the tracer was detected. The sampling was terminated six hours after injection when discharge was declining, which presumably coincided with temporary storage of tracer. It is therefore possible that dye delivery continued when increased meltwater discharge on 29 August resulted in the reconnection of subglacial storage locations.

Following Experiments 5 and 6 no dye was recovered at the sampling point. Zero tracer recovery can result from the slow release of extremely diluted tracer concentrations from subglacial or englacial storage into the main drainage system (Theakstone and Knudsen, 1981; Willis et al., 1990). Consequently, tracer concentrations emerge at the snout below the detection limit and/or after sampling in the proglacial stream has terminated. This delayed and/or diluted tracer return is more likely in highly distributed systems such as a linked-cavity system (Kamb, 1987). However, since Glacier de Tsanfleuron is underlain by permeable limestone bedrock, dye from Experiments 5 and 6 may not have been detected at the glacier snout due to meltwater drainage into a subglacial sinkhole. The tracer could have disappeared into a sinkhole of the karst system and emerged in a non-monitored area. Evidence from the supraglacial snowmelt record and discharge measurements at the glacier snout (Section 4.4.2) suggest that the catchment area of the proglacial stream comprises only about 4 - 5 % of the entire glacier surface. This finding suggests that injection points 5 and 6 were located outside of the proglacial stream catchment area and meltwater from this area of the glacier was routed into the subglacial bedrock.

5.2.2.3 Dispersivity

As noted in Section 3.2.4.4, in a channel of even roughness and hydraulic radius, the dispersion coefficient (D) is approximately proportional to v (Fischer, 1968; Behrens et al., 1975; Maloszewski, 1992) allowing calculation of dispersivity ($d = D/v$, Section 3.2.4.4). The dispersivity (d) reflects the flow divergence within the drainage passageway between injection and sampling site. All breakthrough curves from the moulin injections showed high dispersivities, ranging from between 23 and 80 m (Table 5.2). Dispersivities > 10 m

generally indicate flow through hydraulically inefficient, distributed drainage systems (Hubbard and Nienow, 1997).

5.2.2.4 Variation of velocity with discharge

The relationship between velocity and dicharge (v-Q relationship) has previously been used to infer whether subglacial drainage occurs under pressurised or atmospheric (open) conditions (Seaberg et al., 1988; Willis et al., 1990; Nienow et al., 1996b; Schuler, 2002a). The relationship between Q and v is linear, if the hydraulic geometry of the channels throughout the time period of observation remains constant. Under open-channel conditions, an increase of Q would cause an increase of the hydraulic geometry, followed by increased flow velocities. This would result therefore in a curvature of the v-Q relationship plot (Figure 5.6). The characteristic of this curvature condition is influenced by the hydraulic radius of the drainage systems (Fountain, 1993; Kohler, 1995)

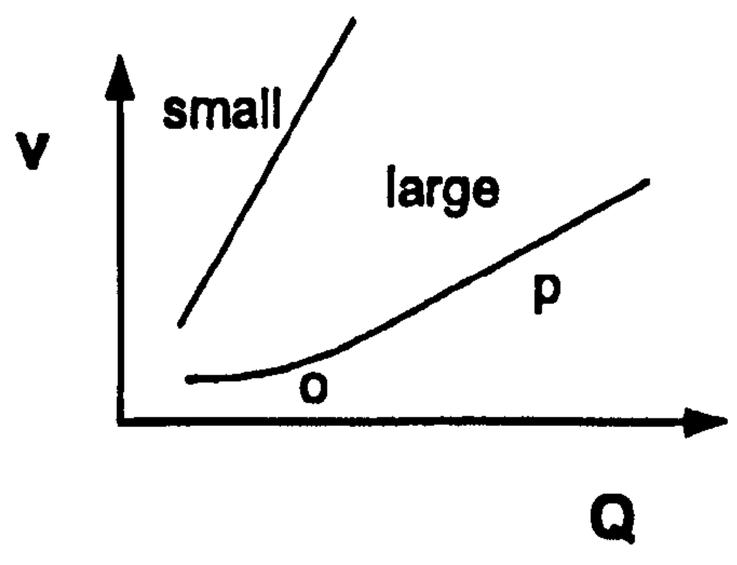

Figure 5.6: Principle of the velocity-discharge relationship for a small and a large drainage system. "o" and "p" indicate sections of water flow in open and pressurised systems (after Schuler, 2002a).

Variations in flow velocities through a subglacial drainage system result from changes of the drainage-system hydraulic structure and/or changes in discharge through the system (Nienow et al., 1996b). At Glacier de Tsanfleuron, there was no correlation found between variations of velocity with discharge and despite a significant discharge decrease, the velocity scarcely varies. This may indicate that at higher discharges a more complex system is used and flow velocities necessarily increase.

5.2.3 Repeated tracer tests

Repeated injections were made into Moulins B and Ciii (Figure 5.1) on different days, using rhodamine WT for the earlier and sodium-fluoresceein for the latter experiments

(Table 5.4 and Figure 5.7). The tracer breakthrough curves from Moulin B (Experiments 1, 28 August and Experiment 4, 29 August) both show multiple-peaks and are highly dispersed with similar timing in onset of tracer recovery. Table 5.4 shows that the flow velocity resulting from Experiment 1 (0.040 ms-1), is about twice as high as for Experiment 4 (0.024 ms-1) but meltwater input to the moulin and the mean bulk discharge at the snout during the tracer test were significantly higher for the latter experiment. The lower mean flow velocity and the higher dispersivity in Experiment 4 at a higher discharge suggest that the tracer was routed through a more complex system than during Experiment 1. Higher mean v at lower Q conditions (Experiments 1 and 4) suggests that the tracer is routed through a more complex system when Q is higher, this is supported by the increased value of inferred d (41 and 77 m respectively). At higher discharges more flow routes, Nye-channels and cavities, became activated perhaps causing a delayed tracer emergence at the glacier snout.

Mean flow velocities obtained from the repeated tracer tests into Moulin C_{iii}, Experiments 3 and 8 (Table 5.4), remained the same, even though the mean discharge was significantly higher during Experiment 3. These findings differ from the behaviour in channelised drainage systems. Given stable hydraulic subglacial conditions, the flow velocity is thought to be directly proportional to the discharge, regardless whether pressurised or atmospheric flow conditions occur (Nienow et al., 1996a). This reflects that at Glacier de Tsanfleuron, the tracer spends most of its transit time in cavities and not in Nye-channels. It is therefore suggested that the extremely slow passage through cavities controls the overall tracer transport. As a result, flow velocities change very little during low and high discharges.

Table 5.4: Repeated tracer injections into Moulins B and C_{iii}.

Injection No.	Moulin	Injection time	Discharge into crevasse [l s^{-1}]*	Mean discharge [m^3s^{-1}]**	Mean flow velocity [ms^{-1}]***	Dispersivity [m]	Tracer recovery [%]****
1	B	28/08/01 15:07	0.10	0.075	0.040	41.2	60
4	B	29/08/01 11:14	0.20	0.116	0.024	76.8	90
3	C_{iii}	29/08/01 11:08	0.50	0.116	0.026	49.4	75
8	C_{iii}	31/08/01 12:05	0.20	0.014	0.026	23.0	2

* estimated

** Mean proglacial discharge during the time of tracer recovery, measured at 15-minute intervals.

*** Determined by fitting the advection-dispersion model CXTFIT 2.1 provided by the U.S. Salinity Laboratory to the individual tracer return curves (Toride et al., 1999).

**** The calculated tracer recovery rates are unreliable because of potential capture losses at the snout and discharge estimation errors (Sections 3.2.4.4 and 3.3.2) but provide useful indicators for the estimation of englacial/subglacial storage and other losses from the system.

Experiment 3 was undertaken under conditions of significantly higher melt and discharge than Experiment 8. This had a significant impact on the recovery rates (75% and 2 % respectively) but did not greatly impact on the starting time and tailing of tracer recovery (Figure 5.7). Both return curves show several peaks suggesting several flow passageways. Peaks occurred at different times, but the overall shape of the return curves and their tailing appeared broadly similar, implying that on both days the water travelled through the same passageways, perhaps at slightly different proportions. This is also emphasised by the flow velocities, which were the same for both curves (0.026 ms^{-1}). From this result, it is suggested that no evolution of englacial and subglacial passageways has taken place between 29 and 31 August.

To summarise, the quantitative analyses of the tracer return curves discussed above re enforces the concept of an inefficient, subglacial drainage system.

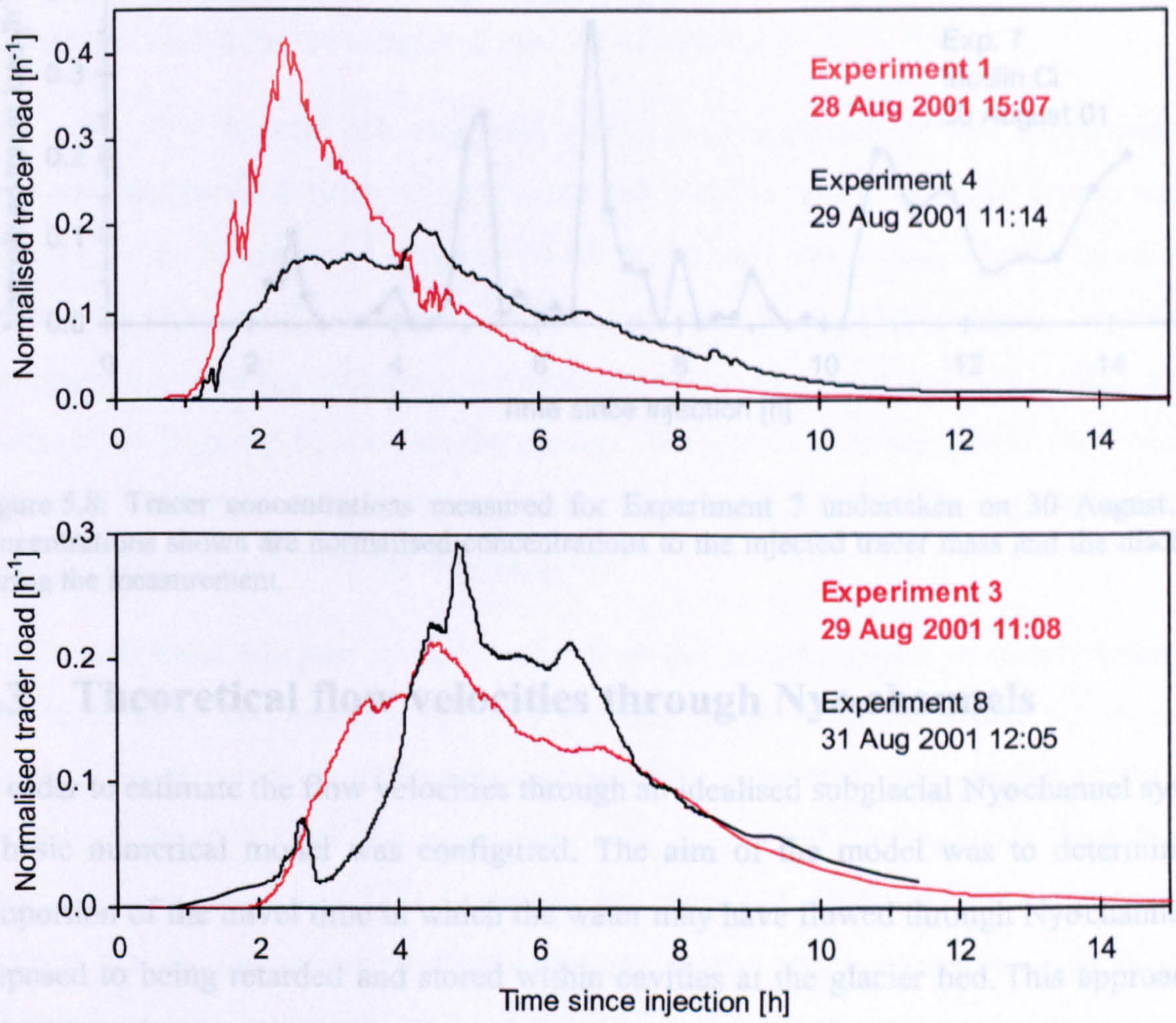

Figure 5.7: Normalised tracer return curves from (a) Experiments 1and 4 and (b) Experiments 3 and 8 undertaken between 28 and 31 August (for further information refer to Table 5.1).

5.2.4 Lithium returns

The lithium concentrations measured from Experiment 7 appear to be random and are unlike a typical tracer breakthrough curve (Figure 5.8). Of the 43 samples taken, the concentrations of 33 samples were above background, varying between 0.1 and 3.0 µg l^{-1}. Elevated concentrations for 77 % of the samples give clear evidence for the existence of a flow connection between the injection and detection site. The tracer return from Experiment 9, undertaken one day later at the same moulin, confirms this link (Figure 5.3). However, the relatively low concentrations detected and the irregular tracer output was possibly a result of tracer storage in subglacial cavities and subsequent periodic release into the main flowpath. Therefore, the curve resulting from the LiCl Experiment 7 could not be used to obtain quantitative information concerning the subglacial drainage conditions.

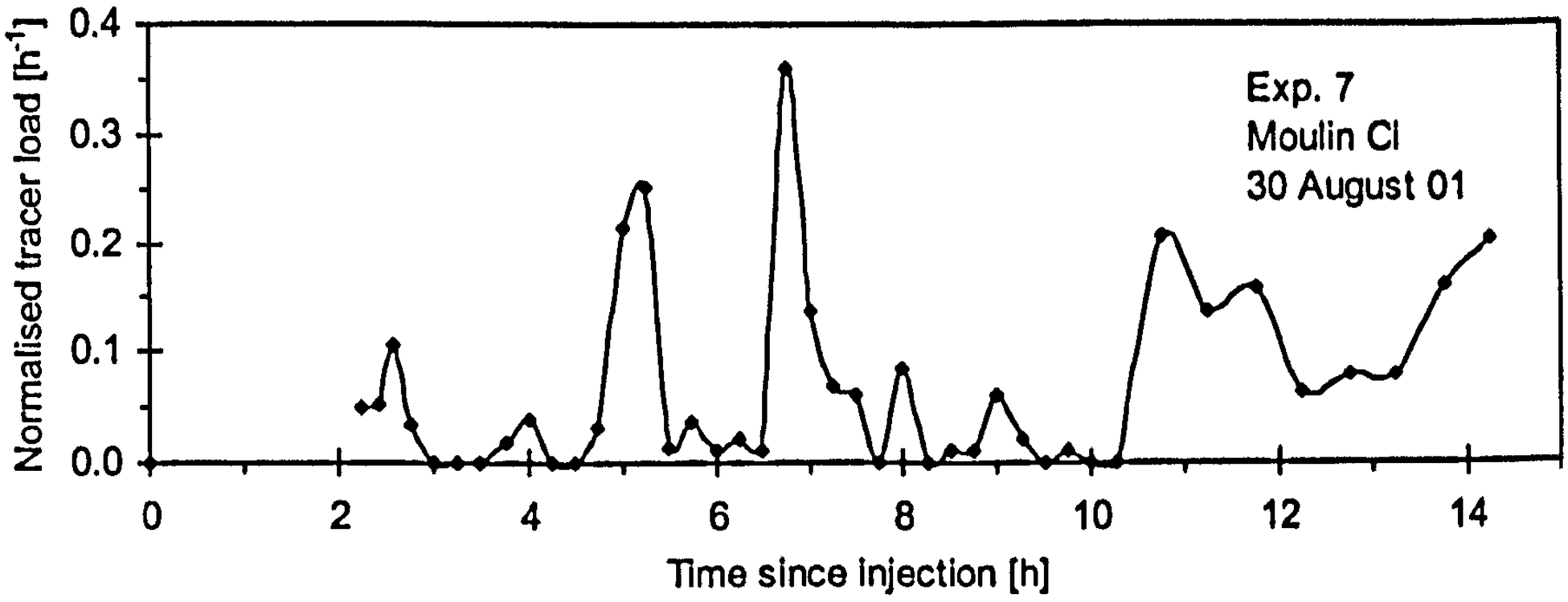

Figure 5.8: Tracer concentrations measured for Experiment 7 undertaken on 30 August. The concentrations shown are normalised concentrations to the injected tracer mass and the discharge during the measurement.

5.3 Theoretical flow velocities through Nye-channels

In order to estimate the flow velocities through an idealised subglacial Nye-channel system, a basic numerical model was configured. The aim of the model was to determine the proportion of the travel time in which the water may have flowed through Nye-channels as opposed to being retarded and stored within cavities at the glacier bed. This approach of using flow-theory of turbulent flow has been applied in previous studies to determine the influence of various parameters such as channel geometry, hydraulic gradient and roughness characteristics in order to explain observed water flow velocities through subglacial drainage systems (Iken and Bindschadler, 1986; Seaberg et al., 1988; Willis et al., 1990; Hock and Hooke, 1993). Here, it is adopted to estimate flow velocities through the subglacial drainage system independently from dye tracer experiments. This allows comparison of theoretical flow velocities with measured flow velocities from dye tracer experiments. Parameters such as straight-line flow distance, elevation gradient between injection and detection point, roughness of the bedrock and width and depth of the channel (from the glacier forefield) were adopted for the model.

5.3.1 Model description

This section describes the model that was used to calculate variations of flow velocities through a system of Nye-channels. The known parameters of the model are elevation difference and straight horizontal flow distance between injection and sampling points.

Four parameters (ice thickness, Manning "n" for Nye-channels, channel width and channel depth) were altered for the subglacial passage of meltwater.

The water flow through the englacial system was neglected on the supposition that meltwater spends the majority of travel time within the subglacial drainage system and only a short time in the englacial system, relative to the total travel time. This is based on the appearance of a heavily crevassed lower tongue area of the glacier due to which water apparently travelled approximately vertically down to the glacier bed. The model setup is illustrated in (Figure 5.9) showing the passage of water entering the glacier via moulins or crevasses at the injection point then, passing through the englacial drainage system before being routed subglacially to the sampling point.

Within subglacial drainage systems water flow can be pressurised, or under atmospheric conditions when the conduits are only partially filled. Pressurised flow occurs mostly during times of enhanced surface melting and thus, exhaustion and destabilisation of the capacity of the subglacial drainage passageways (Stone and Clarke, 1996; Gordon et al., 1998; Nienow et al., 1998). However, as suggested from dye tracer experiments (Section 5.2) the pressurised subglacial drainage system may not have occurred during the 2001 melt season. Therefore, flow velocities in Nye-channels were modelled by applying variable parameters to the Manning-Gauckler-Strickler-equation under atmospheric conditions (Williams, G.P. 1970, cited in Röthlisberger, 1972):

$$v_{pre} = \frac{R^{2/3} \cdot S^{1/2}}{n}, \qquad (5.1)$$

where v_{pre} represents the predicted water velocity in the conduit, R the hydraulic radius of the channel, S the hydraulic gradient and n the Manning roughness coefficient. R was derived from:

$$R = \frac{A}{p}, \qquad (5.2)$$

where A is the cross-sectional area and p the wetted perimeter of the conduit.

5.3.2 Model application

Modelling flow velocities through a system of Nyc-channels using the Manning-Gauckler-Strickler-equation requires values for the hydraulic gradient, roughness parameter for the Nye-channels (Manning *n*) and the hydraulic radius of the channel. Considering the conditions of the subglacial drainage system at Glacier de Tsanfleuron, three values (minimum, maximum and mean) were chosen for each parameter as given in Table5.5. The criteria for selection of the end members and the mean for each of the parameters are explained below.

Table 5.5: End members and one intermediate value of variable parameters as used for the model application.

Variable parameters	Minimum	Mean	Maximum
1. Slope	8°	10°	12°
2. Manning "n" for Nye-channels	0.01 $m^{-1/3}s$	0.02 $m^{-1/3}s$	0.03 $m^{-1/3}s$
3. Channel width	0.03 m	0.09 m	0.3 m
4. Channel depth	0.01 m	0.08 m	0.2 m

Minimum, maximum and mean slope angles were calculated using the altitude at the injection and sampling points (2600 and 2450 m a.m.s.l.) to obtain the maximum possible ice thickness. The maximum possible ice thickness would equate to a slope angle of zero degrees. Utilising ice-core measurement data (Hubbard et al., 2003), the minimum and maximum ice thickness (between 40 and 80 m) was determined and used to obtain the approximate altitude difference between glacier bed, immediately beneath the injection area and the sampling area at the glacier snout. From this, a slope angle of between 8 and 12 degrees was calculated Figure 5.9.

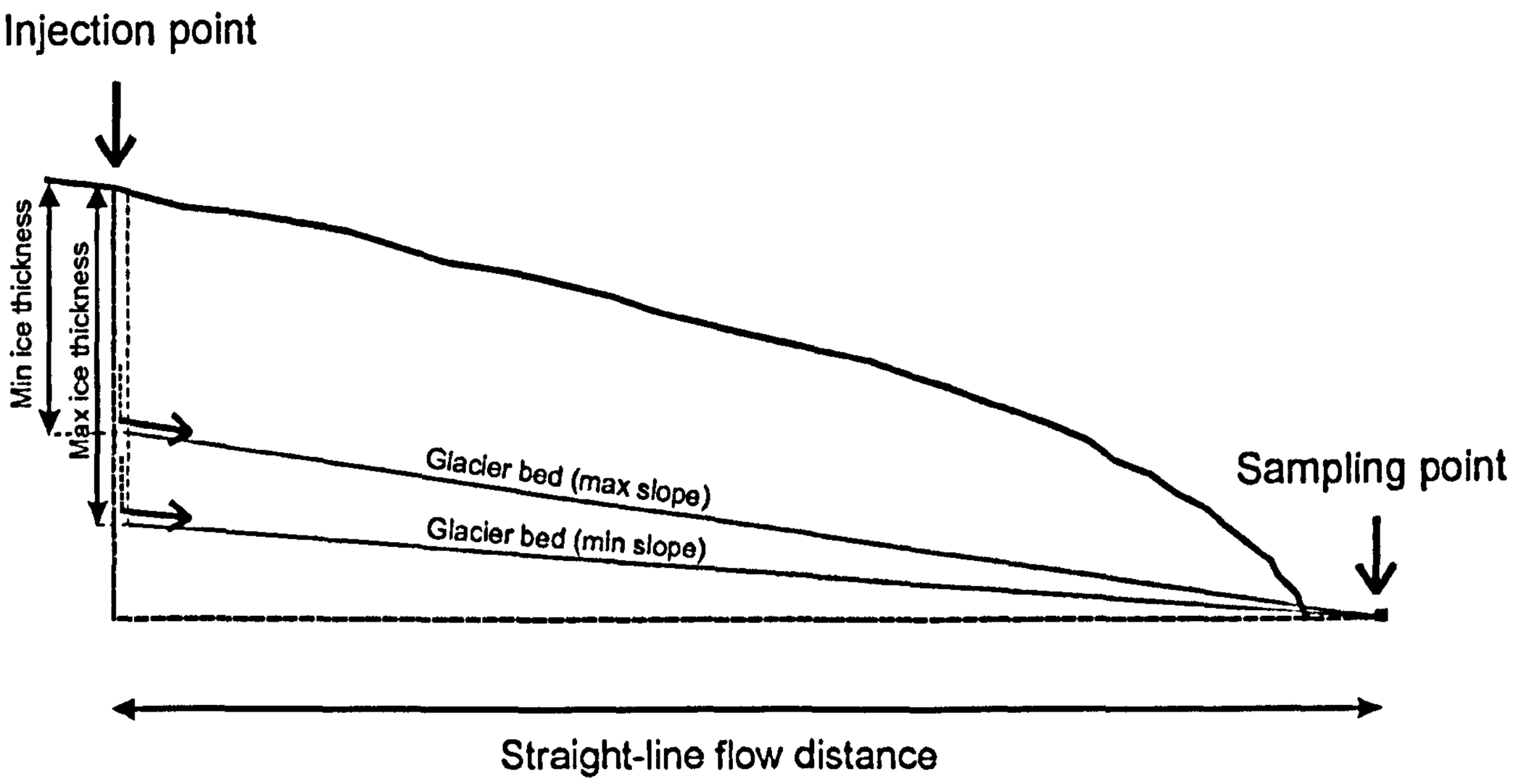

Figure 5.9: Sketch demonstrating gradient determination of glacier bed as used to estimate Nye-channel flow velocities.

Manning's *n* is an empirically derived parameter to quantify channel roughness. Röthlisberger (1972) suggested 0.01 $m^{-1/3}s$ as a value of *n* for straight, smooth pipes, 0.02 $m^{-1/3}s$ for channels of "medium roughness" and 0.1 $m^{-1/3}s$ for "boulder-strewn" channels. Seaberg et al. (1988) used a roughness coefficient *n* of 0.2 $m^{-1/3}s$ to describe characteristic flow along irregular sinuous channels over boulder-strewn bedrock that is both roughened by plucking and smoothed by glacial abrasion. The Nye-channels at Glacier de Tsanfleuron are not boulder-strewn, so that values as high as 0.1 $m^{-1/3}s$ or above can be excluded. In previous applications concerning subglacial properties at several other glaciers, (Bates et al., 2003) used Manning *n* values of 0.03 $m^{-1/3}s$ for Nye-channels at Glacier de Tsanfleuron, (Fountain, 1993) used 0.04 $m^{-1/3}s$ for a system of linked-cavities or paths of interconnected debris and (Willis et al., 1990) used 0.05 $m^{-1/3}s$ for a smooth-walled, straight ice-bound channel. This demonstrates that the range of the subglacial roughness varies between glaciers. From the above argument, and the fairly smooth nature of the limestone, a roughness coefficient for the Nye-channels at Glacier de Tsanfleuron of between 0.01 $m^{-1/3}s$ and 0.03 $m^{-1/3}s$ appears appropriate.

The width and depth of 57 randomly chosen Nye-channels was measured in the proglacial area. From these measurements, Nye-channels at Glacier de Tsanfleuron are found to have a mean width of 0.09 m (standard deviation, σ = 0.05) and a mean depth of 0.08 m

(standard deviation, $\sigma = 0.06$). The channel width ranged between 0.03 and 0.3 m and the channel depth between 0.01 and 0.2 m, the model parameters were chosen accordingly.

The appearance of the exposed Nye-channels observed in the proglacial area (Figure 5.10 and Appendix C) and their close width to depth ratio of 1.0 : 0.9 (Figure 5.11) suggests that these channels were frequently completely water filled. Otherwise, commonly low water levels would probably have caused a V-shaped erosion and therefore ratios of larger depths than widths. However, the discharges measured at the glacier snout and the low snow-line during the 2001 melt-season imply that the channels may not have been completely filled even during times of high melting in the summer 2001.

Figure 5.10: Nye-channels in the proglacial area of Glacier de Tsanfleuron.

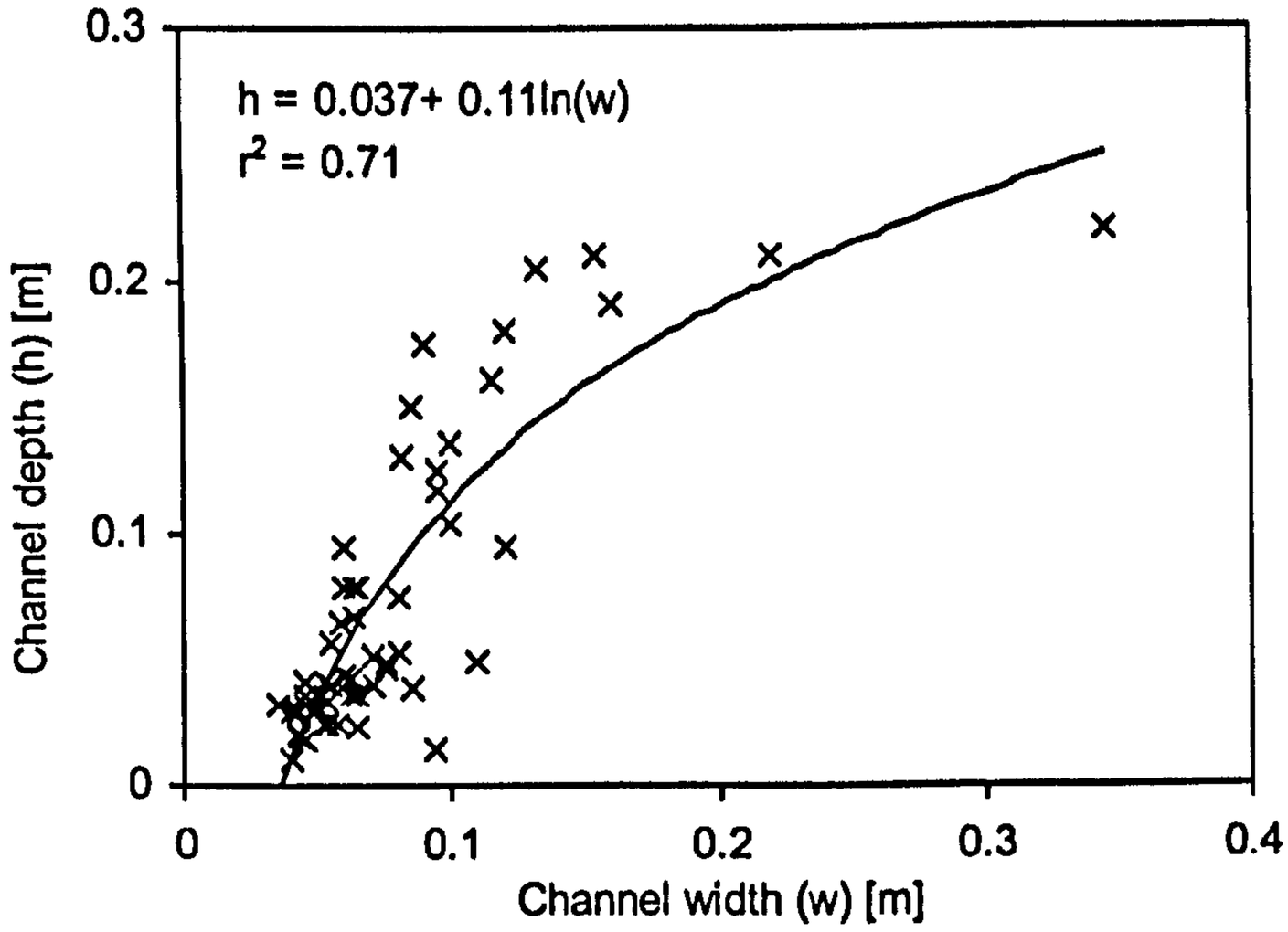

Figure 5.11: Logarithmic correlation between channel width and channel depth, $r^2 = 0.71$.

The values for each parameter were applied to the model in all 81 possible combinations and statistically analysed.

5.3.3 Model results and further considerations

The statistics for the modelled water flow velocities through a subglacial Nye-channel system is summarised in Table 5.6. Careful characterisation of the predicted data is necessary to evaluate whether subglacial flow velocities can be modelled using values obtained from hydraulic reconstruction of the subglacial conditions.

Table 5.6: Statistical characteristics of the predicted flow velocities through Nye-channels.

Statistical property	Flow velocity [m s^{-1}]
Minimum	0.4
Maximum	9.0
Mean	2.2
Median	1.7
Standard deviation	1.8
Kurtosis	3.4
Skewness	1.8

The 81 modelled water flow velocities range from 0.4 to 9.0 ms^{-1}. The relatively high kurtosis of 3.4 suggests a distinct peak around the mean and the positive skewness value of

1.8 implies an asymmetric distribution of data towards the left (lower values). The presentation of the modelled results, in groups of similar flow velocity, graphically demonstrates this data distribution (Figure 5.12). It also shows that about 40 % of the predicted data range between 0.5 and 1.5 ms^{-1}, about 70 % between 0.5 and 2.5 ms^{-1} and only about 10 % exceed velocities over 4.5 ms^{-1}. This suggests that the hydraulic conditions in Nye-channels, as modelled using the observed channel characteristics at Glacier de Tsanfleuron, produce flow velocities that are most likely around the arithmetic mean. Fastest predicted flow velocities relate to large channel width and/or depth and low channel roughness, whereas lowest predicted flow velocities relate to a low channel depth and high channel roughness.

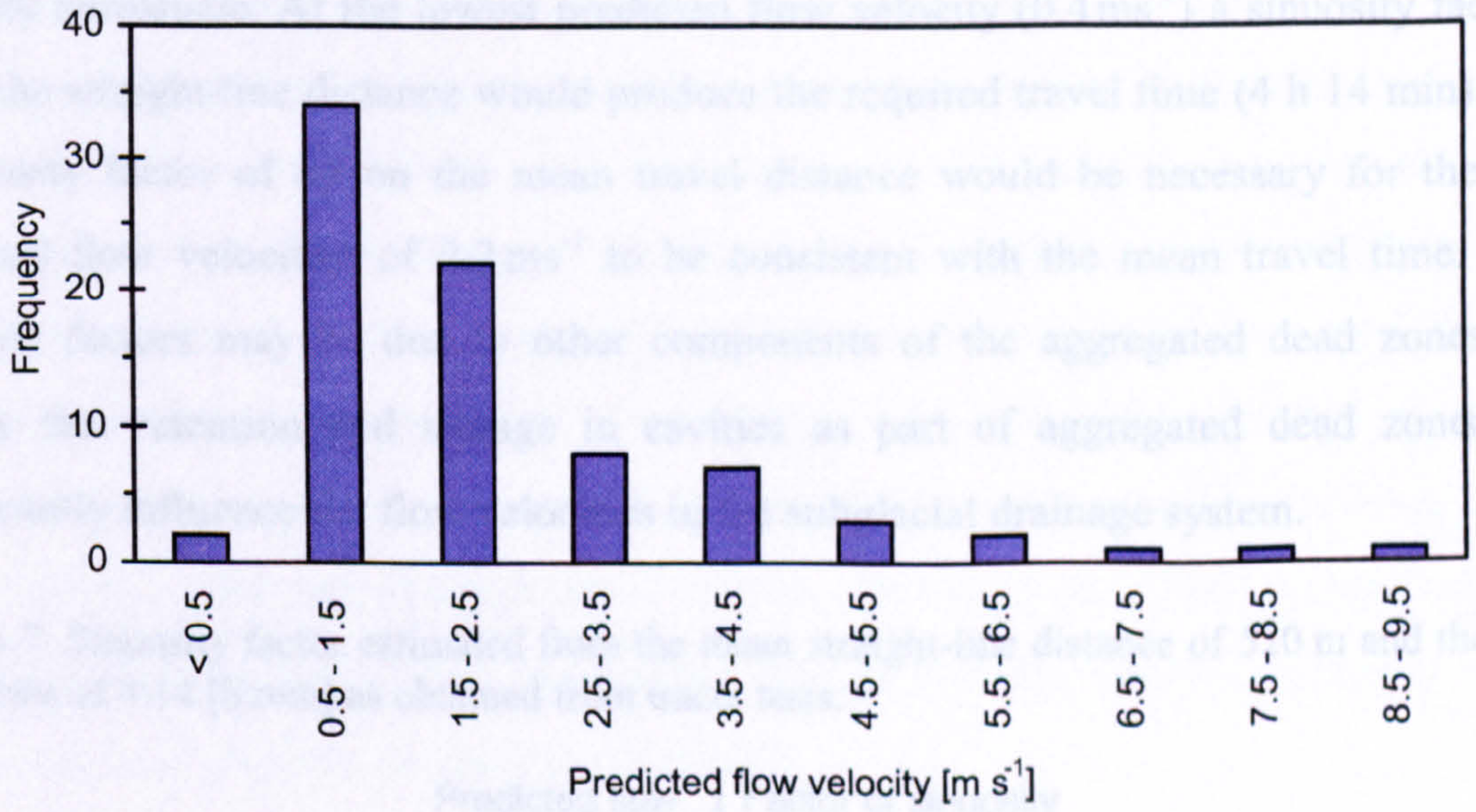

Figure 5.12: Frequency of predicted flow velocities through Nye-channels (n = 81).

The calculated flow velocities through a Nye-channel system were compared with the measured flow velocities (Table 5.2). Regardless of which parameter combination was used, the predicted flow velocities were always significantly faster than the observed values. The predicted mean flow velocity (2.2 ms^{-1}) is more than two orders of magnitude higher than the observed mean flow velocity from tracer tests (0.04 ms^{-1}).

In any natural flow system elements such as channel sinuosity, storage and ponding have an effect on the water flow. These elements have been amalgamated in the hydrological term of aggregated dead zones (Young and Wallis, 1993). Due to the inability to measure or observe the individual components, subglacial aggregated dead zones are impossible to define, but the aggregated dead zones can be considered to be a virtual sinuosity (time

taken by flow divided by time taken for direct flow by the shortest path) in the following paragraph. It is unlikely for a subglacial Nye-channel drainage system to develop straight flow routes between injection and detection points, the channel sinuosity, expressing the additional length of the flowpath was the only parameter taken into account. The parameter for sinuosity was included for comparison of measured and modelled flow velocities.

Sinuosity factors on the mean straight-line distance obtained from tracer experiments (520 m) at different predicted flow velocity that would increase the travel distance, so that the travel time of 4 h 14 min (mean travel time obtained from tracer experiments) resulted, are presented in Table 5.7. From the inspection of the Nye-channels in the proglacial area at Glacier de Tsanfleuron, it is suggested that factors of sinuosity greater than 4are probably unrealistic. At the lowest predicted flow velocity ($0.4\,ms^{-1}$) a sinuosity factor of 12 on the straight-line distance would produce the required travel time (4 h 14 min). Also, a sinuosity factor of 65 on the mean travel distance would be necessary for the mean predicted flow velocities of $2.2\,ms^{-1}$ to be consistent with the mean travel time. These sinuosity factors may be due to other components of the aggregated dead zones. This implies that retention and storage in cavities as part of aggregated dead zones must significantly influence the flow velocities in the subglacial drainage system.

Table 5.7: Sinuosity factor estimated from the mean straight-line distance of 520 m and the mean travel time of 4:14 [h:mm] as obtained from tracer tests.

Predicted flow velocity [ms^{-1}]	Factor of sinuosity
0.4*	12
1.0	29
1.5	44
2.0	59
2.2**	65

* Maximum predicted flow velocity
** Mean predicted flow velocity

Under a maximum sinuosity of factor 4 the proportion of time that water flows through Nye-channels as opposed to its time spend in cavities was calculated (Table5.8). At the highest predicted flow velocities ($0.4\,ms^{-1}$) the water would spend 34 % of the travel time in Nye-channels and 66 % in cavities respectively. Using the mean predicted flow velocity of $2.2\,ms^{-1}$ for this calculation, water would theoretically spend only about 6% of its travel time in Nye-channels and 94 % in cavities.

Table 5.8: Estimated proportion of time water flows in Nye-channels as opposed to in cavities. The calculation is based on the mean straight-line distance of 520 m, a sinuosity factor of four (therefore, a total flow distance of 2080 m) and the mean travel time of 4:14 [h:mm] as obtained from tracer tests.

Predicted flow velocity [ms^{-1}]	Proportion of time in a Nye-channel [%]	Proportion of time spend in a cavity [%]
0.4*	34	66
1.0	14	86
1.5	9	91
2.2**	6	94

* Maximum predicted flow velocity
** Mean predicted flow velocity

In order to compare the proportion of the travel distance that the water may have spend in Nye-channels as opposed to in cavities, the mean travel time of 4 h 14min as obtained from tracer tests was predicted by combinations of Nye-channel flow with cavity flow. The flow distance within cavities or Nye-channels was constrained by the total travel time and the inferred flow velocities for each of the drainage types. Consistent to previous calculations, a mean straight-line travel distance of 520 m and a sinuosity factor of 4 were inferred. Flow velocities considered for the passage of Nye-channels were adopted from modelled flow velocities (Section 5.3.3) and flow velocities of 0.01 and 0.007 are used as possible velocities through cavities as interpreted as such from tracer tests at Storglaciären, Sweden (Hooke et al., 1988) and Midtdalsbreen, Norway (Willis et al., 1990) respectively. The proportion of distance that water would flow through Nye-channels as opposed to cavities at different flow velocities is shown in Table 5.9.

Table 5.9: The proportion of the travel distance that water flows in Nye-channels, opposed to cavity-flow. The mean travel time of 4:14 [h:mm] as observed from tracer tests is assuming the mean straight-line distance of 520 m, a sinuosity factor of 4 (therefore, a total flow distance of 2080 m) and varying flow velocities through Nye-channels and cavities.

Flow velocity Nye channel [ms^{-1}]	Flow velocity cavity [ms^{-1}]	Proportion of Nye-channel travel distance [%]	Cavity travel distance [%]
0.4*	0.007	97	3
1.0	0.007	96	4
1.5	0.007	95	5
2.2**	0.007	95	5
0.4*	0.01	52	48
1.0	0.01	52	48
1.5	0.01	51	49
2.2**	0.01	51	49

* Maximum predicted flow velocity
** Mean predicted flow velocity

Under the consideration that flow velocities through the cavities of 0.007 ms^{-1} and velocities through Nye-channels of between 0.4 and 2.2 ms^{-1}, the proportional distance that water spends in cavities is only 3 % to 5 %. It is remarkable that variations of the flow velocities through Nye-channels of more than an order of magnitude do not have a great impact on the proportion of the distance that water spends in cavities or Nye-channels. Water flow velocities through cavities of 0.01 ms^{-1} and varying velocities through Nye-channels resulted in the proportional distance of 48 % to 49 % that water spends in cavities as opposed to in Nye-channels. These results imply that the proportional distance that the water spends in cavities and Nye-channels respectively, is controlled by the water flow velocity in cavities and that the conditions in Nye channels, responsible for velocity variations are inconsequential.

5.4 The role of sinkholes

The number and size of sinkholes beneath Glacier de Tsanfleuron is unknown, but from the discrepancy between meltwater production at the glacier surface and the discharge volume at the proglacial stream (Section 4.5) it is apparent, that only a small proportion of supraglacially generated meltwater exits at the glacier snout. Some of the water may be temporarily stored in englacial or subglacial cavities, but most of it probably runs off through the karst system beneath the glacier. This finding is also supported by (i) the observation of a number of sinkholes in the glacier forefield (Sharp et al., 1989) and (ii) a flow connection, detected by dye tracing, from a sinkhole in the forefield to a spring (Source de Glarey), SE of Glacier de Tsanfleuron, at an altitude of about 1500 m a.m.s.l. (Masotti, 1991). Thus, it is very likely that sinkholes also exist beneath the present glacier. Sinkholes beneath the glacier will influence the subglacial flow conditions by influencing the likelihood and magnitude of pressurised subglacial conditions Generally, water beneath a glacier becomes pressurised if the water inputs exceeds the available capacity of the subglacial drainage system (Hubbard et al., 1995; Gordon et al., 1998). During high meltwater input water can be forced out of available channels and distributed across the glacier bed. This may decouple the glacier or parts of it from its bed, resulting in enhanced basal motion due to reduced frictional drag (e.g. Iken, 1981; Iken and Bindschadler, 1986; Kamb, 1987; Hooke et al., 1989; Iken and Truffer, 1997; Fischer et al., 1999; Mair et al., 2002; Bingham et al., 2003).

If sinkholes are present beneath the glacier, water is released at these points and atmospheric flow conditions occur. Therefore, the spatial extent of pressurised subglacial conditions during times of high water input is dependent on the density and capacity of sinkholes. At low sinkhole densities pressurised conditions are more likely and the observation of transient ice flow phenomena such as "spring events" and diurnal cyclicity would be expected (Iken and Bindschadler, 1986; Hooke, 1989; Mair et al., 2001; Harper et al., 2002).

During the 2001 melt-season the glacier's dynamics, as related to its hydrological characteristics were studied and are explained in Chapter 6.

5.5 Discussion

Findings from dye tracing

The obtained low flow velocities from the tracer tests of between 0.02 and 0.05 ms^{-1} and dispersivities of between 32 and 80 m respectively suggest that the water in the subglacial drainage system is routed through a hydraulically inefficient subglacial drainage system (Willis et al., 1990; Hock and Hook, 1993; Nienow et al., 1998) (Chapter 3.2.4.4). Variations in flow velocities through a subglacial drainage system result from changes in the drainage-system hydraulic structure and/or changes in discharge through the system (Nienow et al., 1996c). It appears that at Glacier de Tsanfleuron flow velocities are either controlled by the system complexity or by the time that water is delayed by cavity flow.

Low recovery rates during times of low discharge indicate temporary storage of the tracer, possibly due to the disconnection of cavities during the tracer transit; cavities were perhaps reconnected at times of higher discharge. The high dispersion of the tracer return curve, indicated by high dispersivities (23 to 80 m) may be a result of long residence times in cavities during the passage of the tracer through the glacier and its gradual release back into the main hydrological system. However, the described flow characteristics could possibly also have resulted from flow through thin subglacial films (Weertman, 1972, 1983). The observation of laminated carbonate crusts in the forefield of Glacier de Tsanfleuron(Sharp et al., 1989; Hubbard and Sharp, 1993; Hubbard and Hubbard, 1998) suggests that such subglacial films have existed in the past. They probably formed during the refreezing of subglacial meltwater resulting in solute concentration and mineral precipitation (Hubbard

and Hubbard, 1998). A detailed explanation of such geochemical processes is given by Hallet (1976). Furthermore, inefficient water drainage as observed from tracer experiments could result in retardation and storage in the englacial system as opposed to in the subglacial drainage system (e.g. Fountain, 1993).

The detection of flow connections between moulins and the proglacial stream at lower altitudes (Moulins A to C, 2585 to 2615 m a.m.s.l.), but no apparent connection between the upper Moulins D (about 2640 m a.m.s.l.) supports a similar, but slightly larger proglacial stream catchment area than the estimated area of between 2500 and 2600m a.m.s.l. (about 4 % of the glacier surface area). This 4 % proportion was estimated from the quantities of supraglacial meltwater production and the measured discharge quantity in the proglacial stream (Section 4.5). Moulins C are at about 2615 m a.m.s.l., therefore it is necessary to extend the proposed proglacial catchment area to an altitude range of 2500 to 2620 m a.m.s.l., which covers about 5 % of the proglacial stream catchment area. It is concluded that meltwater of the remaining 95 % surface area are drained through the karst bedrock system.

Findings from numerical modelling

Modelled flow velocities through Nye-channels generated flow velocities of between 0.4 and 9.0 ms^{-1} (n = 81). These values overestimate the measured mean flow velocities from 0.02 ms^{-1} to 0.05 ms^{-1} (n = 7) obtained from tracer tests by more than two orders of magnitude. The sinuosity of Nye-channels as it would occur naturally, cannot explain this discrepancy adequately. With the consideration of a drainage network consisting of cavities and Nye-channels accounting for storage and retention effects in cavities, measured transit times were projected realistically. It also demonstrated that in such a linked-cavity configuration water would spend the minority of its transit time in Nye-channels as opposed to in cavities. Similar findings led Walder (1986) to the conclusion that the time water flows through the connections between cavities can be ignored. This concurs with the mapping achieved by Sharp et al. (1989) that approximately 64 % of the distance of the drainage passage ways are Nye-channels. The complementary use of experimental tracer results and theoretical findings that are based on observations of drainage conditions in the glacier forefield indicate that the present subglacial drainage system probably has a similar configuration to the former glacier bed that is exposed in the proglacial area.

However, the model calculations were highly simplified and possible impacts on water flow characteristics due to englacial drainage were not specifically taken into account. It has been realised that englacial routing of water may have an important impact (Fountain, 1993). Because of the inaccessibility of the glacier bed it remains difficult to differentiate between subglacial and englacial flow processes. The results from this study indicate that storage and retention largely effects water flow through the glacier. These storage effects could have been present in both englacial and subglacial drainage systems.

5.6 Conclusions

The aims of this chapter were to characterise the flow conditions of the subglacial drainage system of Glacier de Tsanfleuron during the 2001 melt-season. The conclusions were drawn from quantitative analyses of tracer experiments and from theoretical calculations of Nye-channel flow velocities, mainly based on conditions observed in the glacier forefield.

The flow characteristics obtained from dye tracer experiments are low flow velocities (0.02 to 0.05 ms^{-1}) and high dispersion (dispersivity of between 23 and 80 m). This suggests that the water is subglacial drained hydraulically inefficiently (Willis et al., 1990; Hock and Hooke, 1993; Nienow et al., 1998). Low recovery rates during times of low discharge imply transitory storage of the tracer, perhaps due to the disconnection of cavities during the tracer transit, cavities were perhaps reconnected at times of higher discharge. An inefficient drainage system with similarly low flow velocities can be projected theoretically by assuming a cavity system linked by Nye-channels in which the water travels most of the distance through Nye-channels, but is significantly delayed in cavities, due to temporary storage processes (Section 5.3). This is in agreement with the configuration of the former glacier bed that is exposed in the proglacial area. However, precipitated carbonate crusts that have also been observed in the forefield of Glacier de Tsanfleuron suggest that subglacial water films exist subglacially temporarily (Sharp et al., 1989; Hubbard and Hubbard, 1998). Film flow can occur due to meltwater produced at the ice-bedrock interface by frictional and geothermal heat generation (Weertman, 1972, 1983). Film flow would probably also occur when the capacity of the Nye-channel-cavity network is exceeded. This would result in overflowing drainage passageways and storage spaces and therefore increasing subglacial water pressure. If the subglacial water pressure increases enough and over an area large enough to decouple the glacier from its bed, increased rates

of basal sliding due to reduced frictional drag could result. As discussed in Section 5.4, the spatial extent of subglacial water pressures is also controlled by the density of subglacial sinkholes. Impacts that the subglacial drainage conditions may have had on glacier dynamics are discussed in Chapter 6. The results from glacier surface dynamics may also elucidate whether film flow has existed temporarily at the glacier bed during the summer of 2001.

6 Ice dynamics at Glacier de Tsanfleuron 2001

6.1 Introduction

This chapter presents and interprets the results of the surveying programme undertaken at Glacier de Tsanfleuron during the 2001 melt season to determine seasonal variations in ice dynamics. This is of major interest because variations in glacier motion are to a great extent related to changes of the hydrological conditions at the ice-bed interface. The links between glacier motion and subglacial hydrology have been recognised in the literature (Chapter 2.5.3). However, the impact of a linked-cavity subglacial drainage system on intra-seasonal variations in glacier sliding and thus dynamics is unknown. Accordingly this study uses measurements of surface motion at Glacier de Tsanfleuron to determine links between ice motion and the glacier hydrology of the linked-cavity drainage system at Glacier de Tsanfleuron.

More specifically, the aims of this study were to determine

(i) whether there was a seasonal variation in glacier surface motion during the 2001 melt season;

(ii) whether any variations in surface motion are related to variations in meltwater production at the glacier surface and

(iii) whether variations in surface motion are coupled with changes in subglacial drainage conditions.

In order to address these aims, a stake network of 26 stakes was set-up across the glacier and the position of the stakes surveyed regularly. The results of this survey are presented in Section 6.2. Short-term spatial and temporal variations in ice dynamics between late June and late August are presented in Section 6.3. The degree to which the ice-dynamics reflects changes in the glacio-hydrological system is discussed in Section 6.4. Section 6.5 summarises the findings of the investigations into ice dynamics during the course of the 2001 melt-season.

6.2 Survey results

Graphed time series data of horizontal glacier surface velocities and vertical displacements for all available measurements from all stakes are provided in Appendix D. The horizontal surface velocities appeared to be highly variable throughout the melt season at all stakes. The amplitudes varied between 1 cm d^{-1} and 11 cm d^{-1} (40 m a^{-1}). In order to glean useful information from the survey of the marker stakes during the 2001 field season at Glacier de Tsanfleuron more detailed analyses were required. In Table 6.1 mean horizontal surface velocities are presented. These values were obtained from the first (26 June 2001) and the last (21 or 24 August 2001) survey of each individual stake. Mean horizontal surface velocities of the individual stakes vary from 1.8 cm d^{-1} (Stake $65S_1$, 2745 m a.m.s.l) to 5.6 cm d^{-1} (Stake 10, 2640 m a.m.s.l) and these velocities are generally higher at lower altitudes than at higher altitudes. In general stakes at lower altitudes moved faster than stakes at higher altitudes. This is not an unusual trend and has been observed at other glaciers (Hodge,1974; Willis, 1995) (Chapter 2). The relatively fast velocity of Stake 15 and the unexpectedly slow velocity of Stake 25 S_2 can perhaps be explained by this location in a highly crevassed area where an irregular pattern of surface movement would be expected due to the opening of crevasses.

An overview of the surface dynamics was gained by extrapolating the horizontal surface velocities of the individual stakes (Figure 6.1b). The surface velocities as presented in Figure 6.1b, were produced using the graphics software "SURFER" (Golden Software, Inc.). This type of data presentation by interpolation between individual data points (stakes) and glacier margins gives a useful visualisation of the data in the relevant area, but it must be borne in mind that the only real data points are the stake positions for which data was collected. Velocities at glacier margins were considered to be negligible suggesting values of 0 m d^{-1} along the glacier boundaries. This is clearly not the real case but provides a fair approximation since this is consistent with the standard model of glacier motion (Benn & Evans, 1998). The SURFER plot does not indicate the suggested error at each data point and can only be considered valid with the confidence that the errors do not exceed the presented value. The error analysis procedure was presented in Section 3.4.3 and the specific error at each measuring point is shown by error bars (Appendix D). These figures demonstrate that the measurement errors were only significant for measurement intervals

of less then three days. This suggests that the data generated from a period of more than 60 days as shown in Figure 6.1b can be interpreted with a high degree of confidence.

Table 6.1: Mean intra-seasonal horizontal surface velocities of the individual stakes from the stake network at Glacier de Tsanfleuron during the 2001 melt season (End June – End August).

Stake name	Mean horizontal velocity [cm d^{-1}]
10	5.2
$15N_1$	5.6
$15S_1$	4.9
20	4.2
$25N_1$	4.0
$25S_1$	3.2
$25S_2$	4.5
30	4.3
$35N_1$	3.9
$35S_1$	4.2
$35S_2$	2.6
40	4.0
$45N_1$	3.5
$45S_1$	3.3
$45S_2$	2.4
$45S_3$	1.9
50	3.4
$55N_1$	2.9
$55S_1$	3.0
60	2.9
$65S_1$	1.8
$70N_1$	2.5
70	2.8
$70S_1$	2.4
80	3.0
$80S_1$	3.1

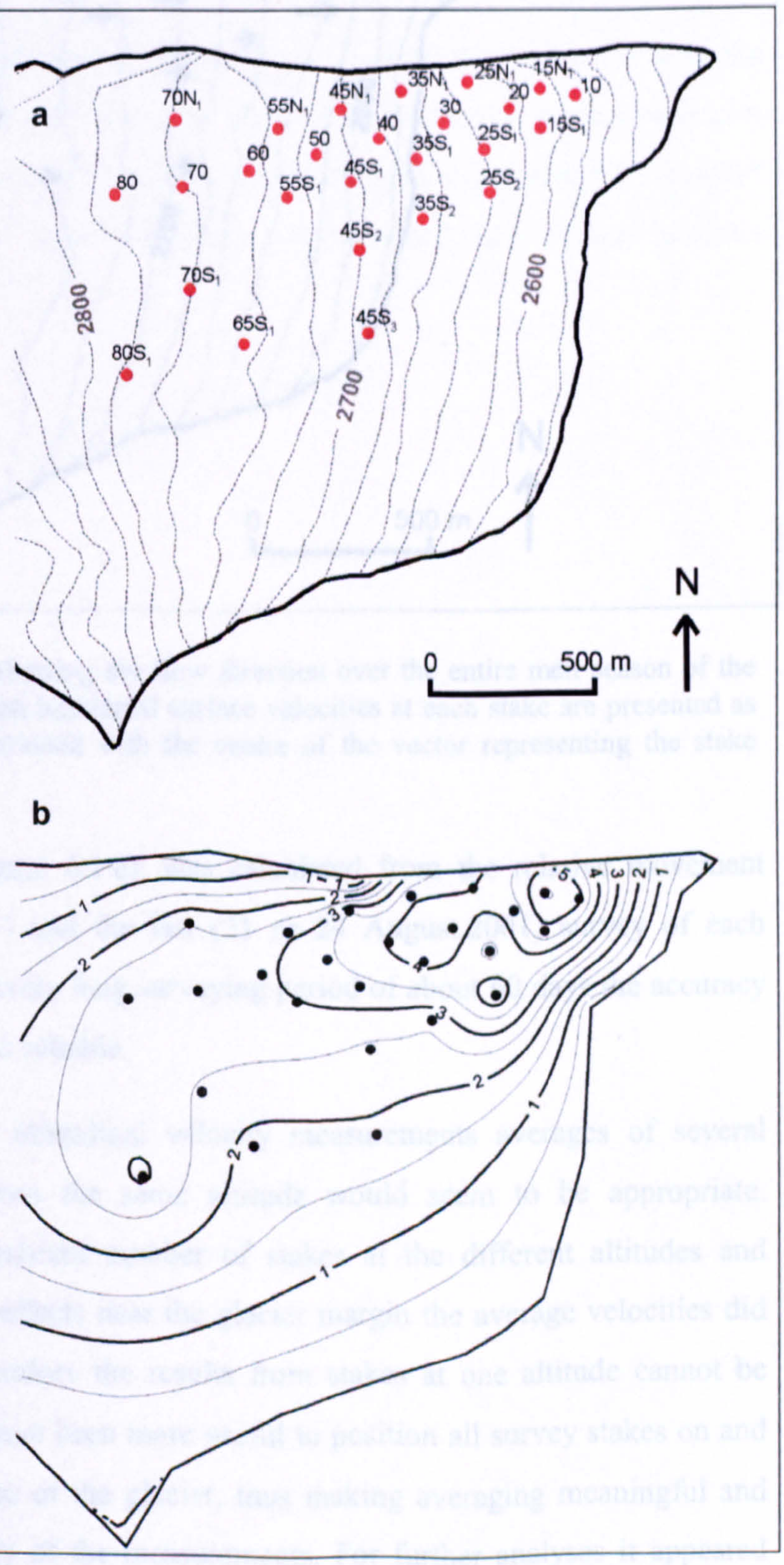

Figure 6.1: (a) Stake network at Glacier de Tsanfleuron during the 2001 melt season; (b) mean horizontal surface velocity distribution from late June to late August 2001. The plot was interpolated from individual stake measurements at locations as indicated; (c) continued below: Vector arrows of the individual stakes.

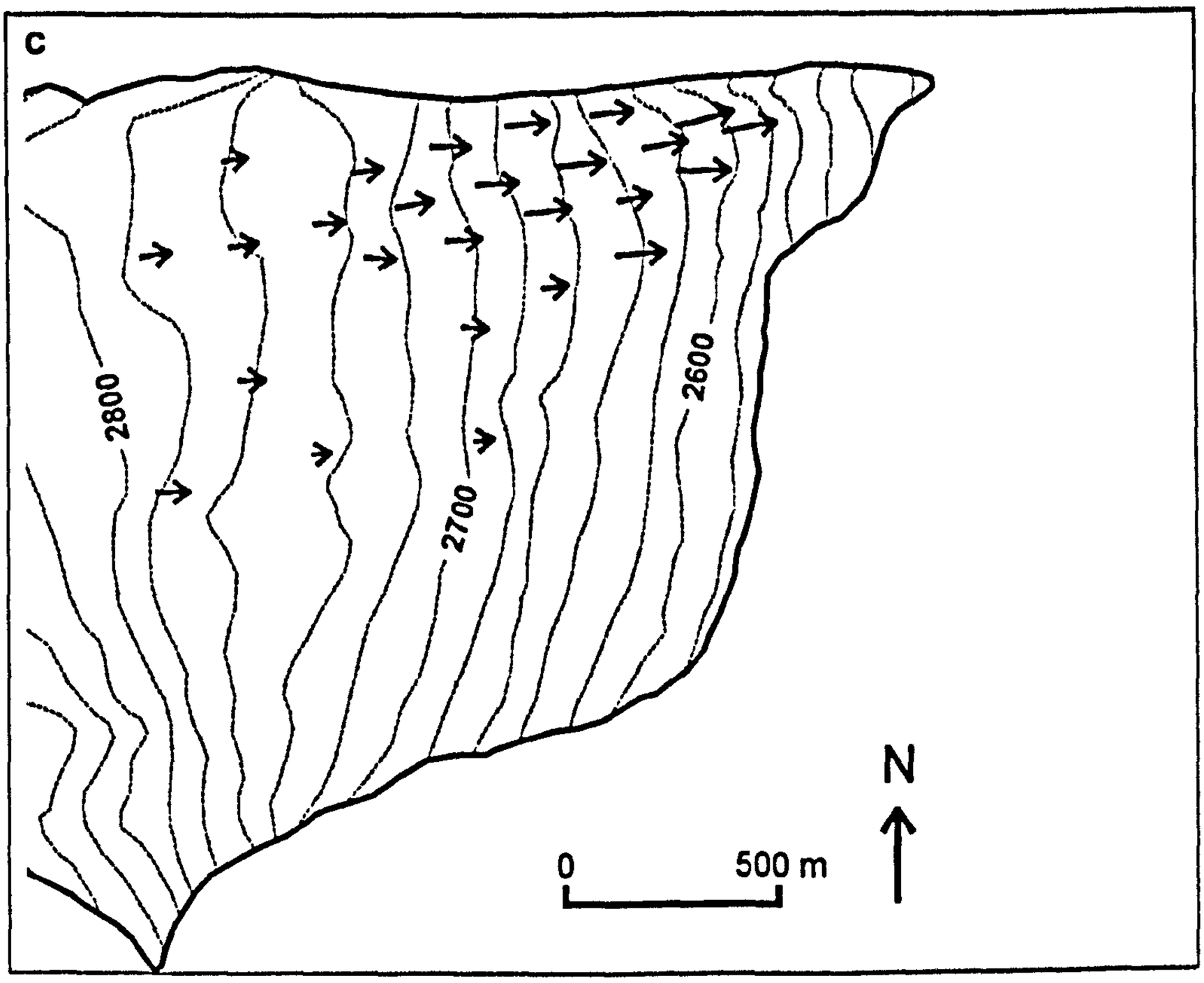

Figure 6.1 cont.: c) Vector arrows showing the flow direction over the entire melt season of the individual stakes. The measured mean horizontal surface velocities at each stake are presented as vectors scaled by velocity and positioned with the centre of the vector representing the stake location

The direction of movement (Figure 6.1 c), was calculated from the relative movement between the first (26 June 2001) and the last (21 or 24 August 2001) survey of each individual stake. Due to the relatively long surveying period of about 60 days the accuracy of the direction is considered to be reliable.

To minimise the errors of the altitudinal velocity measurements averages of several velocity stake measurements from the same altitude would seem to be appropriate. Unfortunately, due to the inconsistent number of stakes at the different altitudes and significant variations due to lag effects near the glacier margin the average velocities did not prove to be meaningful, therefore the results from stakes at one altitude cannot be averaged. In hindsight it would have been more useful to position all survey stakes on and a few metres from the centre line of the glacier, thus making averaging meaningful and therefore increasing the reliability of the measurements. For further analyses it appeared reasonable to concentrate on the stakes at the centre line of the stake network. These stakes are along the centre of the main tongue (probably where the ice is thickest, this is assumed

from observations of the extension of the proglacial valley shape). The centre stakes were evenly spaced up-glacier, 200 m apart and at an altitude range from 2590 m a.m.s.l. to 2780 m a.m.s.l. Overall, the centre stakes were the fastest moving stakes at Glacier de Tsanfleuron during the melt period from the end of June to the end of August 2001.

The results of the horizontal glacier surface velocities and vertical displacements from the centre line of the stake network are presented in Figure 6.2. Horizontal surface velocities are highly variable at all stakes with a decreasing trend throughout the season for most of the stakes. As shown in Figure 6.2 error bars decrease at increasing measurement intervals (see also Figure 3.1.4, Chapter 3).

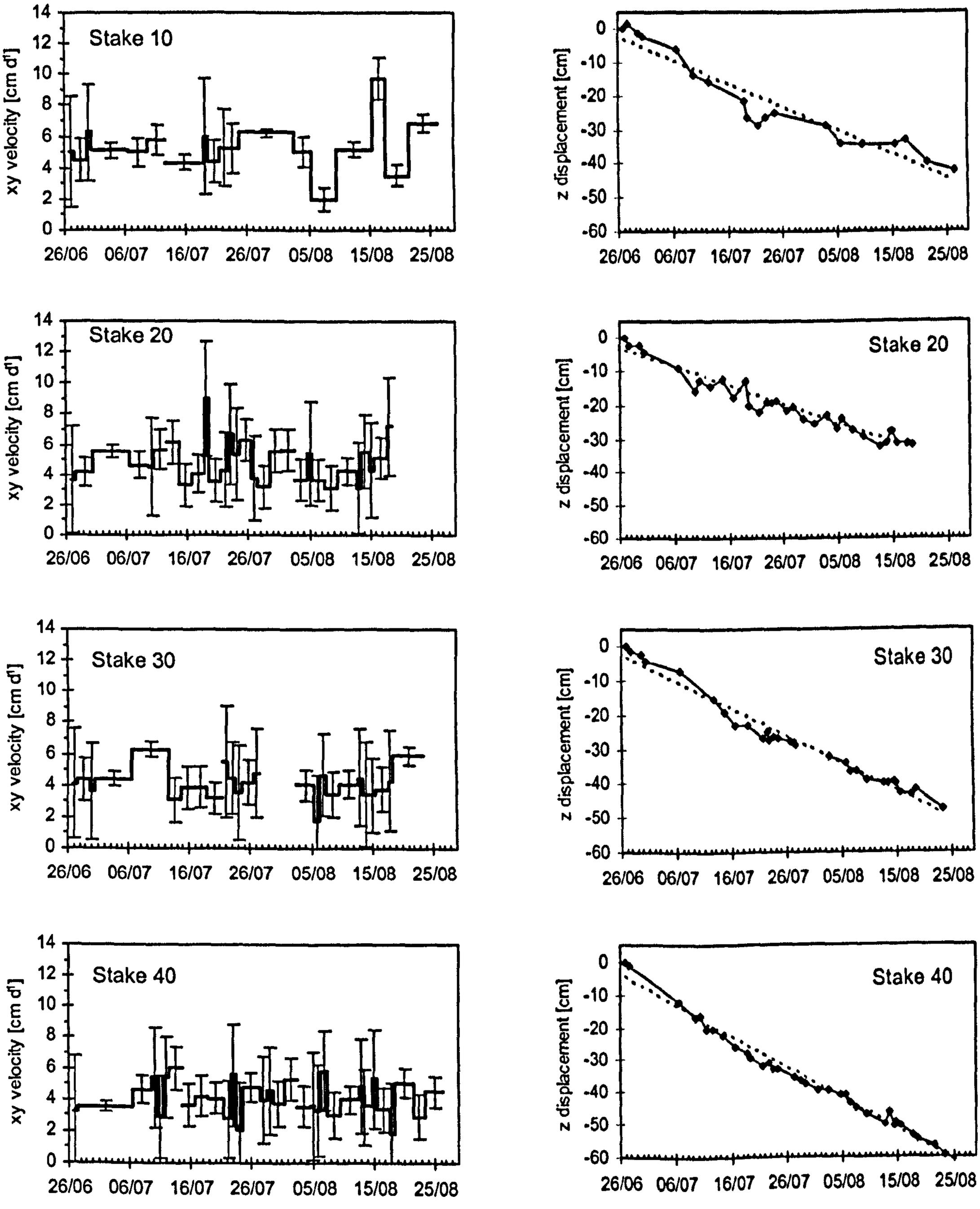

Figure 6.2: Horizontal glacier surface velocities and vertical displacements for the four lower stakes on the centre line of the stake network. Each velocity value is plotted as a horizontal line over the time interval over which it was measured.

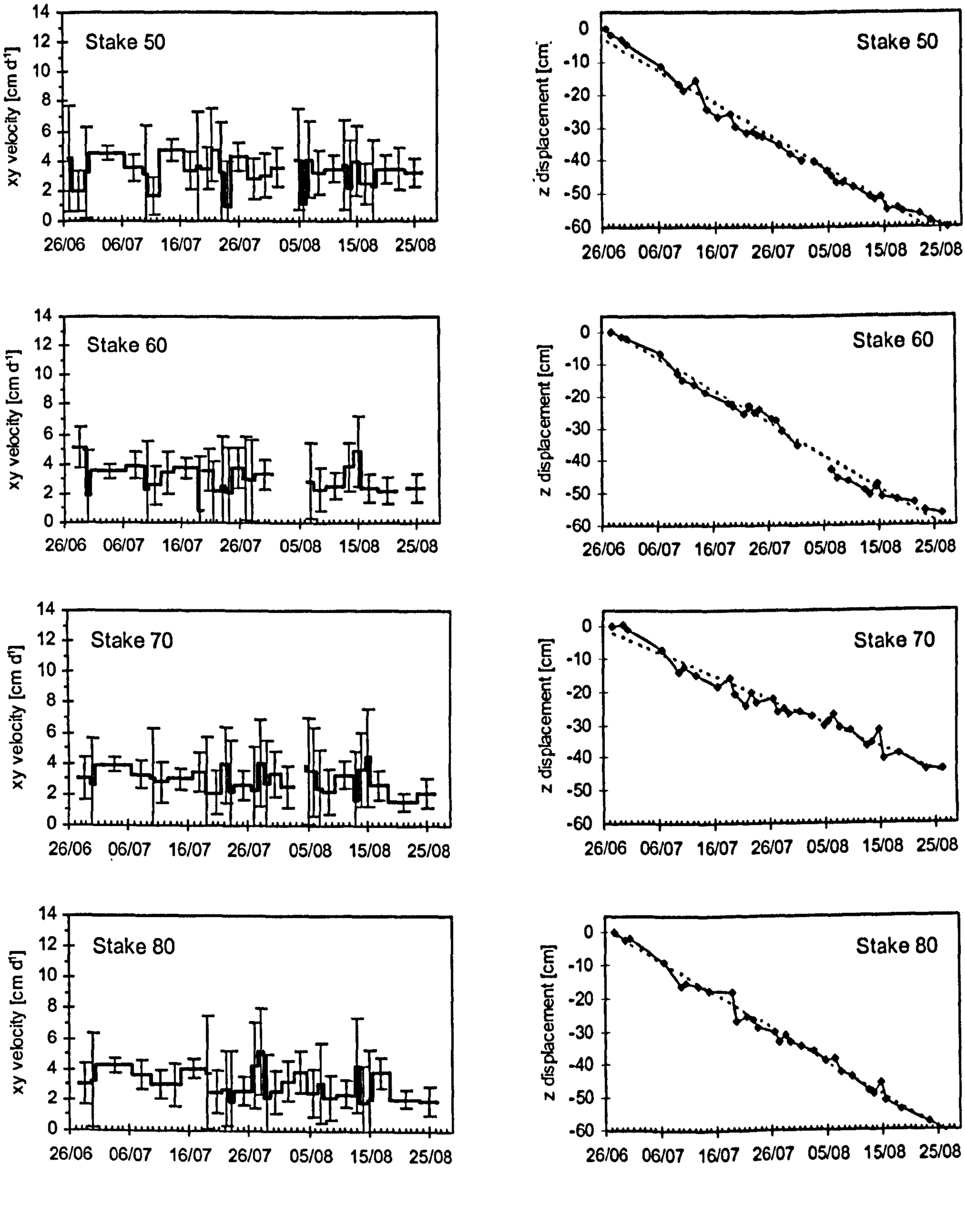

Figure 6.2 cont.: Horizontal glacier surface velocities and vertical displacements for the four upper stakes on the centre line of the stake network. Each velocity value is plotted as a horizontal line over the time interval over which it was measured.

The average of the mean horizontal surface velocities of all centre line stakes from the start to the end of the survey period (26/06 - 24/08/2001) provides a mean intra-seasonal surface velocity of 4 cm d^{-1} or 15 m a^{-1} respectively. Horizontal surface velocity variations at many

glaciers show larger daily amplitudes at lower stakes than at upper stakes (Iken et al., 1983; Harrison et al., 1986; Krimmel and Rasmussen, 1986; Clarke, 1991; Willis et al., 1996) (Section 2.5.4). This trend was not observed at Glacier de Tsanfleuron. Also, the daily amplitude of horizontal velocity variations at many glaciers tends to be larger towards the end of a melt season (Iken et al., 1983; Harrison et al., 1986; Krimmel and Rasmussen, 1986; Clarke, 1991; Willis et al., 1996). At Glacier de Tsanfleuron the amplitudes did not vary in any observable systematic manner throughout the 2001 melt season.

Horizontal surface velocities of the centre stakes as presented in Figure 6.2 seem generally to be highly variable and to vary in a non-systematic way. Some synchronicity in motion events at different stakes may be suggested, but intra-seasonal temporal patterns of increased or reduced surface velocities for neighbouring stakes and the observed variations can not clearly be defined. This may be affected by irregular surveying intervals that make it difficult to clearly observe temporal patterns in motion events. In order to elucidate useful information from undertaken surveys, data presentation for equal surveying intervals was required. Horizontal glacier surface velocities at surveying intervals of approximately one week for the centre stakes are presented in Figure 6.3. According to these measurements, the horizontal surface velocities at lower altitudes (Stakes 10 to 40) are generally faster than at higher altitudes (Stakes 50 to 80). The trend (dashed) line of the horizontal surface flow velocity of the lower stakes reduces insignificantly during the field season and varies considerably (e.g. for Stakes 10 and 20 around 5 cm d^{-1}). However, the upper stakes slowed down significantly e.g. Stakes 70 and 80 from approximately 4 cm d^{-1} at the end of June to 2 cm d^{-1} at the end of August. Lower stakes (Stakes 10, 30, 40) showed increased velocities after the first week of measurement, whereas the horizontal movement of all upper stakes slowed down after the first week of increased motion. This could be interpreted as a kinematic wave of high surface flow velocities moving down-glacier. However, to justify the interpretation of kinematic waves a greater number of stakes showing such patterns would need to be observed. There is a high degree of synchronicity for the general pattern of horizontal surface flow velocities for the upper stakes that shows a decreasing trend. There is also synchronicity between Stakes 20 and 30. The weekly velocity pattern of Stake 10 is highly variable which may be due to the location of this stake in close proximity to a crevasse. Weekly intervals of the horizontal surface velocity of Stake 40 are very steady over the field season following a velocity increase after the first week.

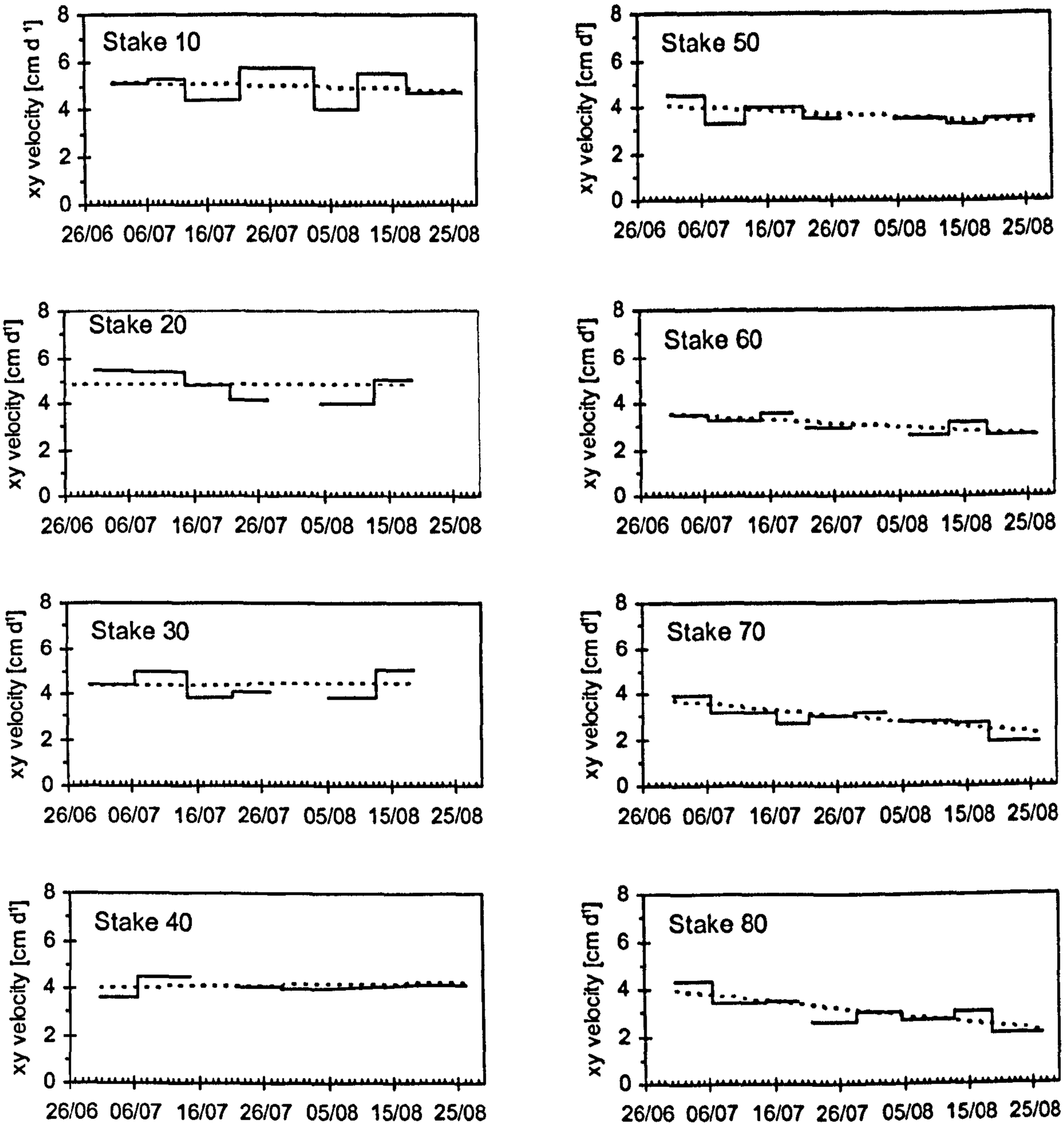

Figure 6.3: Horizontal glacier surface velocities at approximately weekly surveying intervals. The error of the measurements is about 0.5 cm d^{-1} of the measured value (Chapter 3.4.3) and therefore negligible. The dashed line indicates the trend throughout the measurement period.

6.3 Intra-seasonal variations in glacier surface velocities

Intra-seasonal fluctuations in glacier surface motion can provide critical information about basal conditions of the glacier due to the coupling between glacier hydrology and dynamics. (Meier, 1960; Iken et al., 1983; Iken and Bindschadler, 1986).

6.3.1 Horizontal motion

In order to recognise intra-seasonal trends of motion mean horizontal surface velocities of the centre line stakes for three weekly periods were compared. A rational choice of the most complete data sets at the start and end of the observation period and an intermediate week was made to give an accurate assessment. The weeks of comparison are at the start of July (30/06 - 06/07), mid/end of July (21/07 - 27/07) and mid/end of August (14/08 - 21/08). The stake positions at the beginning and end of these weeks were used to calculate the horizontal surface velocity (Figure 6.4).

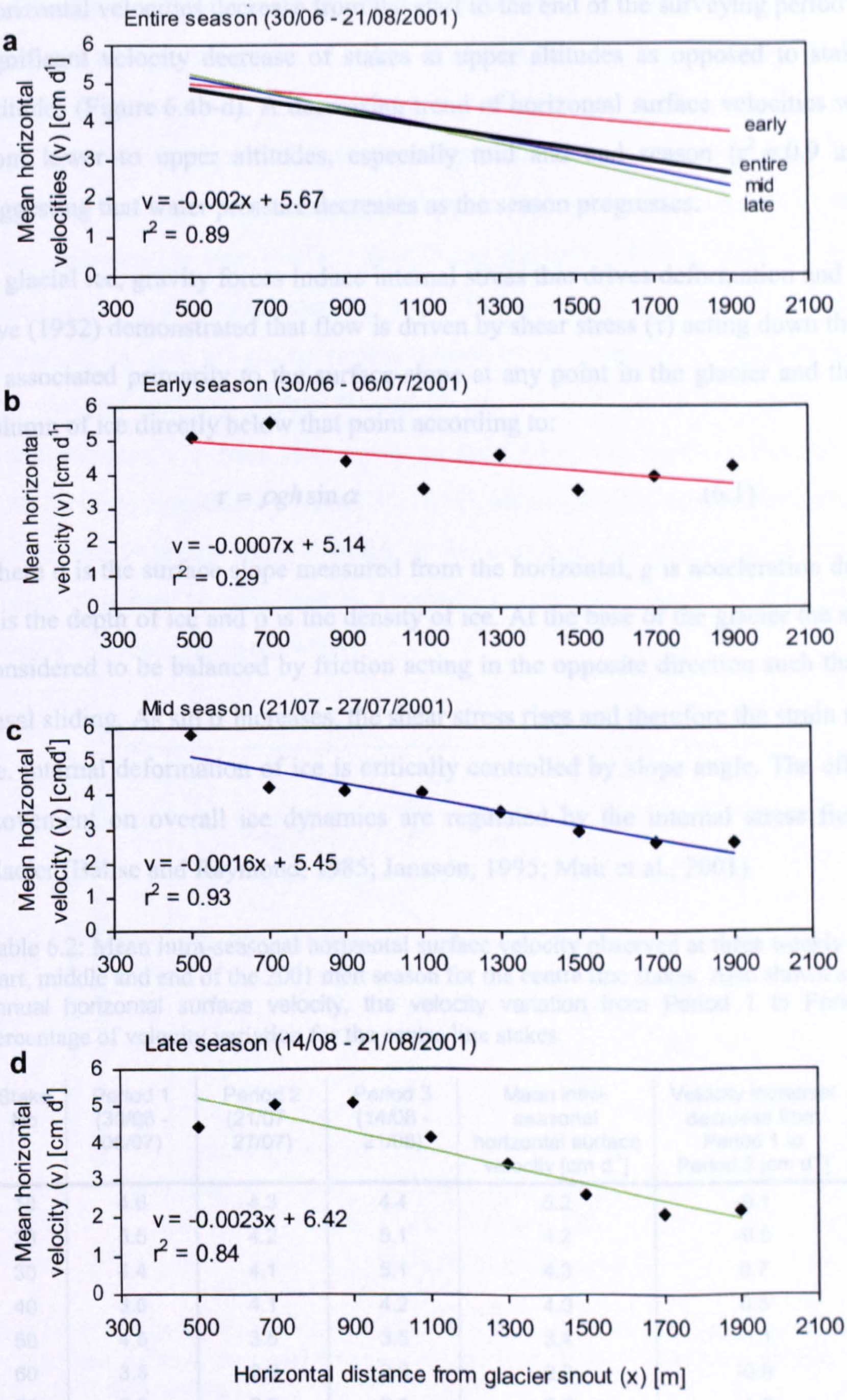

Figure 6.4: Mean horizontal surface velocities of the centre line stakes for weekly periods (a) for the entire field season, (b) at the start of July (30/06 - 06/07), (c) mid/end of July (21/07 - 27/07) and (d) mid/end of August (14/08 - 21/08).

Horizontal velocities decrease from the start to the end of the surveying period with a more significant velocity decrease of stakes at upper altitudes as opposed to stakes at lower altitudes (Figure 6.4b-d). A decreasing trend of horizontal surface velocities was observed from lower to upper altitudes, especially mid and end season ($r^2 = 0.9$ and $r^2 = 0.8$), suggesting that water pressure decreases as the season progresses.

In glacial ice, gravity forces induce internal stress that drives deformation and glacial flow. Nye (1952) demonstrated that flow is driven by shear stress (τ) acting down the glacier and is associated primarily to the surface slope at any point in the glacier and the depth of a column of ice directly below that point according to:

$$\tau = \rho g h \sin \alpha \qquad (6.1)$$

where α is the surface slope measured from the horizontal, g is acceleration due to gravity, h is the depth of ice and ρ is the density of ice. At the base of the glacier the shear stress is considered to be balanced by friction acting in the opposite direction such that there is no basal sliding. As sin α increases, the shear stress rises and therefore the strain rate increases i.e. internal deformation of ice is critically controlled by slope angle. The effects of basal movement on overall ice dynamics are regulated by the internal stress field inside the glacier (Balise and Raymond, 1985; Jansson, 1995; Mair et al., 2001).

Table 6.2: Mean intra-seasonal horizontal surface velocity observed at three weekly periods at the start, middle and end of the 2001 melt season for the centre line stakes. Also shown ar e mean intra-annual horizontal surface velocity, the velocity variation from Period 1 to Period 3 and the percentage of velocity variation for the centre line stakes.

Stake No	Period 1 (30/06 - 06/07)	Period 2 (21/07 - 27/07)	Period 3 (14/08 - 21/08)	Mean intra-seasonal horizontal surface velocity [cm d^{-1}]	Velocity increase/ decrease from Period 1 to Period 3 [cm d^{-1}]	Velocity variation [%]*
10	4.6	4.3	4.4	5.2	-0.1	-2.3
20	5.5	4.2	5.1	4.2	-0.5	-10.9
30	4.4	4.1	5.1	4.3	0.7	16.5
40	3.6	4.1	4.2	4.0	0.6	15.0
50	4.5	3.5	3.5	3.4	-1.1	-31.4
60	3.5	2.9	2.6	2.9	-0.9	-30.6
70	3.9	2.6	2.1	2.8	-1.8	-64.9
80	4.3	2.1	2.2	3.0	-2.1	-68.7

* Percentage of horizontal surface velocity increase/ decrease from mean intra-annual horizontal surface velocity

Analyses of mean horizontal surface velocities of the centre line stakes for three weekly periods at the start, middle and end of the 2001 melt-season (Table 6.2 and Figure 6.4)

demonstrate a greater decrease of mean horizontal velocities of the stakes at higher altitudes. Lower stakes (Stakes 10 and 20) show a slight velocity decrease from Period 1 to Period 3, whereas the horizontal velocity decrease of stakes from upper altitudes (Stakes 70-80) is more significant. This becomes especially apparent when plotting the percentage of velocity increases or decreases (of the mean seasonal surface velocity) of the centre line stakes between the start (30/06 - 06/07) and the end (14/08 - 21/08) of the 2001 melt season (Figure 6.5). During start and end of the field season, stakes at low altitudes (Stakes 10 and 20) indicate the glacier surface motion has decreased by about 2-11 % of the mean intra-seasonal velocity. Stakes 30 and 40 are the only centre line stakes that show an overall increase of surface velocity during the field season. Surface velocities of Stakes 50 to 80 decrease significantly (about 30-70 %), although meltwater production at the glacier surface and therefore water delivery to the englacial and subglacial drainage system is greater. This may be explained by a reduction in pressure due to melting of ice that was stored in cavities during the winter.

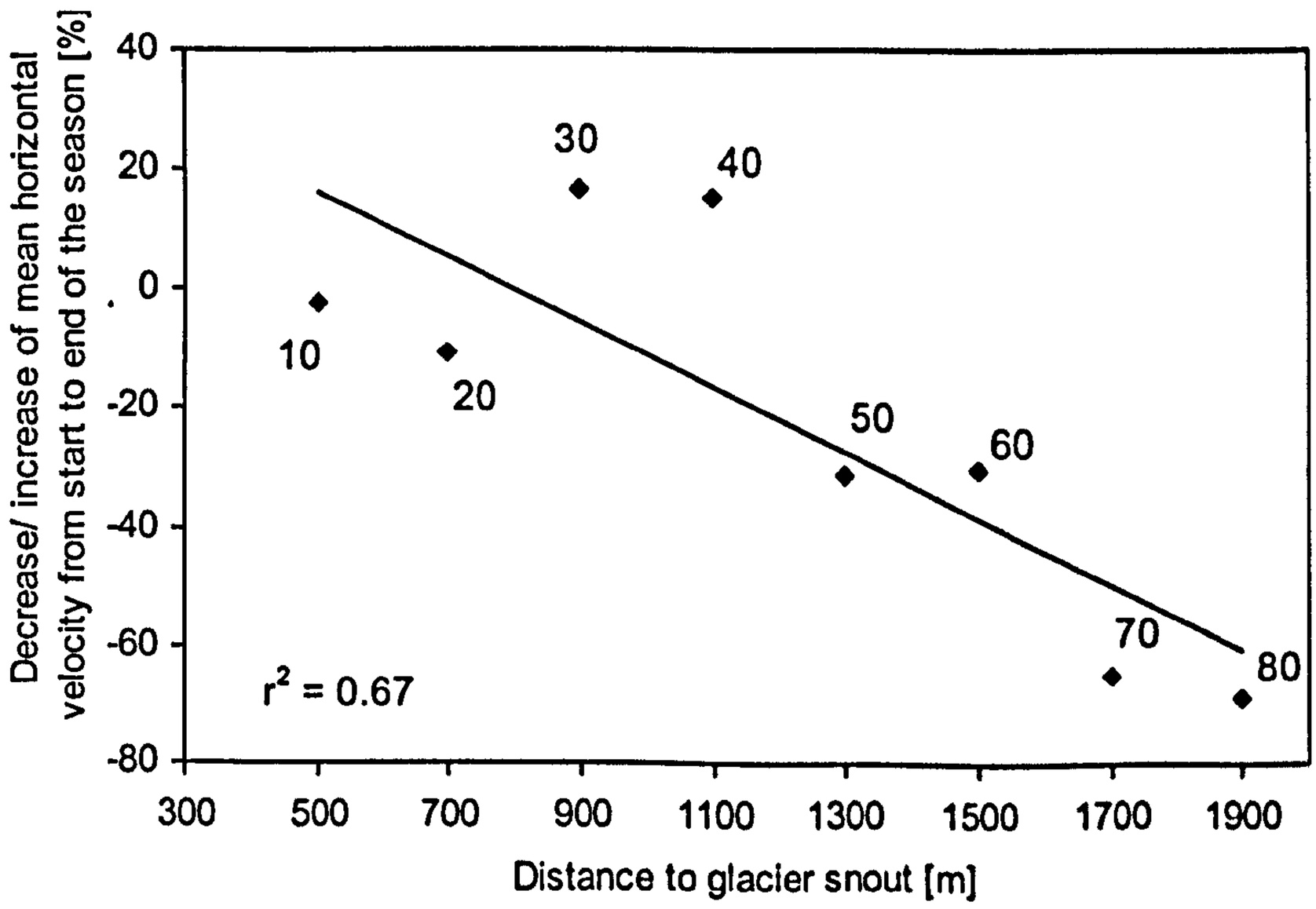

Figure 6.5: Percentage of velocity increases or decreases of the mean seasonal surface velocity of the analysed stakes at the centre line between the start (30/06 - 06/07) and the end (14/08 - 21/08) of the 2001 melt season.

At many temperate glaciers a temporal increase of horizontal velocities has been observed, often during the early melt period ("spring events") (Iken and Bindschadler, 1986; Hooke, 1989; Mair et al., 2001; Harper et al., 2002). Such speed-up events are related to increased basal water pressures that destabilise the glacier bed over large areas, thus decoupling the

glacier from its bed and increasing basal sliding. Spring events can be identified from a period of enhanced glacier surface velocities caused by the increased basal sliding velocity.

The velocity data from the survey at Glacier de Tsanfleuron was inspected for speed-up events, but no obvious increased surface velocities over an area that impacted on several velocity stakes were detected. This suggests that, although a high quantity of meltwater input due to high surface melting in July and August occurred, there was no pressure build-up at the glacier bed during the 2001 melt season. It is possible that the survey of the stake network was not accurate enough to detect speed-up events. Reliable measurements at daily intervals using a reliable method (perhaps differential GPS) may be useful.

Spatial variations in basal drag are often caused by variations in subglacial drainage conditions (Hooke et al., 1989; Van der Veen and Whillans, 1993; Iken and Truffer, 1997). At Glacier de Tsanfleuron, there are no clear spatial patterns of enhanced surface velocities propagating down-glacier ("kinematic waves"). Such kinematic waves were examined at a number of other temperate glaciers during the melt-season (e.g. Schimpp, 1958; Hodge, 1974; Iken and Bindschadler, 1986; Kamb and Engelhardt, 1987; Krimmel and Vaughn, 1987). Spatial variations of the horizontal surface motion of stakes situated at similar altitudes also do not show correlated patterns of horizontal surface motion.

6.3.2 Vertical motion

Speed-up events, showing increased horizontal glacier movement, are often accompanied by vertical uplifts (Lliboutry, 1968; Iken and Bindschadler, 1986; Shoemaker, 1986; Hooke, 1989; Iverson et al., 1995; Mair et al., 2001; Gudmundsson, 2002). At Glacier de Tsanfleuron at many of the observed stakes a slight vertical uplift is noticeable at around 14 August, but no apparent horizontal surface velocity increase during this apparent phase of uplift was observed (Figure 6.2 and Appendix D).

6.3.3 Discussion

It has often been observed that horizontal surface velocities at lower altitudes are lower than at higher altitudes, but the more significant decrease of velocities of stakes from upper altitudes was unexpected. The velocity reduction at upper altitudes and on the glacier plateau is more significant than at lower altitudes. This may be explained by disconnection of lower parts of the glacier from upper parts due to the development of crevasses, thus

reducing shear stress and hence traction at higher plateau altitudes. Another possible reason for this phenomena could be plastic deformation of the ice. Subglacial cavities fill with ice during winter when there is no meltwater available to keep drainage passageways clear. The ice in cavities would start melting with the onset of the melt season. However, due to ice in the cavities, the drainage system would pressurise quicker in the early melt season. This could explain faster flow velocities at the upper stakes at the start of the season, and that the ice movement at these locations then slows down when the ice in cavities melts and the pressure drops. This effect is also more likely to occur at higher altitudes because plateau cavities at upper altitudes of the glacier are liable to be much smaller and less developed than at lower altitudes near the snout, due to the lesser volumes of water at the glacier head.

6.4 Glacio-hydrological impacts

6.4.1 Meltwater input and glacier motion

The data was analysed to determine whether any variations in surface motion are related to variations in meltwater production at the glacier surface (Figure 6.6).

During the period of observation melt rates do not show a trend of significant increase or decrease (Figure 6.6), although significant amplitude changes occur that are high on days with high air temperatures and clear sky. Melt rates below zero (16 July, 20 July) indicate snow accumulation due to snowfall. The snowfall event on 11 August is not reflected in the data because the thin snow layer melted before the next measurement was undertaken, ablation was not measured on this day.

The lack of a trend for snowmelt throughout the melt season can perhaps explain why there is no significant response of glacier motion to melting. Any possible relationships seen in the data reflect multiple processes including increased plastic deformation as well as increased water flow at the higher temperatures.

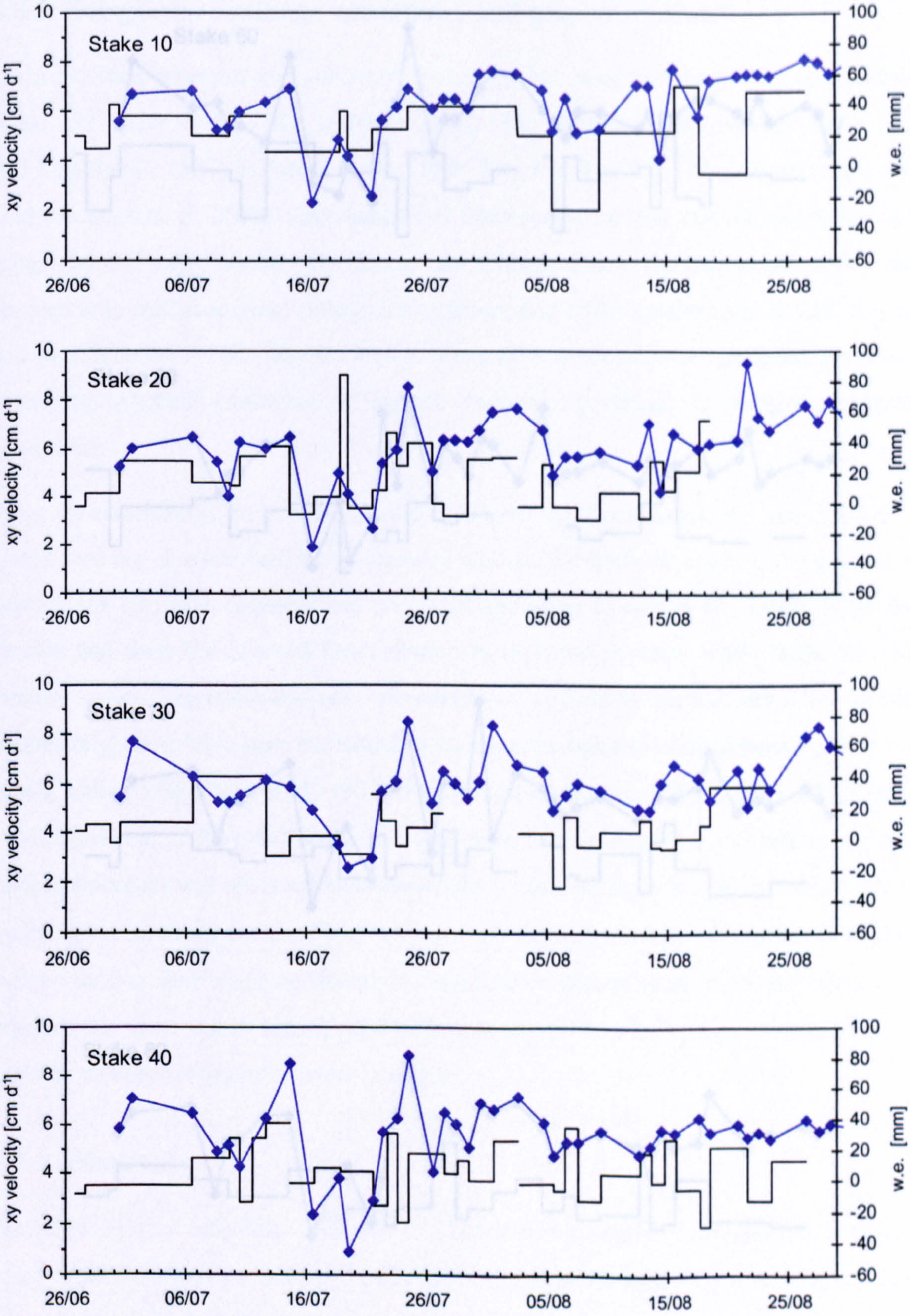

Figure 6.6: Horizontal surface velocities and melt rates for the centre line stakes. Negative melt rates occur due to snow accumulation (snowfall).

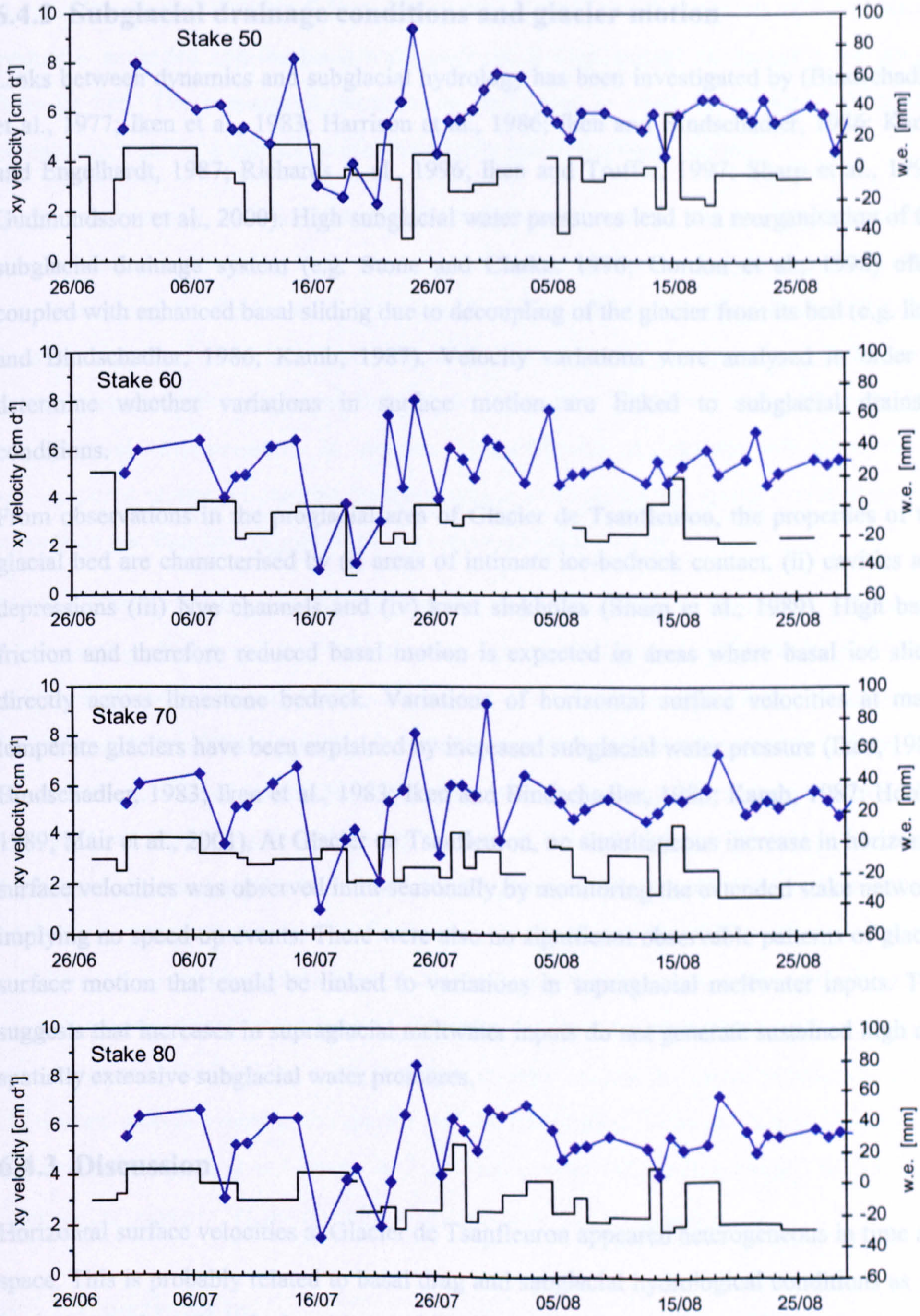

Figure 6.6 cont.: Horizontal surface velocities and melt rates for the centre line stakes. Negative melt rates occur due to snow accumulation (snowfall).

6.4.2 Subglacial drainage conditions and glacier motion

Links between dynamics and subglacial hydrology has been investigated by (Bindschadler et al., 1977; Iken et al., 1983; Harrison et al., 1986; Iken and Bindschadler, 1986; Kamb and Engelhardt, 1987; Richards et al., 1996; Iken and Truffer, 1997; Sharp et al., 1998; Gudmundsson et al., 2000). High subglacial water pressures lead to a reorganisation of the subglacial drainage system (e.g. Stone and Clarke, 1996; Gordon et al., 1998) often coupled with enhanced basal sliding due to decoupling of the glacier from its bed (e.g. Iken and Bindschadler, 1986; Kamb, 1987). Velocity variations were analysed in order to determine whether variations in surface motion are linked to subglacial drainage conditions.

From observations in the proglacial area of Glacier de Tsanfleuron, the properties of the glacial bed are characterised by (i) areas of intimate ice-bedrock contact, (ii) cavities and depressions (iii) Nye channels and (iv) karst sinkholes (Sharp et al., 1989). High basal friction and therefore reduced basal motion is expected in areas where basal ice slides directly across limestone bedrock. Variations of horizontal surface velocities at many temperate glaciers have been explained by increased subglacial water pressure (Iken, 1981; Bindschadler, 1983; Iken et al., 1983; Iken and Bindschadler, 1986; Kamb, 1987; Hooke, 1989; Mair et al., 2001). At Glacier de Tsanfleuron, no simultaneous increase in horizontal surface velocities was observed intra-seasonally by monitoring the extended stake network, implying no speed-up events. There were also no significant observable patterns of glacier surface motion that could be linked to variations in supraglacial meltwater inputs. This suggests that increases in supraglacial meltwater inputs do not generate sustained high and spatially extensive subglacial water pressures.

6.4.3 Discussion

Horizontal surface velocities at Glacier de Tsanfleuron appeared heterogeneous in time and space. This is probably related to basal drag and subglacial hydrological conditions as has been observed at other glaciers (Iken and Truffer, 1997; Fischer et al., 1999).

From observations in the proglacial area, Sharp et al. (1989) proposed that the basal sliding activity of Glacier de Tsanfleuron is independent of basal meltwater flow so long as the water is drained through cavities and Nye-channels under atmospheric pressure. Sharp et

al., (1989) assumed that the sliding velocity would rise once the capacity of this drainage system is exceeded and the basal water pressure is high enough to decouple the glacier from its bed. The pressurised extrusion of meltwater to areas of intimate ice-bedrock contact can result in a thin water film temporally increasing basal motion.

It remains uncertain whether pressurised conditions to separate the glacier from its bed, thus enhancing basal sliding have occurred in the subglacial drainage system temporarily at any time during the field season. Clearly and as discussed in Chapter 5 (Section 5.4), the density of sinkholes in the karst beneath the glacier will greatly influence the water pressure regime in the subglacial drainage system and the likelihood of significant periods of high basal water pressures. In addition, the distribution of sinkholes will determine the spatial extent of any pressurised drainage, which will control the spatial extent of ice bed separation and thus the magnitude of any enhanced basal sliding.

Hubbard (2002) investigated the characteristics of basal motion at Glacier de Tsanfleuron by measuring sliding rate in a frontal cavity during a 6-day survey period in 2000 melt-season. His results showed that the ice motion was temporally variable and characterised by infrequent but distinct periods of relatively rapid motion (about 1 cm d^{-1}) with periods of slow or no motion lasting from minutes up to hours long. These non-uniform basal velocities were interpreted as stick-slip motion. If stick-slip motion occurs at the glacier bed, these patterns may be transferred to the glacier surface causing a variable staccato surface movement. The surface motion measurements during the 2001 melt-season may be indicative of such stick-slip sliding resulting in highly variable horizontal surface velocities as presented in Figure 6.2. Unfortunately, the coupling length between glacier bed and surface is poorly constrained and it therefore remains unclear the extent to which brief and short-lived motion events at the glacier bed are transmitted to the ice surface. In addition, the velocities observed at Glacier de Tsanfleuron were not reliable enough to determine whether the apparent "stick-slip" characteristics were real or apparent.

6.5 Conclusions

During the 2001 melt-season, the motion of Glacier de Tsanfleuron was apparently not affected by changes within the glaciers drainage system. There were no speed-up events observed which could have implied spatially extensive pressurised subglacial drainage conditions. The melt-season was characterised by a late onset of melting, but high melt-

rates were typically observed during July and August. The lack of speed-up events is either a result of limited supraglacial water inputs or a high density of karst sinkholes resulting in negligible basal pressures. The observations suggest that slip-stick motion is the characteristic flow mechanism at Glacier de Tsanfleuron. Lower areas of the glacier move faster than upper areas, which can be explained by the increased slope angle at lower parts of the glacier.

For future observations of ice motion it would be useful to investigate glacier motion during hydrologically different ablation seasons than that observed during the 2001 season. The dynamic response of the glacier in a year with high melt-rates and ablation up to relatively high altitudes would help determine whether the volume of supraglacial runoff or the presence of the subglacial karst was the critical control on basal water pressures and thus the lack of speed-up events in 2001. Long term and intra-annual investigations of glacier motion would provide information on seasonal flow characteristics and in particular, how summer motion compares with winter motion. This information would also help to clarify whether the motion of Glacier de Tsanfleuron is mainly independent of glacier hydrology.

A hypothetical glacial system with similar Nye-channel cavity configuration as at Glacier de Tsanfleuron, but without the underlying karst would be expected to behave in a similar manner to a "normal" impermeable bed glacier. However, hydraulic pressurisation could probably only occur after saturation of the capacity of the Nye-channel cavity system has been achieved. Sharp et al. (1989) argued that the Kamb model (Kamb et al., 1987) (which suggests glacial movement is fundamentally influenced by basal water pressure and ice thickness; these parameters are related in impermeable bed systems) was applicable because the low basal pressure at Glacier de Tsanfleuron was due to the Nye channel and linked-cavity network on the glacier bed as well as the thin ice of Glacier de Tsanfleuron. However, Sharp appears to have, to a large extent, neglected the karstic bedrock which accounts for the loss of perhaps the order of 95 % (see Chapter 5) of the basal water (Chapter 4), the major reason for low subglacial pressures and hence limited movement.

The bed of Glacier de Tsanfleuron can be considered as a complex area of slippery and sticky spots (Fischer and Clarke, 1997; Iken and Truffer, 1997; Fischer et al., 1999). And basal sliding occurs locally when the basal shear traction exceeds frictional drag at the bed. Sliding is enhanced in areas where a meltwater film causes a decrease in friction at the bed-ice interface. There would appear to be little evidence to suggest that film flow occurred at any time at Glacier de Tsanfleuron during the 2001 ablation season.

7 Conclusions

7.1 Introduction

The drainage system of a glacier from the snow/ ice surface through the glacier to its bed is inaccessible and highly complex. In order to investigate the drainage characteristics and hydrological impacts on the motion of Glacier de Tsanfleuron, an interdisciplinary research approach was used. Aims of this thesis were (as outlined in Chapter 1) to investigate

(i) intra-seasonal variations in drainage conditions within the supraglacial snowpack and its effect for the meltwater delivery to the englacial and subglacial drainage system.

(ii) the extent to which subglacial drainage conditions, as observed in the deglaciated proglacial bedrock, are representative of the current subglacial drainage conditions.

(iii) the extent to which meltwater drainage into the glacier emerges from the snout of Glacier de Tsanfleuron and what role karst sinkholes play for subglacial hydrology.

(iv) the extent to which intra-seasonal variations in glacier hydrology impact on the ice dynamics due to variations in water pressure and basal sliding.

These aims were addressed by utilising a variety of different techniques during the 2001 melt-season at Glacier de Tsanfleuron (Table 7.1). The various sources of field data were subsequently analysed and used in an attempt to address the main aims of this thesis.

Table 7.1: Areas of investigation and techniques used for this PhD project to generate data that delivers information towards a better understanding of hydrological processes of a glacier overlying a linked-cavity drainage system.

Area of investigation	Techniques emphasised to generate data
Snowpack hydrology	i) Dye tracing at the snow surface and at the snow-ice interface ii) Water level monitoring at the snow-ice interface iii) Air temperature recording iv) Ablation measurements
Subglacial hydrology	v) Dye tracing vi) Discharge gauging vii) Basic numerical modelling
Glacier dynamics	viii) Survey of a stake network

This chapter summarises these main findings of this thesis (Section 7.2), outlines the implications of the main findings (Section 7.3) and gives some recommendations for future research (Section 7.4).

7.2 Summary of the main conclusions

7.2.1 Snow hydrology

The results presented in Chapter 4 demonstrate that dye tracing can be used effectively to generate information on the drainage system in the snowpack. In this study, travel times through the snowpack (0.08 to 0.32 mh^{-1}) were found more than an order of magnitude slower than the flow at the water-saturated snow-ice interface (7.7 mh^{-1} and 12.2 mh^{-1}). This is probably due to reduced permeability resulting from smaller grain sizes, the presence of ice lenses and the lower water content of the unsaturated snowpack (Wakahama, 1968; Colbeck, 1979; Marsh, 1990). Therefore, meltwater input to the englacial drainage system is significantly delayed by snow. Additionally, decreasing time lags between the water level at the snow-ice interface (W) and temperature (T) minima were detected. This was most significantly demonstrated during a 7-day period where the time lags between minima decreased from 7h 30mins to 0h 45mins from a decreasing snowpack of 0.8 m to 0.4 m. These results suggest that water passes faster through thinner snowpacks; whereas due to its water storage capacity in thicker snowpack a buffering

effect occurs. This supports Colbeck's (1974) suggestion of the thickness of the saturated layer at the snow-ice interface to be proportional to the runoff from the snowpack. The snow-ice interface presents a linking element at the transition for supraglacial and englacial hydrological processes. Due to snowpack decrease during the melt season, the impacts on glacial hydrology are highest at the start of the melt season. The lag times between the water level at the snow-ice interface (W) and bulk discharge (Q) minima decreased from 5h 45mins to 2h 0mins, demonstrating decreased storage times of meltwater at the snow ice interface. Even though a general pattern of the evolution of meltwater flow through snowpacks from the limited number of experiments was not possible, the obtained tracer return curves generally generated broader and more dispersed curves in the thicker than in the thinner snowpack. This may indicate more efficient drainage as the melt season progresses, but due to the complexity of influencing factors further detailed studies are required for evidence.

7.2.2 Subglacial hydrology

The unseasonally thick snowpack made subglacial investigations extremely problematic and dye tracer experiments were not possible before the end of August. However, significant findings concerning the subglacial water drainage system were obtained from dye tracer experiments and basic modelling. Low flow velocities (between 0.02 to 0.05 ms^{-1}) and high dispersivities (23 to 80 m) reflect that meltwater is routed through an inefficient drainage system (Willis et al., 1990; Hock and Hooke, 1993; Nienow et al., 1998). Low recovery rates during times of low discharge imply temporary storage of the tracer, possibly due to the disconnection of cavities during the tracer transit; cavities were perhaps reconnected at times of higher discharge. This suggests a subglacial drainage system consisting of cavities linked by Nye-channels at least beneath the lower tongue of Glacier de Tsanfleuron, similar to the configuration as observed in the forefield. Flow velocities through the subglacial drainage system appeared to be independent from discharge variation indicating that at higher discharges a more complex system is used resulting in higher dispersivities, but not necessarily in increased flow velocities.

Using a basic model, flow velocities through a Nye-channel system were projected theoretically. This demonstrated that water flow is significantly delayed in cavities, due to temporary storage processes. Flow velocities as low as those obtained from dye tracer

experiments cannot result from subglacial drainage dominated by Nye-channel flow, although 51 to 83 % of the subglacial area consists of Nye channels (Sharp et al., 1989). Thus, it is concluded that subglacial meltwater travels most of the distance in Nye channels, but spends most of the time in cavities. This is in agreement with the configuration of the former glacier bed that is exposed in the proglacial area. However, the carbonate crusts as observed in the proglacial area probably resulted from film flow that may have occurred at high surface melt rates and during times when the capacity of the Nye-channel-cavity network was exceeded (Sharp et al., 1989; Hubbard and Hubbard, 1998). This would, as has been observed at other temperate glaciers (Iken et al., 1983; Iken and Bindschadler, 1986; Mair et al., 2001) result in increased subglacial water pressures and thus increased basal motion.

However, the spatial extent of subglacial water pressures and therefore the likelihood of a response in glacier motion, at Glacier de Tsanfleuron, is also influenced by the density of subglacial sinkholes. From the spatial analysis of tracer experiments across the lower tongue area with positive return below 2620 m a.m.s.l. and negative results (no returns) above this altitude, it is proposed that the proglacial stream catchment area covers only about 6 % (uncorrected for errors, see Chapter 4) of the glacier surface. The rest of the meltwater produced at the glacier surface (approximately 96 %) is suggested to runoff through the karst system beneath the glacier. Discharge quantities between 22 July and 23 August of 2.8×10^5 m^3 in the proglacial stream compared with the meltwater produced at the surface of the glacier tongue between 2500 and 2600 m a.m.s.l. of 3.0×10^5 m^3 are in agreement but represent only a very small area of the glacier surface (approximately 5 %). This also suggests that a proportion of about 95 % is lost to runoff through the karst. Both considerations support the supposition that about 95 % of total glacial melt runs off through the underlying karst.

7.2.3 Dynamics

The average of the mean horizontal surface velocities of all centre line stakes from the start to the end of the survey period (26/06 - 24/08/2001) provides a mean intra-seasonal surface velocity of 4 cm d^{-1} or 15 m a^{-1} respectively. Mean horizontal surface velocities of the individual stakes vary from 1.8 cm d^{-1} (Stake 65S$_1$) to 5.6 cm d^{-1} (Stake 10) and these velocities are generally higher at lower altitudes than at higher altitudes as has also been

observed on other glaciers (Elliston, 1973; Hodge, 1974; Hooke et al., 1989). Horizontal surface velocities of the centre line stakes were highly variable with a decreasing trend for most of the stakes. Weekly analysis of the survey data eliminated systematic errors. The analysis demonstrated a high degree of synchronicity of the horizontal surface flow velocities for upper stakes with a significantly decreasing trend during the field season (velocity decreased by approximately half), whereas horizontal flow velocities of lower stakes reduced only insignificantly. This may be explained by a possible reduction of pressure in the Nye channels throughout the melt season at higher altitudes due to the melting of ice that formed in cavities during the winter.

During the 2001 melt-season the motion of Glacier de Tsanfleuron was probably independent from the glaciers basal hydrology, as the capacity of the subglacial Nye-channel system was not exceeded. This is based on the observation of no speed-up periods that would be linked to subglacial water pressures. Whether pressurised conditions have occurred in the subglacial drainage system at other times remains uncertain. It is more likely that stick-slip motion (Fischer and Clarke, 1997) due to frictional drag with no spatial or temporal patterns is typical for Glacier de Tsanfleuron. This assumption is also supported by Hubbard (2002), who investigated the characteristics of basal motion at Glacier de Tsanfleuron by measuring sliding rate in a frontal cavity. From infrequent but distinct periods of relatively rapid motion Hubbard interpreted these non-uniform basal velocities as stick-slip motion.

7.3 Implications of the research

The data set that was collected during the 2001 melt season at Glacier de Tsanfleuron covers a broad research area and enables us to answer the open questions explored by this research. Implications of glacio-hydrological processes from the combination of the used research methods are outlined below.

7.3.1 Intra-seasonal variations of snowpack drainage conditions

Dye tracing experiments at the snow surface and at the snow-ice interface as well as monitoring the water level at the snow-ice interface provided information about the drainage conditions of the supraglacial snowpack. Meltwater percolates slowly through the snowpack (at Glacier de Tsanfleuron during summer 2001 at about 0.08 to 0.32 mh^{-1}) with

velocity variations depending on the occurrence of ice layers, snow grain size and water saturation (Wakahama, 1968; Colbeck, 1979; Marsh, 1990). Flow velocities at the water-saturated snow-ice interface at Glacier de Tsanfleuron during summer 2001 increased by an order of magnitude. Consulting the available data, valuable conclusions about the seasonal development of snowpack hydrology are not possible. It has been demonstrated that the processes are complex and the effectiveness of meltwater routing is related to the development of flowpaths, meltwater generation at the snow surface, snowpack thickness, diurnal temperature cycle and seasonal changes. Meltwater generation at the snow surface and percolation through the snowpack is responding to short-term temperature variations. This is clearly reflected by diurnal water level variations at the snow-ice interface and thus will directly affect meltwater inputs to the englacial and subglacial drainage systems. Despite large quantities of water generated at the glacier surface through snowmelt in July and August this was not reflected in the measured dynamic response of the glacier. No "speed-up" event as commonly observed at other glaciers was detected during the course of the summer (e.g. Iken et al., 1983; Mair et al., 2002).

7.3.2 Subglacial drainage conditions

Dye tracer experiments suggests that the subglacial drainage system at Glacier de Tsanfleuron is hydrologically inefficient and similar configured as the former subglacial drainage system exposed in the glacier forefield as observed by Sharp et al. (1989).

However, the underlying karst system appears to play a major role in the subglacial drainage conditions at Glacier de Tsanfleuron. These conditions are perhaps unique since approximately 95 % of subglacial water is drained to the karst. If this large quantity of meltwater was not lost to the karst and entered the subglacial hydrological system considerably different glacier dynamics would be expected.

The availability of a Nye-channel-cavity drainage system has, perhaps, also a critical influence on the meltwater drainage at the start of the melt season. Flowpaths at temperate glaciers overlying impermeable bedrock commonly close due to ice pressure and inadequate drainage during the winter and thus need to develop again from the bases of moulins and crevasses at the onset of the melt-season (Hooke, 1998). Over the course of the melt period, more meltwater quantities enter the subglacial drainage system and induce transient high subglacial water pressures. This causes channels to evolve rapidly (Nienow

et al., 1998). In contrast, at Glacier de Tsanfleuron the subglacial and karst drainage system remains over winter and meltwater can directly be drained effectively from the start of the melt season. The dye tracing results suggest that at high discharges more drainage routes are activated.

7.3.3 The proglacial stream catchment area

Dye tracer tests and the comparison between ablation and discharge quantities showed that only approximately 6 % of the glacier drains to the proglacial stream at the glacier snout, the remaining 94 % (see Chapter 4) being lost to the underlying karst. The spatial extent of pressurised subglacial conditions during times of high water input is reliant on the density and capacity of sinkholes. At low sinkhole densities, pressurised conditions are more likely and the observation of transient ice flow phenomena such as "spring events" and diurnal cyclicity would be expected (Iken and Bindschadler, 1986; Hooke, 1989; Mair et al., 2001; Harper et al., 2002).

7.3.4 Ice dynamics and the impacts of glacier hydrology on glacier motion

From the glacier dynamics observations, it has been suggested that during summer 2001 subglacial channels did not overflow sufficiently to separate the glacier from its bed and enhance basal glacier sliding. The subglacial drainage system may not have been pressurised preventing decoupling of the glacier (or a part of it) from its bed that would have resulted in increased basal sliding that would have caused speed-up events. This suggests that high water pressures in the subglacial system have been prevented by: (i) high conveyance of the existing drainage system consisting of a network of Nye-channels and linked-cavities; (ii) a large number of sinkholes that drain meltwater efficiently into the karst bedrock; or (iii) insufficient water inputs during the 2001 melt-season. Thus, it is apparent that in the case of Glacier de Tsanfleuron the karst bedrock plays a critical role in restricting widespread speed-up events as opposed to glaciers sitting on impermeable lithologies. Although the 2001 melt-season was characterised by a late onset of melting, generally high melt-rates occurred during July and August. The dye tracer experiments in this study suggested that most meltwater drains through the underlying karst and the subglacial system does not get highly pressurised because bulk discharge is routed away from the glacier bed into the karst. Therefore, despite being a distributed drainage system,

as discharge rises, water pressure is not responding as would be expected on an impermeable bedded glacier.

From research in the forefield of the glacier, Sharp (1989) suggested that the subglacial drainage system of Glacier de Tsanfleuron consist of a linked-cavity system as described by Kamb (1987). Sharp suggested that there is low subglacial pressure due to the existence of Nye channels and relatively thin ice. Hence, pressurised conditions would only occur if the discharge exceeds 5 $m^3 s^{-1}$ (Sharp, 1989). From features of the visible palco-glacial bed (Sharp et al., 1989, Hubbard and Hubbard, 1998) there is evidence that pressurised conditions must have occurred sometime in the past. When the glacier was of larger size and volume, larger amounts of meltwater would have drained subglacially, increasing the chance of highly pressurised subglacial conditions occurring during times of high meltwater inputs. It remains unknown whether pressurised conditions sufficient to have a significant impact on glacier dynamics would occur again beneath Glacier de Tsanfleuron during a melt season with higher melt rates than during the 2001 season. However, Sharp appears to have, to a large extent, neglected the karstic bedrock which accounts for the loss of approximately 95 % of the basal water, which may be the major reason for low subglacial pressures and hence limited movement.

7.3.5 Summary of the main findings

Large amounts of melt in July and August (mean snowpack depth reduces from of 3.7 m to 0.4 m) deliver great amounts of water to the englacial and subglacial systems. Normally one would expect this to have a major influence upon the glaciers dynamics due to increased water pressure at the glacier bed. However, the capacity of the Nye-channel and cavity configuration seemed large enough to prevent pressurising the system. Perhaps more important is the loss of approximately 95 % of basal water into the bedrock karst system. This is reflected in relatively low proglacial discharges (< 0.6 $m^3 s^{-1}$) from a limited catchment area. Hence, on Glacier de Tsanfleuron there is no clear dynamic response to seasonal meltwater inputs (at least in the 2001 melt season). The system does not become destabilised due to subglacial water pressure over a large enough area for widespread velocity enhancements to take place. Surface ice velocity observations during this research and direct measurements of basal motion from marginal cavities (Hubbard, 2002) suggested stick-slip motion to occur at the basal margins at Glacier de Tsanfleuron. Such

brief motion patterns may be transferred from the basal margins to the glacier surface. To clarify whether this is likely to occur at Glacier de Tsanfleuron the coupling length between glacier bed and surface needs to be investigated and constrained.

7.4 Recommendations for future research

7.4.1 Instrumentation

Accurate snowmelt measurements at the snow surface are desirable, because the quantity of meltwater generated at the glacier surface influences flow velocities through the snowpack (Colbeck, 1978). Water table measurements at the snow-ice interface and ablation measurements can provide information about storage and delay of meltwater flow. For the effective coupling of meltwater generation with water table variations at the snow-ice interface, measurement of surface melt rates at a higher resolution than from daily stake readings would be ideal. This could be achieved by using an ultrasonic depth gauge (UDG).

Combination of lysimeter measurements and dye tracer experiments could give quantitive information about flow velocities and meltwater delivery from the snowpack to the englacial drainage system during the diurnal cycle. The combination of lysimeter measurements with velocity measurements from dye tracing could help elucidate any relationship between snowmelt and diurnal bulk discharge variations.

Thermistor-chains especially in cold snowpacks would be useful for detecting both freezing and refreezing processes that may influence surface meltwater production and its transport through the snowpack.

Redesign of the fluorometer head/sensor to enable tracer concentration measurements at lower water levels than the 4 cm that the borehole fluorometer requires at the moment. If the detection depth could be reduced this might eliminate the need for a "detection pool" and enable direct measurements as meltwater drains from the snowpack at the snow-ice interface.

Also, it would be useful to establish meteorological stations on the glacier to obtain meteorological information regarding parameters such as solar radiation, precipitation, wind intensity, evaporation and relative humidity that influence the snowpack. But it must be stressed that the complexity of the heterogeneous snowpack requires good temporal melt-rate data collection to coincide with data from in-situ meteorological stations.

Geophones, connected to real-time data loggers, strategically placed on the glacier surface may also be used to detect ice-quake activity data. These data might then be used to identify weather "stick-slip" events are real (Kavanaugh and Clarke, 2001) and related to changes in the prevailing hydrological conditions.

7.4.2 Data collection

Dye tracing in snowpack was found to be a valuable method that can give further insight into meltwater flow processes within supraglacial snowpacks (although, there is room for improvements of the method as suggested in Section 4.8.2). Moulin experiments to investigate subglacial drainage characteristics have again been shown to provide useful information about a hydrological system that is otherwise would be inaccessible. Observations in years with different hydrological or climatical characteristics such as differences in snowline retreat, cold or warm summers and thick or thin winter snowpack demonstrate that a single season may be unrepresentative of the "normal" year. In order to obtain a clearer picture, similar research should be carried out over several seasons.

A series of experiments into the same moulin or borehole at different discharge levels and different water levels would prove useful to see if there is any variation in velocity with varying discharge at different water levels, e.g. (Hubbard et al., 1995). These would then illustrate whether water pressure is fluctuating with discharge and water level.

To clarify whether the position of the snowline (Nienow et al., 1998) had an influence on the subglacial drainage system, further investigations of subglacial flow conditions are required in years with other hydrological characteristics, e.g. repeated tracer experiments into the same moulin during a daily discharge cycle which are subsequently compared. Furthermore, to elucidate the development of the subglacial drainage system throughout the melt season, repeated experiments in a seasonal time scale could give valuable information. The inference is that the position of the snowline may significantly influence the size of the subglacial conduits (Fountain, 1996). To further study intra-seasonal variations and flow behaviour of meltwater within a linked-cavity system it would be useful to undertake extensive dye tracer experiments in a defined area of the glacier with no karst sinkholes.

Appendices

Appendix A: Calibration of the field fluorometer

In order to obtain accurate estimates of dye concentrations, the Turner 10 field fluorometers require calibration. The calibration of both Turner fluorometers was undertaken before the experiments during the field season. Prior to the field season about 500 ml of standard solutions (30000 $\mu g\ l^{-1}$ and 3000 $\mu g\ l^{-1}$) were prepared with deionised water in the lab. These standards allowed easy preparation of accurate calibration solutions in the field for the whole range of concentrations expected during the measurements. Using a pipet (1 ml) for small quantities and a glass graduate cylinder (10 ml) for larger quantities, different volumes of the standard solution were measured and subsequently diluted with clear stream water in a glass volumetric flask (1000 ml) to prepare calibration solutions of 3, 15, 30 and 45 $\mu g\ l^{-1}$. The stream water was cleared from sediments by filtering (Whatman 542 filter paper pore size 2.7 µm). For the calibration the flow cuvette of the fluorometer was sealed at one side and calibration solutions were then poured in at the other side. A total of five calibration concentrations (including a blank) were each measured three times to obtain a calibration function by linear regression (Figure A.2). In between using the various calibration solutions the fluorometer cuvette was cleaned by flushing with clear stream water, purging previous tracer contamination.

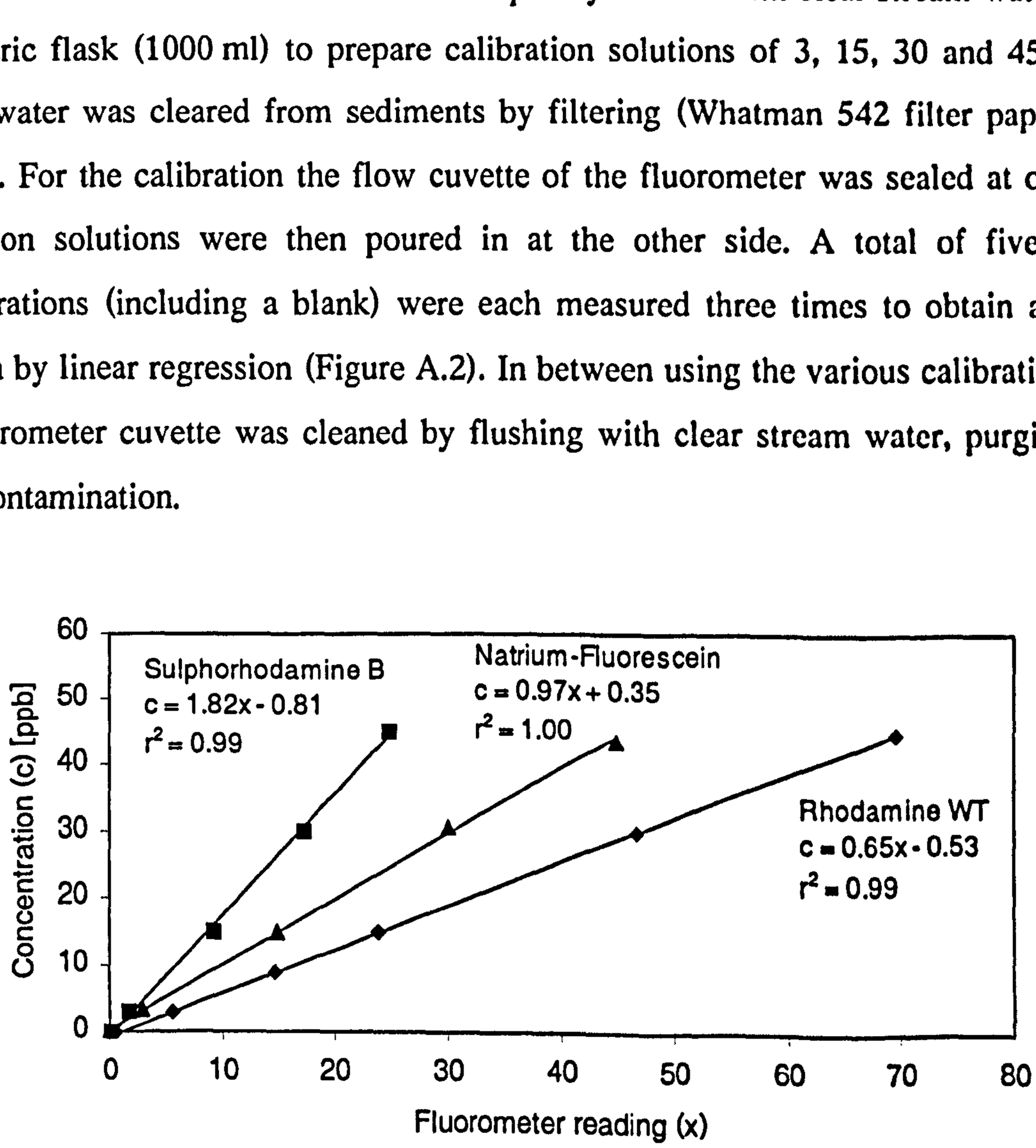

Figure A.1: Calibration curves for rhodamine WT, sulphorhodamine B and sodium-fluorescein for the Turner 10 field fluorometer.

Appendix B: Snow density

To obtain the density of the snowpack a pit was dug and vertical samples taken in the pit wall from the snow surface down to the glacier ice using a stainless steel snow-density measuring tube of 10 cm diameter and a precise spring balance. From the sample length and weight the snow density and water equivalent was calculated.

Table A.1: Densities of the upper 30 to 50 cm of the snowpack

Date	Stake location (see Figure A.3)	Altitude [m a.m.s.l]	Density of the upper 30 to 50 cm of the snowpack [kg m^{-3}]
29/06/2001	50	2710	477
30/06/2001	30	2650	514
02/07/2001	200 m below 10	2560	490
02/07/2001	201 m below 10	2560	459
14/07/2001	40	2690	586
21/07/2001	10	2590	563
21/07/2001	30	2650	554
26/07/2001	20	2630	564
31/07/2001	$55S_1$	2730	470
05/08/2001	20	2650	479
07/08/2001	$35S_1$	2670	562
13/08/2001	20	2650	499
17/08/2001	20	2650	534
21/08/2001	$55S_1$	2730	532
21/08/2001	$55N_1$	2750	597
22/08/2001	50	2710	541
Average			530

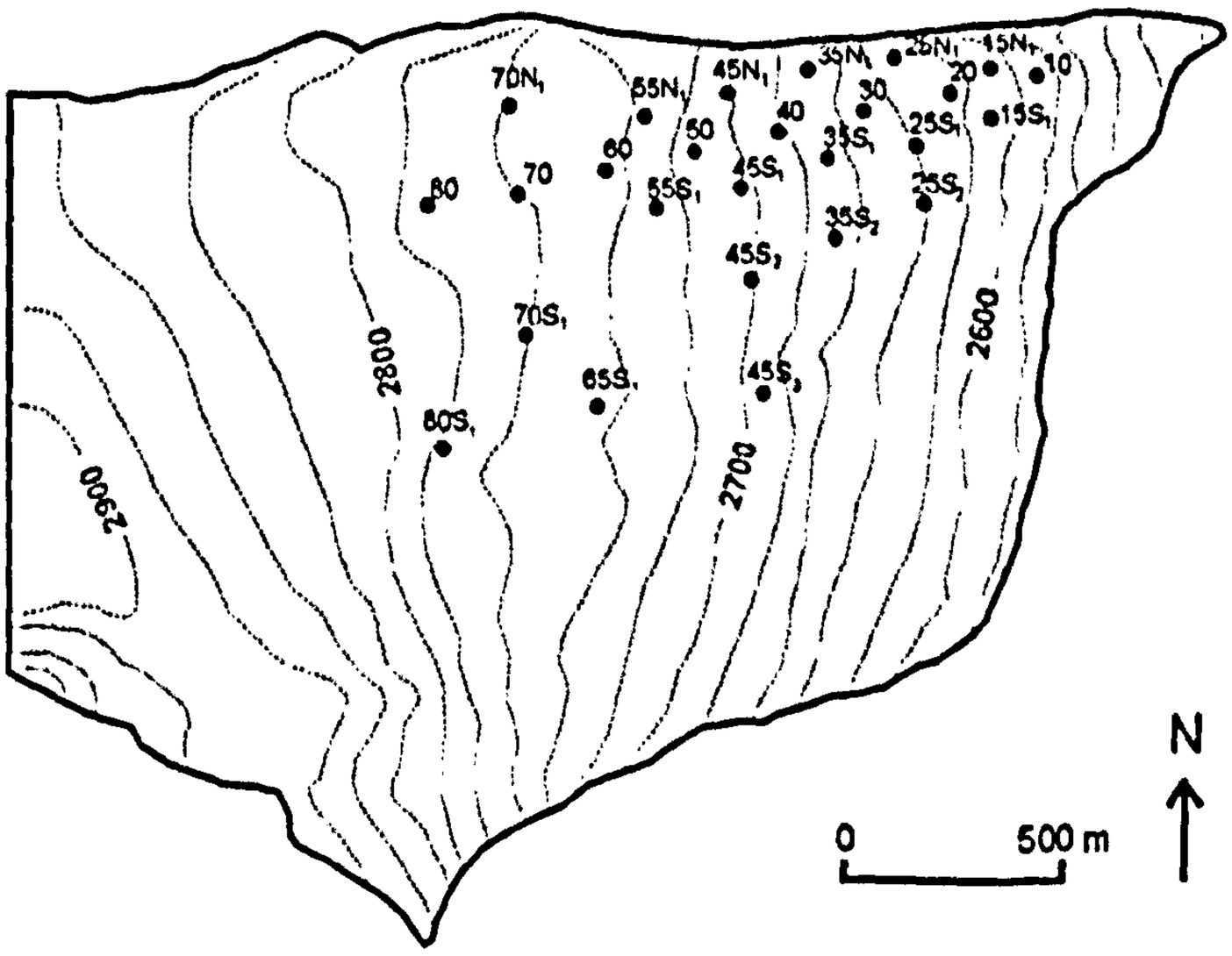

Figure A.2: The stake network across Glacier de Tsanfleuron.

Appendix C: Nye Channels in the proglacial area of Glacier de Tsanfleuron

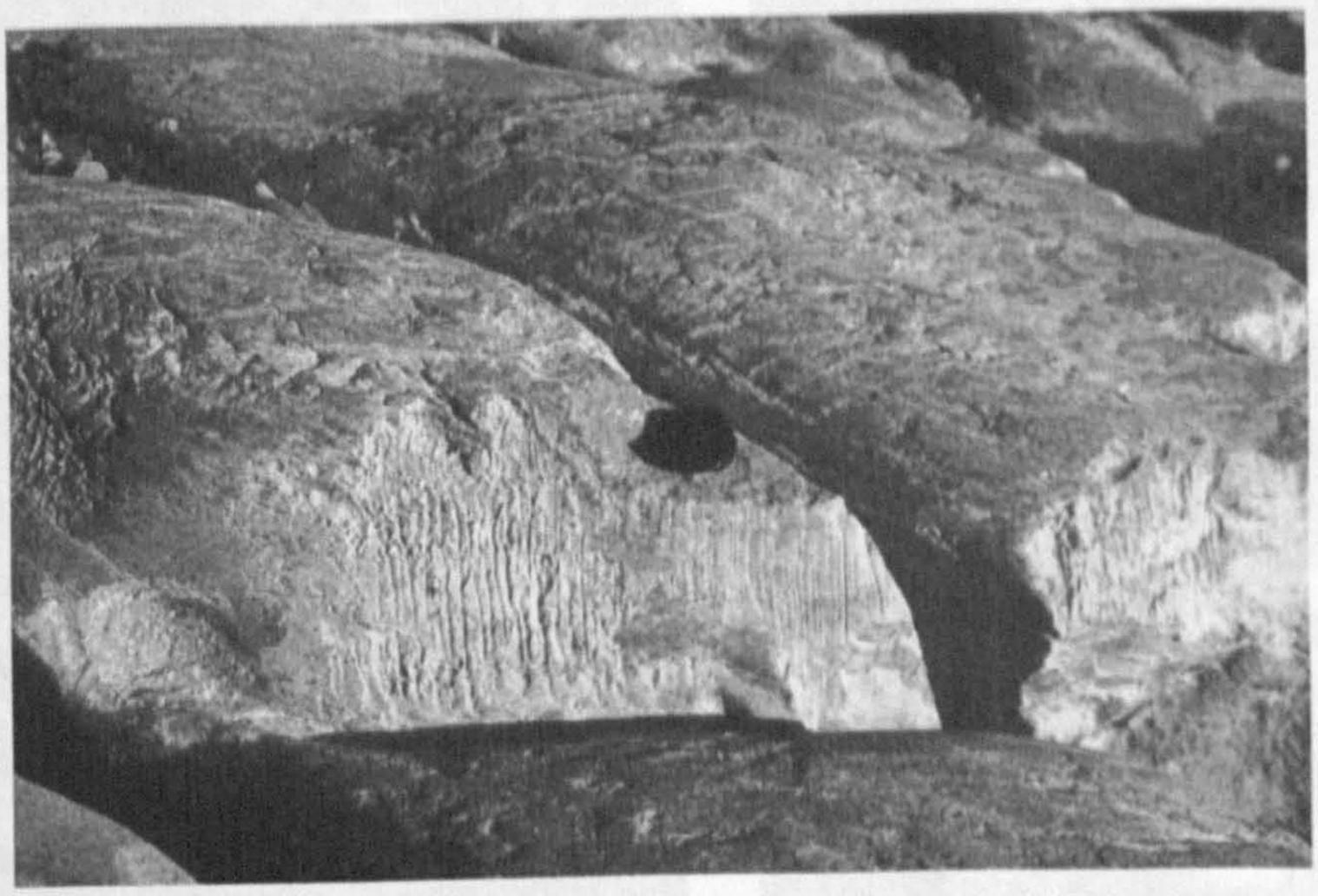

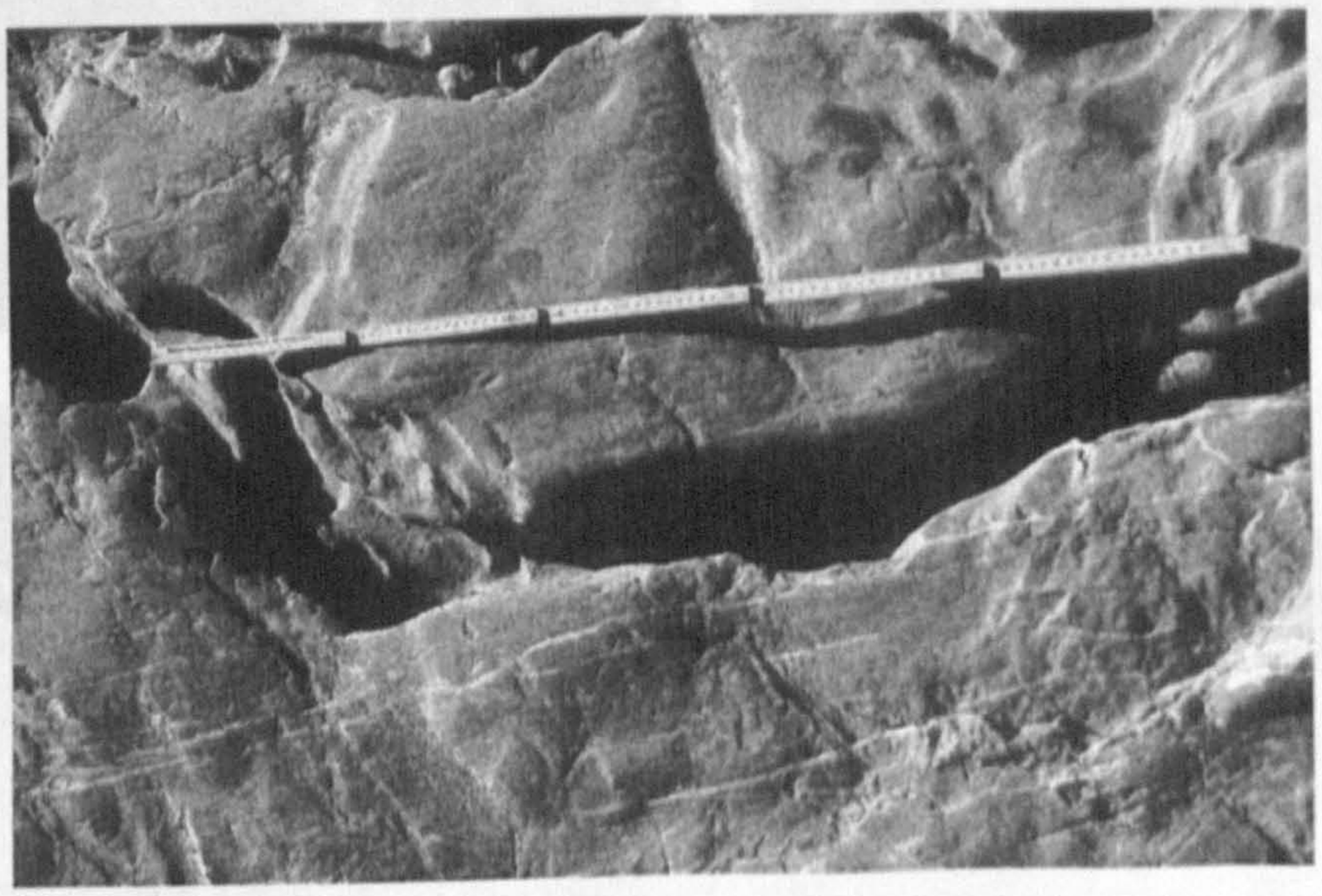

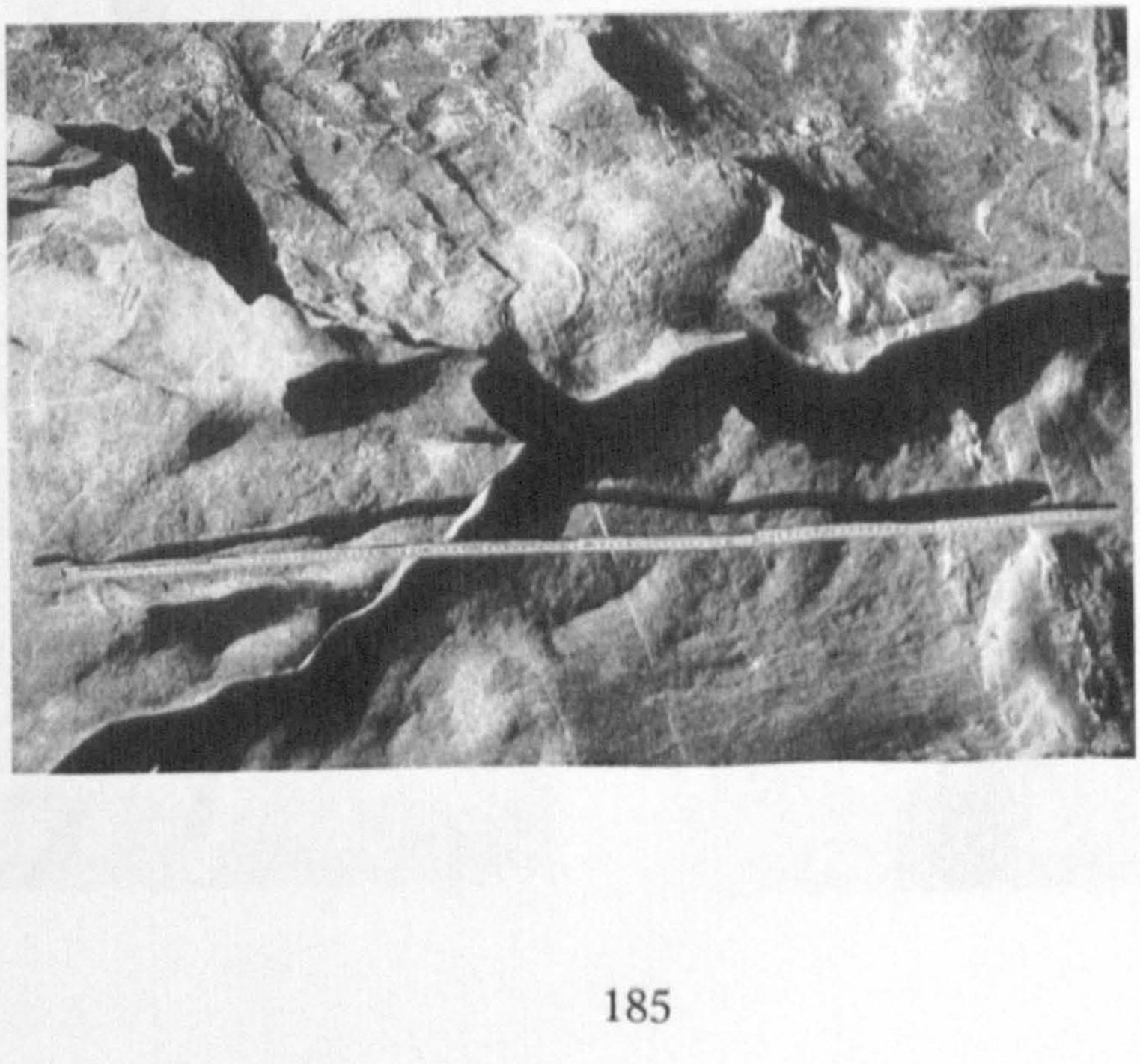

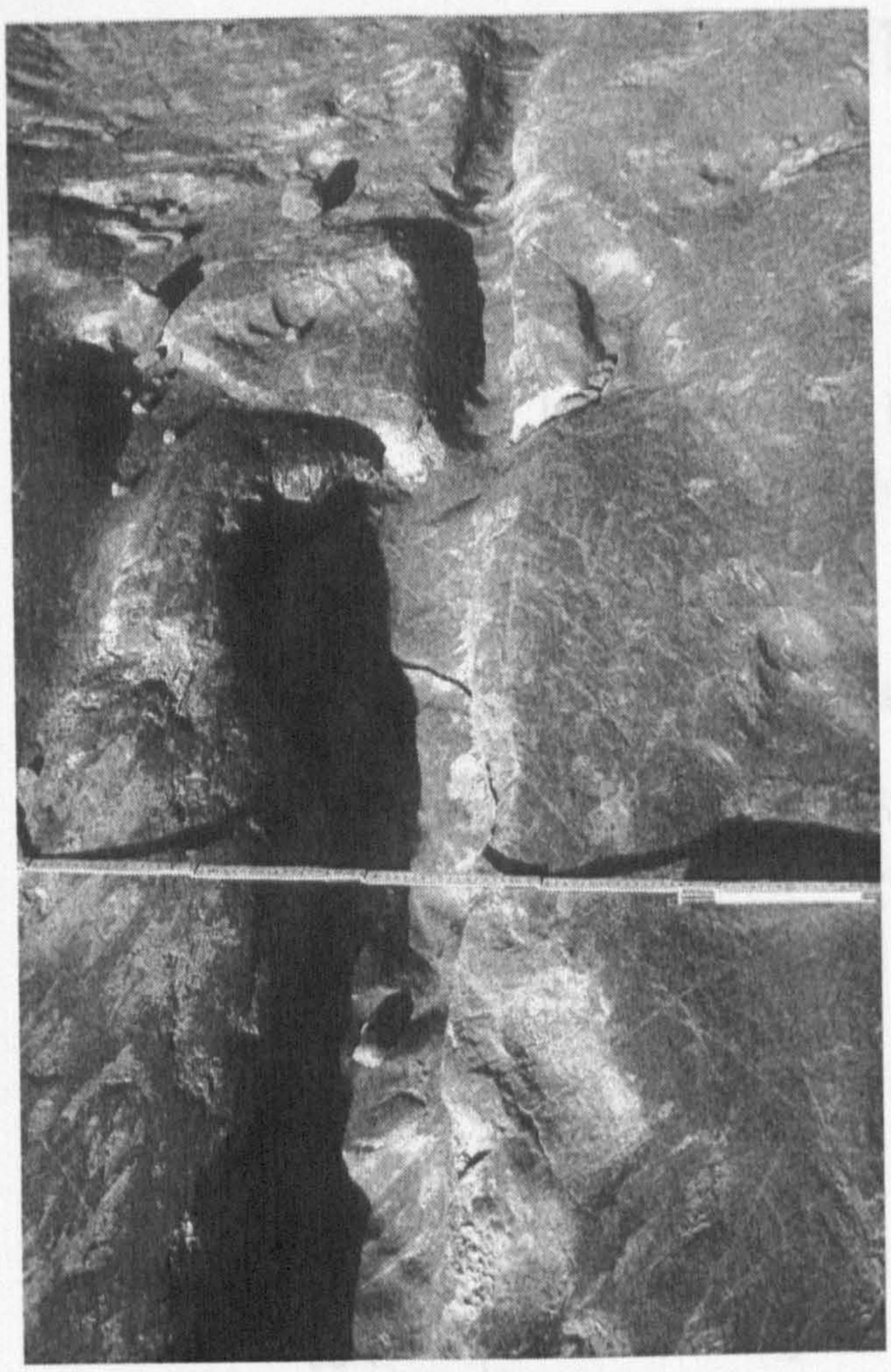

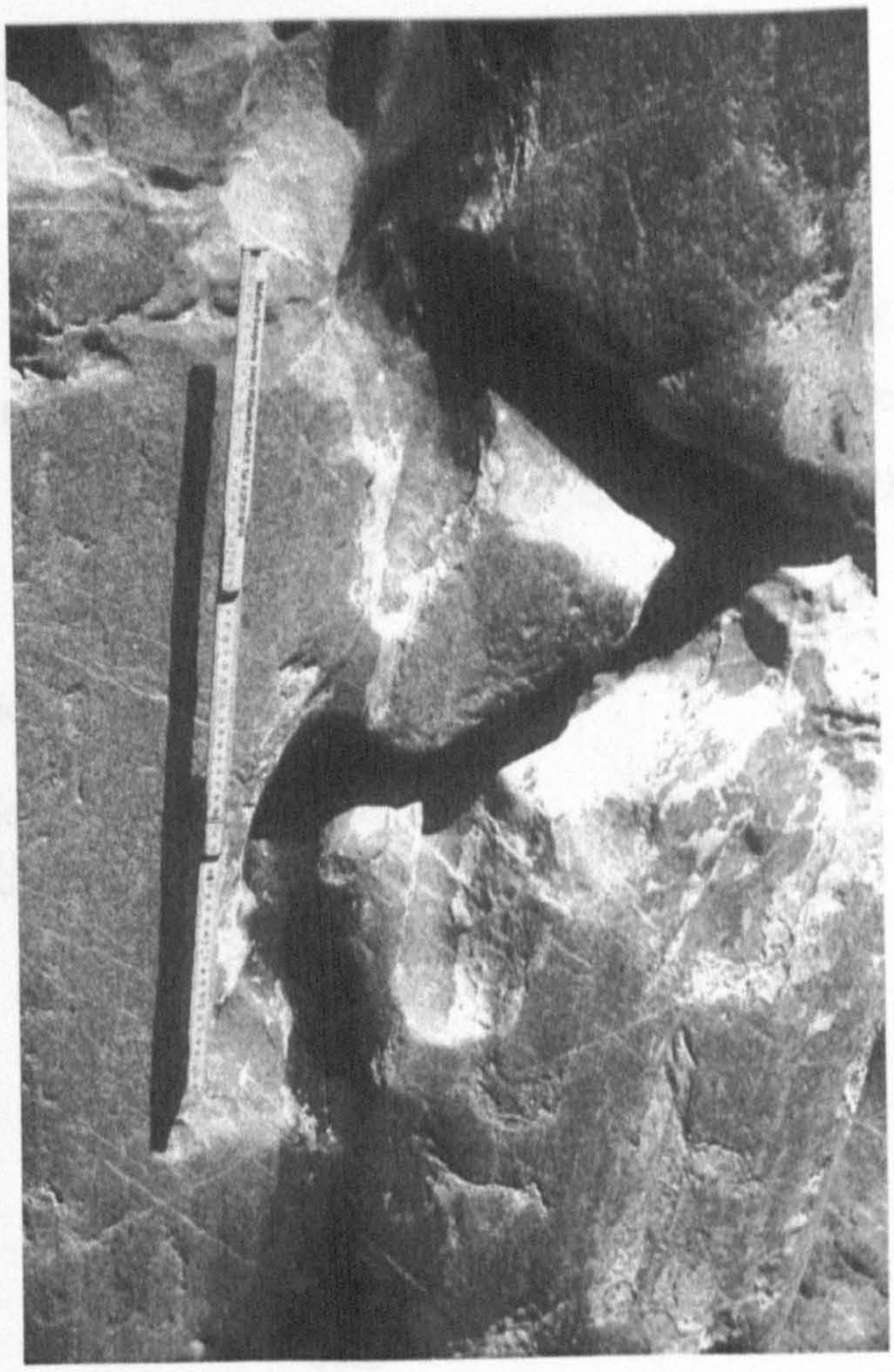

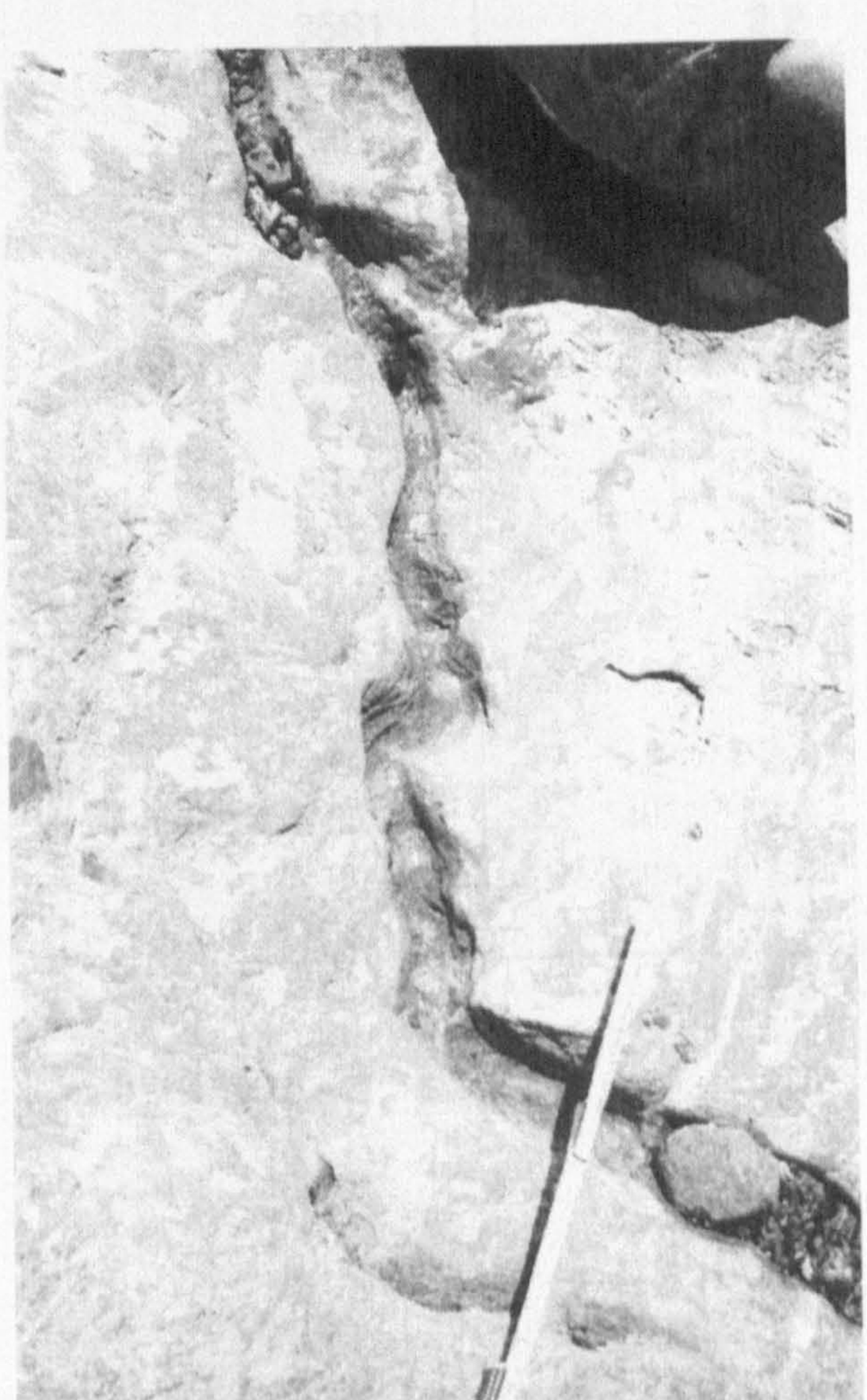

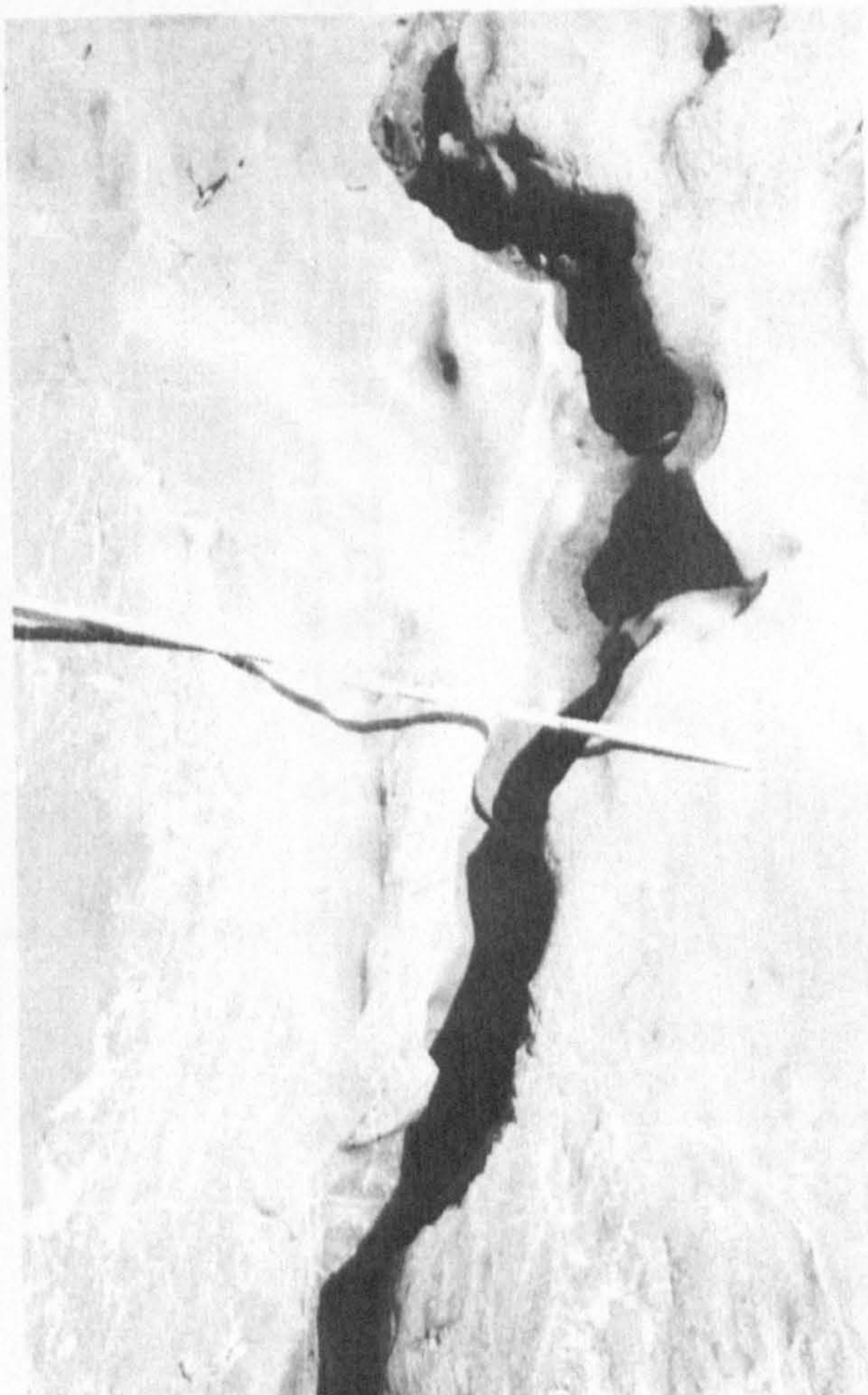

Appendix D: Horizontal flow velocities of all stakes

Survey precision

The position of all stakes was measured at least twice and the mean of the resulting xy-coordinates was used to calculate the planar stake position. The uncertainty of the xy-coordinates was calculated as a mean value using the two available xy-positions from all measurements at each stake.

Table A.2: Reproducibility estimate of the xy position of the surveying stakes.

Stake	Mean xy uncertainty [cm] between Survey 1 and Survey 2	Standard deviation
10	3.4	2.66
15N1	3.2	2.40
15S2	2.3	2.08
20	2.0	1.23
25N1	1.6	1.20
25S1	2.3	2.32
25S2	2.7	1.65
30	1.2	1.07
35N1	1.2	0.93
35S1	2.2	1.75
35S2	2.0	1.63
40	1.7	1.77
45N1	1.0	0.93
45S1	1.2	1.03
45S2	2.3	1.57
45S3	2.7	1.84
50	1.2	1.06
55N1	1.2	1.75
55S1	1.9	1.33
60	0.8	0.73
65S1	2.7	2.29
70N1	1.5	1.02
70	2.1	1.92
70S1	2.3	2.01
80	1.5	1.18
80S1	3.7	2.94
mean	2.0	1.63

Survey results

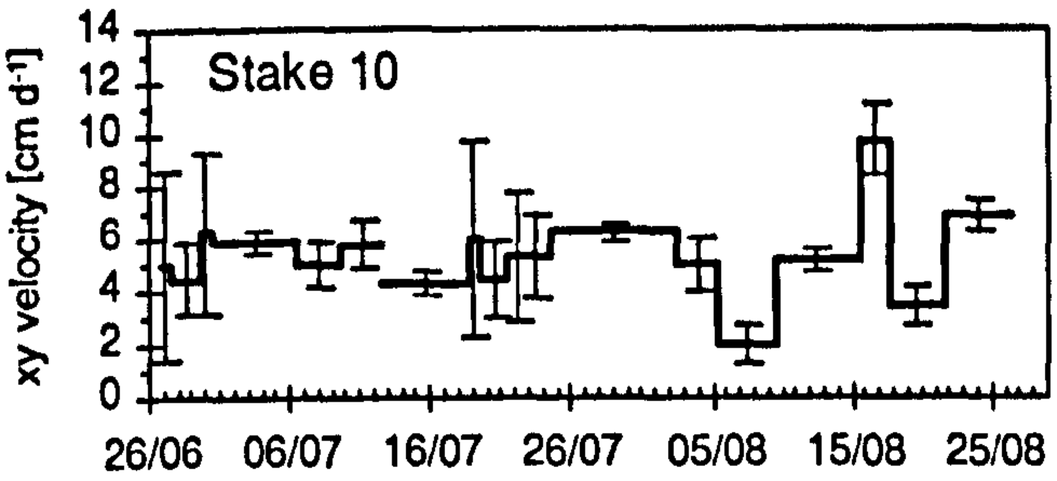

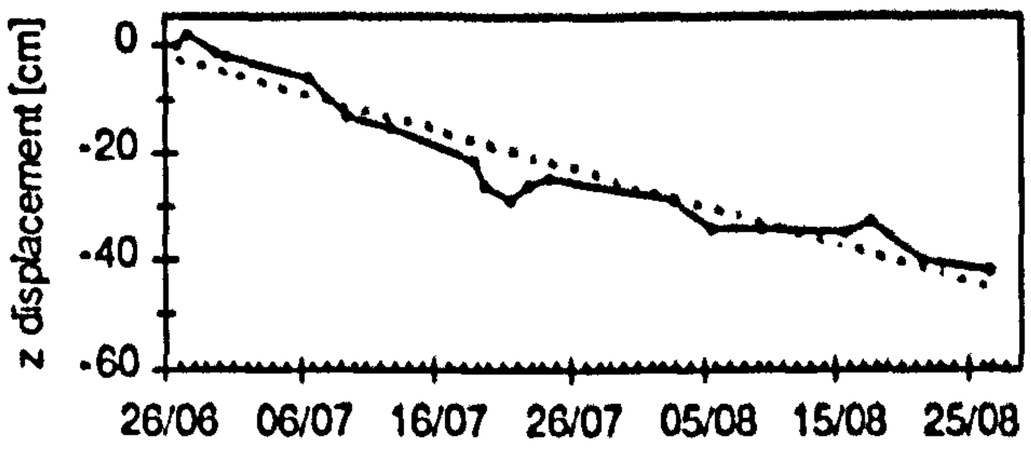

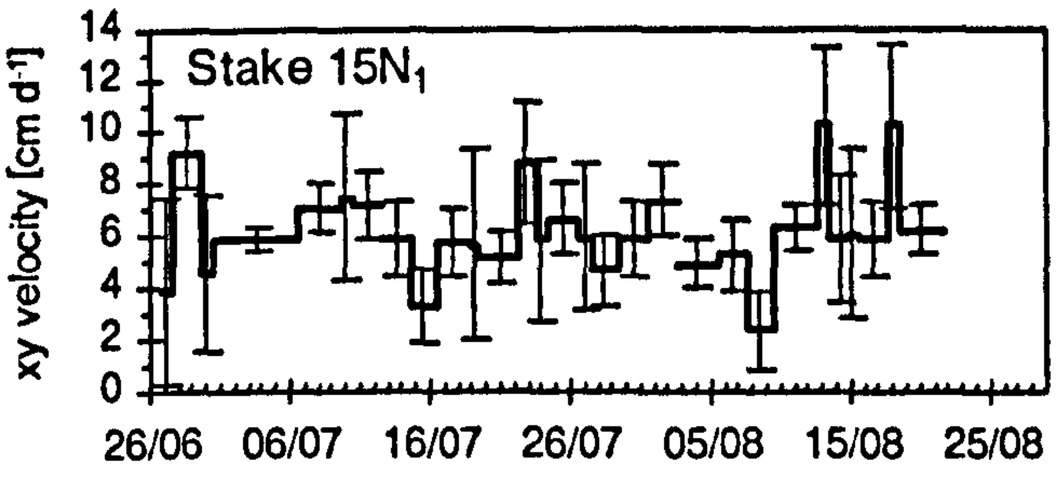

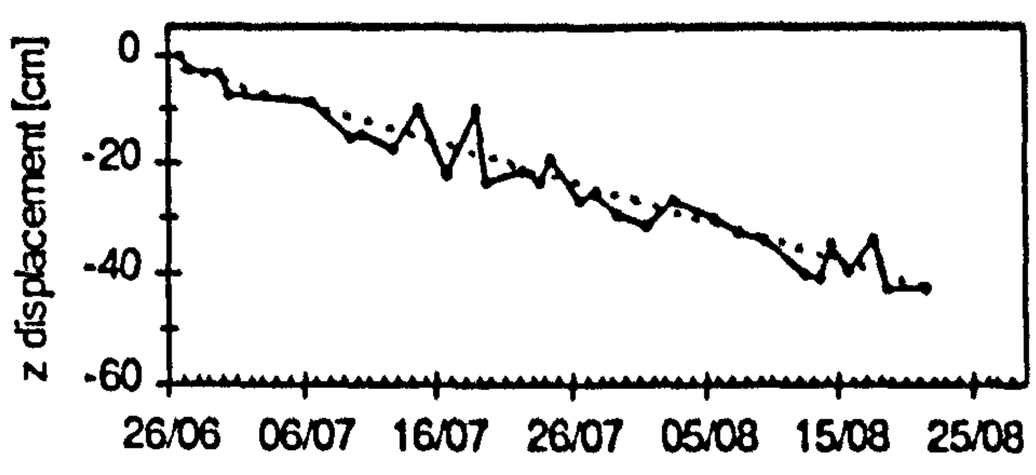

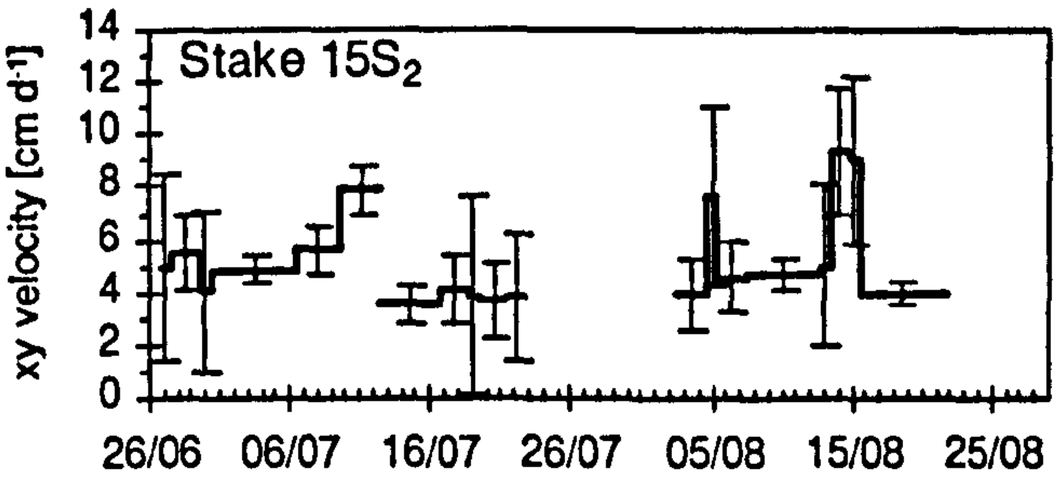

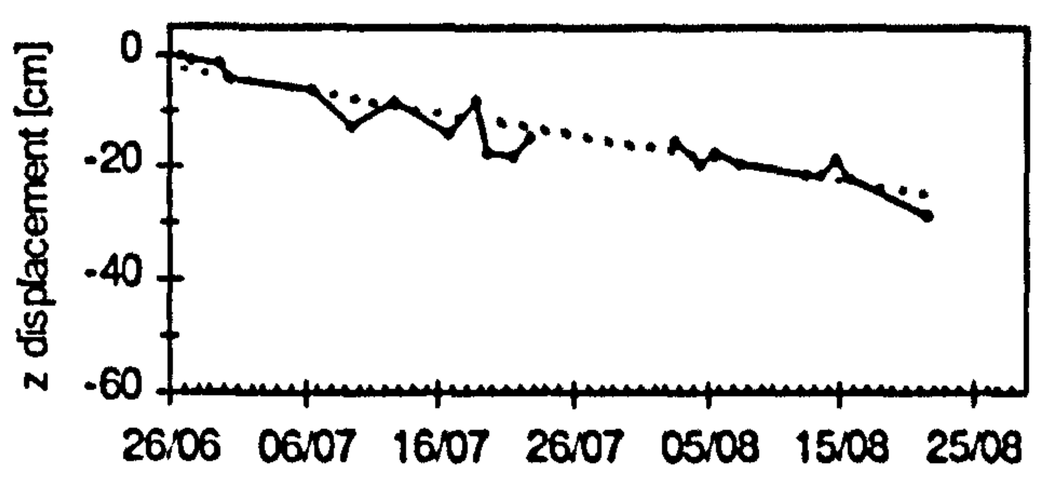

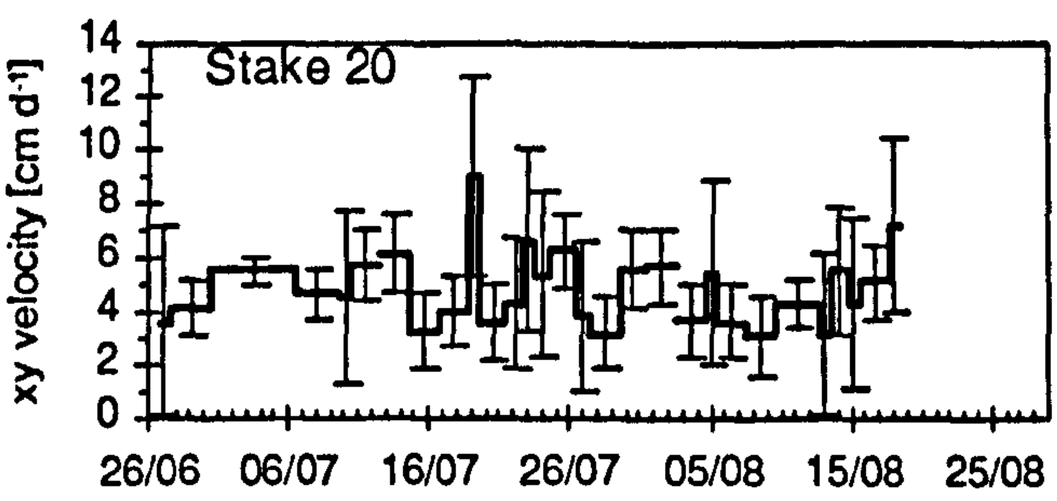

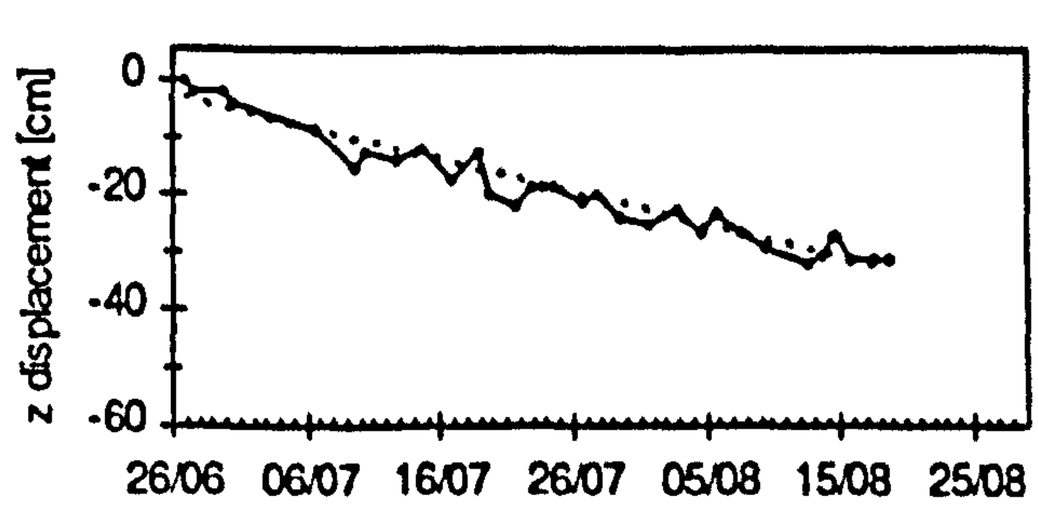

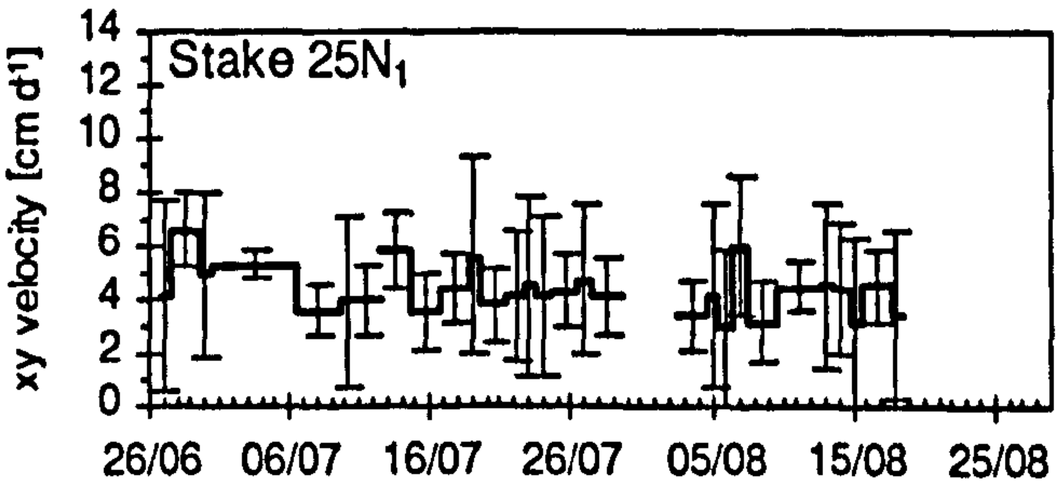

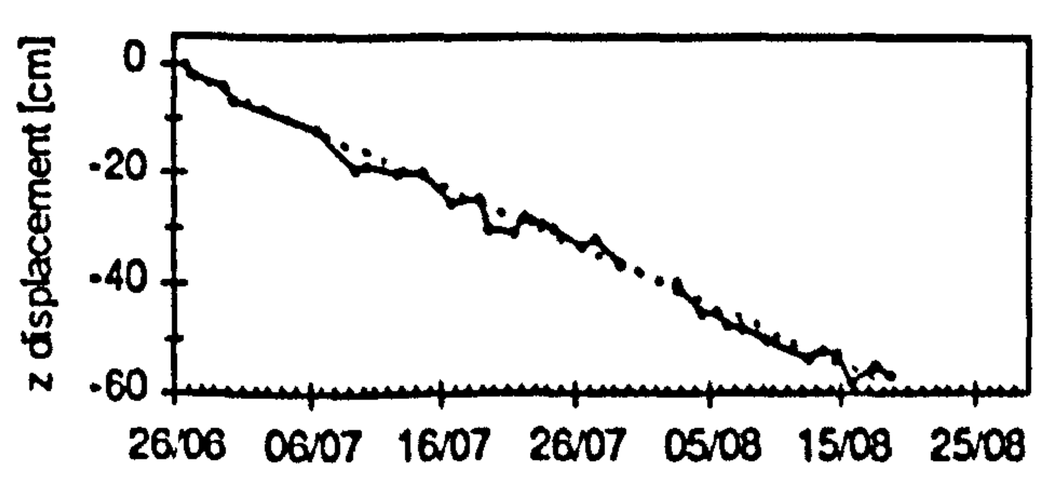

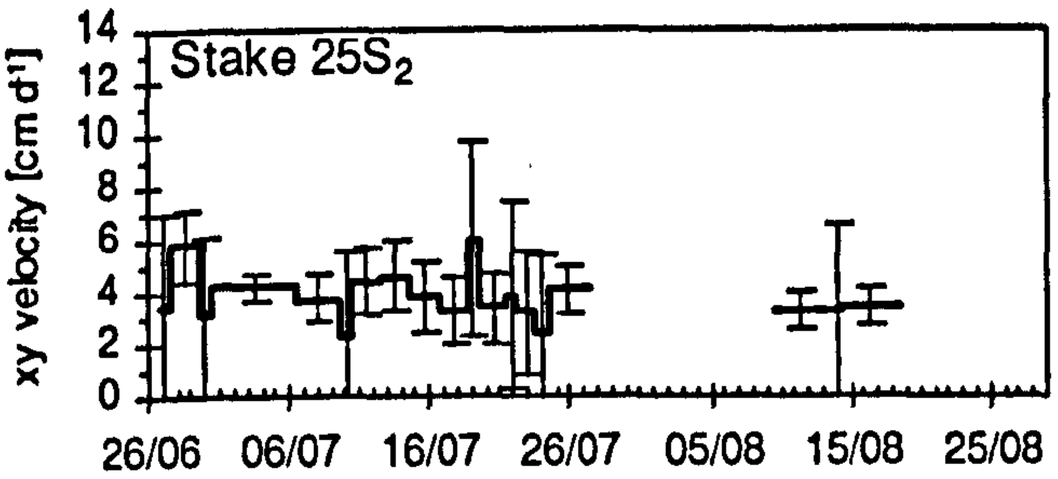
Stake 25S2
xy velocity [cm d-1]
14
12
10
8
6
4
2
0
26/06
06/07
16/07
26/07
05/08
15/08
25/08

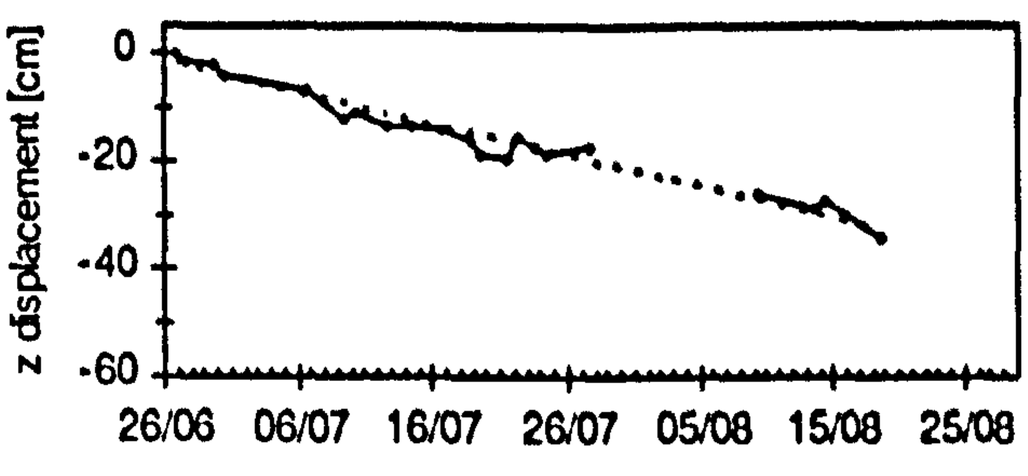
z displacement [cm]
0
-20
-40
-60
26/06
06/07
16/07
26/07
05/08
15/08
25/08

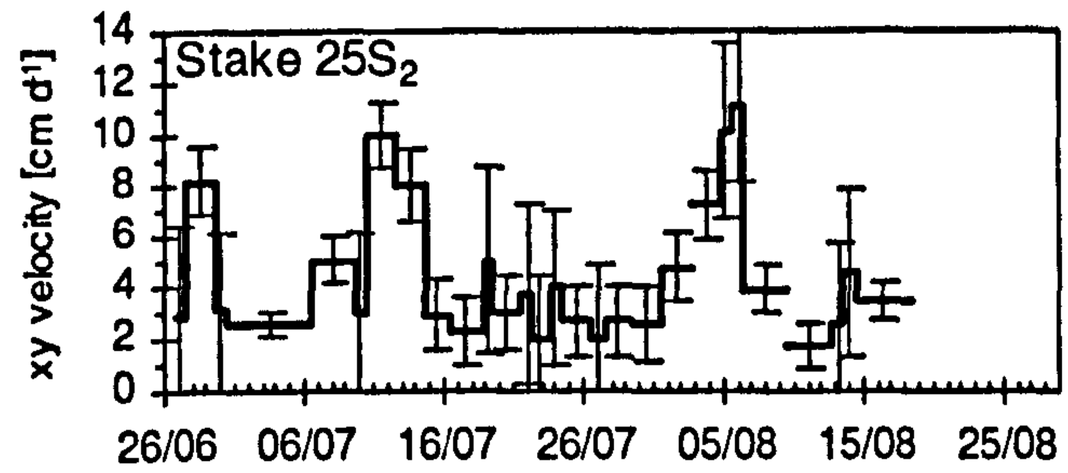
Stake 25S2
xy velocity [cm d-1]
14
12
10
8
6
4
2
0
26/06
06/07
16/07
26/07
05/08
15/08
25/08

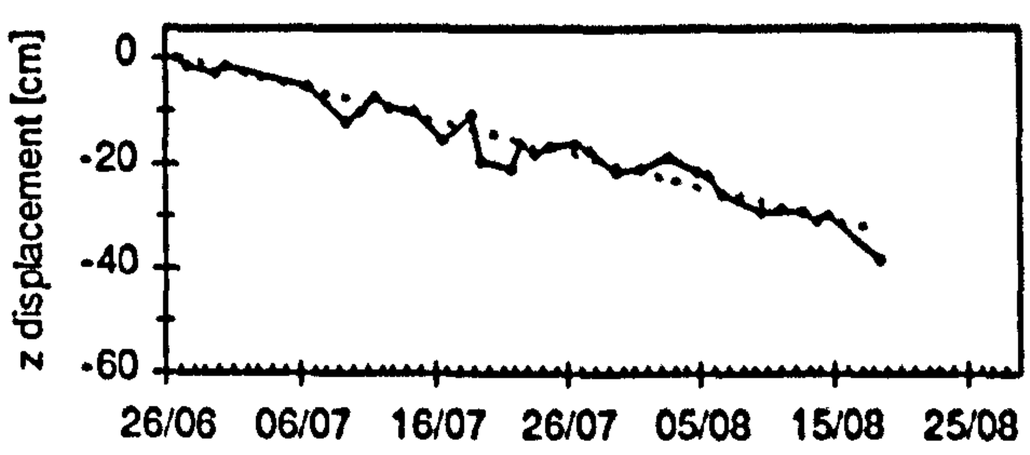
z displacement [cm]
0
-20
-40
-60
26/06
06/07
16/07
26/07
05/08
15/08
25/08

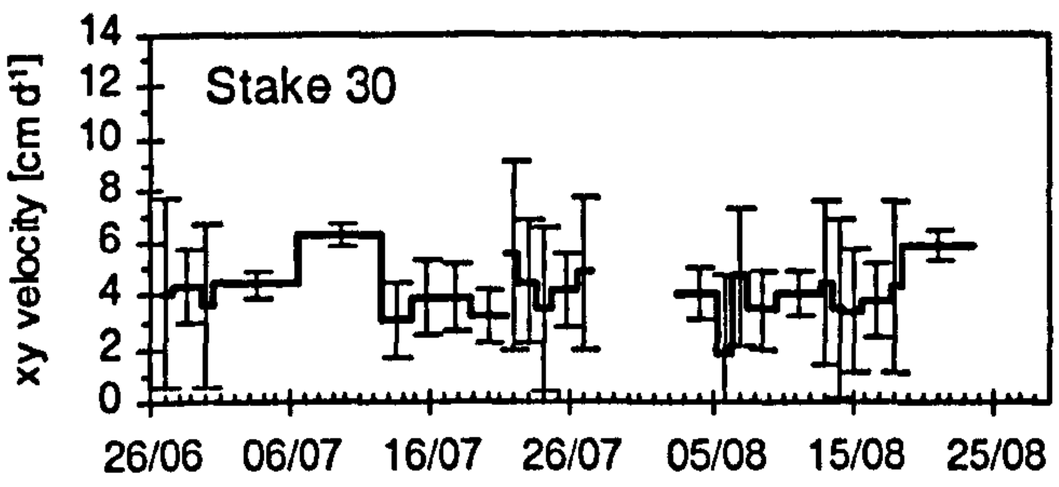
Stake 30
xy velocity [cm d-1]
14
12
10
8
6
4
2
0
26/06
06/07
16/07
26/07
05/08
15/08
25/08

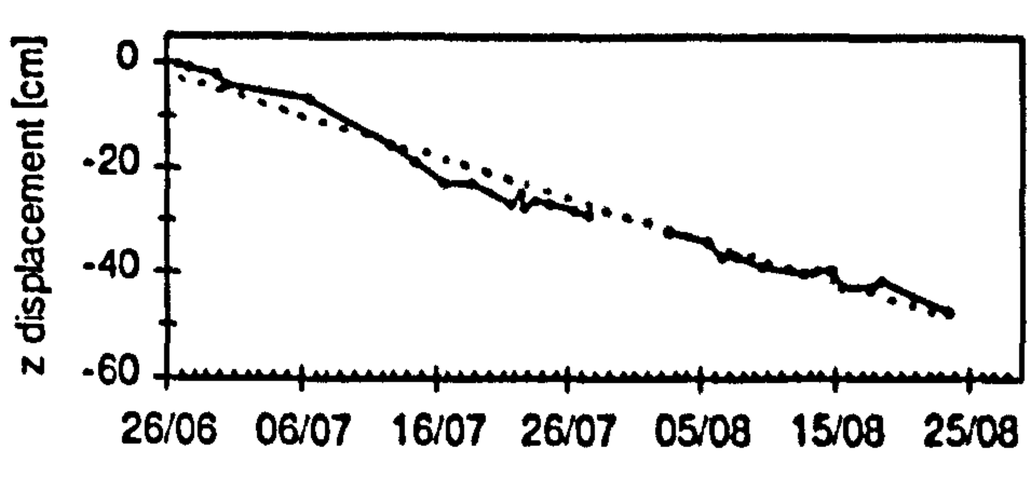
z displacement [cm]
0
-20
-40
-60
26/06
06/07
16/07
26/07
05/08
15/08
25/08

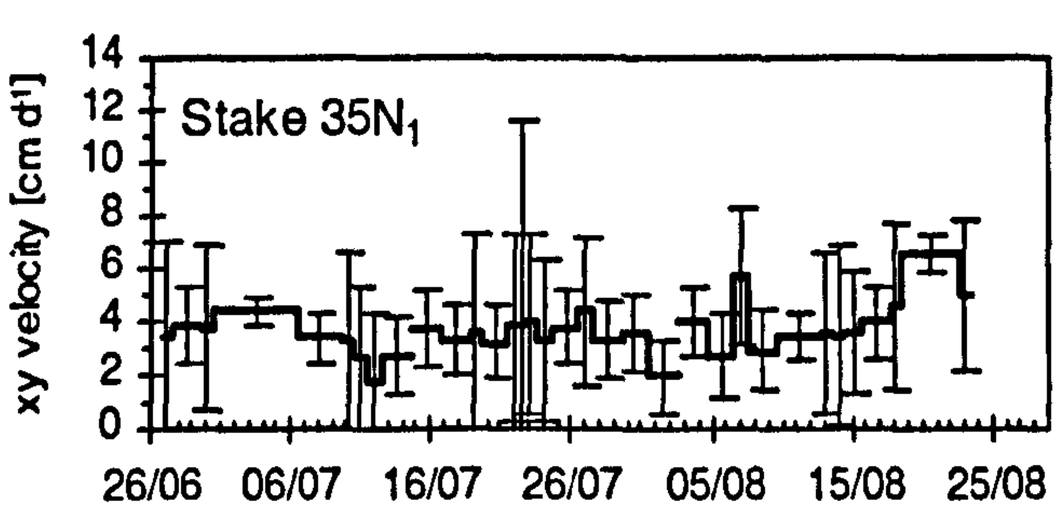
Stake 35N1
xy velocity [cm d-1]
14
12
10
8
6
4
2
0
26/06
06/07
16/07
26/07
05/08
15/08
25/08

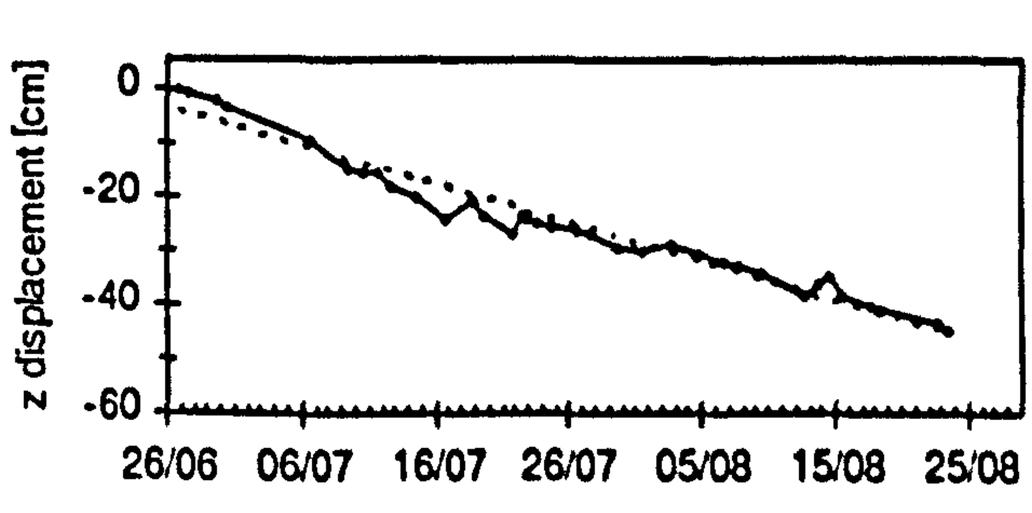
z displacement [cm]
0
-20
-40
-60
26/06
06/07
16/07
26/07
05/08
15/08
25/08

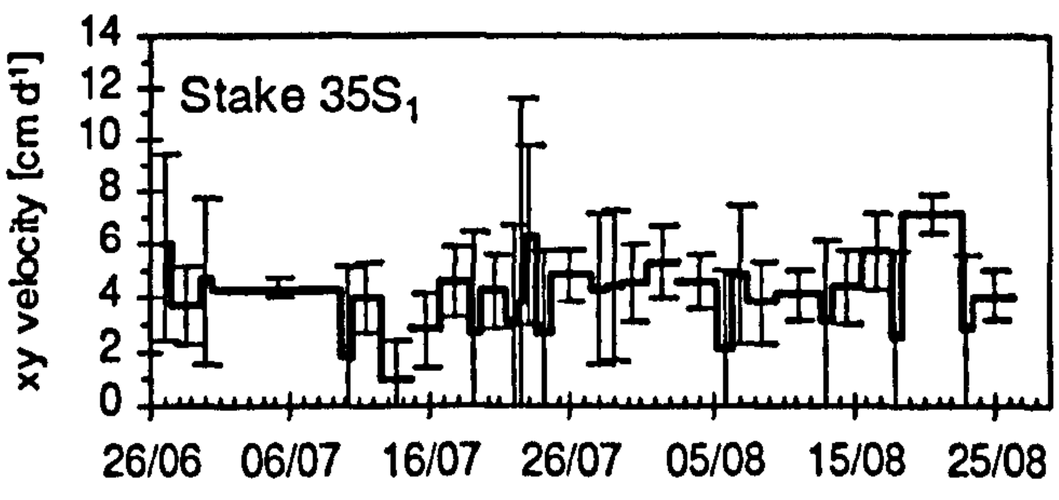
Stake 35S1
xy velocity [cm d-1]
14
12
10
8
6
4
2
0
26/06
06/07
16/07
26/07
05/08
15/08
25/08

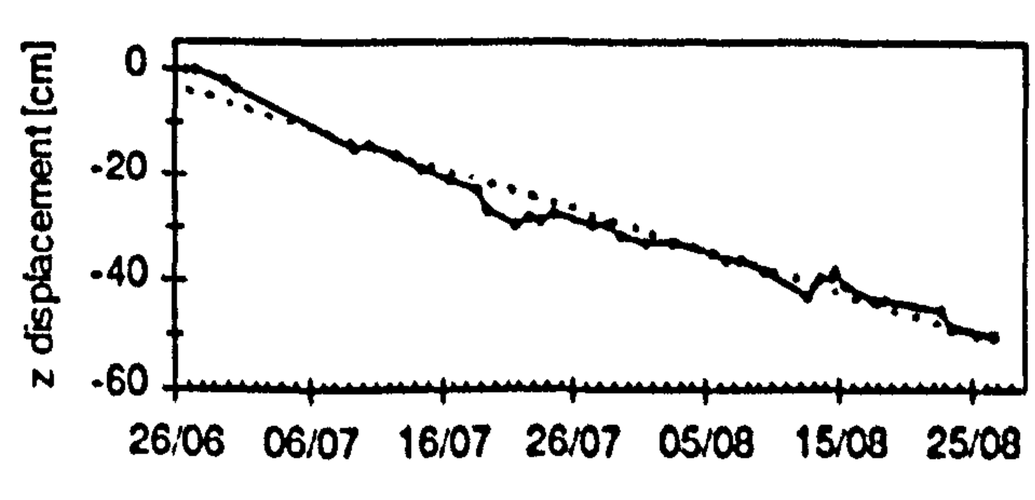
z displacement [cm]
0
-20
-40
-60
26/06
06/07
16/07
26/07
05/08
15/08
25/08

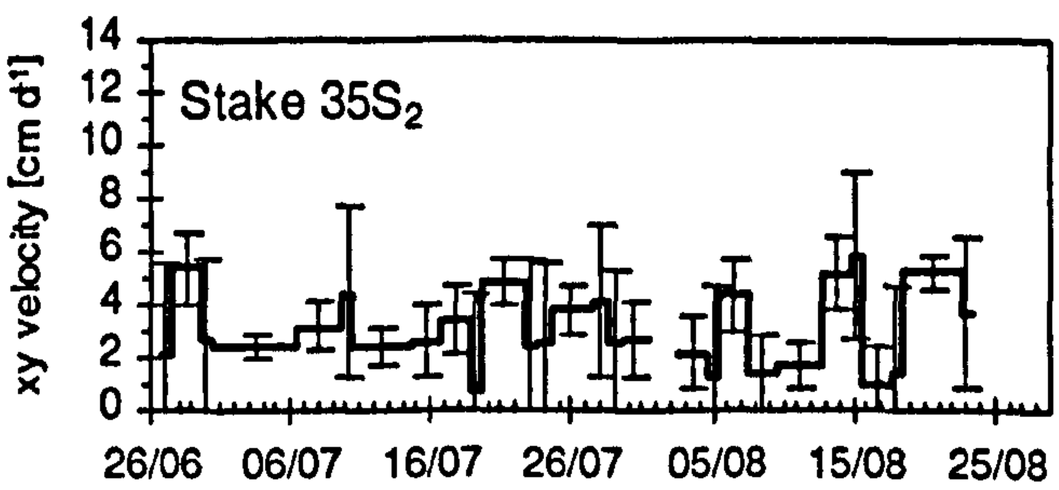
Stake 35S2
xy velocity [cm d-1]
14
12
10
8
6
4
2
0
26/06
06/07
16/07
26/07
05/08
15/08
25/08

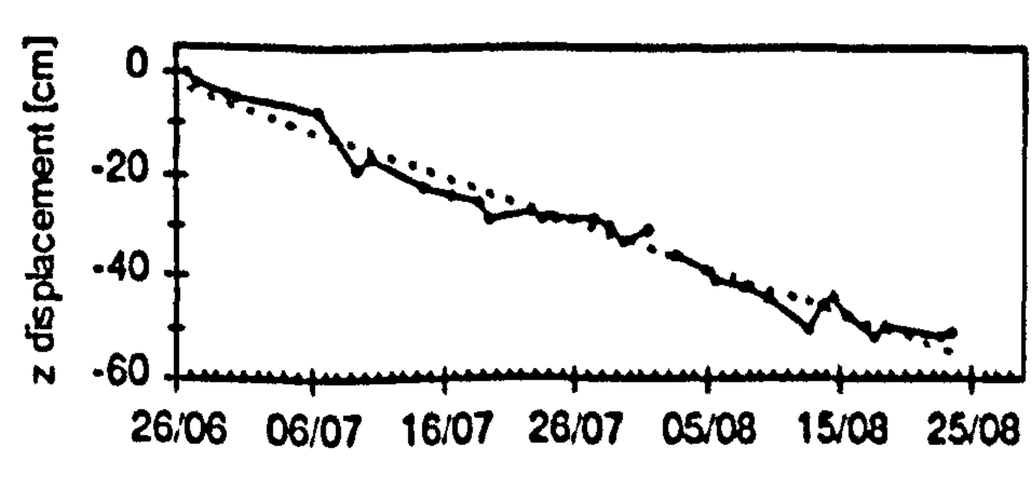
z displacement [cm]
0
-20
-40
-60
26/06
06/07
16/07
26/07
05/08
15/08
25/08

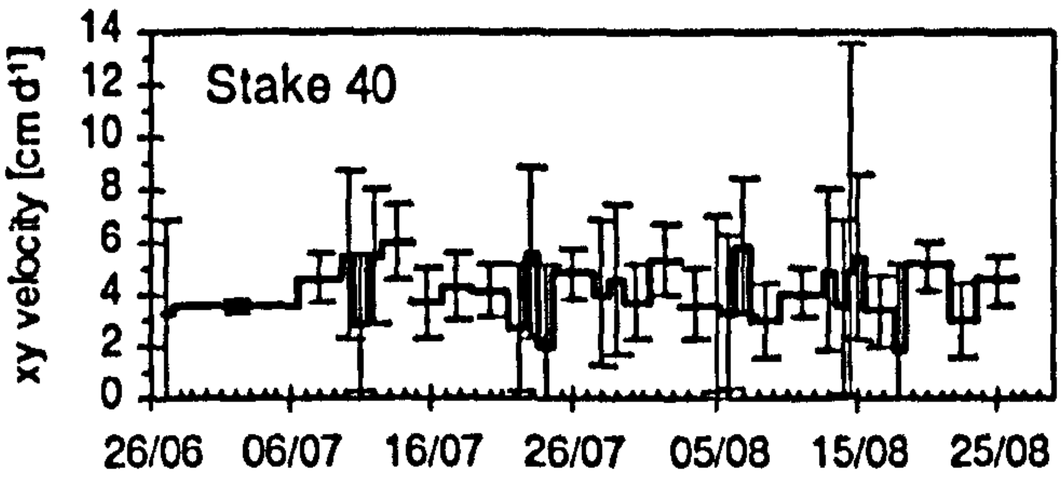
Stake 40
xy velocity [cm d-1]
0
2
4
6
8
10
12
14
26/06
06/07
16/07
26/07
05/08
15/08
25/08

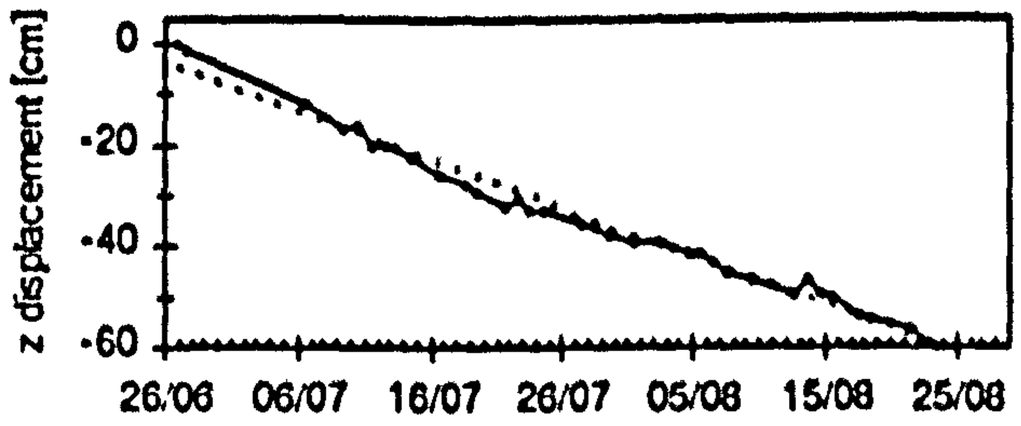
z displacement [cm]
0
-20
-40
-60
26/06
06/07
16/07
26/07
05/08
15/08
25/08

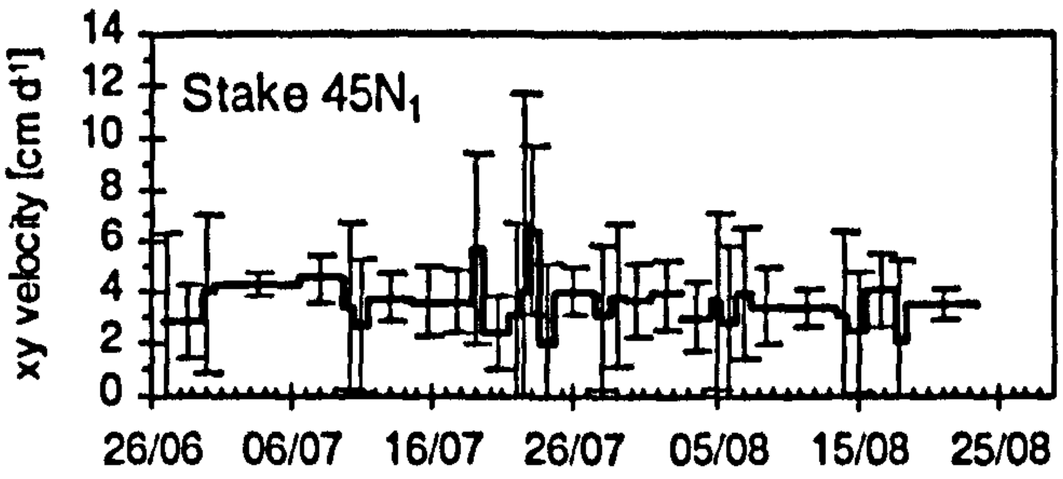
Stake 45N1
xy velocity [cm d-1]
0
2
4
6
8
10
12
14
26/06
06/07
16/07
26/07
05/08
15/08
25/08

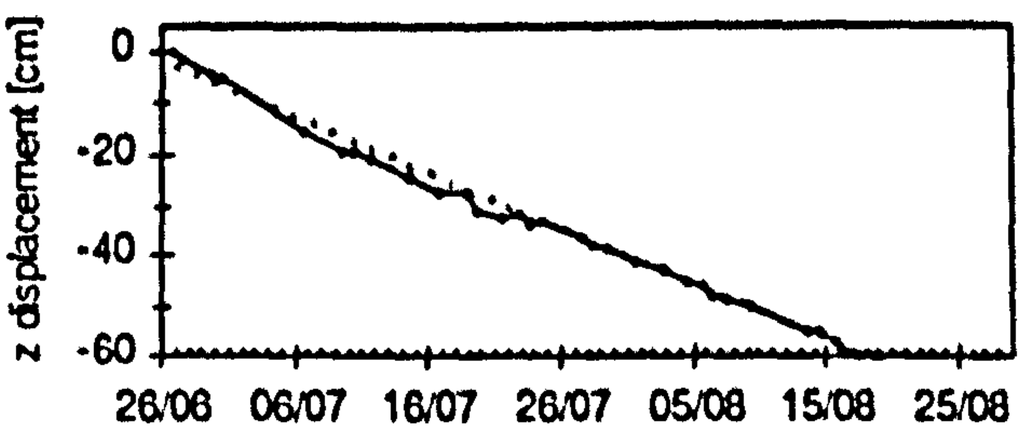
z displacement [cm]
0
-20
-40
-60
26/06
06/07
16/07
26/07
05/08
15/08
25/08

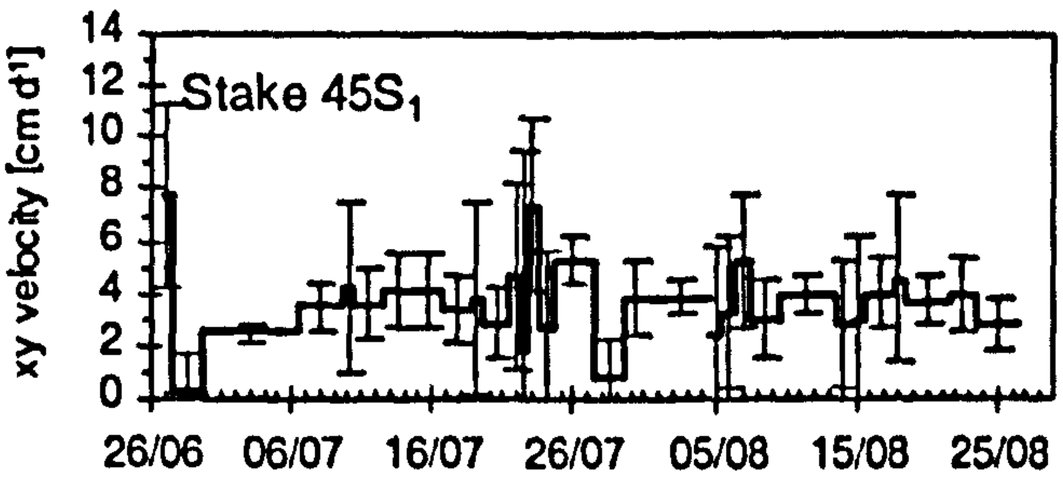
Stake 45S1
xy velocity [cm d-1]
0
2
4
6
8
10
12
14
26/06
06/07
16/07
26/07
05/08
15/08
25/08

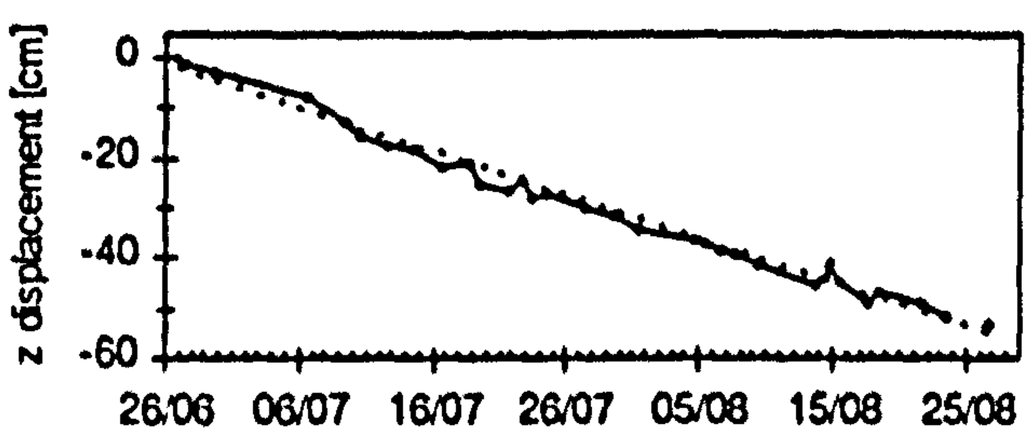
z displacement [cm]
0
-20
-40
-60
26/06
06/07
16/07
26/07
05/08
15/08
25/08

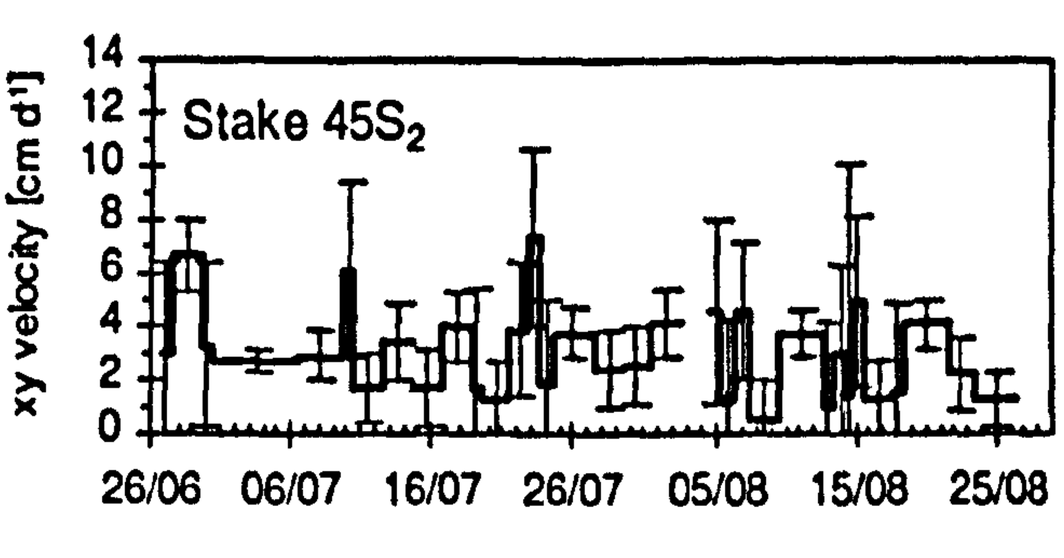
Stake 45S2
xy velocity [cm d-1]
0
2
4
6
8
10
12
14
26/06
06/07
16/07
26/07
05/08
15/08
25/08

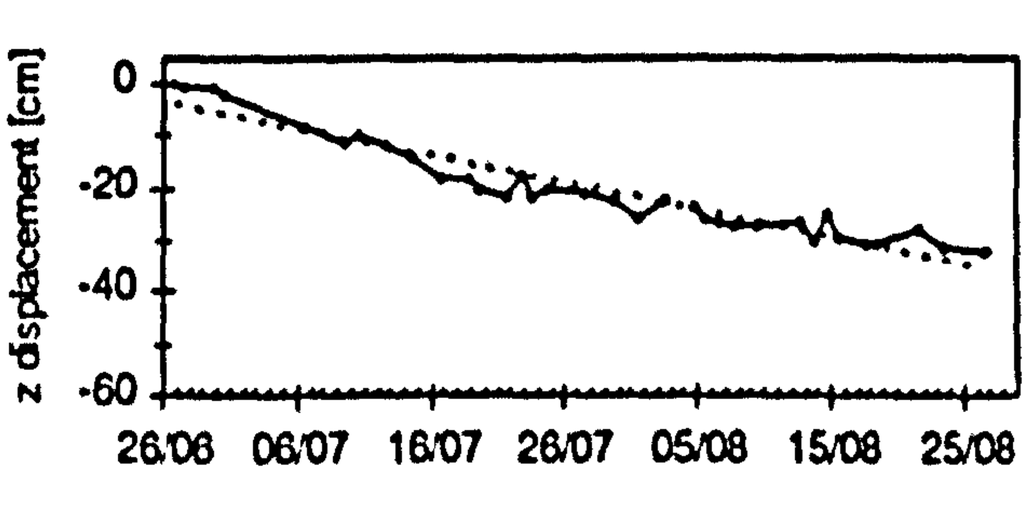
z displacement [cm]
0
-20
-40
-60
26/06
06/07
16/07
26/07
05/08
15/08
25/08

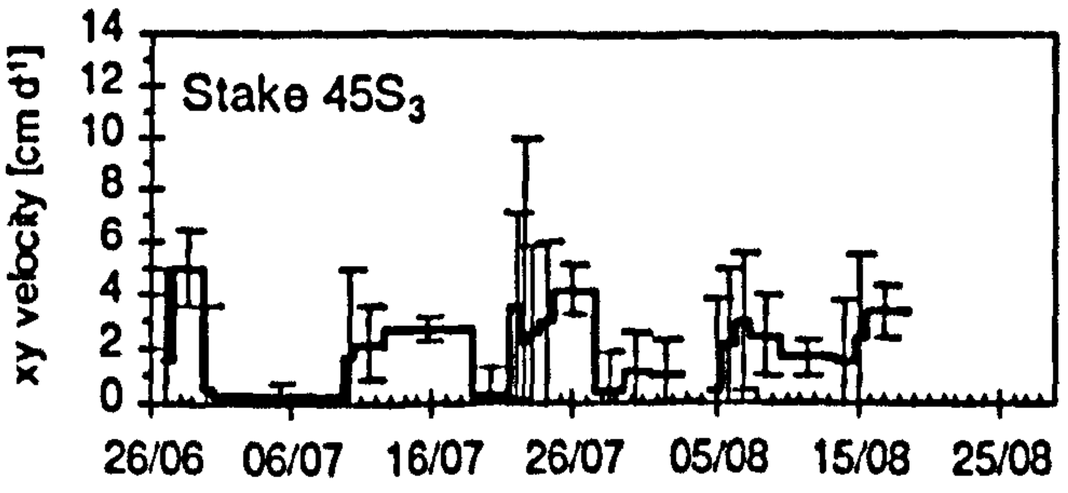
Stake 45S3
xy velocity [cm d-1]
0
2
4
6
8
10
12
14
26/06
06/07
16/07
26/07
05/08
15/08
25/08

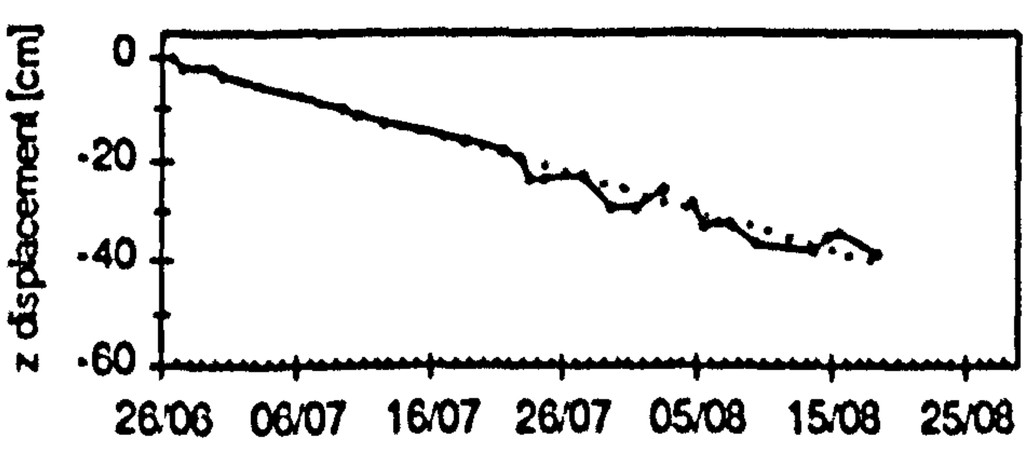
z displacement [cm]
0
-20
-40
-60
26/06
06/07
16/07
26/07
05/08
15/08
25/08

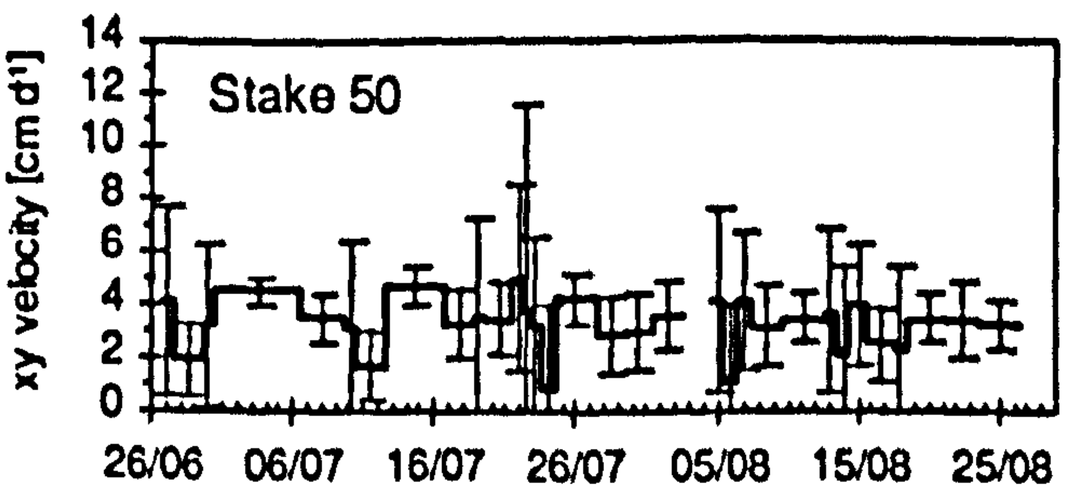
Stake 50
xy velocity [cm d-1]
0
2
4
6
8
10
12
14
26/06
06/07
16/07
26/07
05/08
15/08
25/08

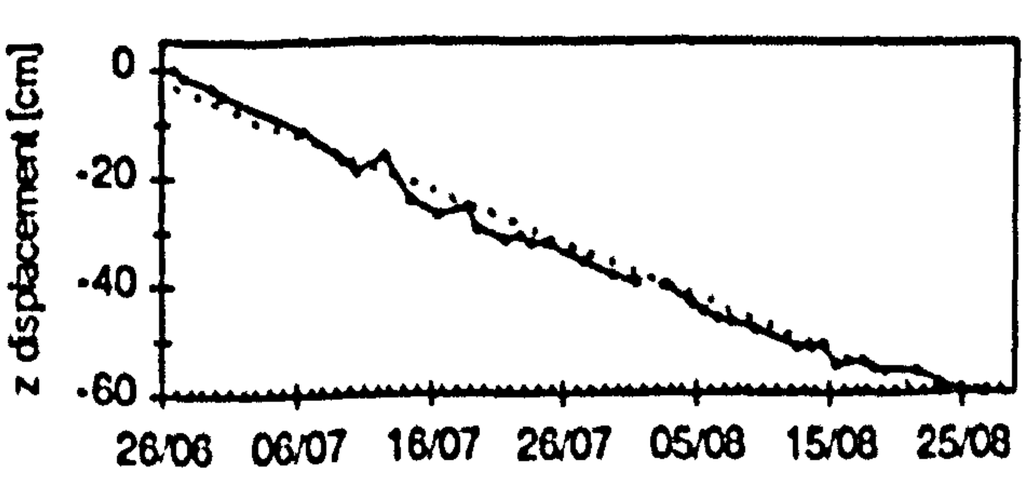
z displacement [cm]
0
-20
-40
-60
26/06
06/07
16/07
26/07
05/08
15/08
25/08

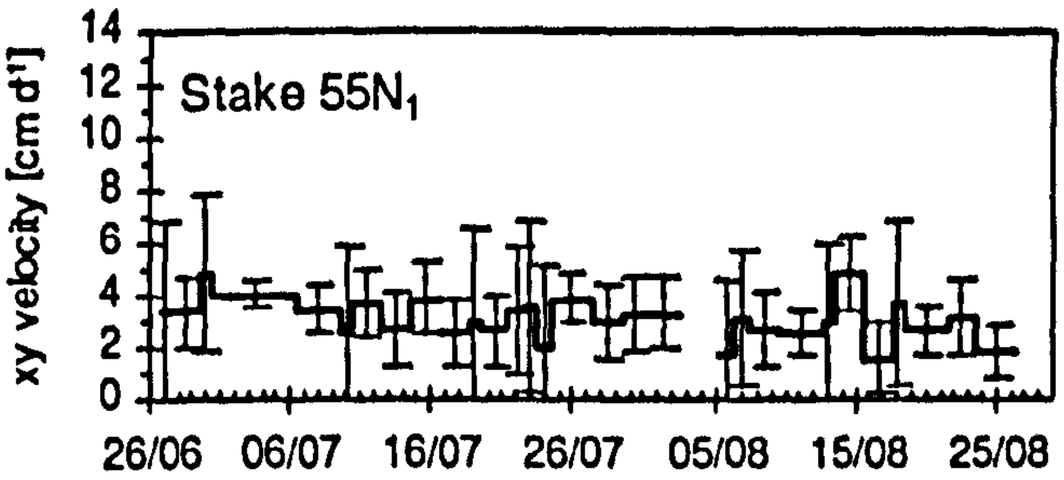
Stake 55N1
xy velocity [cm d-1]
14
12
10
8
6
4
2
0
26/06 06/07 16/07 26/07 05/08 15/08 25/08

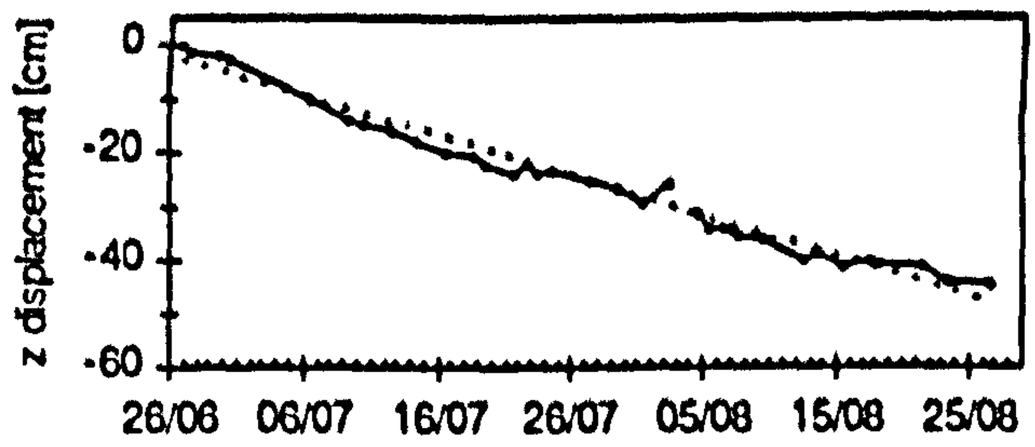
z displacement [cm]
0
-20
-40
-60
26/06 06/07 16/07 26/07 05/08 15/08 25/08

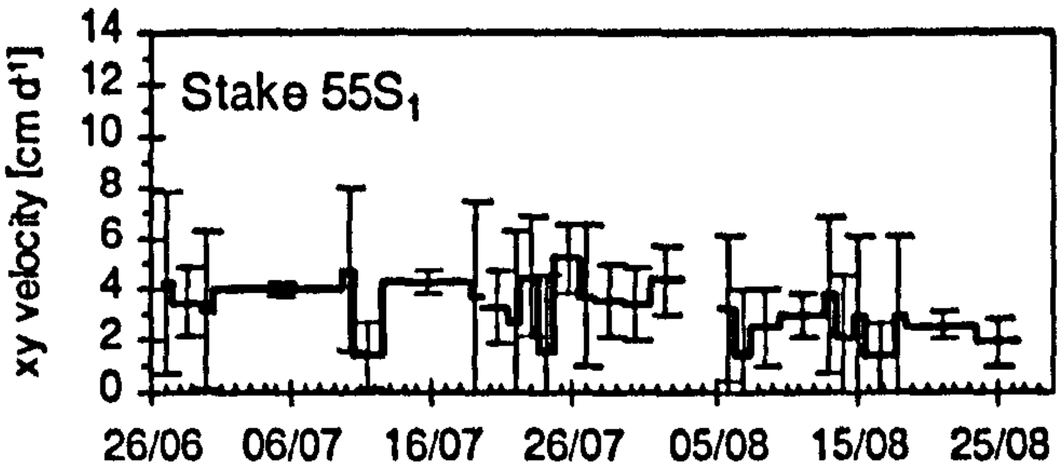
Stake 55S1
xy velocity [cm d-1]
14
12
10
8
6
4
2
0
26/06 06/07 16/07 26/07 05/08 15/08 25/08

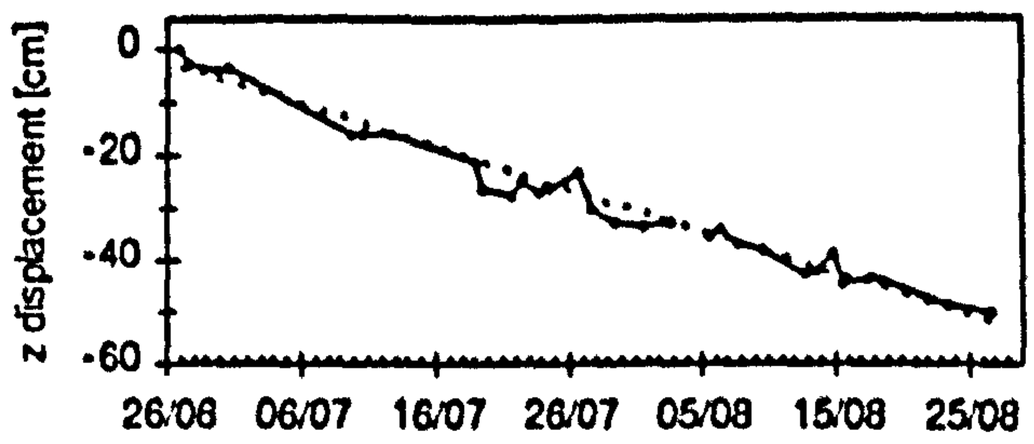
z displacement [cm]
0
-20
-40
-60
26/06 06/07 16/07 26/07 05/08 15/08 25/08

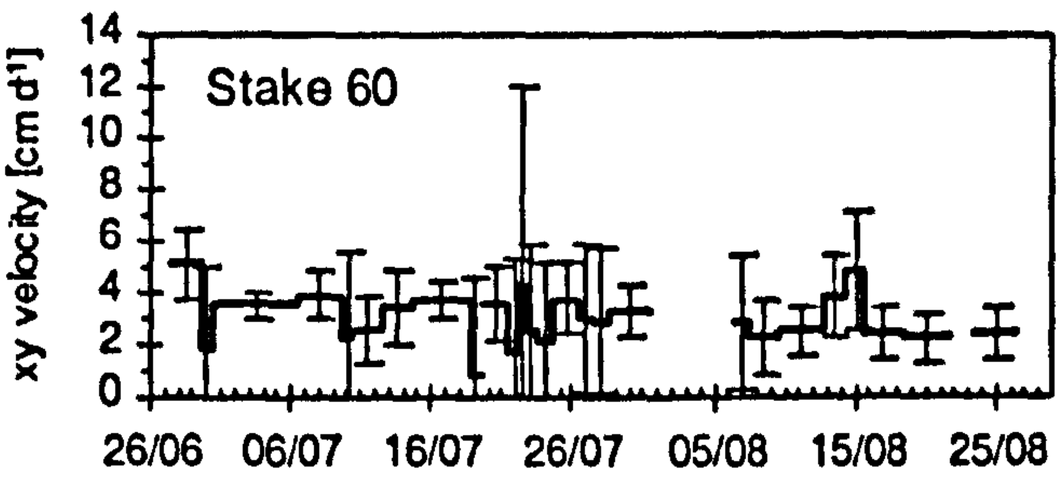
Stake 60
xy velocity [cm d-1]
14
12
10
8
6
4
2
0
26/06 06/07 16/07 26/07 05/08 15/08 25/08

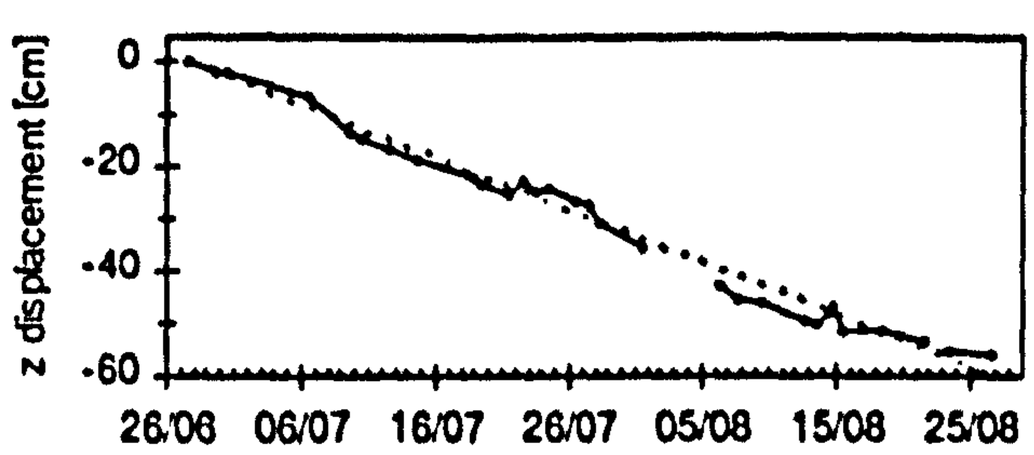
z displacement [cm]
0
-20
-40
-60
26/06 06/07 16/07 26/07 05/08 15/08 25/08

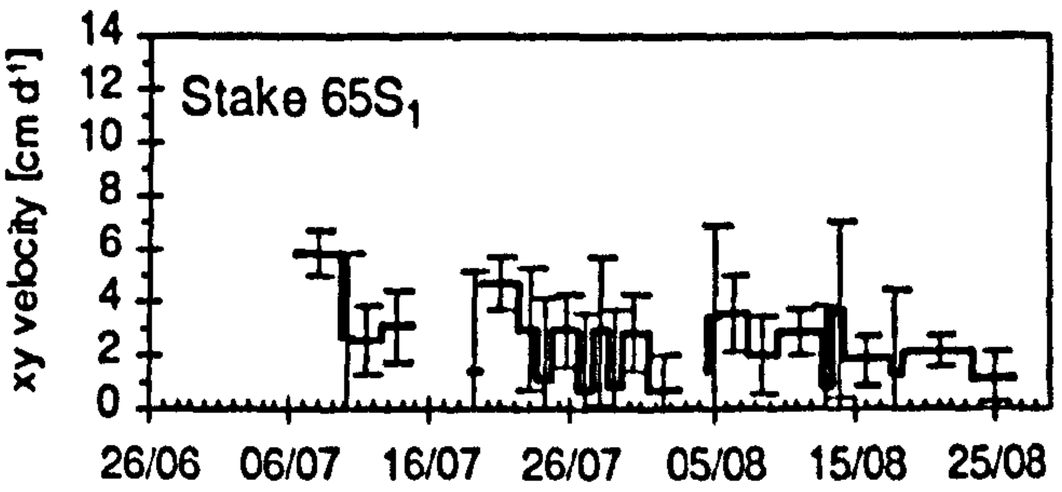
Stake 65S1
xy velocity [cm d-1]
14
12
10
8
6
4
2
0
26/06 06/07 16/07 26/07 05/08 15/08 25/08

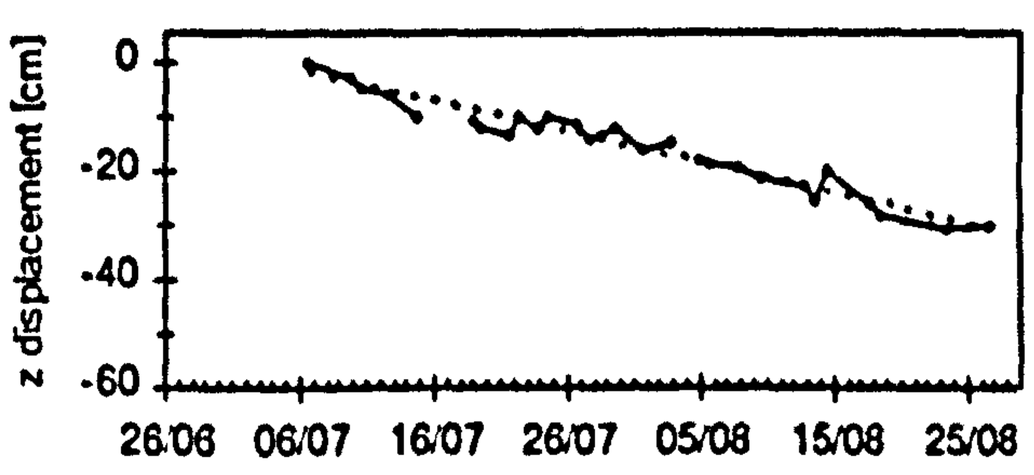
z displacement [cm]
0
-20
-40
-60
26/06 06/07 16/07 26/07 05/08 15/08 25/08

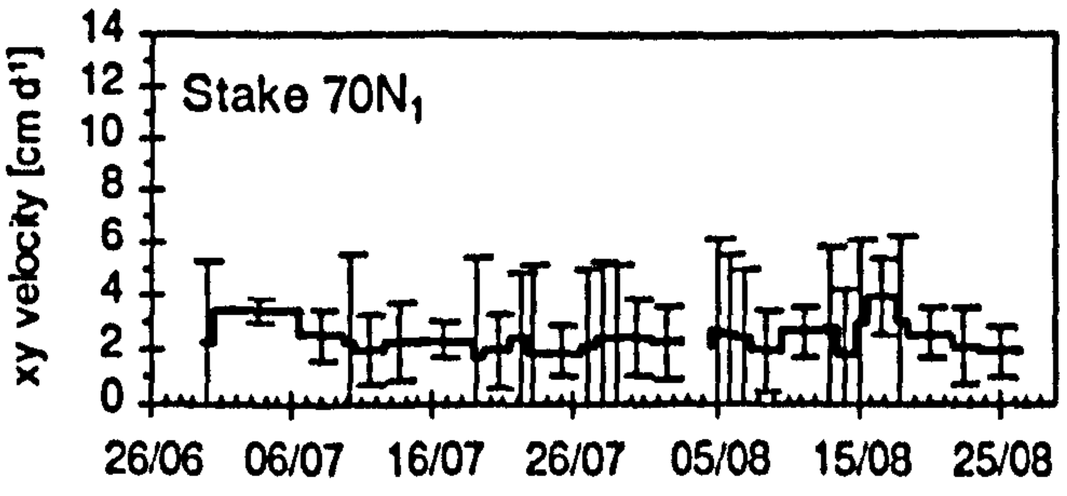
Stake 70N1
xy velocity [cm d-1]
14
12
10
8
6
4
2
0
26/06 06/07 16/07 26/07 05/08 15/08 25/08

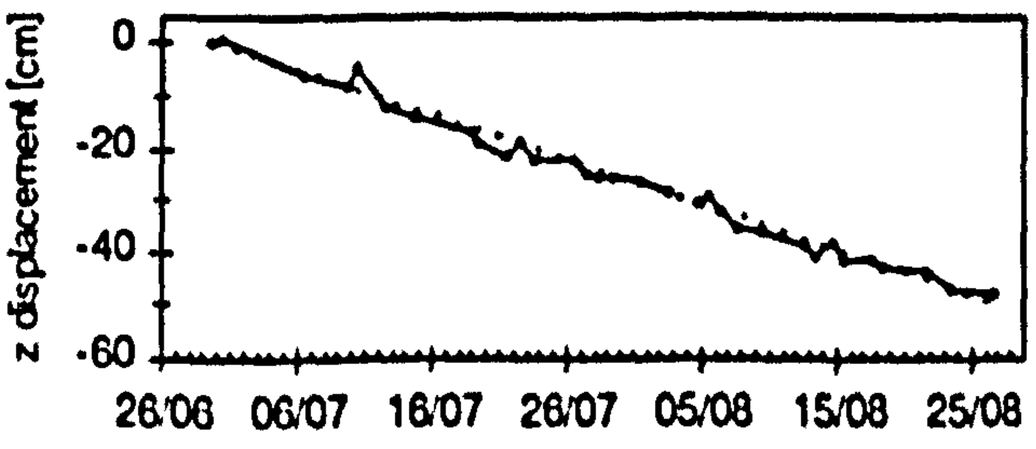
z displacement [cm]
0
-20
-40
-60
26/06 06/07 16/07 26/07 05/08 15/08 25/08

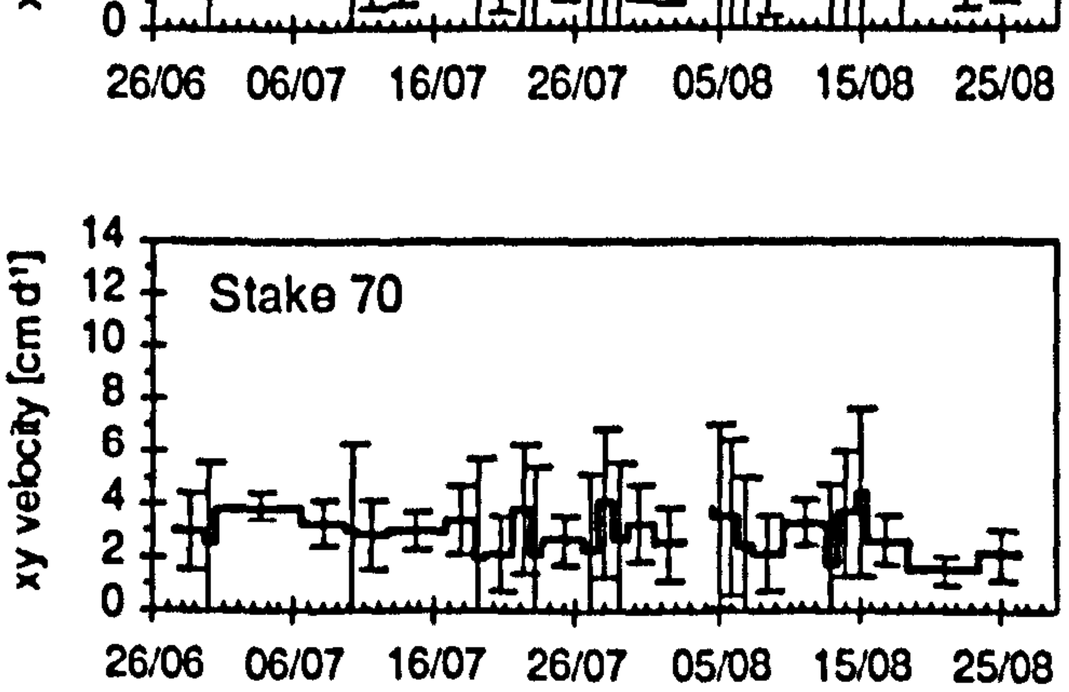
Stake 70
xy velocity [cm d-1]
14
12
10
8
6
4
2
0
26/06 06/07 16/07 26/07 05/08 15/08 25/08

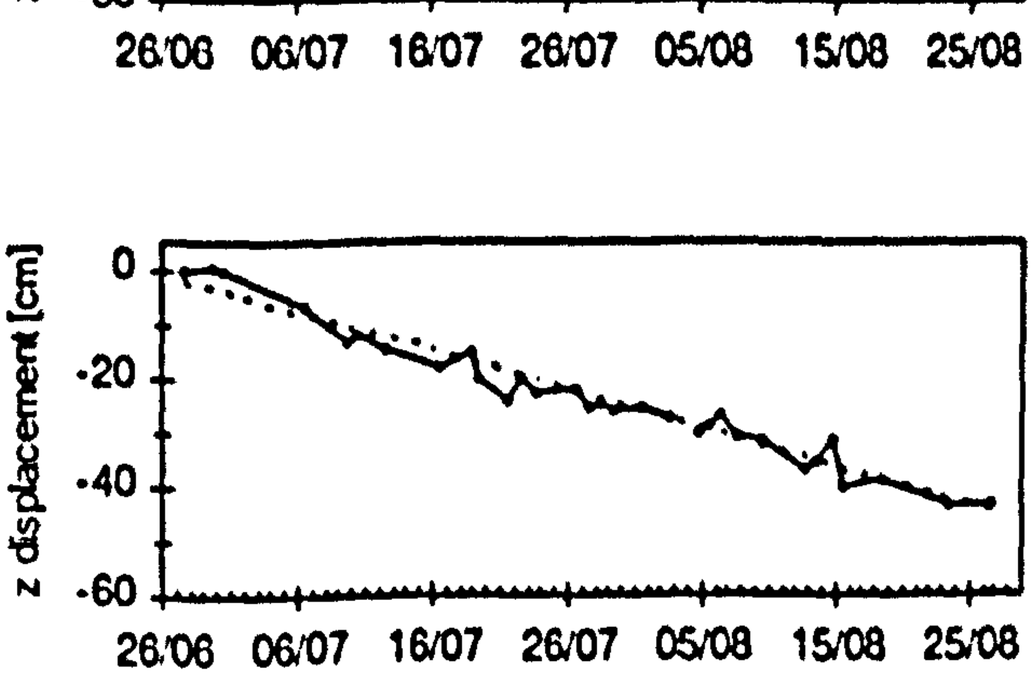
z displacement [cm]
0
-20
-40
-60
26/06 06/07 16/07 26/07 05/08 15/08 25/08

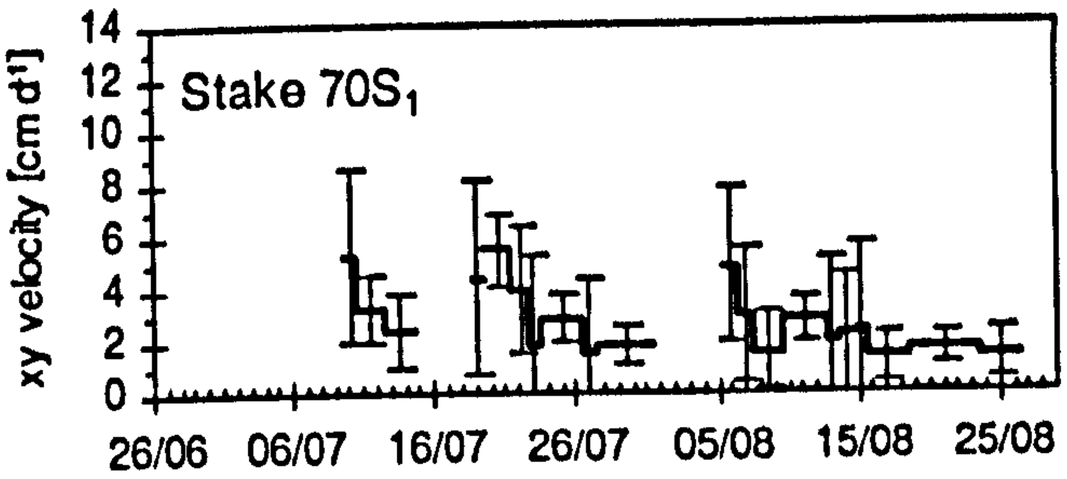
Stake 70S1
xy velocity [cm d-1]
14
12
10
8
6
4
2
0
26/06
06/07
16/07
26/07
05/08
15/08
25/08

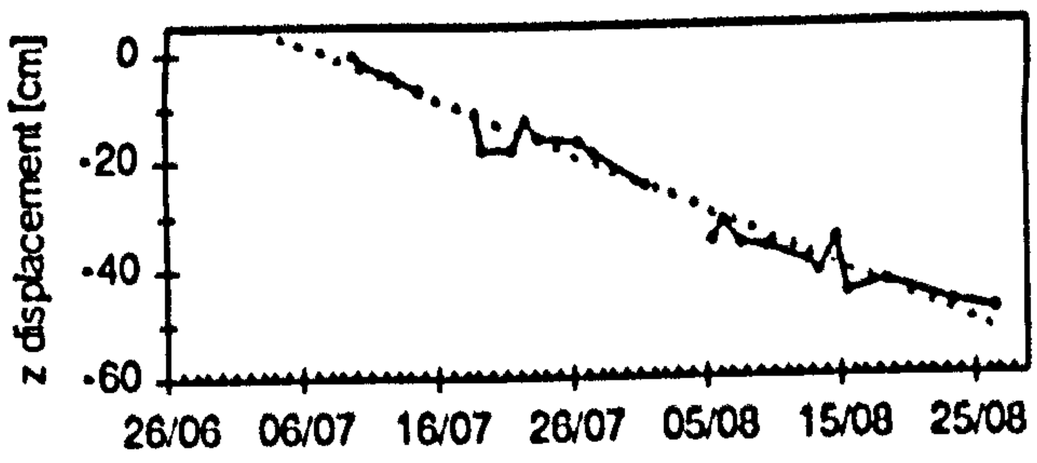
z displacement [cm]
0
-20
-40
-60
26/06
06/07
16/07
26/07
05/08
15/08
25/08

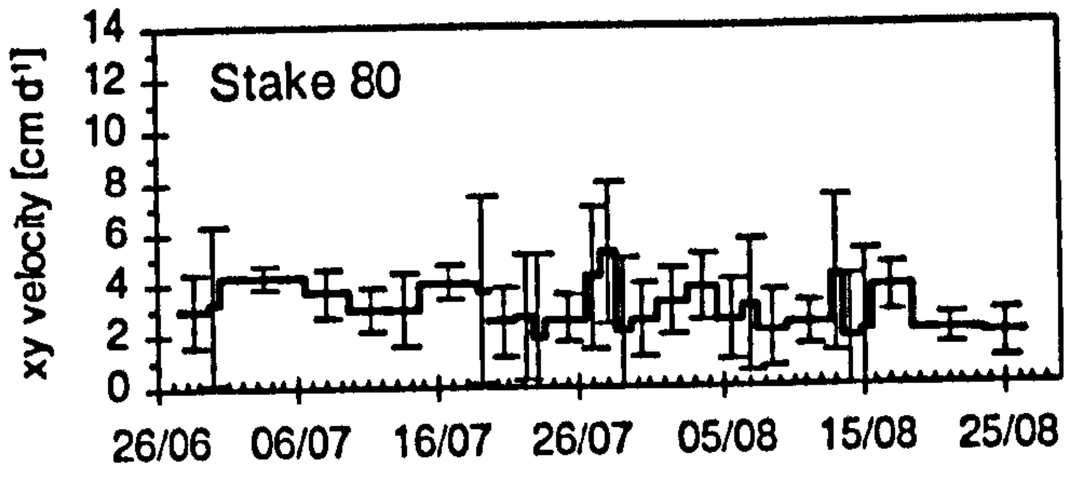
Stake 80
xy velocity [cm d-1]
14
12
10
8
6
4
2
0
26/06
06/07
16/07
26/07
05/08
15/08
25/08

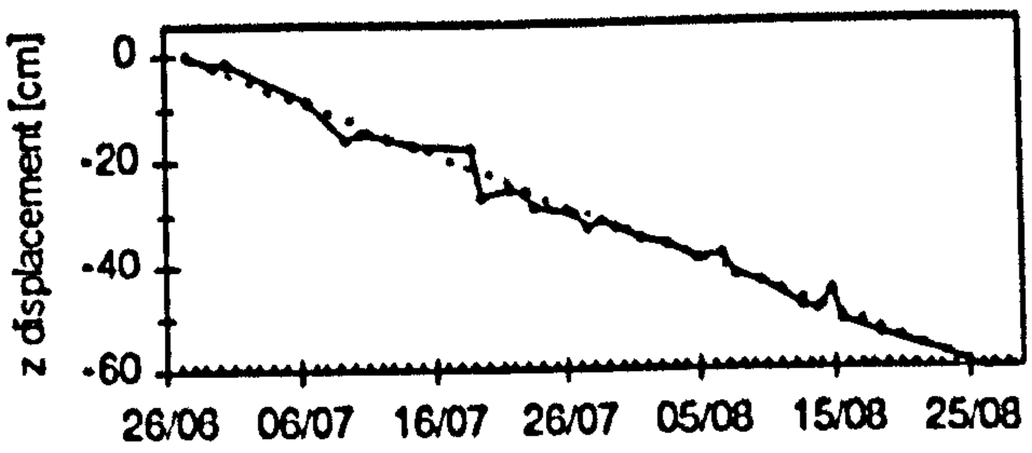
z displacement [cm]
0
-20
-40
-60
26/06
06/07
16/07
26/07
05/08
15/08
25/08

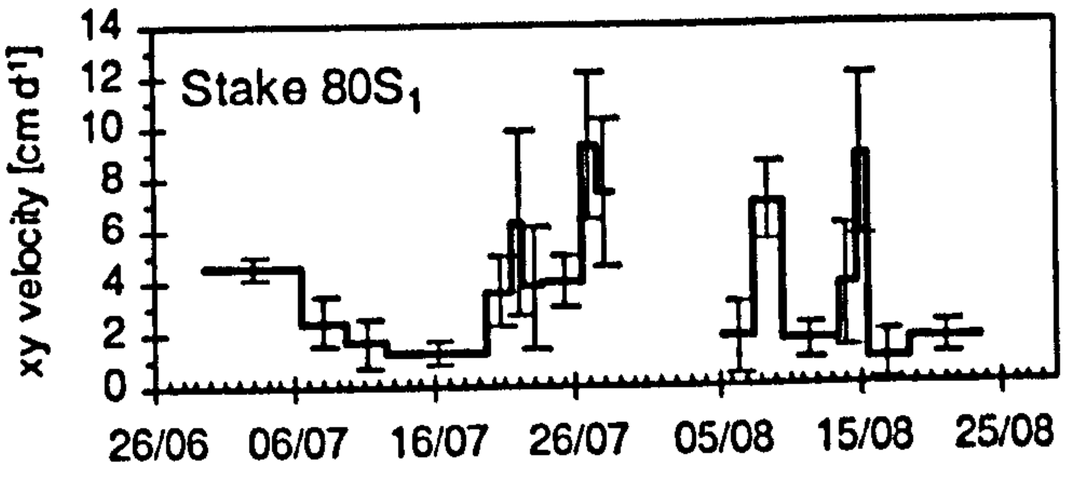
Stake 80S1
xy velocity [cm d-1]
14
12
10
8
6
4
2
0
26/06
06/07
16/07
26/07
05/08
15/08
25/08

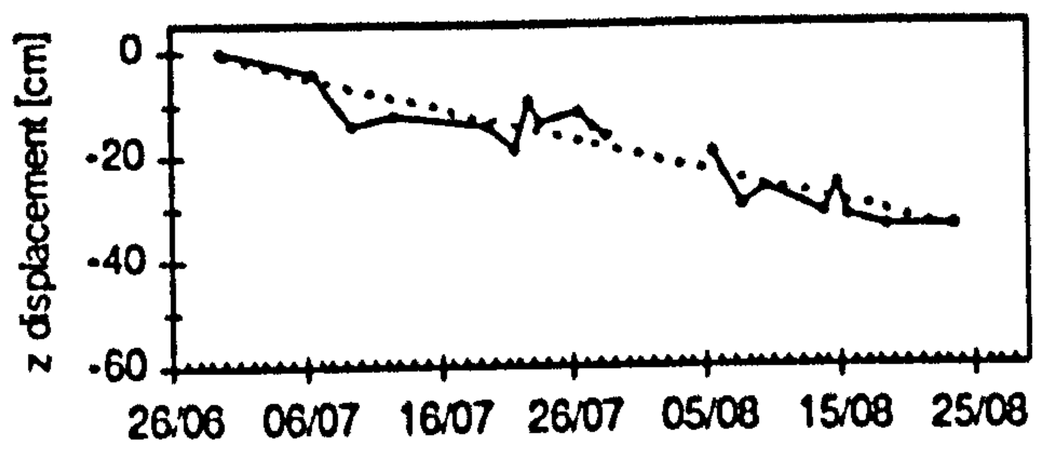
z displacement [cm]
0
-20
-40
-60
26/06
06/07
16/07
26/07
05/08
15/08
25/08

References

Albert, M., Koh, G., and Perron, F., 1999: Radar investigations of melt pathways in a natural snowpack. *Hydrological Processes,* 13: 2991-3000.

Albert, M. R. and Perron, F. E., 2000: Ice layer and surface crust permeability in a seasonal snow pack. *Hydrological Processes,* 14: 3207-3214.

Alley, R. B., 1989: Water-pressure coupling of sliding and bed deformation: II. Velocity-depth profiles. *Journal of Glaciology,* 35: 119-129.

Alley, R. B., 2003: Stabilizing feedbacks in glacier-bed erosion. *Nature,* 424: 758 - 760.

Ambach, W., Behrens, H., Bergmann, H., and Moser, H., 1972: Markierungsversuche am inneren Abflussystem des Hintereisferners (Ötztaler Alpen). *Zeitschrift für Gletscherkunde und Glazialgeologie,* 8: 137-145.

Ambach, W. and Eisner, H., 1979: Ein Tracerexperiment zum Schmelzwasserfluß in der Wassertafel eines temperierten Gletschers. *Zeitschrift für Gletscherkunde und Glazialgeologie,* 15: 229-234.

Ambach, W., Blumthaler, M., and Kirchlechner, P., 1981: Application of the gravity flow theory to the percolation of melt water through firn. *Journal of Glaciology,* 27: 67-75.

Anderson, R. S., Hallet, B., Walder, J. S., and Aubry, B. F., 1982: Observations in a cavity beneath Grinnell Glacier. *Earth Surface Processes and Landforms,* 7: 63-70.

Andreason, J. O., 1985: Seasonal surface velocity variations on a sub-polar glacier in West Greenland. *Journal of Glaciology,* 31: 319-323.

Andreason, J.-O., 1983: Basal sliding at the margin of the glacier Austre Okstindsbreen, Nordland, Norway. *Arctic and Alpine Research,* 15: 333-338.

Arnold, N., Richards, K., Willis, I., and Sharp, M., 1998: Initial results from a distributed, physically based model of glacier hydrology. *Hydrological Processes,* 12: 191-220.

Baker, D., Escher-Vetter, H., Moser, H., Oerter, H., and Reinwarth, O., 1982: A glacier discharge model based on results from field studies of energy balance, water storage and fow. *IAHS Publ.,* 138, Wallingford, Oxfordshire.

Balise, M. J. and Raymond, C. F., 1985: Transfer of basal sliding variations to the surface of a linearly viscous glacier. *Journal of Glaciology,* 31: 308-318.

Bates, P. D., Siegert, M. J., Lee, V., Hubbard, B. P., and Nienow, P. W., 2003: Numerical simulation of three-dimensional velocity fields in pressurised and non-pressurised Nye channels. *Annals of Glaciology,* 37: 281-285.

Behrens, H., Bergmann, H., Moser, H., Rauert, W., Stichler, W., Ambach, W., Eisner, H., and Pessl, K., 1971: Study of the discharge of alpine glaciers by means of environmental isotopes and dye tracers. *Zeitschrift für Gletscherkunde und Glazialgeologie,* 7: 79-101.

Behrens, H., Bergmann, H., Moser, H., Ambach, W., and Jochum, O., 1975: On the water channels of the internal drainage system of the Hintereisferner, Ötztal Alps, Austria. *Journal of Glaciology,* 14: 375-382.

Behrens, H., Moser, H., Oerter, H., Bergmann, H., Ambach, W., Eisner, H., Kirchlechner, P., and Schneider, H., 1979: Neue Ergebnisse zur Bewegung des Schmelzwassers im Firnkörper des Akkumulaitonsgebietes eines Alpengletschers (Kesselwandferner, Ötztaler Alpen). *Zeitschrift für Gletscherkunde und Glazialgeologie,* 15: 219-228.

Behrens, H., Oerter, H., and Reinwarth, O., 1982: Results of tracer experiments with fluorescent dyes on Vernagtferner (Ötztal Alps, Austria) from 1974-1982. *Zeitschrift für Gletscherkunde und Glazialgeologie,* 18: 65-83.

Bencala, K. E., Rathbun, R. E., Jackman, A. P., Kennedy, V. C., Zellweger, G. W., and Avanzino, R. J., 1983: Rhodamine WT dye losses in a mountain stream environment. *American Water Resources Association, Water Resources Bulletin,* 19: 943-950.

Benn, & Evans, D. (1998): Glaciers and Glaciation, Arnold, London: 734.

Betterton, M. D., 2001: Theory of structure formation in snowfields motivated by penitentes, suncups, and dirt cones. *Physical Review E,* 6305: art. no. 056129.

Bindschadler, R., 1983: The importance of pressurized subglacial water in separation and sliding at the glacier bed. *Journal of Glaciology,* 29: 3-19.

Bindschadler, R. A., Raymond, C. F., and Crosson, R., 1977: Geometry and dynamics of a surge-type glacier. *Journal of Glaciology,* 18: 181-194.

Bingham, R. G., 2003: The hydrology and dynamics of a High Arctic Glacier: PhD thesis, University of Glasgow, 254.

Bingham, R. G., Nienow, P. W., and Sharp, M. J., 2003: Intra-annual and intra-seasonal flow dynamics of a High Arctic polythermal valley glacier. *Annals of Glaciology,* 37: 181-188.

Björnsson, H., 1998: Hydrological characteristics of the drainage system beneath a surging glacier. *Nature,* 395: 771-774.

Blake, E. W. and Clarke, G. K. C., 1992: Interpretation of borehole-inclinometer data: a general theory applied to a new instrument. *Journal of Glaciology,* 38: 113-124.

Blake, E. W., Fischer, U. H., and Clarke, G. K. C., 1994: Direct measurement of sliding at the glacier bed. *Journal of Glaciology,* 40: 595-599.

Boon, S., Sharp, M. J., and Nienow, P. W., 2003: Impact of an extreme melt event on the hydrology and runoff of a high Arctic glacier. *Hydrological Processes,* 17: 1051-1072.

Boulton, G. S., 1974: Processes and patterns of glacial erosion. *In* Coates, D. R. (ed.), *Glacial Geomorphology*. Binghamton, N.Y.: State University of New York, 41-87.

Boulton, G. S. and Jones, A. S., 1979: Stability of temperate ice caps and ice sheets resting on beds of deformable sediment. *Journal of Glaciology,* 24: 29-43.

Boulton, G. S. and Hindmarsh, R. C. A., 1987: Sediment deformation beneath glaciers: Rheological and geological consequences. *Journal of Geophysical Research,* 92: 9059-9082.

Braithwaite, R. J. and Olesen, O. B., 1989: Calculation of glacier ablation from air temperature, West Greenland. *In* Oerlemans, J. (ed.), *Glacier fluctuations and climatic change, Glaciology and Quaternary geology*. Dordrecht: Kluwer, 219-233.

Brown, G. H., 2002: Glacier meltwater hydrochemistry. *Applied Geochemistry,* 17: 855-883.

Brugman, M. M., 1986: *Water flow at the base of a surging glacier.* Ph.D. thesis, California Institute of Technology, Pasadena.

Burkishmer, M., 1983: Investigations of glacier hydrological systems using dye tracer techniques: Observations at Pasterzengletscher, Austria. *Journal of Glaciology,* 29: 403-416.

Clarke, G. K. C., 1982: Glacier Outburst Floods from Hazard Lake, Yukon Territory, and the Problem of Flood Magnitude Prediction. *Journal of Glaciology,* 28: 3-21.

Clarke, G. K. C., Collins, S. G., and Thompson, D. E., 1984: Flow, thermal structure, and subglacial conditions of a surge-type glacier. *Canadian Journal of Earth Sciences,* 21: 232-240.

Clarke, G. K. C., 2003: Hydraulics of subglacial outburst floods: new insights from the Spring-Hutter formulation. *Journal of Glaciology,* 49: 299-313.

Clarke, T. S., 1991: Glacier dynamics in the Susitna River basin, Alaska, USA. *Journal of Glaciology,* 37: 97-106.

Climate in Switzerland, 2004: available: http://www.about.ch/geograppy/climate/.

Colbeck, S. C., 1972: A theory of water percolation in snow. *Journal of Glaciology,* 11: 369-385.

Colbeck, S. C., 1974: Water flow through snow overlying an impermeable boundary. *Water Resources Research,* 10: 119-123.

Colbeck, S. C., 1975: A theory of water flow through a layered snowpack. *Water Resources Research,* 11: 261-266.

Colbeck, S. C., 1976: An analysis of water flow in dry snow. *Water Resources Research,* 12: 523-527.

Colbeck, S. C., 1977: Short-term forecasting of water run-off from snow and ice. *Journal of Glaciology,* 19: 571-587.

Colbeck, S. C., 1978: The physical aspects of water flow through snow. *Advances in Hydroscience,* 11: 165-206.

Colbeck, S. C., 1979: Water flow through heterogeneous snow. *Cold Regions Science Technology,* 1: 37-45.

Colbeck, S. C. and Anderson, E. A., 1982: The permeability of a melting snow cover. *Water Resources Research,* 18: 904-908.

Colbeck, S. C., 1986: Classification of seasonal snow cover crystals. *Water Resources Research,* 22: 59-70.

Colbeck, S. C., Akitaya, E., Armstrong, R., Grubler, H., Lafeuille, J., Lied, K., McClung, D., and Morris, E., 1990: *The international classification for seasonal snow on the ground*

Collins, D. N., 1979: Hydrochemistry of meltwaters draining from an alpine glacier. *Arctic and Alpine Research,* 11: 307-324.

Collins, D. N., 1982a: Flow-routing of meltwater in an Alpine glacier as indicated by dye tracer tests. *Beiträge zur Geologie der Schweiz-Hydrologie,* 28: 523-534.

Collins, D. N., 1982b: Water storage in an Alpine glacier. *IAHS Publ.*, 138, Wallingford, Oxfordshire.

Convey, H. and Raymond, C. F., 1993: Snow stability during rain. *Journal of Glaciology,* 39: 635-642.

Convey, H. and Benedict, R., 1994: Infiltration of water into snow. *Water Resources Research,* 30: 641-649.

Copland, L., Harbor, J., Gordon, S., and Sharp, M., 1997a: The use of borehole video in investigating the hydrology of a temperate glacier. *Hydrological Processes,* 11: 211-224.

Copland, L., Harbor, J., and Sharp, M., 1997b: Borehole video observation of englacial and basal ice conditions in a temperate valley glacier. *Annals of Glaciology,* 24: 277-282.

Denoth, A., 1999: Wet snow pendular regime: the amount of water in ring-shaped configurations. *Cold Regions Science and Technology,* 30: 13-18.

Dunne, T., Price, A. G., and Colbeck, S. C., 1976: The generation of runoff from subarctic snowpacks. *Water Resources Research,* 12: 677-685.

Elliston, G. R., 1973: *Water movement through the Gornergletscher. Symposium on the Hydrology of Glaciers. Cambridge, 7-13 September, 1969.* Glaciological Society, Publication No. 95

Engelhardt, H. F., Harrison, W. D., and Kamb, B., 1978: Basal sliding and conditions at the glacier bed as revealed by bore-hole photography. *Journal of Glaciology,* 20: 469-508.

Erickson, T. A., Williams, M. W., and Sommerfeld, R. A., 2000: Spatial Statistics of Snowmelt. *In* Bentley et al. (ed.), *Computational Methods in Water Resources XIII.* Rotterdam: Balkema.

Fairchild, I. J., Bradby, L., Sharp, M., and Tison, J.-L., 1994: Hydrolchemistry of carbonate terrains in alpine glacial settings. *Earth Surface Processes and Landforms,* 19: 33-54.

Fairchild, I. J., Killawee, J. A., Sharp, M., Spiro, B., Hubbard, B., Lorrain, R. D., and Tison, J.-L., 1999: Solute generation and transfer from a chemically reactive alpine glacial-proglacial system. *Earth Surface Processes and Landforms,* 24: 1189-1211.

Fischer, H. B., 1968: *Methods for predicting dispersion coefficients in natural stream, with applications to lower reaches of the Green and Duwamish Rivers, Washington.* United States Geological Survey, Professional Paper 528-A, Washington, DC.

Fischer, U. H. and Clarke, G. K. C., 1994: Plowing of Subglacial Sediment. *Journal of Glaciology,* 40: 97-106.

Fischer, U. H. and Clarke, G. K. C., 1997: Stick-slip sliding behaviour at the base of a glacier. *Annals of Glaciology,* 24: 390-396.

Fischer, U. H., Iverson, N. R., Hanson, B., Hooke, R. L., and Jansson, P., 1998: Estimation of hydraulic properties of subglacial till from ploughmeter measurements. *Journal of Glaciology,* 44: 517-522.

Fischer, U. H., Clarke, G. K. C., and Blatter, H., 1999: Evidence for temporally varying "sticky spots" at the base of Trapridge Glacier, Yukon Territory, Canada. *Journal of Glaciology,* 45: 352-360.

Fischer, U. H. and Clarke, G. K. C., 2001: Review of subglacial hydro-mechanical coupling: Trapridge Glacier, Yukon Territory, Canada. *Quaternary International,* 86: 29-43.

Forel, F. A., 1898: Circulation des eaux dans le Glacier du Rhône. *Spelunca, Bulletin de la Societé de Spéléologie,* 4: 156-158.

Fountain, A. and Walder, J. S., 1998: Water flow through temperate glaciers. *Reviews of Geophysics,* 36: 299-328.

Fountain, A. G., 1989: The storage of water in, and hydraulic characteristics of, the firn of South Cascade Glacier, Washington, U.S.A. *Annals of Glaciology,* 13: 69-75.

Fountain, A. G., 1993: Geometry and flow conditions of subglacial meltwater at South Cascade Glacier, Washington State, USA: an analysis of tracer injections. *Journal of Glaciology,* 139: 143-156.

Fountain, A. G., 1994: Borehole water-level variations and implications for the subglacial hydraulics of South Cascade Glacier, Washington State, U.S.A. *Journal of Glaciology,* 40: 293-304.

Fountain, A. G., 1996: Effect of snow and firn hydrology on the physical and chemical characteristics of glacial runoff. *Hydrological Processes,* 10: 509-521.

Fowler, A. C., 1987: Sliding with cavity formation. *Journal of Glaciology,* 33: 255-267.

Fowler, A. C., 1999: Breaking the seal at Grimsvötn, Iceland. *Journal of Glaciology,* 45: 506-516.

Freeze, R. A. and Cherry, J. A., 1979: *Groundwater.* London: Prentice Hall.

Geomagnetism-Group, 2000: GGUN-FL fluorometer - User Manual. *Institute of Geology, University of Neuchâtel, Switzerland.*

Gerdel, R. W., 1954: The transmission of water through snow. *Transactions, American Geophysical Union,* 35: 457-485.

Gordon, S., Sharp, M., Hubbard, B., Smart, C., Ketterling, B., and Willis, I., 1998: Seasonal reorganisation of subglacial drainage inferred from measurements in boreholes. *Hydrological Processes,* 12: 105-133.

Grust, K., 1998: *Einsatzmöglichkeiten von künstlichen Tracern in der Glazialhydrologie.* Diplomarbeit (unpublished), Department für Hydrologie, Albert-Ludwigs-Universität Freiburg, Freiburg.

Grust, K., in press: Oberflächengewässer - surface water. *In* Käss, W. (ed.), *Hydrogeologische Markierungstechnik*: Balkema, Rotterdam/Brookefield.

Gudmundsson, G. H., Iken, A., and Funk, M., 1997: Measurements of ice deformation at the confluence area of Unteraargletscher, Bernese Alps, Switzerland. *Journal of Glaciology,* 43: 548-556.

Gudmundsson, G. H., Bassi, A., Vonmoos, M., Bauder, A., Fischer, U. H., and Funk, M., 2000: High resolution measurements of temporal and spatial variations in surface velocities of Unteraargletscher, Bernese Alps, Switzerland. *Annals of Glaciology,* 31: 63-68.

Gudmundsson, G. H., 2002: Observations of a reversal in vertical and horizontal strain- rate regime during a motion event on Unteraargletscher, Bernese Alps, Switzerland. *Journal of Glaciology,* 48: 566-574.

Gurnell, A., Hannah, D., and Lawler, D., 1996: Suspended sediment yield from glacier basins. In Walling, D. E. and Webb, B. E. (eds.), Erosion and sediment yield: global and regional perspectives. Proceedings of the Exeter Symposium, July 1996. Wallingford, Oxfordshire: *IAHS Publ.* 236, 97-104.

Gurnell, A. M., 1993: How many reservoirs? An analysis of flow recessions from a glacier basin. *Journal of Glaciology,* 39: 409-414.

Hagen, J. O., Wold, B., Liestøl, O., Østrem, G., and Sollid, J. L., 1983: Subglacial processes at Bondhusbreen, Norway: preliminary results. *Annals of Glaciology,* 4: 91-98.

Hallet, B., 1976: Deposits formed by subglacial precipitation of $CaCO_3$. *Geological Society of America Bulletin,* 87: 1003-1015.

Hallet, B. and Anderson, R., 1980: Detailed glacial geomorphology of a proglacial bedrock area at Castleguard Glacier, Alberta, Canada. *Zeitschrift für Gletscherkunde und Glazialgeologie,* 16: 171-184.

Hannah, D. M., Gurnell, A. M., and McGregor, G. R., 1999: A methodology for investigation of the seasonal evolution in proglacial hydrograph form. *Hydrological Processes,* 13: 2603-2621.

Hannah, D. M., Smith, B. P. G., Gurnell, A. M., and McGregor, G. R., 2000: An approach to hydrograph classification. *Hydrological Processes,* 14: 317-338.

Hanson, B., Hooke, R. L., and Grace, E. M., 1998: Short-term velocity and water-pressure variations down-glacier from a riegel, Storglaciären, Sweden. *Journal of Glaciology,* 44: 359-367.

Hantz, D. and Lliboutry, L., 1983: Waterways, ice permeability at depth, and water pressures at Glacier D'Argentiére, French Alps. *Journal of Glaciology, 29: 227-239.*

Harbor, J., Sharp, M., Copland, L., Hubbard, B., Nienow, P., and Mair, D., 1997: Influence if subglacial drainage conditions in the velocity distribution within a glacier cross section. *Geology,* 25: 739-742.

Harper, J. T. and Humphrey, N. F., 1995: Borehole video analysis of a temperate glacier's englacial and subglacial structure: implications for glacier flow models. *Geology,* 23: 901-904.

Harper, J. T., Humphrey, N. F., and Greenwood, M. C., 2002: Basal conditions and glacier motion during the winter/spring transition, Worthington Glacier, Alaska, USA. *Journal of Glaciology,* 48: 42-50.

Harrington, R. and Bales, R. C., 1998a: Interannual, seasonal, and spatial patterns of meltwater and solute fluxes in a seasonal snowpack. *Water Resources Research,* 34: 823-831.

Harrison, W. D. and Kamb, B., 1973: Glacier borehole photography. *Journal of Glaciology,* 12: 129-137.

Harrison, W. D., Raymond, C. F., and MacKeith, P., 1986: Short period motion events on Variegated Glacier as observed by automatic photography and seismic methods. *Annals of Glaciology,* 8: 82-89.

Hasnain, S. I., Jose, P. G., Ahmad, S., and Negi, D. C., 2001: Character of the subglacial drainage system in the ablation area of Dokriani glacier, India, as revealed by dye tracer studies. *Journal of Hydrology,* 248: 216-223.

Hay, J. E. and Fitzharris, B. B., 1988: A comparison of the energy-balance and bulk-aerodynamic approaches for estimating glacier melt. *Journal of Glaciology,* 34: 145-153.

Hock, R. and Hooke, R. L., 1993: Evolution of the internal drainage system in the lower part of the ablation area of Storglaciären, Sweden. *Geological Society of America Bulletin,* 105: 537-546.

Hock, R., Iken, A., and Wangler, A., 1999: Tracer experiments and borehole observations in the overdeepening of Aletschgletscher, Switzerland. *Annals of Glaciology,* 28: 253-260.

Hodge, S. M., 1974: Variations in sliding of a temperate glacier. *Journal of Glaciology,* 13: 349-369.

Hodge, S. M., 1979: Direct measurements of basal water pressure: progress and problems. *Journal of Glaciology,* 23: 439-447.

Holmlund, P., 1988: Internal geometry and the evolution of moulins, Storglaciären, Sweden. *Journal of Glaciology,* 34: 242-248.

Hooke, R. B., 1998: *Principles of glacier mechanics*. Upper Saddle River, New Jersey: Prentice Hall.

Hooke, R. L., Brzozowski, J., and Bronge, C., 1983: Seasonal variations in surface velocity, Storglaciären, Sweden. *Geografiska Annaler,* 65 A: 263-277.

Hooke, R. L., 1984: On the role of mechanical energy in maintaining subglacial water conduits at atmospheric pressure. *Journal of Glaciology,* 30: 180-187.

Hooke, R. L., Miller, S. B., and Kohler, J., 1988: Character of the englacial and subglacial drainage system in the upper part of the ablation area of Storglaciären, Sweden. *Journal of Glaciology,* 34: 228-231.

Hooke, R. L., 1989: Englacial and subglacial hydrology: a qualitative review. *Arctic and Alpine Research,* 21: 221-233.

Hooke, R. l., Calla, P., Holmlund, P., Nilsson, M., and Stoeven, A., 1989: A 3 year record of seasonal variations in surface velocity, Storglaciären, Sweden. *Journal of Glaciology,* 35: 253-247.

Hooke, R. L., Laumann, T., and Kohler, J., 1990: Subglacial water pressures and the shape of subglacial conduits. *Journal of Glaciology,* 36: 67-71.

Hubbard, B. and Sharp, M., 1993: Weertman regelation, multiple refreezing events and the isotopic evolution of the basal ice layer. *Journal of Glaciology,* 39: 275-291.

Hubbard, B. and Nienow, P., 1997: Alpine subglacial hydrology. *Quaternary Science Reviews,* 16: 939-955.

Hubbard, B. and Hubbard, A., 1998: Bedrock surface roughness and the distribution of subglacially precipitated carbonate deposits: implications for formation at Glacier de Tsanfleuron, Switzerland. *Earth Surface Processes and Landforms,* 23: 261-270.

Hubbard, B., 2002: Direct measurement of basal motion at a hard-bedded, temperate glacier: Glacier de Tsanfleuron, Switzerland. *Journal of Glaciology,* 48: 1-8.

Hubbard, B., Hubbard, A., Mader, H., Tison, J.-L., Grust, K., and Nienow, P., 2003: Spatial variability in the water content and rheology of temperate glaciers: Glacier de Tsanfleuron, Switzerland. *Annals of Glaciology,* 37: 1-6.

Hubbard, B. P., Sharp, M. J., Willis, I. C., Nielsen, M. K., and Smart, C. C., 1995: Borehole water level variations and the structure of the subglacial hydrological system of Haut Glacier d'Arolla, Valais, Switzerland. *Journal of Glaciology,* 41: 572-583.

Humphrey, N., 1987: *Coupling between water pressure and basal sliding in a linked-cavity hydraulic system*, 170, Wallingford, Oxfordshire.

Iken, A., 1981: The effect of subglacial water pressure on the sliding velocity of a glacier in an idealized numerical model. *Journal of Glaciology,* 27: 407-421.

Iken, A., Röthlisberger, H., Flotron, A., and Haeberli, W., 1983: The uplift of Unteraargletscher at the beginning of the melt season - a consequence of water storage at the bed? *Journal of Glaciology,* 29: 28-47.

Iken, A. and Bindschadler, R. A., 1986: Combined measurements of subglacial water pressure and surface velocity of Findelengletscher, Switzerland: conclusions about drainage system and sliding mechanism. *Journal of Glaciology,* 32: 101-118.

Iken, A., Echelmeyer, K., Harrison, W., and Funk, M., 1993: Mechanisms of fast flow in Jakobshavns Isbræ, West Greenland: Part 1. Measurements of temperature and water level in deep boreholes. *Journal of Glaciology,* 39: 15-25.

Iken, A. and Truffer, M., 1997: The relationship between subglacial water pressure and velocity of Findelengletscher, Switzerland, during advance and retreat. *Journal of Glaciology,* 43: 328-338.

Illangasekare, T. H., Walter, R. J., Meier, M. F., and Pfeffer, W. T., 1990: Modelling of meltwater infiltration in subfreesing snow. *Water Resources Research,* 26: 1001-1012.

Iverson, N. R., Jansson, P., and Hooke, R. l., 1994: In situ measurement of the strength of deforming subglacial till. *Journal of Glaciology,* 40: 497-503.

Iverson, N. R., Hanson, B., Hooke, R. l., and Jansson, P., 1995: Flow mechanism of glaciers on soft beds. *Science,* 267: 80-81.

Iverson, N. R., Cohen, D., Hooyer, T. S., Fischer, U. H., Jackson, M., Moore, P. L., Lappegard, G., and Kohler, J., 2003: Effects of basal debris on glacier flow. *Science,* 301: 81-84.

Jansson, P., 1995: Water pressure and basal sliding, Storglaciären, Sweden. *Journal of Glaciology,* 41: 232-240.

Jordan, E., 1981: Die Gletscher der bolivianischen Anden. Stuttgart: Franz Steiner Verlag.

Jordan, P., 1983: Meltwater movement in a Deep Snowpack - 1. Field observations. *Water Resources Research,* 19: 971-978.

Kamb, B. and LaChapelle, E., 1964: Direct observation of the mechanism of glacier sliding over bedrock. *Journal of Glaciology,* 5: 159-172.

Kamb, B., Raymond, C. F., Harrison, W. D., Engelhardt, H. F., Echelmeyer, K. A., Humphrey, N. F., Brugman, M. M., and Pfeffer, W. T., 1985: Glacier surge mechanism: 1982-1983 surge of Variegated Glacier, Alaska. *Science,* 227: 469-479.

Kamb, B., 1987: Glacier surge mechanism based on linked cavity configuration of the basal water conduit system. *Journal of Glaciology,* 32: 9083-9100.

Kamb, B. and Engelhardt, H. F., 1987: Waves of accelerated motion in a glacier approaching surge: the mini-surges of Variegated Glacier, Alaska, USA. *Journal of Glaciology,* 33: 27-46.

Kamb, B., Engelhardt, H. F., Fahnestock, M. A., Humphrey, N. F., Meier, M. F., and Stone, D., 1994: Mechanical and hydrological basis for the rapid motion of a large tidewater glacier. 2. Interpretation. *Journal of Geophysical Research,* 99: 15231-15244.

Käss, W., 1998: Tracing technique in Geohydrology. Rotterdam: Balkema.

Kattelmann, R. C., 1985: Macropores in snowpacks of Sierra Nevada. *Annals of Glaciology,* 6: 272-273.

Kattelmann, R. C., 1989: Spatial variability of snow-pack outflow at a site in Sierra Nevada, USA. *Annals of Glaciology,* 13: 124-128.

Kattelmann, R. C. and Dozier, J., 1999: Observations of snowpack ripening in the Sierra Nevada, California, U.S.A. *Journal of Glaciology,* 45: 409-416.

Kavanaugh, J. L. and Clarke, G. K. C., 2001: Abrupt glacier motion and reorganization of basal shear stress following the establishment of a connected drainage system. *Journal of Glaciology,* 47: 472-480.

Kohler, J., 1992: *Glacial hydrology of Storglaciären, northern Sweden*, University of Minnesota College, Minnesota, USA.

Kohler, J., 1995: Determining the extent of pressureized flow beneath Storglaciären, Sweden, using results of tracer experiments and measurements of input and output discharge. *Journal of Glaciology*, 41: 217-231.

Kreft, A. and Zuber, A., 1978: On the physical meaning of the dispersion equation and its solutions for different initial and boundary conditions. *Chemical Engineering Science*, 33: 1471-1480.

Krimmel, R. M., Tangborn, W. V., and Meier, M. F., 1973: Water flow through a temperate glacier, The Role of Snow and Ice in Hydrology. Proceedings of symposia held at Banff, September 1972. Wallingford, Oxfordshire: *IAHS Publ.* 107, 401-416.

Krimmel, R. M. and Rasmussen, L. A., 1986: Using sequential photography to estimate ice velocity at the terminus of Columbia Glacier, Alaska. *Annals of Glaciology*, 8: 117-123.

Krimmel, R. M. and Vaughn, B. H., 1987: Columbia Glacier, Alaska: changes in velocity 1977-1986. *Journal of Geophysical Research*, 92: 8961-8968.

Lang, H., Schädler, B., and Davidson, G., 1977: Hydrological investigations on the Ewigschneefeld - Grosser Aletschglescher: ablation, meltwater infiltration, water table in firn, heat balance. *Zeitschrift für Gletscherkunde und Glazialgeologie*, 12: 109-124.

Lang, H., Leibundgut, C., and Festel, E., 1979: Results from tracer experiments on the water flow through the Aletschgletscher. *Zeitschrift für Gletscherkunde und Glazialgeologie*, 16: 209-218.

Lang, H. and Braun, L. N., 1990: On the information content of air temperature in the context of snow melt estimation. Proceedings of the Strbské Pleso Symposium, Czechoslovakia, 1988. *In* Molnar, L. (ed.), *Hydrology of mountainous areas.* International Association of Hydrological Sciences 190, 347-354.

Langham, E. J., 1975: *The mechanism of rotting of ice layers within a structured snowpack*, 114, Wallingford, Oxfordshire.

Langham, E. J., 1981: Physics and properties of snowcover. *In* Gray, D. M. and Male, D. H. (eds.), *Handbook of Snow*. Toronto: Pergamon Press, 275-337.

Lehning, M., Bartelt, P., Brown, B., Russi, T., Stockli, U., and Zimmerli, M., 1999: SNOWPACK model calculations for avalanche warning based upon a new network of weather and snow stations. *Cold Regions Science and Technology*, 30: 145-157.

Lehning, M., Bartelt, P., Brown, B., and Fierz, C., 2002a: A physical SNOWPACK model for the Swiss avalanche warning. Part III: meteorological forcing, thin layer formation and evaluation. *Cold Regions Science and Technology*, 35: 169-184.

Lehning, M., Bartelt, P., Brown, B., Fierz, C., and Satyawali, P. K., 2002b: A physical SNOWPACK model for the Swiss avalanche warning. Part II: Snow microstructure. *Cold Regions Science and Technology*, 35: 147-167.

Leica Geosystems, 2003: *Users manual for the Total Geodimeter System (TGS) 400*. Leica Geosystems AG, Heerbrugg, Switzerland.

Lliboutry, L., 1971: Permeability, brine content and temperature of temperate ice. *Journal of Glaciology*, 10: 15-30.

Lliboutry, L. A., 1968: General theory of subglacial cavitation and sliding of temperate glaciers. *Journal of Glaciology,* 7: 21-58.

Mair, D., Nienow, P., Willis, I., and Sharp, M., 2001: Spatial patterns of glacier motion during a high-velocity event: Haut Glacier d'Arolla, Switzerland. *Journal of Glaciology,* 47: 9-20.

Mair, D., Nienow, P., Sharp, M., Wohlleben, T., and Willis, I., 2002: Influence of subglacial drainage system evolution on glacier surface motion: Haut Glacier d'Arolla. *Journal of Geophysical Research-Solid Earth,* 107: art. no. 2175.

Male, D. H., 1980: The seasonal snowcover. *In* Colbeck, S. C. (ed.), *Dynamics of Snow and Ice Masses*. New York: Academic Press, 305-395.

Male, D. H. and Gray, D. M., 1981: Snowcover ablation and runoff. *In* Male, D. H. and Gray, D. M. (eds.), *Handbook of Snow*. Toronto: Pergamon Press, 360-436.

Maloszewski, P., 1992: Mathematical modelling of tracer transport in different aquifers: Results from ATH test fields. *In* Hötzl , H. and Werner, A. (eds.), *Tracer Hydrology*. Rotterdam: Balkema, 25-30.

Marquardt, D., 1963: An algorithm for least-squares estimation of nonlinear parameters. *Journal of the Society for Industrial and Applied Mathematics,* 11: 431-441.

Marsh, P. and Woo, M., 1984a: Wetting front advance and freezing of meltwater within a snow cover 1. Observations in the Canadian Arctic. *Water Resources Research,* 20: 1853-1864.

Marsh, P. and Woo, M., 1984b: Wetting front advance and freezing of meltwater within a snow cover 2. A simulation model. *Water Resources Research,* 20: 1865-1874.

Marsh, P., 1990: Snow hydrology. *In* Prowse, T. D. and Ommanney, C. S. L. (eds.), *Northern Hydrology: Canadian Perspectives*. Saskatoon, Saskatchewan (Canada): Minister of Supply and Services Canada NHRI Science Report No.1, 37-61.

Marsh, P., 1999: Snowcover formation and melt: recent advances and future prospects. *Hydrological Processes,* 13: 2117-2134.

Masotti, D., 1991: Contribution à l'étude scientifique du karst de Tsanfleuron, Valais. *Actes du 9. Congrès national de la SSS*: 173-176.

Mathews, W. H., 1963: Discharge of a glacial stream. *IAHS Publ.,* 163, Wallingford, Oxfordshire.

McKay, G. A. and Gray, D. M., 1981: The distribution of snowcover. *In* Gray, D. M. and Male, D. H. (eds.), *Handbook of Snow*. New York: Pergamon Press, 153-190.

Meier, M. F., 1960: Mode of flow of Saskatchawen Glacier, Alberta, Canada. *United States Geological Survey Professional Paper,* 351: 16-18.

Meier, M. F. and Tangborn, W. V., 1961: Distinctive characteristics of glacier runoff. *United States Geological Survey Professional Paper,* 424: 14-16.

Meier, M. F., 1973: Hydraulics and hydrology of glaciers, The role of snow and ice in hydrology. Wallingford, Oxfordshire: *IAHS Publ.* 107, 353-369.

Mercanton, P. L., 1916: Vermessungen am Rhônegletscher, Mensurations au Glacier du Rhône, 1874-1915. *Neue Denkschriften der Schweizerischen Naturforschenden Gesellschaft*, 52, Zürich.

Moeri, T. and Leibundgut, C., 1986: Winter dye tracer experiments on the Findelengletscher (Canton Wallis, Switzerland). *Zeitschrift für Gletscherkunde und Glazialgeologie,* 22: 33-41.

Moreau, L., 2003: Documentary film: The ice flow of Argentiére glacier in the area of an ice fall (oral presentation). *Alpine Glaciology Meeting (AGM), 13/03-14/03/2003 Grenoble.*

Morris, E. M., 1989: Turbulent transfer over snow and ice. *Journal of Hydrology,* 105: 205-223.

Mortimer, C. E., 1987: *Chemie*. Stuttgart: Georg Thieme Verlag.

Nakawo, M. and Hayakawa, N., 1998: *Snow and ice science in hydrology*: Institute for Hydrospheric-Atmospheric Science, Nagoya University and United Nations Educational Scientific Organisation.

Ng, F., 2000: Canals under sediment-based ice-sheets. *Annals of Glaciology,* 30: 146-152.

Nienow, P., Sharp, M., and Willis, I., 1996a: Temporal switching between englacial and subglacial drainage pathways: dye tracer evidence from the Haut Glacier d'Arolla, Switzerland. *Geografiska Annaler,* 78 A: 51-60.

Nienow, P., Sharp, M., and Willis, I., 1996b: Sampling-rate effects on the properties of dye breakthrough curves from glaciers. *Journal of Glaciology,* 42: 184-189.

Nienow, P., Sharp, M., and Willis, I. C., 1996c: Velocity-discharge relationships derived from dye tracer experiments in glacial meltwaters: implications for subglacial flow conditions. *Hydrological Processes,* 10: 1411-1426.

Nienow, P., 1997: Hydrological influences on basal flow dynamics in valley glaciers. *Final Report. Nerc Research Fellowship GT5/93/AAPS/1.*

Nienow, P., Sharp, M., and Willis, I., 1998: Seasonal changes in the morphology of the subglacial drainage system, Haut Glacier d'Arolla, Switzerland. *Earth Surface Processes and Landforms,* 23: 825-843.

Nienow, P. W., 1993: *Dye tracer investigations of glacier hydrological systems*. PhD thesis, Department of Geography, University of Cambridge, Cambridge.

Nye, J. F. and Frank, F. C., 1973: Hydrology of the intergranular veins in a temperate glacier.Symposium on the Hydrology of Glaciers. Proceedings of the symposium held at Cambridge, England, 7-13 September 1969,. *IAHS Publ.*, 95, Wallingford, Oxfordshire.

Nye, J. F., 1976: Water flow in glaciers: Jökulhlaups, tunnels and veins. *Journal of Glaciology,* 17: 181-204.

Nye, N. F., 1973: Water at the bed of a glacier. *Symposium on the hydrology of glaciers*, 95: 189-194.

Oerter, H. and Moser, H., 1982: Water storage and drainage within the firn of a temperate glacier (Vernagtferner, Ötztal Alps, Austria). *Hydrological Aspects of Alpine and High-Mountain Areas,* 138: 71-81.

Office fédéral de topographie, 1992a: Carte nationale de la Suisse, 1:25000. St-Léonard, No. 1286.

Office fédéral de topographie, 1992b: Carte nationale de la Suisse, 1:25000. Les Diablerets, 1285.

Ohmura, A., 2001: Physical basis for the temperature-based melt-index method. *Journal of Applied Meteorology,* 40: 753-761.

Østrem, G. and Brugman, M., 1991: Glacier mass-balance measurements: *NHRI Science Report* No.4.

Paterson, W. S. B., 1994: The physics of glaciers. Third ed. New York: Pergamon.

Pfeffer, W. T., Illangasekare, T. H., and Meier, M. F., 1990: Analysis and modelling of melt-water refreezing in dry snow. *Journal of Glaciology,* 36: 238-246.

Pfeffer, W. T., Meier, M. F., and T.H., I., 1991: Retention of Greenland runoff by refreezing: implications for projected future sea level change. *Journal of Geophysical Research,* 96: 22117-22124.

Pfeffer, W. T. and Humphrey, N. F., 1996: Determination of timing and location of water movement and ice-layer formation by temperature measurements in sub-freezing snow. *Journal of Glaciology,* 42: 292-304.

Pohjola, V. A., 1994: TV-video observations of englacial voids in Storglaciären, Sweden. *Journal of Glaciology,* 40: 231-240.

Raymond, C. F., 1971: Flow in a transverse section of Athabasca Glacier, Alberta, Canada. *Journal of Glaciology,* 10: 55-84.

Raymond, C. F. and Harrison, W. D., 1975: Some observations on the behaviour or the liquid and gas phases in temperate glacier ice. *Journal of Glaciology,* 14: 213-233.

Raymond, C. F., 1980: Temperate valley glaciers. *In* Colbeck, S. C. (ed.), *Dynamics of Snow and Ice Masses*. London: Academic Press, INC., 80-139.

Reynaud, L., 1987: The November 1986 survey of the Grand Moulin on the Mer de Glace, Mont Blanc Massif, France. *Journal of Glaciology,* 33: 130-131.

Richards, K., Sharp, M., Arnold, N., Gurnell, A., Clark, M., Tranter, M., Nienow, P., Brown, G., Willis, I., and Lawson, W., 1996: An integrated approach to modelling hydrology and water quality in glacierized catchments. *Hydrological Processes,* 10: 479-508.

Röthlisberger, H., 1972: Water pressure in intra- and subglacial channels. *Journal of Glaciology,* 11: 177-203.

Röthlisberger, H., 1980: Gletscherbewegung und Wasserabfluss. *Wasser, Energie, Luft - Eau, énergie, air,* 72: 290-294.

Röthlisberger, H. and Lang, H., 1987: Glacial hydrology. *In* Gurnell, *A. M. and Clark, M. J. (eds.), Glacio-fluvial sediment transfer: An Alpine perspective*. Hoboken, N.J.: John Wiley and Sons, 207-284.

Schimpp, O., 1958: *Der Eishaushalt am Hintereisferner in den Jahren 1952-53 und 1953-54*, 4, Wallingford, Oxfordshire.

Schmidt, R. A., 1982: Properties of blowing snow. *Reviews of Geophysics and Space Physics,* 20: 39-44.

Schneebeli, M., 1995: Development and stability of preferential flow paths in a layered snowpack, 228, Wallingford, Oxfordshire.

Schneebeli, M., Pielmeier, C., and Johnson, J. B., 1999: Measuring snow microstructure and hardness using a high resolution penetrometer. *Cold Regions Science and Technology,* 30: 101-114.

Schneider, T., 1999: Water movement in the firn of Storglaciären, Sweden. *Journal of Glaciology,* 45: 286-294.

Schneider, T., 2000: Hydrological processes in the wet-snow of glaciers - a review. *Zeitschrift für Gletscherkunde und Glazialgeologie,* 36.

Schneider, T., 2001: Hydrological processes in firn on Storglaciären, Sweden: PhD thesis, Stockholm University.

Schommer, P., 1978: Rechnerische Nachbildung von Wasserspiegelganglinien im Firn und Vergleich mit Feldmessungen im Ewigschneefeld (Schweizer Alpen). *Zeitschrift für Gletscherkunde und Glazialgeologie,* 14: 173-190.

Schuler, T., 1997: Hydrologie eines randtropischen Gletschers. Diplomarbeit (unpublished), Institut für Hydrologie, Albert-Ludwigs-Universität Freiburg, Freiburg.

Schuler, T., 2002: Investigation of water drainage through an alpine glacier by tracer experiments and numerical modeling. Mitteilung, 177, Versuchsanstalt für Wasserbau, Hydrologie und Glaziologie der ETH Zürich, Gloriastrasse 37-39, ETH-Zentrum, CH-8092, Zürich.

Seaberg, S. Z., Seaberg, J. Z., Hooke, R. L., and Wieberg, D. W., 1988: Character of the englacial and subglacial drainage system in the lower part of the ablation area of Storglaciären, Sweden, as revealed by dye-trace studies. *Journal of Glaciology,* 34: 217-227.

Seligman, G., 1936: Snow structures and ski fields. London: Macmillan.

Sellers, S., 1999: Theory of water transport in melting snow with a moving surface. *Cold Regions Science and Technology,* 31: 47-57.

Sharp, M., Gemmell, J. C., and Tison, J.-L., 1989: Structure and stability of the former subglacial drainage system of the Glacier de Tsanfleuron, Switzerland. *Earth Surface Processes and Landforms,* 14: 119-134.

Sharp, M., Richards, K., Willis, I., Arbold, N., Nienow, P., Lawson, W., and Tison, J.-L., 1993: Geometry, bed topography and drainage system structure of the Haut Glacier d'Arolla, Switzerland. *Earth Surface Processes and Landforms,* 18: 557-571.

Sharp, M., Richards, K. S., and Tranter, M., 1998: *Glacier Hydrology and Hydrochemistry - Advances in Hydrological Processes*. Chichester: John Wiley and Sons Ltd.

Shimizu, H., 1970: Air permeability of deposited snow. *Low Temperature Science Series A,* 20: 1-32.

Shoemaker, E. M., 1986: Subglacial hydrology for an ice-sheet resting on a deformable aquifer. *Journal of Glaciology,* 32: 20-30.

Shreve, R. L., 1972: Movement of water in glaciers. *Journal of Glaciology,* 11: 205-214.

Shreve, R. L., 1985: Late Wisconsin ice-surface profile calculated from esker paths and types, Katahdin esker system, Maine. *Quaternary Research,* 23: 27-37.

Singh, P., Spitzbart, G., Hübl, H., and Weinmeister, H. W., 1999: Importance of ice layers on liquid water storage within a snowpack. *Hydrological Processes,* 13: 1799-1805.

Smart, P. L. and Laidlaw, I. M. S., 1977: An evaluation of some fluorescent dyes for water tracing. *Water Resources Research,* 13: 15-33.

Sommerfeld, R. A., Bales, R. C., and Mast, A., 1994: Spacial statistics of snowmelt flow: data from lysimeters and aerial photos. *Geophysical Research Letters,* 21: 2821-2824.

Spring, U., 1980: Intraglacialer Wasserabfluss: Theorie und Modellrechnung. Mitteilung 48, Versuchsanstalt für Wasserbau, Hydrologie und Glaziologie der ETH Zürich. [contact address: Gloriastrasse 37-39, ETH-Zentrum, CH-8092 Zürich]

Stenborg, T., 1969: Studies of the internal drainage of glaciers. *Geografiska Annaler,* 51 A: 13-41.

Stenborg, T., 1973: Some viewpoints on the internal drainage of glaciers. *Symposium on the hydraulics of glaciers*, Publication No. 95: 117-130.

Stone, D. B., Clarke, G. K. C., and Blake, E. W., 1993: Subglacial measurement of turbidity and electrical conductivity. *Journal of Glaciology,* 39: 327-340.

Stone, D. B. and Clarke, G. K. C., 1996: In situ measurements of basal water quality and pressure as an indicator of the character of subglacial drainage systems. *Hydrological Processes,* 10: 615-628.

Sturm, M. and Holmgren, J., 1993: Rain-induced water percolation in snow as detected using heat flux transducers. *Water Resources Research,* 29: 2323-2334.

Sugiyama, S. and Gudmundsson, G. H., 2003: Diurnal variations in vertical strain observed in a temperate valley glacier. *Geophysical Research Letters,* 30: art. no. 1090.

Swift, D. A., 2002: Provenance of suspended sediment in subglacial drainage systems. PhD thesis, Department of Geography and Topographic Science, University of Glasgow, Glasgow.

Swift, D. A., Nienow, P. W., Spedding, N., and Hoey, T. B., 2002: Geomorphic implications of subglacial drainage configuration: rates of suspended sediment evacuation controlled by seasonal drainage system evolution. *Sedimentary Geology,* 149: 5-19.

Taylor, G., 1954: The dispersion of matter in turbulent flow through a pipe. *Proceedings of the Royal Society of London,* A223: 446-468.

Theakstone, W. H., 1967: Basal sliding and movement near the margin of the Glacier Østerdalsisen, Norway. *Journal of Glaciology,* 6: 805-816.

Theakstone, W. H. and Knudsen, N. T., 1981: Dye tracer tests of water movement at the glacier Austre Okstinbreen, Norway. *Norsk Geografisk Tidskrift,* 35: 21-28.

Toride, N., Leij, F., and van Genuchten, M. T., 1999: The CXTFIT code for estimating transport parameters from laboratory or field experiments, version 2.1. *Technical Report,* 137. U.S. Department of Agriculture, Riverside, California.

Tranter, M., Brown, G. H., Hodson, A. J., and Gurnell, A. M., 1996: Hydrochemistry as an indicator of subglacial drainage system structure: a comparison of Alpine and sub-polar environments. *Hydrological Processes,* 10: 541-556.

Turner, 1997: Model 10-AU-005-CE Fluorometer, User's Manual. Sunnyvale, CA: Turner Designs. [contact address: 845 W. Maude Ave., Sunnyvale, CA 94086, USA]

Van der Veen, C. J. and Whillans, I. M., 1993: Location of mechanical controls on Columbia Glacier, Alaska, U.S.A., prior to its rapid retreat. *Arctic and Alpine Research,* 25: 99-105.

Van der Veen, C. J., 1999: *Fundamentals of Glacier Dynamics*. Rotterdam: Balkema.

Vivian, R. and Bocquet, G., 1973: Subglacial cavitation phenomena under the Glacier d'Argentière, Mont Blanc, France. *Journal of Glaciology,* 12: 439-451.

Vivian, R., 1980: The nature of the ice-rock interface: the results of investigation on 20 000 m2 of the rock bed of temperate glaciers. *Journal of Glaciology,* 25: 267-277.

Vortmann, G. and Timeus, G., 1910: L'applicazione del cloruro di litio nelle indagine d'irologia sotterranea. Le origini del Timavo. *Bolletino della Societa adriaticadi di science naturali, Trieste,* 25: 233-237.

Wakahama, G., 1968: The metamorphism of wet snow, 79, Wallingford, Oxfordshire.

Wakahama, G., 1975: The role of meltwater in densification processes of snow and firn, 114, Wallingford, Oxfordshire.

Walder, J. S. and Hallet, B., 1979: Geometry of former subglacial water channels and cavities. *Journal of Glaciology,* 23: 335-346.

Walder, J. S., 1982: Stability of sheet flow of water beneath temperate glaciers and implications for glacier surging. *Journal of Glaciology,* 28: 273-293.

Walder, J. S., 1986: Hydraulics of subglacial cavities. *Journal of Glaciology,* 32: 439-445.

Walder, J. S. and Fowler, A., 1994: Channelised subglacial drainage over a deformable bed. *Journal of Glaciology,* 40: 3-15.

Wankiewicz, A., 1979: A review of water movement in snow. *In* Colbeck, S. C. and Ray, M. (eds.), *Proceedings Meeting of Modelling Snow Cover Runoff, Sept. 26-28 1978.* Hanover, NH, USA, 223-252.

Warren, S. G., 1982: Optical properties of snow. *Reviews of Geophysics and Space Physics,* 20: 67-89.

Weertman, J., 1957: On the sliding of glaciers. *Journal of Glaciology,* 3: 33-38.

Weertman, J., 1964: The theory of glacier sliding. *Journal of Glaciology,* 5: 287-303.

Weertman, J., 1972: General theory of water flow at the base of a glacier or ice sheet. *Reviews of Geophysics and Space Physics,* 10: 287-333.

Weertman, J., 1983: Basal water film, basal water pressure, and velocity of traveling waves on glaciers. *Journal of Glaciology,* 29: 20-27.

Weertman, J. and Birchfield, G. E., 1983: Stability of sheet water flow under a glacier. *Journal of Glaciology,* 29: 374-382.

Weischet, W., 1991: *Einführung in die Allgemeine Klimatologie*. Stuttgart: Teubner.

Williams, M. W., Sommerfield, R., Massman, S., and Rikkers, M., 1999: Correlation lengths of meltwater flow through ripe snowpacks, Colorado Front Range, USA. *Hydrological Processes,* 13: 1807-1826.

Willis, I., 1995: Intra-annual variations in glacier motion: a review. *Progress in Physical Geography,* 19: 61-106.

Willis, I. C., Sharp, M. J., and Richards, K. S., 1990: Configuration of the drainage system of Midtdalsbreen, Norway, as indicated by dye-tracing experiments. *Journal of Glaciology,* 36: 89-101.

Willis, I. C., Richards, K. S., and Sharp, M. J., 1996: Links between proglacial stream suspended sediment dynamics, glacier hydrology and glacier motion at Midtdalsbreen, Norway. *Hydrological Processes,* 10: 629-648.